UNIVERSIDADE FEDERAL DO PARANÁ

CAROLINE KOZAK

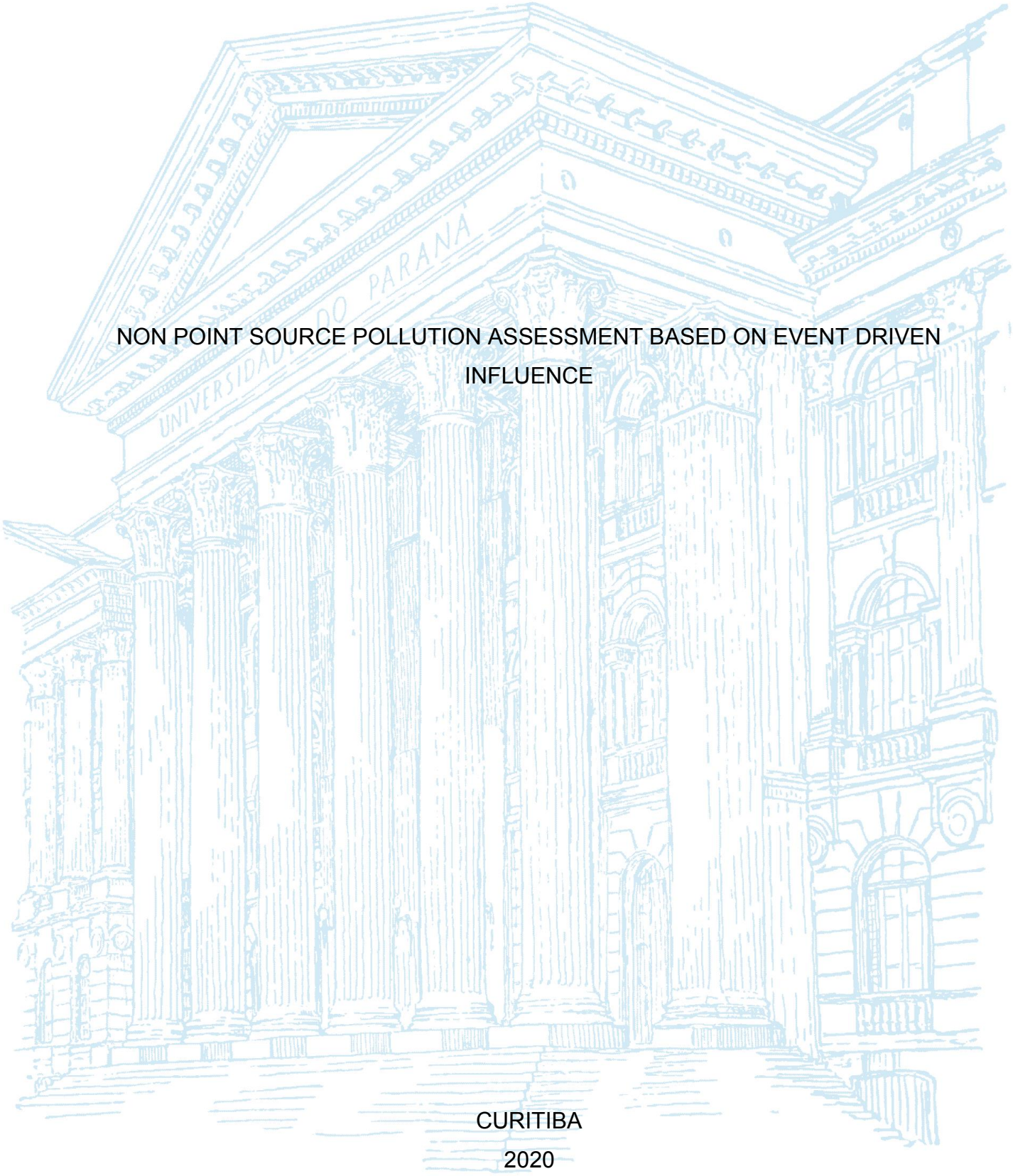

NON POINT SOURCE POLLUTION ASSESSMENT BASED ON EVENT DRIVEN INFLUENCE

CURITIBA

2020

CAROLINE KOZAK

NON POINT SOURCE POLLUTION ASSESSMENT BASED ON EVENT DRIVEN INFLUENCE

Tese apresentada ao curso de Pós-Graduação em Engenharia de Recursos Hídricos e Ambiental, Setor de Tecnologia, Universidade Federal do Paraná, como requisito parcial à obtenção do título de Doutor em Engenharia de Recursos Hídricos e Ambiental.

Orientador: Prof. Dr. Cristovão Vicente Scapulatempo Fernandes.

Coorientador: Prof. Dr. Sérgio Michelotto Braga.

Coorientador: Prof. Dr. Júlio César Rodrigues de Azevedo.

CURITIBA

2020

Catalogação na Fonte: Sistema de Bibliotecas, UFPR
Biblioteca de Ciência e Tecnologia

K88n Kozak, Caroline
Non point source pollution assessment based on event driven influence [recurso eletrônico] / Caroline Kozak. – Curitiba, 2020.

Tese - Universidade Federal do Paraná, Setor de Tecnologia, Programa de Pós-Graduação em Engenharia de Recursos Hídricos e Ambiental (PPGERHA), 2020.

Orientador: Cristovão Vicente Scapulatempo Fernandes.
Coorientador: Sérgio Michelloto Braga.
Coorientador: Júlio César Rodrigues de Azevedo.

1. Água - Qualidade. 2. Água - Poluição. 3. Desenvolvimento de recursos hídricos. I. Universidade Federal do Paraná. II. Fernandes, Cristovão Vicente Scapulatempo. IV. Braga, Sérgio Michelloto. V. Azevedo, Júlio César Rodrigues de. VI. Título.

CDD: 354.36

Bibliotecária: Vanusa Maciel CRB- 9/1928

APPROVAL MINUTE

The Examining Board is designated by the Faculty of the Graduate Program of the Federal University of Paraná in ENGENHARIA DE RECURSOS HÍDRICOS E AMBIENTAL where invited to argue the DISSERTATION of PHILOSOPHY DOCTOR by **CAROLINE KOZAK** , entitled: **Non point source pollution assessment based on event driven influence**, under the supervision of Dr. CRISTOVÃO VICENTE SCAPULATEMPO FERNANDES, which and after assessment of the candidate and the work, the Examining Board decided for the APPROVAL in the present rite.

The granting of the title of philosophy doctor is contingent upon the fulfillment of all the requirements indicated by the Examining Board and terms determined in the regulation of the Graduate Program.

CURITIBA, November 30th, 2020.

Eletronic Signature
30/11/2020 16:45:12.0
CRISTOVÃO VICENTE SCAPULATEMPO FERNANDES
President of the Examining Board

Eletronic Signature
07/12/2020 13:39:11.0
MARCO TADEU GRASSI
External Member (UNIVERSIDADE FEDERAL DO PARANÁ)

Eletronic Signature
01/12/2020 05:22:13.0
STEPHAN HILGERT
External Member (KARLSRUHE INSTITUTE OF TECHNOLOGY)

Eletronic Signature
03/12/2020 15:04:10.0
PAULO TARSO SANCHES DE OLIVEIRA
External Member (UNIVERSIDADE FEDERAL DO MATO GROSSO DO SUL)

Eletronic Signature
01/12/2020 14:52:39.0
REGINA TIEMY KISHI
Internal Member (UNIVERSIDADE FEDERAL DO PARANÁ)

Eletronic Signature
01/12/2020 10:57:59.0
SADEGH PARTANI
External Member (BOJNORD UNIVERSITY)

I dedicate this thesis to my husband, Jorge William Pedroso Silveira, who gave me wings to fly and, patiently, waited for me to return.

ACKNOWLEDGEMENTS

À Deus, pela dádiva da vida, e pelos desafios colocados no meu caminho, que me fizeram sair da minha zona de conforto e chegar até aqui.

À minha família pelo apoio incondicional.

Um agradecimento especial ao meu marido, Jorge Silveira, que me deu todo suporte técnico e emocional para que a execução deste trabalho desse certo, apoiando e defendendo todas as minhas decisões. Obrigada por tudo, mas principalmente, pela paciência, pelos sorrisos e pelo aprendizado diário.

Aos amigos que sempre estiveram por perto e foram tão importantes durante toda esta jornada, nas pessoas de Ana Paula Muhlenhoff, Artur Andrade, Bárbara Alves de Lima, Danieli Mara Ferreira, Carlos Eduardo Barquilha, Juliana Leithold, Luciane Lemos do Prado, Marcelo Coelho, Naiara Mottim Justino, Suelen Chami e Victória Monteiro Zanona. Infelizmente não consigo nomear a todos, mas com certeza minha gratidão é enorme e eterna, e vocês sabem disso.

Um agradecimento especial à Bruna Polli e Ellen Caroline Baettker, irmãs que a vida me deu e que sem dúvida tem grande influência no meu caminho, me dando suporte e sobretudo carinho mesmo quando eu menos merecia.

À sociedade brasileira.

À CAPES, CNPq e Fundação Araucária por todo suporte financeiro disponibilizado durante o período de desenvolvimento e execução desta pesquisa.

À Universidade Federal do Paraná e ao PPGERHA pela infraestrutura e pela oportunidade de me proporcionar uma educação pública e de qualidade

Aos membros da minha banca de avaliação, professores Regina Tiemy Kishi, Marco Tadeu Grassi, Paulo Tarso Sanches de Oliveira e os pesquisadores Stephan Hilgert e Sadegh Partani, pela disposição em acompanhar o desenvolvimento da pesquisa e dedicação ao ler este trabalho, contribuindo sempre significativamente para a sua evolução. Meu muito obrigada.

Um agradecimento especial à Luciane Lemos do Prado, Bárbara Alves de Lima e Rubia Bottini por toda ajuda, sugestão, apoio técnico-científico, ensinamentos e conversas durante a execução do trabalho no Laboratório de Engenharia Ambiental Francisco Borsari Neto (LABEAM), no Laboratório de Estudos Avançados em Química Ambiental (LEAQUA) e no Núcleo Interdisciplinar de Pesquisa em Tecnologias Ambientais (NIPTA).

A todo grupo de discentes e docentes PPGERHA que de alguma forma fizeram parte da minha evolução pessoal.

A professora Regina Kishi, em nome de todos os integrantes do Projeto Água e Ação, que me fizeram voltar a sonhar, fazer e realizar novamente.

Ao Leandro Stival por toda ajuda e suporte técnico no LaTeX.

Às minhas pupilas Fernanda Batista Guimarães Cipriano e Mayara Powrosnek que me deram todo o suporte laboratorial durante as análises e que me ensinaram tanto sobre orientação, relações pessoais e sobre a vida. Ao Lucas Przygoda que foi meu braço direito durante todos esses anos. Obrigada por todas idas ao campo, instalação de equipamentos, testes, erros, choros, risadas e parceira. Sem vocês este trabalho não seria possível.

À Dona Neusa, uma mulher extraordinária, forte e guerreira, que vive o Rio Barigui durante sua vida toda e me ajudou durante a campanha de escoamento de base. Obrigada pela simpatia, alegria e confiança. A senhora é um grande exemplo de vida e espero, que um dia, meu trabalho possa proporcionar melhores condições para os rios urbanos.

Aos meus co-orientadores, Sérgio Braga e Júlio Azevedo, por toda ajuda fornecida com infraestrutura, dando condições para que cada detalhe desejado neste trabalho fosse passível de ser realizado.

E por fim, mas não menos importante, todo meu agradecimento e carinho eterno ao meu orientador Cristovão Fernandes, um ser humano singular, principalmente por nunca deixar de acreditar. Obrigada por todos os momentos que vivemos durante essa parceria, inclusive as brigas. Obrigada por me ensinar sobre qualidade da água, sobre a idiossincrasias da vida e das pessoas e sobre sempre levantar mais uma vez porque “The fights still remains”.

"A educação não transforma o mundo. A educação muda as pessoas e as pessoas transformam o mundo"
(Paulo Freire)

"... But the fighter still remains"
(The Boxer - Simon and Garfunkel)

RESUMO

A ocorrência de eventos de chuva causa a lavagem das áreas superficiais de uma bacia hidrográfica e, consequentemente, o carreamento de poluentes para o corpo hídrico. Esta forma de fonte de poluição é chamada de fonte não pontual (FNP) e, devido a sua relação com a ocorrência de chuvas pode ser considerada mais difícil de ser monitorada do que as fontes pontuais. O tipo de poluente introduzido em um corpo hídrico pela FNP está relacionado com as características de uso do solo da bacia, assim como a forma que estes poluentes serão carreados está relacionado com as características hidrológicas dos eventos de chuva. Portanto, uma das formas de avaliar a contribuição de poluição por FNP é associando a concentração (mg L^{-1}) com a vazão (m^3 s^{-1}) e assim fazendo estimativas de carga (kg d^{-1}) da dinâmica dos poluentes, usando da estratégia de monitoramento integrado de chuva e vazão. As diferenças de uso do solo de cada área de drenagem da bacia refletem diferentemente na qualidade da água dos rios sendo, também, propagadas a jusante. Assim, realizar o monitoramento de dois locais consecutivos de uma bacia hidrográfica, considerando a dinâmica de transporte de poluentes por FNP entre eles, ainda não é efetivamente explorado na literatura. Assim, o objetivo deste trabalho é avaliar quali-quantitativamente a poluição de FNP influenciada pelos eventos de chuva em dois pontos de monitoramento consecutivos. Além disso também, será feita a avaliação da magnitude do aporte de poluente durante os eventos de chuva em comparação com o perfil de base do rio. Estes objetivos estão baseados na hipótese de que as distintas configurações de uso do solo em cada área de drenagem exercem influência significativa na contribuição da poluição carreada pelo escoamento superficial na bacia hidrográfica durante os eventos de chuva. Assim, a estratégia usada foi i) o uso de amostradores automáticos para coletar amostras de água do rio durante a ascensão e recessão dos hidrogramas, ii) o monitoramento de dois pontos consecutivos no rio (entrada e saída) e iii) a quantificação de distintos conjuntos de parâmetros de qualidade da água. A área de estudo foi a Bacia do Rio Barigui, na sua porção norte, em que os pontos estão localizados em Almirante Tamandaré (BA1) e no Parque Tingui (BA2). Para a coleta dos eventos de chuva, foram utilizados amostradores automáticos, configurados especificamente para cada ponto de monitoramento. Os conjuntos de parâmetros de qualidade da água (PQA) analisados foram: (i) tradicional (nitrogênio, fósforo, sólidos e carbono), (ii) matéria orgânica dissolvida (MOD), (iii) contaminantes emergentes (CE) e (iv) metais. Além disso, foram realizadas coletas sem a ocorrência de chuvas para delinear o fluxo de base dos rios, fazendo a análise dos mesmos conjuntos de parâmetros. Como resultado, foram monitorados 8 eventos de chuva, dos quais 3 eventos ocorreram em BA1 e 5 eventos em BA2. Portanto, existem 3 eventos de chuva que representam a entrada e saída entre os pontos BA1-BA2, denominado de influência da área incremental. De maneira geral, os resultados mostraram que as características dos eventos de chuva têm grande influência no carreamento dos poluentes, dos quais se destacam a intensidade da chuva, principalmente no ponto BA1, e a quantidade de dias secos antecedentes, principalmente no ponto BA2. Em termos quantitativos, os PQA indicam que o ponto BA2 recebe maior aporte de poluentes que o ponto BA1, onde BA1 recebe influência de FNP de poluição como lavagem de áreas vegetadas e/ou de agricultura, processos erosivos e formação geológica do solo, enquanto o ponto BA2, além de receber a influência de montante, recebe contribuições da lavagem das áreas urbanizadas, galerias e descarga de estação de tratamento de esgoto. Os parâmetros tradicionais mais relevantes medidos foram COD and SS, que respectivamente rep-

resentam uma carga introduzida de 74.10 ton day^{-1} e 196.27 ton day^{-1} em BA1, e 903.95 ton day^{-1} e 5,332.87 ton day^{-1} em BA2. A dinâmica da MOD mostrou que os eventos de chuva favorecem o carreamento de material com características mais refratárias para o corpo hídrico. Os CEs indicaram a influência da ocupação antrópica onde a cafeína e fármacos foram os contaminantes de maior ocorrência durante os eventos de chuva (100% de ocorrência para cafeína e naproxeno, e 42-100% de ocorrência para ibuprofeno). Os elementos inorgânicos, ou metais analisados na fração dissolvida tiveram maiores concentrações medidas durante o escoamento de base do que durante os eventos de chuva, indicando a influência da formação geológica da região; enquanto para os elementos da fração total apresentaram maiores concentrações durante os eventos de chuva, indicando o potencial transporte de poluentes aderidos às partículas para jusante. Desta forma, a principal contribuição desta tese foi verificar e confirmar a influência das mudanças de uso do solo ocorrida entre os pontos BA1 e BA2, com a diminuição de áreas vegetadas e o aumento de áreas urbanizadas, pela análise dos múltiplos PQA considerando a estratégia de análise da área incremental. Assim, destaca-se que os processos de FNP de poluição exercem influência na qualidade da água dos rios e devem ser considerados para a melhoria da gestão dos recursos hídricos.

Palavras-chaves: Monitoramento e Avaliação. Qualidade da água. Gestão de Recursos Hídricos. Fonte não pontual de poluição. Área incremental.

ABSTRACT

Rainfall episodes occurrence causes surface wash-off in the watershed and, consequently, pollutant carrying into the water bodies. This kind of pollution source is called a non-point source (NPS) and, due to its relation with rainfall occurrence, it can be considered more difficult to monitor than point sources. The type of pollutant introduced into the water body by NPS is related to the watershed land use, as well as, pollutants transport that will be carried in is related to the hydrological characteristics of rainfall events. Therefore, one of the ways to assess the contribution of NPS pollution is to associate the concentration (mg L^{-1}) with the flow (m^3 s^{-1}) and them to produce load estimation (kg d^{-1}) of pollutant dynamics, using rainfall and flow integrated monitoring strategy. The differences in land use in each drainage area reflect differently on the river water quality, and consequently, they are propagated downstream. Thus, monitoring two consecutive locations in a watershed, considering the pollutant dynamics of transport by FNP between them, is not yet effectively explored in the literature. Thus, the main aim of this research is to assess quali-quantitatively NPS pollution influenced by rainfall events at two consecutive monitoring points. In addition, an assessment will be made of the magnitude of the pollutant input during rain events compared to the base profile of the river. These objectives are based on the hypothesis that the different land use, in each drainage area, have a significant influence on the pollution contribution carried by runoff in the watershed during rainfall events. Thus, the strategy used was i) to use automatic samplers to collect water samples from the river during the hydrographs rising and recession, ii) to monitor two consecutive sites in the river (input and output), and iii) to quantify distinct water quality parameters. The study area was Barigui River Watershed, in its northern portion, where monitoring points were located in Almirante Tamandaré (BA1) and Parque Tingui (BA2). For rainfall discretization, automatic samplers were used, configured specifically for each monitoring point. The sets of water quality parameters (WQP) analyzed were: (i) traditional (nitrogen, phosphorus, solids and carbon); (ii) dissolved organic matter (DOM); (iii) emerging contaminants (EmerC) and (iv) metals. Additionally, campaigns without rainfall occurrence were performed, to outline river base flow. As a result, 8 rain events were monitored, of which 3 events occurred in BA1 and 5 events in BA2. Therefore, there are 3 rainfall episodes that represent the input and output between points BA1-BA2, called of incremental area influence. In general, results showed that hydrological characteristics had a great influence on pollutants behavior of which rainfall intensity especially at point BA1, and antecedent dry days especially at point BA2. In quantitative terms, WQP indicates that point BA2 receives a greater contribution of pollutants than point BA1, where BA1 is influenced by NPS pollution, such as washing-off from vegetated areas and/or agriculture, erosion processes and geological formation of the soil, while point BA receives upstream influence, washing-off from urbanized areas, galleries, and wastewater treatment plant discharge. The most relevant traditional parameters measured were COD and SS, which respectively represent an introduced load of 74.10 ton day^{-1} and 196.27 ton day^{-1} in BA1, and 903.95 ton day^{-1} and 5,332.87 ton day^{-1} in BA2. The DOM dynamics showed that rainfall events favor the carrying of material with more refractory characteristics for the water body. The EmerC indicated human activities influence, where caffeine and pharmaceuticals were the most frequent contaminants during rainfall events (100 % occurrence for caffeine and naproxen, and 42-100 % occurrence for ibuprofen). The inorganic elements, or metals analyzed in the dissolved

fraction, had higher concentrations during the baseflow than during rainfall events, indicating geological formation influence of the region; while for the total fraction had greater magnitude during rainfall events, indicating the potential transport of pollutants adhered to the particles downstream. Thus, the overall contribution is to proper assess the impact of changes in the incremental land use between two monitoring sites , with vegetated areas decrease and urbanized areas increase, by the analysis of multiple WQP, especially from anthropic influence to highlight the relevance of adequate assessment of NPS pollution on river water quality that should be considered to improve water resources management.

Key words: Monitoring and Assessment. Water Quality. Water Resources Management. Non point sources of pollution. Incremental Area.

LIST OF FIGURES

Figure 1 – Three pillars of NPS assessment . . . 29
Figure 2 – Strategy to monitor NPS contribution and transport considering a control volume . . 30
Figure 3 – Schematic representation of thesis subdivision . . . 32

Figure 4 – Urbanization effects in the surface runoff . . . 35
Figure 5 – Adaptive monitoring approach; (a) Represent hydrological context with and without rainfall occurrence; (b) Represent high-frequency monitoring all the time; (c) Represent adaptive monitoring focusing when there are periods of interest . . . 39
Figure 6 – Schematic representation of the pollutograph: (a) hydrograph: flow variation over time; (b) pollutograph: flow and concentration over time with similar pattern; (c) pollutograph: flow and concentration over time with opposite pattern . . . 42
Figure 7 – EMC curve representation and zone identification . . . 43
Figure 8 – Hysteresis patterns: (A) clockwise loop; (B) anticlockwise loop; (C) no hysteresis pattern; (D) figure-eight-shape loops . . . 45
Figure 9 – Plot of ΔC vs. ΔR for hysteresis loop and pattern of flow and concentration . . . 46
Figure 10 – Emerging contaminants interaction in the environment and potential human health risks . . . 55
Figure 11 – Potential pollution sources of emerging contaminants into the water body and human exposure . . . 55

Figure 12 – Barigui Watershed and, BA1 and BA2 monitoring sites localization . . . 71
Figure 13 – Land use classification for Barigui Watershed . . . 72
Figure 14 – Land use classification zoom for BA1 and BA2 drainage areas . . . 73
Figure 15 – Soil classification on the BA1 and BA2 monitoring sites . . . 74
Figure 16 – BA1 hydrograph in 2018. Data used was collect from rainfall station located in BA1. White space represent lack of data . . . 75
Figure 17 – BA2 hydrograph in 2018. Data used was collect from rainfall and meteorological station located in BA2. White space represent lack of data . . . 76
Figure 18 – Schematic representation of the hydrological characteristics calculated from hydrograph 77
Figure 19 – Almirante Tamandaré monitoring point. (a) improvement in structures to collect samples; (b) ruler to read water level; (c) SBn automatic sampler; (d) SBn storage/ (e) Monitoring site . . . 79
Figure 20 – Tingui monitoring point. (a) ruler to read water level; (b) SBn automatic sampler; (c) SBn storage . . . 80
Figure 21 – Programming logistical of SBn sampling based on flow rate schedule . . . 81
Figure 22 – BA1-2 intermediate monitoring site localization . . . 82
Figure 23 – Barigui Watershed slope, ranging between 1,100 m (hot colors) and 850 meters (cold colors) . . . 83
Figure 24 – Schematic representation of the cross section area in BA1 (up) and BA2 (down) . . . 84

Figure 25 – UV-Vis scan from 200 to 600 nm with specific absorbance's location of the $SUVA_{254}$, A_{285}/DOC, E_2/E_3 and E_3/E_4 . Black arrow indicates absorbance in 254 nm for the $SUVA_{254}$ calculation; Red arrow indicates absorbances in 285 nm for the A_{285}/DOC calculation; Grey lines indicate absorbances in 300 nm and 400 nm for the ratio A_{300}/A_{400} (E_3/E_4) calculation; Blue lines indicate absorbances in 250 nm and 365 nm for the ratio A_{250}/A_{365} (E_2/E_3) calculation 86
Figure 26 – Peak and indices identification on EEM representation. White rectangles represent the specific region where peak A, C, T_1, T_2 and B are measured. A peak is identified as the highest intensity value, measured in Raman Units (r.u.). Locations of emission intensities used to calculate HIX (pink circles, λ_{Ex} 254 nm), BIX (cian points, λ_{Ex} 310 nm) and FI (light gray points, λ_{Ex} 370 nm) are indicated 87
Figure 27 – Molecular structures of the pharmaceutical emerging contaminants considered in this study 90
Figure 28 – Molecular structures of the PCPs emerging contaminants considered in this study . . 91
Figure 29 – Molecular structures of the sterol emerging contaminants considered in this study . . 91
Figure 30 – Graphical Abstract of the results subdivision, considering hydrological characteristics and water quality parameters 92
Figure 31 – Hydrographs for rainfall events collected in BA1 and BA2 monitoring sites 95
Figure 32 – Scores and loadings from PCA of rainfall episodes and hydrological characteristics . . 98
Figure 33 – Water volume transported (V_{transp}) (black bar) and surface runoff (SRun) (grey bar) proportions during the rainfall episode monitored in BA1 and BA2 99
Figure 34 – Dendrogram of the hydrological characteristics measured in the rainfall episodes . . . 102
Figure 35 – Linear Fit of the groups identified in the Cluster analysis 103
Figure 36 – Box plot of the conventional water quality parameters for baseline campaign 106
Figure 37 – N-NH_4^+ and TN concentration along baseline campaign 108
Figure 38 – PO_4^{3-} and TP concentration along baseline campaign 108
Figure 39 – DOC and COD concentration along baseline campaign 109
Figure 40 – Turbidity and SS concentration along baseline campaign 109
Figure 41 – Pollutographs from BA1 monitoring site in E1, E2 and E4, respectively along the horizontal axis 110
Figure 42 – Pollutographs from BA2 monitoring site in E1, E2, E3, E4 and E5, respectively along the horizontal axis 111
Figure 43 – EMC curves during rainfall episodes in BA1 and BA2 116
Figure 44 – Overall EMC and load values for the WQP measured in the five diffuse pollution events and baseline 118
Figure 45 – EMC changes in BA1 during rainfall episodes. Positive values indicates input mass and negative values indicate dilution effects. 119
Figure 46 – EMC changes in BA2 during rainfall episodes monitored. Positive values indicate input mass and negative values indicate dilution effects 121
Figure 47 – WQP increment between control volume (BA2-BA1) during E1 (grey), E2 (green) and E4 (blue). 122
Figure 48 – WQP proportion of contribution from each drainage area 123
Figure 49 – Box plot of EEMs peaks for BA1, BA1-2 and BA2 monitoring sites during baseline campaign 126
Figure 50 – EEMs with the highest peak T_2 intensity measured during baseline campaign 127
Figure 51 – Biplot of A_{285}/DOC and $SUVA_{254}$ values between BA1, BA1-2 and BA2 during baseline campaign 128

Figure 52 – Biplot of FI and BIX values between BA1, BA1-2 and BA2 during baseline campaign 128
Figure 53 – HIX values distribution in BA1, BA1-2 and BA2 during baseline campaign 129
Figure 54 – EEMs peaks distribution along the three rainfall episodes monitored in BA1 129
Figure 55 – EEMs peaks distribution along the five rainfall episodes monitored in BA2 130
Figure 56 – A_{285}/DOC and $SUVA_{254}$ distribution during rainfall episodes monitored in BA1 and BA2. 132
Figure 57 – Biplot FI-BIX and HIX distribution along rainfall episodes monitored in BA1 and BA2.133
Figure 58 – Box plot of EEMs peaks from baseline profile and events monitored in BA1 and BA2 135
Figure 59 – Samples collected during rainfall episodes and assessed for emerging contaminants at BA1 and BA2 monitoring sites 137
Figure 60 – CAF, NAP and TCS behavior along rainfall episodes monitored in BA1 and BA2 sites 141
Figure 61 – NAP, CAF and TCS behavior in rainfall event 2 monitored in BA1 and BA2 142
Figure 62 – EMC curves of emerging contaminants during event 2 143
Figure 63 – Load of emerging contaminants during event 2 in BA1 and BA2 144
Figure 64 – Samples collected and analyzed for metals in BA1 and BA2 145
Figure 65 – Pollutographs of dissolved metals monitored in BA1 and BA2 during rainfall episodes 146
Figure 66 – EMC for dissolved metals analyzed during baseline and rainfall episodes at BA1 and BA2 147
Figure 67 – Pollutographs of total metals monitored in BA1 and BA2 during rainfall episodes . . 149
Figure 68 – EMC for total metals analyzed during baseline and rainfall episodes at BA1 and BA2 150
Figure 69 – Pollutograph of total metals in event 2 at BA1 and BA2 151
Figure 70 – EMC curves of total metals during event 2 in BA1 and BA2 152
Figure 71 – Metals EMC of incremental area on the event 2 153
Figure 72 – Scheme of the similar researches associated to the results sub-sections presented . . . 156

Figure 73 – Average values of hydrological characteristics measured in BA1 and BA2 158
Figure 74 – Average incremental load (ton day^{-1}) of the water quality parameters analyzed in this study: a) conventional - part I; b) conventional - part II; c) emerging contaminants; d) total metals 159
Figure 75 – Relative differences between rainfall events EMC and baseline EMC for a) conventional parameters - part I, b) conventional parameters - part II, c) emerging contaminants, d) dissolved metals, e) total metals 161
Figure 76 – Box plots of the total and dissolved fraction of a) carbon, b) phosphorus, c) nitrogen, d) aluminium, e) calcium, and f) magnesium measured during rainfall episodes 162

LIST OF TABLES

Table 1 – Logic evolution for diffuse pollution assessment . . . 47
Table 2 – UV-Vis absorbance ratios used for CDOM characterization . . . 50
Table 3 – Five main regions in the EEM for identification of the humic- and protein-like compounds 52
Table 4 – Fluorescence indices for assessment of DOM sources and composition . . . 52
Table 5 – Emerging contaminants characteristics considered in this study . . . 61
Table 6 – Monitoring details from previously studies of water quality in rivers . . . 67
Table 7 – Similar studies which evaluated organic matter contribution during rainfall episode . . . 69

Table 8 – Monitoring sites details: drainage area and river length . . . 70
Table 9 – Land use and soil occupation in two monitoring sites in River Barigui . . . 72
Table 10 – Main chemical characterization of Latossol, Cambisol and Argisol soils . . . 73
Table 11 – Total monthly precipitation and average monthly flow from BA1 and BA2 monitoring site during 2018. . . . 75
Table 12 – Rainfall episode classification according to RI, RD and ΔQ . . . 78
Table 13 – Analytical procedures used to determine conventional water quality parameters . . . 85
Table 14 – EmerC categorization and classification, nomenclature and abbreviations used in this thesis . . . 89

Table 15 – Detailing of the rainfall episodes monitored: number of samples collected in each monitoring site, and period of the year which occurred the sampling . . . 94
Table 16 – Hydrological characteristics for the rainfall events analyzed in this study in BA1 and BA2 monitoring site . . . 96
Table 17 – Rainfall episodes parameterization and classification (REClass) proposed, according to RI, RD and ΔQ measured from the hydrograph . . . 96
Table 18 – V_{transp}, SRun and P_{acum} considering the proportions of water volume precipitated and transported . . . 100
Table 19 – Pearson correlation for the hydrological characteristics measured in the five rainfall episode . . . 101
Table 20 – Sample identification (ID) and sampling schedule in the baseline campaign . . . 105
Table 21 – Average ($\overline{x}$) (± standard deviation (σ)), maximum (max) and minimum (min) concentration of the water quality parameters (WQP) in baseline campaign . . . 107
Table 22 – Pollutographs pattern observed for the traditional water quality parameters during rainfall episodes monitored . . . 111
Table 23 – Average (± standard deviation), maximum (max) and minimum (min) concentration of the conventional water quality parameters for rainfall episodes monitored . . . 114
Table 24 – EMC values for the rainfall episodes monitored in BA1 and BA2 . . . 115
Table 25 – EMC values in the peak of each rainfall episode, in BA1 and BA2 . . . 117
Table 26 – Average ($\overline{x}$)(± standard deviation (σ)), maximum (max) and minimum (min) peak intensity of the EEMs in baseline campaign . . . 125
Table 27 – Average (± standard deviation) of peaks A, B, C, T1 and T2 measured in EEMs for all rainfall episodes monitored in BA1 and BA2 . . . 131
Table 28 – Average values of peaks A, B, C, T1 and T2, and humic- and protein-like sum for baseline and rainfall episodes monitored in BA1 and BA2 . . . 134

Table 29 – Percentage of occurrence of the emerging contaminants in the baseline and rainfall episodes monitored in BA1 and BA2 139
Table 30 – CAF, NAP and TCS average ($\overline{x}$)± standard deviation σ, max and min concentration (μg.L^{-1}) in baseline and rainfall episodes monitored 140
Table 31 – Average concentration (± standard deviation) (ppb) of the metals analyzed in BA1 and BA2 during baseline and rainfall episodes 148
Table 32 – Proportion (%) of the pollutant carried into the river until peak flow in BA1 and BA2 152
Table 33 – Calculated loads for conventional water quality parameters, total metals and emerging compounds in BA1 and BA2 160
Table 34 – Selectivity data of the emerging compounds measured in this thesis 165
Table 35 – Linearity and sensitivity of the emerging compounds measured in this thesis 166
Table 36 – Limits of detection (LOD) and quantification (LOQ) for the emerging components measured in samples of this thesis 167
Table 37 – Element identification, calibration curve and correlation coefficient for the inorganic analysis performed in ICP-OES 167
Table 38 – Limits of detection (LOD) and quantification (LOQ) for the inorganic elements (metals) measured in samples of this thesis 168

LIST OF ABBREVIATIONS AND ACRONYMS

A_{285}/DOC	Ratio between Absorbance in 285 nm and Dissolved Organic Carbon
AAS	Acetylsalicylic Acid
ADP	Antecedent Dry Period (day)
AMS	Adaptive monitoring strategy
AS	Salicylic Acid
BA1	Monitoring site located in Almirante Tamandaré City
BA1-2	Monitoring site located in São Jorge WWTs output
BA2	Monitoring site located in Tingui Park, Curitiba City
BeP	Benzylparaben
BIX	Biological Index
BMP	Best Management Practice
BOD	Biochemical Oxygen Demand
BSTFA	N, O-Bis(trimethylsilyl)trifluoroacetamide
Bt	Base time of the hydrograph (hours)
BuP	Butylparaben
βsi	β-Sitosterol
C18	Octadecil
CAF	Caffeine
CAS	Chemical Abstracts Service
CDOM	Chromophoric DOM
CEC	Contaminant of Emerging Concern
CLN	Colestanona
CLT	Cholesterol
COD	Chemical Oxygen Demand
CODd	Dissolved Chemical Oxygen Demand
COPEL	Companhia Paranaense de Energia (in portuguese)
Cot	Concentration Time of the hydrograph (hours)
CPL	Coprostanol
Crt	Critical Time of the Hydrograph (hours)

DL	Detection Limit
DIC	Diclofenac
DO	Dissolved Oxygen
DOC	Dissolved Organic Carbon
DOM	Dissolved Organic Matter
ΔQ	Flow variation ($m^3.s^{-1}$)
E1	Event 1
E2	Event 2
E3	Event 3
E4	Event 4
E5	Event 5
Es1	Estrone
Es2	17β-Estradiol
E. Coli	Escherichia coli
EC	Electrical Conductivity
ED	Event Duration (hours)
EE2	Ethinyl Estradiol
EEM	Excitation-Emission Matrix
EI	Electrons Impact
EMC	Event Mean Concentration
EmerC	Emerging Contaminants
EPL	Epicoprostanol
EPR	Electron Paramagnetic Resonance
EtP	Ethylparaben
FDOM	Fluorescent DOM
FEEMC	Fluorescence Excitation-Emission Matrix Code
FenP	Fenoprofen
FI	Fluorescence Index
FNF	Fenofibrate
FSS	Fixed Suspended Solids
Ft	Falling-limb time of the hydrograph (hours)
FT-ICR/MS	Fourier Transform Ion Cyclotron Resonance - Mass Spectrometer
GC	Gas Chromatography
GemF	Gemfibrozil

HIX	Humification Index
HPLC	High Performance Liquid Chromatography
HS	Humic Substances
ICs	Inorganic Compounds
ICP-OES	Inductively Coupled Plasma Optical Emission Spectrometry
IBU	Ibuprofen
IR	Infrared Spectroscopy
Koc	Partition coefficient between organic carbon and water
Kow	Partition coefficient between octanol and water
LOD	Limit of Detection
LOQ	Limit of Quantification
LME	Electronic Monitoring Laboratory (in portuguese Laboratório de Monitoramento Eletrônico)
Max	First maximum value from a set of data
MeP	Methylparaben
Min	First minimum value from a set of data
MRM	Multiple Reactions Mode
MS	Mass spectrometry
MS/MS	Tandem Mass spectrometry
MTL	Metoprolol
NAD	Nadolol
NAP	Naproxen
n.c.	Not Collected
NMR	Nuclear Magnetic Resonance Spectroscopy
NS	Number of Samples
NPS	Non Point Source
OC	Organic Carbon
OM	Organic Matter
P_{accum}	Accumulated precipitation (mm)
P_{accum} 25%	Accumulated precipitation (mm) until achieve the first 25% of the total rainfall amount
PAH	Polycyclic Aromatic Hidrocarbon or polyaromatic hydrocarbons
PAR	Paracetamol
PCPs	Personal Care Products
pH	potential of Hydrogen
pka	Coefficient of Acid Dissociation

PRL	Propanolol
PrP	Propylparaben
PS	Point source
Q_{base}	Base flow ($m^3.s^{-1}$)
QL	Quantitation Limit
Q_{max}	Maximum flow ($m^3.s^{-1}$)
RD	Rainfall Duration (hours)
RD 25%	Rainfall Duration until achieve the first 25% of the total rainfall amount
RClass	Rainfall classification according to WHO (2008)
REClass	Rainfall episodes classification
RI	Rainfall Intensity ($mm.h^{-1}$)
rpm	Rotation per minute
Rt	Rising-limb time of the hydrograph (hours)
r.u.	Raman Units
SANEPAR	Paraná Sanitation Company
SBn	Automatic sample with distinct schedule to collect samples in rainfall episode developed on LME by Professor Sergio Braga
SPE	Solid Phase Extration
SRP	Soluble Reactive Phosphorus
SRun	Surface Runoff (m^3)
SSC	Suspended Sediment Concentration
STI	Stigmasterol
$SUVA_{254}$	specific ultraviolet absorbance in 254 nm
TCS	Triclosan / Irgasan
TDP	Total Dissolved Phosphorus
TKN	Total Kjedahl Nitrogen
TMCS	TriMethylChloroSilane
TMDL	Total Maximum Daily Load
TN	Total Nitrogen
TOC	Total Organic Carbon
TP	Total Phosphorus
TPP	Total Particulate Phosphorus
TRP	Total Reactive Phosphorus
TSS	Total Suspended Solids
UASB	Upflow Anaerobic Sludge Blanket

UV-Vis	Ultra Violet Visible
VSS	Volatile suspended solids
V_{transp}	Volume of water transported (m^3)
WaT	Water Temperature
WQP	Water Quality Parameter
WTP	Water Treatment Station
WWTP	Waste Water Treatment Plant

LIST OF SYMBOLS

Al	Aluminium
$Al_2(SO_4)_3$	Aluminium sulfate
Ar	Argon
As	Arsenic
B	Boron
Ba	Barium
C	Carbon
Ca	Calcium
Cd	Cadmium
Cl	Chlorine
Co	Cobalt
Cr	Chromium
Cu	Copper
-C=O	Double bond between carbon and oxygen
-CNO	bond among carbon, nitrogen and oxygen
Fe	Iron
$FeCl_3$	Iron Chloride
H_2SO_4	Sulfuric acid
HCl	Hydrochloric acid
He	Helium
Hg	Mercury
HNO_3 p.a.	Nitric Acid pure
K	Potassium
Mg	Magnesium
Mn	Manganese
N	Nitrogen
Na	Sodium
Ni	Nickel
N-NH_4^+	Ammonium Nitrogen
N-NO_3^-	Ion Nitrate
N-NO_2^-	Ion Nitrite

O	Oxygen
P	Phosphorus
Pb	Lead
PO_4^{3-}	Íon orthophosphate
Si	Silicon
σ	Standard deviation of the data
λ	Wavelength
$\overline{x}$	Average values of the data
Zn	Zinc

CONTENTS

1 INTRODUCTION . . . 27
1.1 Evidence of interest and Strategy . . . 29
1.2 Thesis Hypothesis and Objectives . . . 31
1.3 Thesis Organization . . . 32

2 THEORETICAL BACKGROUND . . . 33
2.1 Diffuse pollution dynamic: non point sources concepts . . . 33
2.1.1 Land use and NPS . . . 34
2.2 What is the best way to assess NPS contribution? . . . 36
2.2.1 Monitoring strategy . . . 36
2.2.2 Hydrological Characteristics . . . 40
2.2.3 Data Analysis and Assessment . . . 41
2.2.3.1 Pollutograph . . . 41
2.2.3.2 Event Mean Concentration - EMC . . . 42
2.2.3.3 Hysteresis . . . 44
2.2.4 Summary . . . 46
2.3 What are the water quality parameters needed to be measured? . . . 47
2.3.1 Conventional Water Quality Parameters for NPS . . . 47
2.3.2 Spectroscopy Techniques . . . 49
2.3.2.1 UV-Vis absorbances . . . 49
2.3.2.2 Fluorescence . . . 51
2.3.3 Emerging Contaminants . . . 54
2.3.3.1 Pharmaceutical . . . 56
2.3.3.2 Caffeine (CAF) . . . 58
2.3.3.3 Personal Care Products (PCPs) . . . 58
2.3.3.4 Sterol . . . 59
2.3.4 Inorganic Elements (IEs) or Metals . . . 62
2.3.5 Summary . . . 65
2.4 Where are we? . . . 65

3 MATERIAL AND METHODS . . . 70
3.1 The Barigui Watershed . . . 70
3.2 Land use . . . 70
3.2.1 Geology . . . 72
3.3 Hydrological Characteristics . . . 74
3.3.1 Rainfall Episodes Classification - REClass . . . 78
3.4 Monitoring Strategy for NPS Conditions . . . 79
3.4.1 Infrastructure . . . 79
3.4.2 Automatic Sampler - SBn . . . 80
3.4.3 Baseline Conditions . . . 82
3.4.4 Control Volume . . . 83
3.5 Water Quality Parameters . . . 85
3.5.1 Conventional Water Quality Parameters . . . 85

3.5.2 Dissolved Organic Matter (DOM) . . . 86
3.5.3 Inorganic Elements (IEs) . . . 87
3.5.4 Emerging Contaminants (EmerC) . . . 88

4 RESULTS AND DISCUSSION . . . 92
4.1 **Rainfall episodes assessment** . . . 94
4.1.1 Rainfall Episodes . . . 94
4.1.2 Influence of the hydrological characteristics on discharge behavior . . . 99
4.1.3 Summary . . . 103
4.2 **Conventional Water Quality Parameters** . . . 105
4.2.1 Baseline . . . 105
4.2.2 Pollutographs . . . 109
4.2.3 EMC . . . 115
4.2.4 Baseline and Rainfall Episodes . . . 117
4.2.4.1 BA1 . . . 118
4.2.4.2 BA2 . . . 120
4.2.5 Control Volume: BA2 - BA1 . . . 121
4.2.6 Summary . . . 124
4.3 **DOM dynamics** . . . 125
4.3.1 Baseline . . . 125
4.3.2 Rainfall . . . 127
4.3.3 DOM dynamics in the control volume defined . . . 133
4.3.4 Summary . . . 136
4.4 **Emerging Contaminants** . . . 137
4.4.1 Occurrence . . . 137
4.4.2 CAF, NAP and TCS behavior . . . 140
4.4.3 Summary . . . 144
4.5 **Metals** . . . 145
4.5.1 Dissolved Fraction . . . 146
4.5.2 Total Fraction . . . 149
4.5.3 Metals dynamics . . . 151
4.5.4 Summary . . . 153
4.6 Summary of the Chapter . . . 155

5 FINAL REFLECTIONS . . . 157
5.1 How is the impact of land use? . . . 157
5.2 How much pollutant load is carried into the river during the rainfall episodes? . . . 158
5.3 How distant are we from the baseline conditions? . . . 160
5.4 Where does the pollution go? . . . 162
5.5 Future strategy research questions . . . 163

6 APPENDIX . . . 165
6.1 Materials and Methods . . . 165
6.1.1 Quality control of emerging contaminants analysis . . . 165
6.1.2 Quality control of inorganic elements analysis . . . 165
6.1.3 Fluorescence Excitation-Emission Matrix Code - FEEMC . . . 166

Bibliography . . . 169

1 INTRODUCTION

> *"The decision based on information is a better qualified decision. The river basins management involves a large number of social and political aspects, and this characteristic often induces to a mistaken assessment of what the "management mission" is. The last goal of the management process is to make decisions about water resources uses and implement them effectively. However important social factors are, such as public participation, conducting orientation campaigns, promoting environmental education programs and others, it is inescapable that good quality decisions depend on information and analytical tools to give them support."*
>
> Porto and Porto (2008)

The water resources planning and management Brazilian law (Federal Law number 9433 from 8^{th} January, 1997) provides conditions, requirements and considerations for adequate water assessment for planning and action. The main goal is to always guarantee enough water quantity for the future generations, and therefore the proper quality for use. As a consequence, the management strategy have to integrate quantity and quality considering the land use changes along the time. To ensure these purposes, five instruments have been defined: (i) water resources plan, (ii) proper right of use, (iii) charging for water use, (iv) water classification, and (v) information system. Each management tool have distinct objectives and must be implemented to guarantee multiple water uses. Despite potential independent application, the requirement of applying all together will improve management efficiency and efficacy (PORTO; PORTO, 2008). The necessity of an assessment based on temporal and spatial challenges are still encouraging.

In this perspective, water monitoring is essential. Usually, it is performed hydrological monitoring programs that involve quantitative and qualitative aspects of the water resources. In Brazil, there are more than twenty-one thousand of monitoring stations, but only about 5 thousand to monitor water quality in the entire national territory, being operated to the National Water Agency and National Net of Water Quality Monitoring (ÁGUAS, 2018). These stations are concentrated in southern, southeastern and coastal regions of northeastern Brazil (ÁGUAS, 2018) with significant lack information about water quality. Rainfall and discharge analysis generally are based on a typical hydrological year, and the main water quality parameters are pH, water temperature (WaT), dissolved oxygen (DO), turbidity and electrical conductivity (EC).

Conventional Brazilian monitoring programs of water quality, without automatic system or high-frequency monitoring, consider monthly (even weekly) campaigns to assess water quality over the year. Generally, it is defined according to the spatial concern of point sources (PS) of pollution, mainly to attend the demands of the water body classification. In general PS approach are referred to 95% flow and concentration frequency curve (ZUCCO et al., 2012; ÁGUAS, 2013a). However, water quality is also associated to more environment aspects as rainfall regimes, surface runoff, geology, surface vegetation cover, land use, anthropic influences, and combination from PS and NPS of pollution.

Yan, Li and Gao (2019) present NPS control from rural and agricultural areas, which represent about half of the total water pollution in China. The authors proposed an framework to identify sources of NPS pollution (export coefficient), and critical and dominant sources areas. They highlighted that these kind of assessment and identification are prerequisite to control water pollution from NPS. In the other perspective, Chen et al. (2018b) present NPS concern from urban areas, where surface dust accumulation

was identified as the key sources of urban NPS. The authors proposed an comparison between rainfall episodes and snow-melt occurrence as driven forces of pollution, because their mechanism of transport are different. Similarly, it was highlight the necessity to identify and to characterize NPS pollution in order to improve a management of water quality.

In United State of America, the Clean Water Act′s provide a total maximum daily load (TMDL) program to control water pollution and decrease pollution sources, and then, to ensure water bodies restoration, protection, and guidelines achievement. TMDL determines maximum load of pollution from PS and NPS, plus a margin of safety, to be discharged in river and do not exceed water quality standards. For each pollutant a TMDL is developed, and specific reductions loads are calculated for each kind of pollutant (USEPA, 2018). Moreover, reasonable best management practice (BMP) to control NPS must be considered and well implemented to achieve the purpose of pollution control (NOVOTNY, 2003).

Brazil have increased monitoring programs for the water resources planning and management purposes, and one appropriated law and standards to ensure this improvement for safety and to establish consensus for adequate management . However, there is a lack of water quality data and quali-quantitative approach to understand the entire process. It is required to proper address PS and NPS, with hydrological regime of rainfall and land use influences into the water system. According to Shen et al. (2020), the solution to environmental problems relies on the implementation of management measures and policies, and there are few applications of watershed BMPs in order to control NPS paradigm.

Each activity developed in a watershed have directly influence into the water quality of the near water resource. It is a cause-effect reaction. Urban areas and agriculture affect water system, in distinct forms, but both under intense impact. Agricultural activities increase the amount of fertilizer, can induce erosion processes and have influence in suspended solids carried into the river (BU et al., 2014; YU et al., 2016). On the other hand, urbanization increase surface runoff directly to water bodies (PORTO; PORTO, 2008; GIRI; QIU, 2016). This kind of pollution sources, named as NPS, has been one of the biggest challenge for the water quality improvement (ÁGUAS, 2013b).

Generally, the urban source is easier to detect because is punctual, than agriculture source due to the mechanisms of pollution transport and input. Therefore, a quali-quantitative monitoring strategy sounds required to understand aspects that have influence in water quality, considering the watershed territory. To monitor, under this perspective, can help to identify priority areas to improve management actions. There is significant contribution to understand the load pollutant as consequence of rainfall episodes (INAMDAR et al., 2011; BRAGA, 2013; SINGH; INAMDAR; MITCHELL, 2015; KOZAK, 2016; ZHOU et al., 2017; MCCARTHY et al., 2018; FRANK; GOEPPERT; GOLDSCHEIDER, 2018). But automatic sampling reveals ideal quali-quantitative strategy to the monitoring system evolution (MORAETIS et al., 2010; BRAGA, 2013; CHEN et al., 2015; RAMOS et al., 2015; YU et al., 2016; RUHALA; ZARNETSKE, 2017; ZULKIFLI; RAHIM; LAU, 2017). However, there are few studies which consider these two above mentioned aspects and land use changes. And it is essential to associate these concepts to detect influence of NPS and their impacts into the river system.

Generally, non-point pollution studies use the intensive monitoring strategy from a single monitoring point (BENDER et al., 2018; KOZAK et al., 2019; GRUDZIEN, 2019; DRUMMOND, 2020), due to the high costs and some difficulties in automated monitoring during rainfall episodes. The Bender et al. (2018), Kozak et al. (2019), Grudzien (2019), Drummond (2020) studies were developed in Brazil, respectively in Rio Grande do Sul State and Paraná State. In all of them, were evaluated just one monitoring site for different reason, as for example, i) few studies which evaluated intra-events effects; ii) absence of non-point sources studies in the watershed; iii) quali-quantative discretization of the hydrograph during rainfall episodes that usually is not conventional in the country, and others.

In contrast, the studies that consider spacial monitoring, with more than one sites, usually assess the rainfall effects, in distinct land use zones or seasons (ZHANG et al., 2018b; FRANK; GOEPPERT; GOLDSCHEIDER, 2018; DONG et al., 2019; MA; LI, 2020). In this strategy, it is common to use high-frequency sensors to collect water quality data (BAUWE et al., 2015; MCCARTHY et al., 2018) producing continuous data series, including therefore, dry and rainy seasons. These studies are generally developed abroad.

However, interestingly, any of these strategies mentioned consider two (or more) monitoring sites consecutively. Therefore, rainfall effects in water quality rivers associated to the watershed land use considering an input and output, and their respective effects along the water body is a gap not well explored in the environmental monitoring and assessment context.

1.1 EVIDENCE OF INTEREST AND STRATEGY

NPS assessment must be based on three pillars: 1) land use, 2) monitoring strategy, and 3) water quality parameters. Figure 1 shows a schematic representation with their specificity.

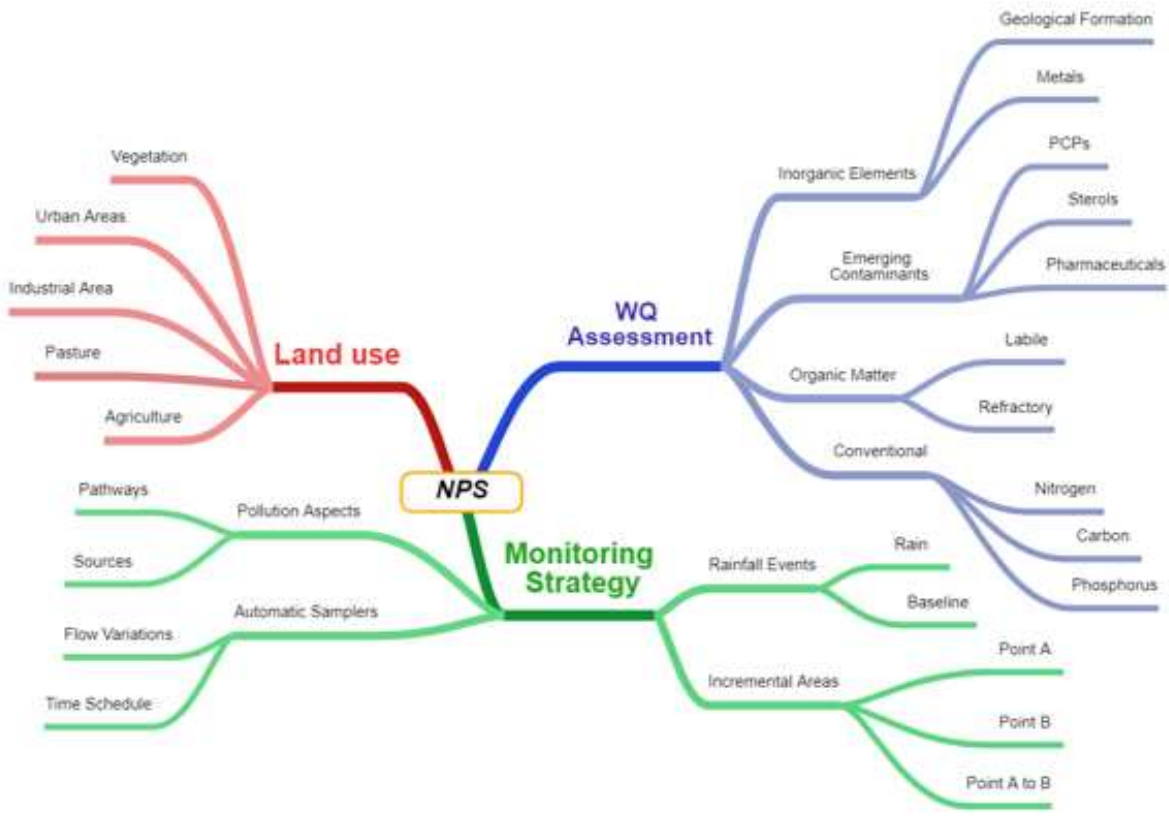

Figure 1 – Three pillars of NPS assessment

Land use characterization is important to identify predominant soil dynamics and changes, representing an association with the pollution build-up and wash-off for river systems. For example, urbanized area represents more inputs of pollution from vehicles and/or wastewater from residences, and larger impervious area, that contribute to the rapid hydrograph rising. Otherwise, a smaller urbanized area (which can be it vegetation or agriculture area) contributes with pollutants from agriculture application

and/or particles from erosion or more infiltration rate, and smaller impervious area that contribute to the slow hydrograph rise. Therefore, to know these aspects and probable pattern and scenarios, helps to determine appropriate monitoring strategy (GIRI; QIU, 2016; OLIVEIRA; MAILLARD; PINTO, 2017; NÓBREGA et al., 2018; MELLO et al., 2018).

The approach chosen must be based on the identification of pollution aspects, both from source and transport mechanism or pathways (CHEN et al., 2018a; YAN; LI; GAO, 2019; MEYER et al., 2019; SHEN et al., 2020). Discretization of rainfall influence over pollutant inputs into the river better assessed using automatic samplers. It can be programmed to collect samples fixed in time or variable by the flow or by water level variations (RAMOS et al., 2015; NICOLAU et al., 2012; KOZAK et al., 2019). Additionally, to compare rainfall effects, it is necessary to know behavior without rainfalls (baseline conditions). Thus it is possible to establish the most relevant scenarios of pollution introduction. Therefore, using these strategies, to define two monitoring points and to determine an control volume it is an interesting approach to monitor behavior considering input, output and land use influences (MEYER et al., 2019; SHEN et al., 2020). Figure 2 present a schematic representation of the strategy used to monitor NPS contribution considering a control volume.

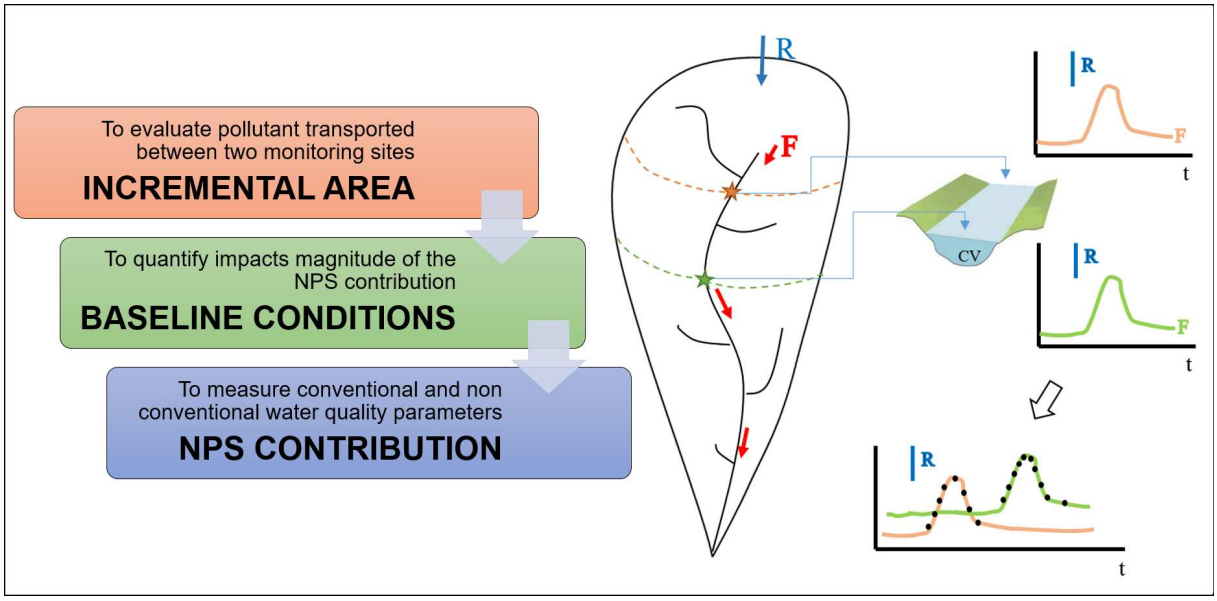

Figure 2 – Strategy to monitor NPS contribution and transport considering a control volume

Then, with these criteria and strategy herein defined, chemistry is a powerful tool/science which allow qualitative characterization of what is happening in the river system: (i) the conventional parameters, which are traditionally used for law regulation, such as right to use the water, licensing and water bodies classification; (ii) The organic matter characterization, which represents a molecular and more direct way of estimating labile and refractory sources and possible interactions that occur in the system; (iii) The emerging contaminants help to identify a PS of pollution during NPS transport, because they are considered pollutant essentially from an anthropogenic source; (iv) the inorganic elements or metals, which in this case represent NPS occurrence, transport and characteristic of the drainage area, because metals were associated to the geological formation.

Therefore, this association of different parameters helps to compose the whole in order to explain, to understand, to evaluate these processes of NPS of pollution or transport of pollution.

1.2 THESIS HYPOTHESIS AND OBJECTIVES

This thesis hypothesis is based on the evidence of interest and strategy presented considering that, **" Distinct land use and soil occupations have significant influence on pollutant contribution by surface runoff in the watershed, considering rainfall events "**. Another additional hypothesis that can be evaluated are:

1. In the drainage area with more proportion of urban land use, antecedent dry period is the determinant factor for the pollutant wash-off
2. In the drainage area with more proportion of agriculture and vegetated areas land use, rainfall intensity (duration and amount of water) is the determinant factor for the pollutant wash-off
3. Load pollution will be bigger in BA2 than in BA1
4. On BA1 will not be detected emerging compounds due to non existence of PS of pollution, while on BA2 will be detected emerging compounds related to human activities due to the WWTS influence
5. Pollutant loads and concentration will be bigger during rainfall episodes than during baseline conditions, in all water quality parameters.
6. Geological formation have significant contribution in the river water quality, mainly during rainfall episodes.

In this context, the main objectives of this thesis are to assess quali-quantitatively NPS pollution during rainfall episodes using two monitoring sites, and to quantify magnitude of the NPS pollution through comparison of baseflow patterns.

Specific objectives are:

1. To evaluate hydrological characteristics in two monitoring site, in terms of rainfall and flow variations, as well as, baseflow scenarios;
2. To use automatic sampling considering rainfall influences and flow variation to discretize hydrograph rise and falling;
3. To investigate conventional water quality parameters, as TN, TP and TSS;
4. To determine organic matter characteristics with dissolved organic carbon (DOC) and spectroscoy techniques;
5. To investigate pollution derived from anthropogenic activities, as emerging compounds;
6. To determine NPS contribution through metals quantification;
7. To assess baseline conditions of the river, without rainfall influences
8. To propose an rainfall events classification

The main contribution is to produce an integration of "photos" to represent a "movie" of the river system during rainfall episodes in terms of water quality, in order to know environment dynamics. Furthermore, these steps are the first one to consider input and output to assess incremental area and land use changes influences. These results can help to improve mathematical modeling representation of NPS sources, to prioritize water resources management in a watershed to reduce and/or avoid water pollution, to understand rainfall process and, therefore, to consider then as an important component of the water resources instruments.

In this sense, some resources question are proposed to support the objectives and hypothesis of this thesis. They are:

- How is the impact of land use?
- How much is the load carried into river during rainfall episodes?
- How distance are we from baseline conditions?
- Where does the pollution go?

1.3 THESIS ORGANIZATION

This thesis is divided in six chapters as presented in Figure 3. This division was proposed to facilitate the theoretical background about NPS pollution, their relevance in the water resources management, and the approach used.

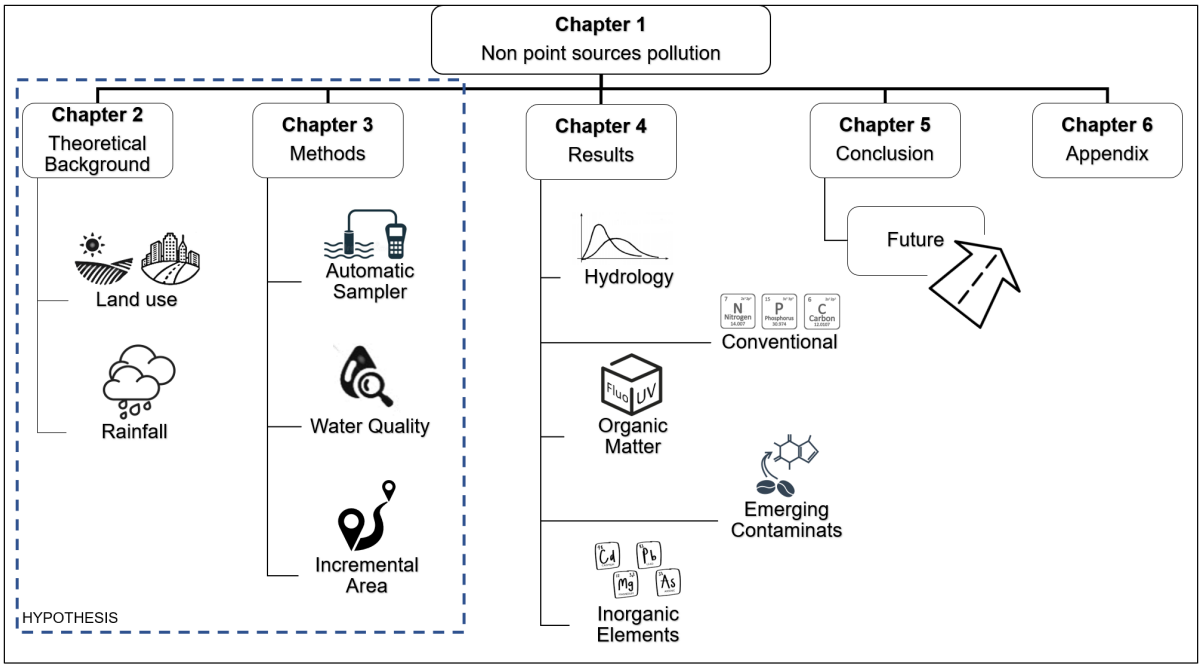

Figure 3 – Schematic representation of thesis subdivision

Chapter 1 introduces the subject, highlighting significance, hypothesis and objectives to study NPS pollution in rivers. Chapter 2 brings NPS concepts associated with land use. Chapter 3 shows methods, strategy and materials used to collect samples and process them. These chapters, so far, based the hypothesis. Chapter 4 presents the results obtained, subdivided in five section in order to improve the understanding of all data performed. Chapter 5 presents answers for the research questions proposed and give future recommendation. Chapter 6 brings together all additional data information which can be necessary.

2 THEORETICAL BACKGROUND

"*Diffuse pollution can be controlled by hundreds of best management practices focusing on different hydrological and land-use components*"

Novotny (2003), page 132

In this chapter will be present concepts about the three pillars of NPS assessment during rainfall episodes: (i) land use changes and patterns just known, (ii) how to assess NPS pollution, in terms of samples collecting and data processing, and (iii) water quality parameters which can be used to assess NPS and, also, PS pollution. This introduction of the concepts it is important to a better clarification about scientific finding and possible applications in this thesis.

2.1 DIFFUSE POLLUTION DYNAMIC: NON POINT SOURCES CONCEPTS

The Brazilian Environment Law (N°. 6.938, August 18th 1981) defines pollution as the degradation of environment quality due to activities which imply damages to health, security and social welfare, adverse conditions to social and economic activities, adversely biota impacts, adversely environment aesthetic and sanitary conditions and, inputs of matter or energy in disagreement to the established standards (BRASIL, 1981). It highlights that there are two main pollution sources: (i) point and (ii) non-point sources or diffuse sources.

PS pollution is when pollutant enters into the river at discrete and identifiable locations. Generally, it is easy to measure their quality and quantity, due to controlled access at a single point. Municipal and industrial wastewater effluents, sewer overflows, bypasses and drainage systems are examples of point sources of pollution. In contrast, NPS pollution is when the pollutant enters indirectly into the river at diffuse, distributed and intermittent way. In comparison to the PS, it is more difficult to identify and to measure their quantity and quality, due to their high spatial and temporal variability, making the attribution complex. NPS can be originated from air, land uses and subsurface zones. Wet and dry deposition from atmosphere, accumulation on impervious surfaces, erosion (e.g. drainage system, channels, stream bank and bottom rivers), leaching, groundwater infiltration, solids accumulation in sewers, sediment release, runoff from silviculture and agriculture, and urban runoff are another examples (USEPA, 1984; NOVOTNY, 2003; OECD, 2017; SPERLING, 2017).

In this context, pollutant are driven by meteorological processes, which are atmospheric transport and precipitation (NOVOTNY, 2003). Rainfall episodes induces hydrological process in a watershed and, consequently, runoff of pollutant from the land surface (OECD, 2017). This contribution depends of the water volume precipitated during rainfall events, concentrations in flow regimes, point contributions (USEPA, 1984), and land use characteristics (NOVOTNY, 2003). Therefore, to understand generation and control of NPS it is necessary to understand watershed dynamic, hydrological conditions, characteristics, processes and possible pathways.

When precipitation occurred on permeable surface, such as vegetated areas and agriculture region, great part of the water will be infiltrated by the soil and subsoil, another part will be retained in the vegetation and/or evapotranspirates. About 20% to 35% of the rainfall will be converted in river

flow, in slow and superficial contribution. Therefore, pesticides and fertilizers applied on surfaces will be introduced into the river system by this pathway. However, precipitation on impermeable surface, such as urbanized areas or compacted soil, about 95% of the rain will be directly converted in runoff, being introduced into the river quickly. Thus, residual urbanized areas such as dust, accumulated materials from atmospheric deposition, residual fuel, and others, will be introduced into the river by this pathway (NOVOTNY, 2003).

Supporting this, Porto and Porto (2008) affirm that the activities developed into watershed are extremely associated to land use changes and, therefore, have a direct effect on degree and type of pollution, either point or non-point influence. Complementary, Bu et al. (2014) affirm that land use itself does not affect water quality, but land use patterns does, changing hydrological and chemical runoff processes in a watershed due to human activities. In this sense, urbanization, agriculture, paddy land, and farmland are some types of these activities developed in a watershed, and causes impacts into the river system. In general, better water quality tendencies are associated to the watersheds with less urbanization and more forests (LEE et al., 2009) during both dry and rainy seasons (BU et al., 2014)

Agricultural activities and urbanization are the primary cause of water degradation, even from PS and NPS (GIRI; QIU, 2016). Zhou et al. (2016a) found higher nitrogen concentration in areas with high proportions of agriculture attributed to non-point sources, while nitrogen ammonia and phosphorus measured in areas with industrial activities and domestic wastewater was associated to point sources. However, the authors highlighted that these pollutant were not proportional to the land use characteristics. Thus, it is essential to understand the entire watershed ecosystem. Pollutant can be originated naturally or from human activities, and will be dependent of chemistry characteristics, volume and concentration (OECD, 2017). Therefore, due to the more complex nature of NPS pollution (GIRI; QIU, 2016), it becomes a great concern for the water resources management (USEPA, 1984).

2.1.1 LAND USE AND NPS

According to EEA (2018), agriculture is the key source of NPS pollution, but urban land, forestry, atmospheric deposition and rural activities can also be important sources. Agricultural activities has been the most widespread cause of diffuse pollution. Activities as crop cultivation, irrigation intensities, livestock facilities, forest cut, silviculture, fertilization and use of pesticides produces significant negative impacts in the water bodies, with high inputs of amounts of nutrients, salts, minerals, organic matter, fecal bacteria's, pesticides, and others, on the aquatic system (USEPA, 1984; NOVOTNY, 2003; MENESES et al., 2015). Some examples of negative impacts are eutrophication, oxygen depletion, fish and biota contamination and mortality, human health impacts, salinization of surfaces water, erosion, sedimentation and silting, and groundwater contamination (SODRÉ, 2012; ANA, 2013; GIRI; QIU, 2016; EEA, 2018)

Urbanization have more visual impacts than agriculture activities. The urban development and fast growth population increase the number of buildings, impervious areas, environmental pressures and wastewater generation, that consequently, have negative impacts in the river system. Effects as floods, decrease in the evapotranspiration, soil compaction, increase in water runoff from roofs, streets, industrial areas and others, which washes a large volume of pollutant into the river. Such pollutant are heavy metals, inorganic chemicals, pesticides, hydrocarbons, sediment, oil, rubber, nutrients, and residues from roofs and tyres (USEPA, 1984; NOVOTNY, 2003; SODRÉ, 2012; ANA, 2013; EEA, 2018; MÜLLER et al., 2019). Figure 4 shows a schematic representation of urbanization effect on the surface runoff. More impervious areas contribute to faster and bigger peak flow while in less impervious areas peak flow is slower and smaller, due to the benefits of infiltration process.

There are many studies focusing on water quality and land use type. Bu et al. (2014) estimated

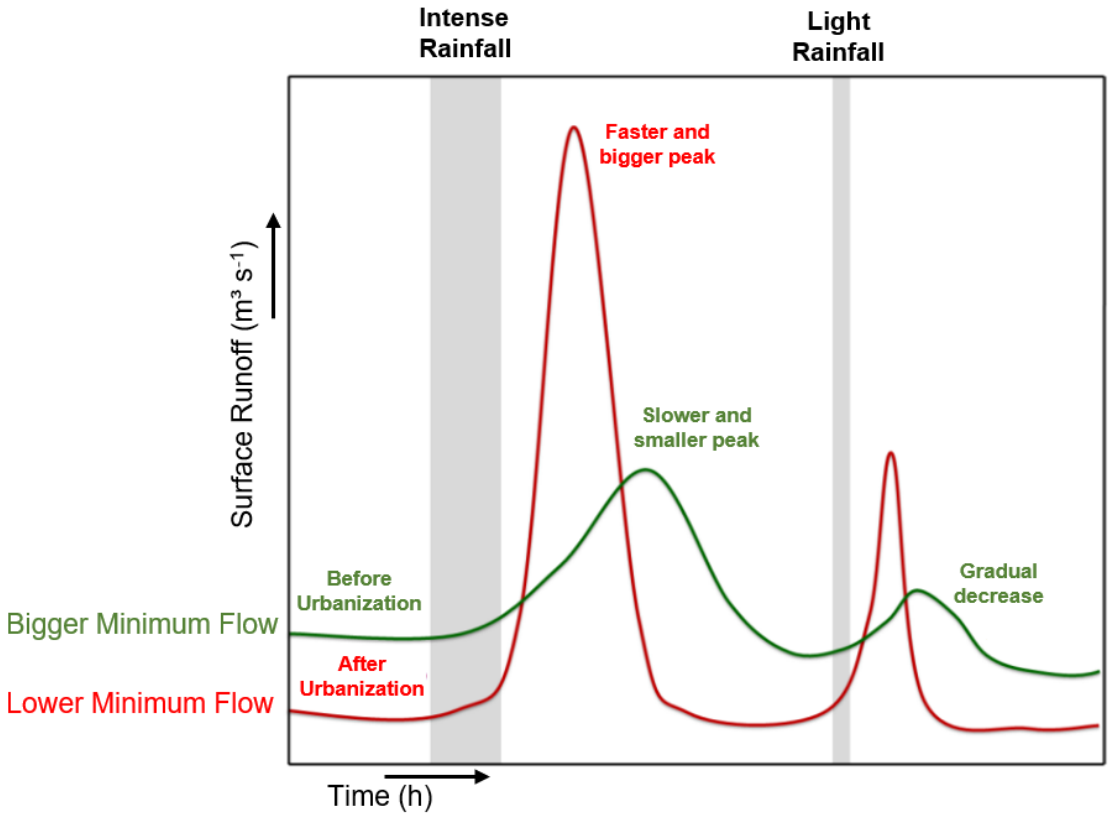

Figure 4 – Urbanization effects in the surface runoff

SOURCE: Adapted from SODRÉ (2012)

the relation between river water quality and land use types, identifying major pollution sources in the Taizi River basin (China) with 13.202 km^2. Regions with more proportions of urbanized areas contributed with organic matter pollution from domestic sewage. Regions with urbanized and agriculture area contributes with nitrogen and phosphorus inputs. Mountain regions with fewer people suffered organic pollution from livestock production, and along the river were evidenced impact of nitrogen pollution from surface runoff due to erosion and sand extraction in the river channel. In the same perspective, Ding et al. (2016) estimated land use pattern for predict water quality in a first and second order rivers, on the Dongjiang River watershed (China), with area of approximately 35.340 km^2. The results suggested that areas composed by orchard, grassland and cropland are related to nitrogen and phosphorus inputs, due to fertilizer use, and urban areas are related to ammoniacal nitrogen, nitrate and phosphorus inputs, due to the potential for impervious areas to accumulate pollutants. Mello et al. (2018) examined land use and land cover influences in water quality in six low-order streams in Sarupaí River basin (Brazil). The analysis indicated that forest land was associated to good water quality, with dissolved oxygen as main predictor, and agriculture land and urban areas were associated to water quality degradation, with strong correlation with total nitrogen, total phosphorus and fecal coliforms. Moreover, information criteria models applied, indicated variation in the water quality during water discharge changes.

Yu et al. (2016) it was verified the influences of dry and rainy season and topographic characteristics in the water quality of the Wei River (China), with 134.3 x 10^4 km^2 of drainage area. The results suggest land use types had more influence in water quality during dry season than during rainy season. This occurs because point sources have more impacts in the watershed, due to urban land, than non-point sources from agriculture land. Additionally, average slope and land use proximity to river were consid-

ered important factors that affect water quality. Nóbrega et al. (2018) identified concentration and output fluxes of carbon and nutrient during baseflow ans stormflow condition Amazon and Cerrado catchments in Brazil, observing changes in land use and land cover (vegetated areas to pasture). The authors found higher concentrations of carbon and nutrient in the pasture land compared to the vegetated land in both catchments, suggesting that native forest contribute to the better water quality in river during baseflow condition. Moreover, higher calcium concentration were found in pasture areas than in native areas, in the Cerrado catchment, during stormflow condition, suggesting that high rainfall rates facilitated leaching of calcium into the river from liming practices. However, for the Amazon catchment, rainfall episodes promotes dilution of the calcium concentration, compared to the baseflow concentration. In terms of fluxes, stormflow condition showed a substantial hydrological pathway for carbon and nutrient losses, being, for example, responsable for 50% of the dissolved organic carbon fluxes in the Amazon pasture. The authors related these losses with the deforestation, reducing infiltration capacity and consequently reflecting in the water quality.

Thus, NPS pollution is essentially associated to the land use of the watershed (OLIVEIRA; MAILLARD; PINTO, 2017). Generally, better water quality tendencies were observed in watersheds having less urbanization and more forests (LEE et al., 2009; ZHOU et al., 2016a), where a combination of many factors and activities in a watershed favor to random contribution for the water body pollution (GIRI; QIU, 2016; BU et al., 2014). Some of these factors are hydrological variations (precipitation and temperature), landscape characteristics (slope and soil types), runoff contributions and patterns, activities developed (farmland, croplands, irrigation and drainage systems), different influences from dry and wet seasons (NÓBREGA et al., 2018; YU et al., 2016; BU et al., 2014; LEE et al., 2009; PORTO; PORTO, 2008). Thus, better catchment management and monitoring can help to a better understanding about the diffuse processes in order to decrease bad effects over the river (OLIVEIRA; MAILLARD; PINTO, 2017; DING et al., 2016).

2.2 WHAT IS THE BEST WAY TO ASSESS NPS CONTRIBUTION?

Generally, to assess the NPS pollution is challenging, due to the multiple sources of contribution, various pathways, climate conditions randomness and lack of guidelines and regulation for diffuse pollution control. Despite not having any general protocol how to monitoring NPS, there is some characteristics and strategies that should be considered during diffuse pollution assessment (MCCARTHY et al., 2018). It refers to: (i) Monitoring strategy; (ii) The relevance of hydrological characteristics; and (iii) Data analysis and assessment

2.2.1 MONITORING STRATEGY

The main concern in NPS pollution studies is related to the monitoring experimental planning. Generally, it must to be during rainfall episodes due to the complex dynamic in these moments associated to concentration-discharge relationships (LLOYD et al., 2016). It is necessary a extensive data acquisition to cover all variables, and, do not underestimate any of them (QUIGLEY JANE CLARY; O'BRIEN, 2009). Then, an integrative monitoring, which considers water quality (mg/L) during specific flow quantity (m^3/s) is a proper approach (BRAGA, 2013).

Selecting suitable technique to monitor and measure is extremely related to the purpose of the monitoring (ZULKIFLI; RAHIM; LAU, 2017). Collecting single samples, automatic sampling (time or

flow conditions) and high frequency monitoring are some of the monitoring strategies. It can have high and low technical sophistication, cost and maintenance. Quigley Jane Clary and O'Brien (2009) highlights that single sampling provides a water quality "snapshot" at a single point in the time, and not properly estimate the pollutant load under significant rainfall episodes. However, many single samples collected at short time intervals can be used to assess pollutographs characteristics and to estimate loads pollutant.

The improvement of automatic sampling better reviewed this strategy, based on tome or flow-weight triggering strategy (DELPLA et al., 2011; BRAGA, 2013; OKAMURA et al., 2013; AICH; ZIMMERMANN; ELSENBEER, 2014; GAO et al., 2014; VISWANATHAN; MOLSON; SCHIRMER, 2015; RAMOS et al., 2015; KOZAK et al., 2019). It can be used as constant time programming (volume proportional to flow rate or to flow volume increment) or constant volume programming (time proportional to flow volume increment) (QUIGLEY JANE CLARY; O'BRIEN, 2009). Therefore, the adequate sampling strategy used during a rainfall episode is important to avoid the first flush bias and to guarantee a better mass emission characterization (LEE et al., 2007)

Delpla et al. (2011) used a runoff water sampling device, considering a predetermined volume (0.6 or 1.2 L). Ramos et al. (2015) used a probe programmed to activate water sampling considering water level variation, with 10 cm on both rising an falling stages of the rainfall episode. And, in the same perspective Kozak et al. (2019) used an automatic sampler operated by a programming code, developed by Braga (2013), that performed sample collection according to water level variations. The initial trigger was 5 cm of water level variation in 10 minutes of interval, and after that 10 cm on both rising and falling hydrograph. This kind of monitoring strategy allowed the quali-quantitative discretization of diffuse pollution inputs. Thus, fixing sampling strategies focus on start samples during these non-permanent events is necessary to avoid the uncertainties and to ensure the better understanding about the load emission in the system (LEE et al., 2007). Therefore, it is clear how complex is to adjust an monitoring strategy to assess NPS dynamics.

As a rule, the most important moment during an rainfall episode is the first portion of the flow, which contains the highest pollutant concentration. This moment is named as first-flush (NOVOTNY, 2003; QUIGLEY JANE CLARY; O'BRIEN, 2009). Current studies have been concerned with the first-flush phenomenon characterization (LEE et al., 2007; ALIAS et al., 2014; METADIER; BERTRAND-KRAJEWSKI, 2012; BLAEN et al., 2016; PENG et al., 2016; MCCARTHY et al., 2018; WISE et al., 2019), with distinct purposes, using different monitoring and sampling strategies. For example, Wise et al. (2019) investigated how rainfall episodes impact the DOC dynamic in dryland regions. They collected samples manually in a concrete channel, which receive runoff from many natural and artificial conveyances draining ten watershed with 2,462 ha in total. It was evaluated four rainfall events. Hydrograph analysis was divided in three phases: (i) phase 1: the beginning of the event, where it were introduced DOC from autochthonous sources, near to the monitoring site; (ii) phase 2: the peak of the event, where occurred the first flush of the allochthonous sources of DOM, which were transported from the impervious area of the urban area. (iii) phase 3: the end of the event, where there was flush of processes allochthonous DOM, from longer or slower flow paths. Thus, although sampling has limited automatic infrastructure, analyses looking at first-flush effects were relevant to identify that during rainfall episodes there is a potential strong impact on river biogeochemistry, due to the concentrated carbon pulses.

In other perspective Mamoon et al. (2019) investigated rainfall runoff from arid regions to examine the first-flush effect in relation to the pollution in six distinct impervious areas. In this case, the study was controlled, using rainfall simulator in a 4.55 m^2 of area. It was generated two rainfall events with 42mm/h during 30 min (flow rate 14 L/min) and 20 mm/h during 30 min (flow rate 7 L/min). The results detected a clear first flush condition for most of the pollutants in the all sites. In the first 40% of surface runoff was found 50% to 72% of total suspended solids, 36% to 90% of total phosphorus, 61% to

86% of total organic carbon, and 6% to 100% of trace metals. Additionally, authors suggest that surface texture is the contributing factor for the first-flush. Thus, it is possible to design an appropriate storm water treatment devices in order to reduce urban pollution. Therefore, regardless of the pollutant type, it is in the first 40% of runoff volume transported during rainfall the most loads of pollutant are washed-off (ALIAS et al., 2014).

Moreover, high-frequency monitoring is a high cost improvement that uses in-situ sensors to monitor water quality parameters at high temporal resolution (LLOYD et al., 2016), obtaining a continuous record of water quality (QUIGLEY JANE CLARY; O'BRIEN, 2009). The advantages is associated to improve understanding about the overall process (BOWES et al., 2015; RUHALA; ZARNETSKE, 2017), such as: (i) discrete measurements at one minute or less intervals, to detect pollutant variability during rainfall events and runoff effects (QUIGLEY JANE CLARY; O'BRIEN, 2009), (ii) to generate high resolution database to investigate seasonal and temporal variations (HALLIDAY et al., 2014; LLOYD et al., 2016).

However, despite the high-frequency monitoring to be a powerful tool, there are some disadvantages associated to their use, as: higher costs in acquisition and installation, more power demands to sensor, datallogers and telemetry systems, more frequent maintenance due to accumulation of sediment, biofilms, environmental factors (pH, temperature, conductivity and turbidity, for example), and more increase the risk of damage during rainfall monitoring due to the higher river velocities in this periods. (BLAEN et al., 2016; GRAYSON; HOLDEN, 2016). Thus, considering that the ideal data set for NPS monitoring and assessment need to capture timing and magnitude variations in pollutant concentrations (QUIGLEY JANE CLARY; O'BRIEN, 2009), this devices could be a great improvement to the monitoring program.

Any and all forms of monitoring should be shaped according to the main objective to be achieved, assessing the necessary infrastructure, human and financial resources available to carry out adequate planning (BEHMEL et al., 2016). Behmel et al. (2016) highlight a sequence of actions for a successful monitoring program, based on stakeholder implications, scientific and, administrative requirements, and policy making action plans. Therefore, it is possible to establish an evolutionary order, starting with a minimum monitoring infrastructure (level 1 - screening evaluation), gradually evolving to a more detailed monitoring (level 2 - performance evaluation) and finally, an advanced one (level 3 - research and design). For example, an initial screening of diffuse contribution in a watershed can be initiated with basic rainfall quantity data, if possible flow and/or water level, and a simple program of sampling to assess water quality in dry and rainy periods. Then, to evaluate the performance, rainfall characteristics, land use details and water quality assessment can be refined and better detailed. Thus, at a more advanced level, with a solid database, it is possible to investigate more detailed processes, such as, system mass balance, land use effects, impacts on water quality, application of water resources management and implementation of diffuse pollution control measures.

In this sense, considering an evolution between levels two and three monitoring program for NPS contribution, Krause et al. (2015) and Blaen et al. (2016) presented an adaptive monitoring strategy (AMS). This kind of monitoring consist in combining high spatial and resolution data acquisition during specific interest periods (KRAUSE et al., 2015) or biogeochemically active periods, such as high flow events (BLAEN et al., 2016). Figure 5 shows the schematic representation of the adaptive monitoring approach. The clear benefit is to concentrate efforts in the most relevant high flow periods, and to produce the best water quality discretization. Blaen et al. (2016) explains that monitoring frequency can be activated based on the variable of interest, such as nutrients, a surrogate variable, such as level, or a combination of variables. Furthermore, the setting of triggers and thresholds for AMP is extremely important. For example, water level variation as a trigger can be used to assess rainfall episodes dynamics, however this

same variable can suffer accidental releases, as sewer discharges or river bank collapse. Therefore, this type of problem should be taken into consideration when choosing the appropriate trigger (BLAEN et al., 2016).

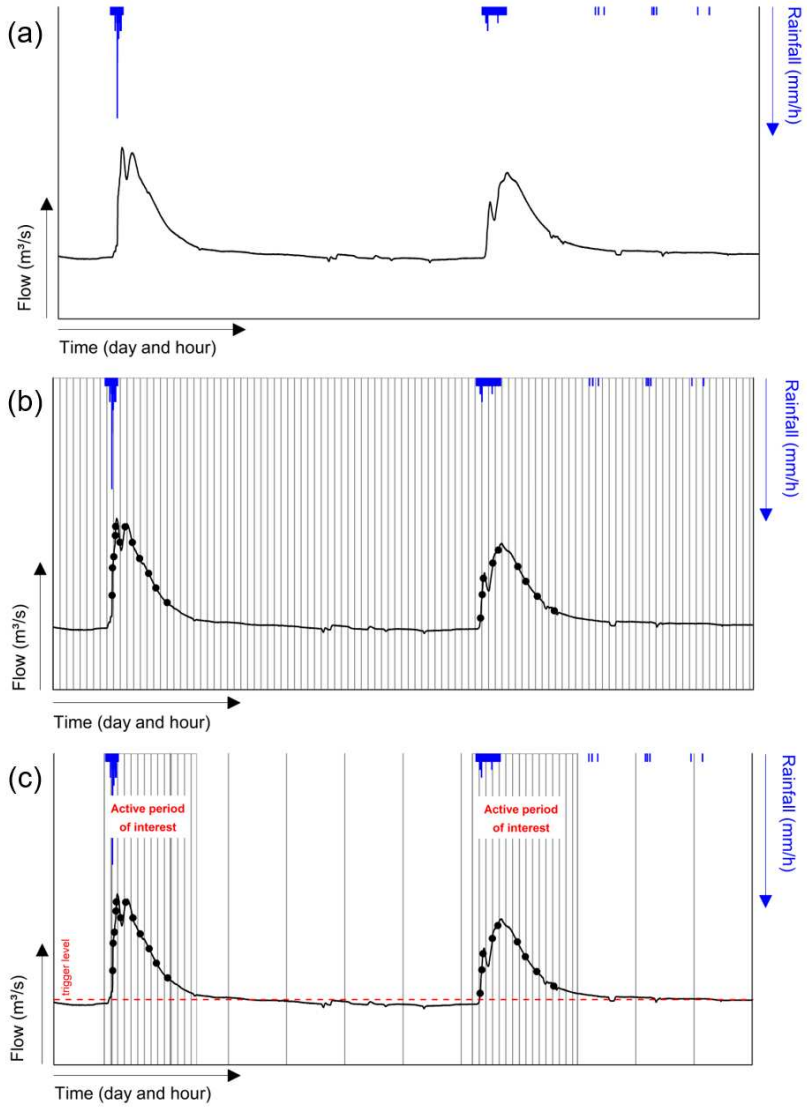

Figure 5 – Adaptive monitoring approach; (a) Represent hydrological context with and without rainfall occurrence; (b) Represent high-frequency monitoring all the time; (c) Represent adaptive monitoring focusing when there are periods of interest

SOURCE: Adapted from Blaen et al. (2016)
NOTE: Black continuous line represents flow, blue bar represents rainfall, black points represent samples, vertical gray lines represent monitoring frequency

There are many kind of sampling and monitoring strategy. Many studies use one or a combination of these approaches presented (LEE et al., 2007; BOWES; SMITH; NEAL, 2009; CARSTEA et al., 2010; DELPLA et al., 2011; METADIER; BERTRAND-KRAJEWSKI, 2012; ALIAS et al., 2014; BRAGA, 2013; BLAEN et al., 2016; DING et al., 2016; YU et al., 2016; FRANK; GOEPPERT; GOLDSCHEIDER, 2018; KOZAK et al., 2019; XIE et al., 2019; WISE et al., 2019; GRUDZIEN, 2019; DRUMMOND, 2020).

Moreover, it is extremely important know all about the system, including watershed characteristics, hydrological serie and trends, land use and soil occupation evolution (BLAEN et al., 2016), to

produce representative information, high data quality and understanding of the processes. Therefore, decreasing uncertainties during the data acquisition also may result lower cost with improved accuracy and variability (LEE et al., 2007). Overall, for the NPS contribution the appropriate monitoring approach it is the one in which the first-flush conditions are evaluated.

2.2.2 HYDROLOGICAL CHARACTERISTICS

To properly establish the relationship between concentration and discharge requiring attention from many researchers. They vary because of the differences land use and hydrological characteristics of the watershed (LLOYD et al., 2016). Each specific rainfall produces different water quality and quantity behavior (KOZAK et al., 2019). Moreover, watershed size, relief aspects as topology and flooded regions, geology, artificial modifications, and land use dynamics are relevant variables.

The hydrological characteristics relevant are (i) rainfall depth (mm), (ii) rainfall intensity (mm/h), (iii) rainfall duration (hours), (iv) rising and falling times (h and/or %), (v) antecedent dry periods, (vi) antecedent cumulated rainfall, (vii) water level (m or cm), (viii) maximum, minimum and average flows during the event(m^3/s), (ix) event duration (days and/or hours), (x) average discharge in 24 hours before rainfall, (xi) volume produced during the event (m^3), (xii) volume of total flow (METADIER; BERTRAND-KRAJEWSKI, 2012; ALIAS et al., 2014; BOWES et al., 2015; BIEROZA; HEATHWAITE, 2015; WIJESIRI et al., 2015; LLOYD et al., 2016; XIE et al., 2019).

Alias et al. (2014) observed residential catchment located in Australia, in order to evaluate the influence of the rainfall episodes in the wash-off process. 23 rainfall events were monitored and total phosphorus (TP), total nitrogen (TN) and, total suspended solids (TSS) were measured. Results indicate that the initial 10% of the wash-off process is influenced by rainfall depth and duration. Moreover, the pollutant accumulated during dry periods have influence in the beginning of the wash-off process, and rainfall intensity during the initial 10% of the event, and after 10% of the effective rainfall have completely different influence in the wash-off process. The authors suggest that lumped rainfall characteristics is inappropriate to investigate the influence on pollutant wash-off. Detailed evaluation of rainfall and discharge moments can help to a better understanding about this process, and consequently, design treatment systems for pollutant loads.

Lloyd et al. (2016) uses high temporal frequency data sensors of nitrate, total phosphorus, turbidity and discharge to investigate storm flow variation in relation to the catchment hydrogeology, rainfall duration, antecedent conditions, land use and season. The study was performed in two distinct field sites in Hampshire Avon catchment, United Kingdom. Results showed that nitrate transported was associate to the rainfall duration, where nitrate rich soil and groundwater is flushed straightforward to the stream during rainfall. However, total phosphorus fluxes were associate to the antecedent condition and surface or near surface sources, because pulses of phosphorus increased with discharge. Otherwise, antecedent conditions is not so important in the sediment/turbidity transported, because it is classified as transport-limited: if there is flow able to transport fine sediment, there will sediment available to be transported.

Xie et al. (2019) observed eight rainfall to assess watershed responses combining monitoring, modelling and statistical analysis in the Zhangjiachong catchment (1.62 km^2), China. Rainfalls classification ranged between medium to extremely heavy, with ranges of total precipitated of 18.2 to 104.7 mm, and intensity of 7.9 to 45.4 mm/h. Results indicate that during medium rainfall episodes, the rainfall characteristics, such as amount and intensity, play a vital role in runoff generation and pollutant transport. And, for extremely rainfall episodes, total phosphorus and sediment release was associated with the flow variables, such as total outflow and peak flow. The authors highlighted that it is difficult to identify these rainfall-runoff controlling factors for NPS pollution. Therefore, it is important to pre-classify rainfall

episodes for the interpretation of the mechanisms drivers.

These studies are examples of how different pathways transport mass into the river system, and that rainfall characteristics produces distinct effect in the each watershed. At the same time, all variables are dependent of the entire system and independent in each singular rainfall episode. Flow and concentrations in each rainfall event have distinct and complex dynamics (METADIER; BERTRAND-KRAJEWSKI, 2012). Thus, hydrological characteristic detailing provide information about the system and the process, being extremely important in the NPS pollution studies.

2.2.3 DATA ANALYSIS AND ASSESSMENT

There are many alternatives to assess and evaluate data of water quality and quantity from NPS studies. Each approach is able to present different kind of information. The most usual graphical methods are pollutographs, event mean concentration (EMC) and hysteresis analysis. From them, it is possible to calculate some indexes to classify and assess the rainfall episodes and pollutant contribution.

2.2.3.1 Pollutograph

The pollutographs highlights pollutant concentration changes over time, and are associated to the hydrographs (6a). On this kind of representative graphic it is possible to observe flow variation (rising and falling) with water quality changes. Hydrological characteristics are extremely useful in pollutograph analysis, in order to assess rise time, peak flow, falling time, water volume transported, and consequently, the behavior of the pollutant observed. Figure 6 shows a schematic representation of the pollutograph. The following situations can happen: (i) the pollutant follows the pattern of the hydrograph, increasing and decreasing along with the flow (6b); (ii) the pollutant has an opposite behavior to that of the hydrograph, decreasing its concentration with increasing flow and increasing concentration with decreasing flow (6c); (iii) there is no pattern establish; (iv) having high variability during the rain event, with no defined pattern. Each situation depends on the characteristics of the basin and the rainfall event.

Delpla et al. (2011) studied the runoff fluxes during storm and shower rainfall events by an adapted monitoring in a experimental field. The pollutographs from both types of rainfall events were divergent, suggesting different impact into receiving water due to distinct rainfall characteristics in winter and autumn. For example, dissolved organic carbon (DOC) reached maximum concentration at the beginning of the shower rainfall, whereas DOC suffered dilution in the storm rainfall, increasing their concentration with rainfall intensity increase. Metadier and Bertrand-Krajewski (2012) presented pollutographs from two monitoring sites (Chassieu and Ecully catchment) in Lyon (France). The authors found a diversity of rainfall episodes and presented the three main typical behavior as (i) small rainfall episodes, where discharge and concentration had similar dynamics and simultaneous variations; (ii) successive rainfall episodes with various flow peaks and concentration stability or dilution; and (iii) strong rainfall episodes with clear dilution effects. To conclude, due to the variables pollutographs generated, the authors highlighted how diverse and complex is interaction of the process, which must be analysed as a continuous time series to ensure further assessment.

Meyer et al. (2019) used an real-time monitoring station for water quality assessment to characterize and classify the pollution sources spectrum. The study was performed in Saarland (Germany), in eight different monitoring site. From pollutographs from site number 1 (river Blies in Reinheim) it was verified that river suffers erosion process during rainfall episodes, due to simultaneously increase of turbidity and bound phosphorus (P). The turbidity pattern was clearly associated to the runoff from soil with previous fertiliser application, and higher amount of bound P than total reactive phosphorus

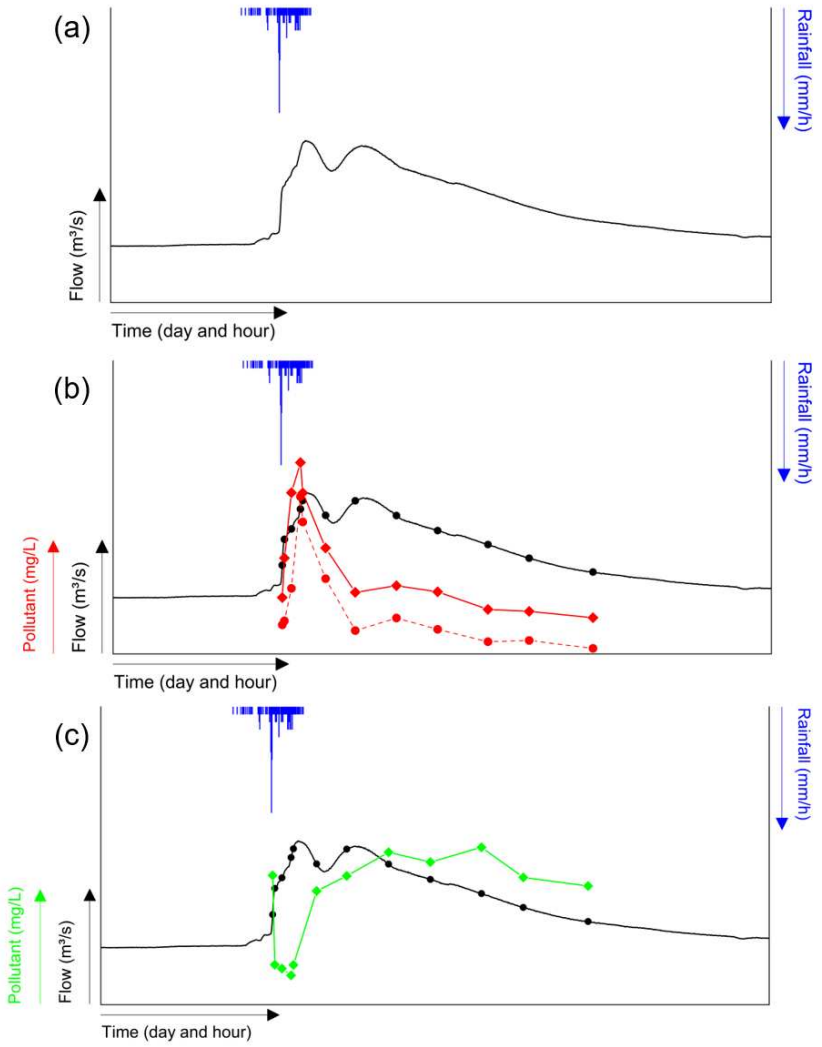

Figure 6 – Schematic representation of the pollutograph: (a) hydrograph: flow variation over time; (b) pollutograph: flow and concentration over time with similar pattern; (c) pollutograph: flow and concentration over time with opposite pattern

SOURCE: The Author (2019)

(TRP) (which suffer dilution during rainfall episodes) corroborate the erosion processes. Interestingly in the same monitoring site, nitrate ($N\text{-}NO_3^-$) concentration suffer dilution during rainfall episodes, and with decreasing of the river discharge, the amount of $N\text{-}NO_3^-$ returned to the usual background values.

2.2.3.2 Event Mean Concentration - EMC

The EMC is mass of pollutant contained in the runoff event by the total volume of flow in the rainfall episode. EMC value is calculated by Equation 2.1

$$EMC = \frac{\sum Q_i C_i}{\sum Q_i} \tag{2.1}$$

where Q_i is the discrete flow measurements on the rainfall hydrograph, and C_i are discrete pollutant concentration measurements on the pollutograph. EMC is the flow-weighted sampling representation (NOVOTNY, 2003), resulting in a single value to represent the entire rainfall episode.

Thus, EMC curves is a dimensionless graph with cumulative pollutant load versus cumulative runoff volume (MCCARTHY et al., 2018). It can be used to evaluate pollutant behavior during rainfall events, in terms of introducting mass into the river. This curve also is called as M(V) curve. Metadier and Bertrand-Krajewski (2012) proposed an classification of the EMC curves in three zones, named zone A, zone B, and zone C. The main purpose is to distinguish load concentration, load attenuation and load dilution during a rainfall episode, being possible to compare distinct events and different watershed. Figure 7 shows schematic representation of the EMC curves with Metadier and Bertrand-Krajewski (2012) classification.

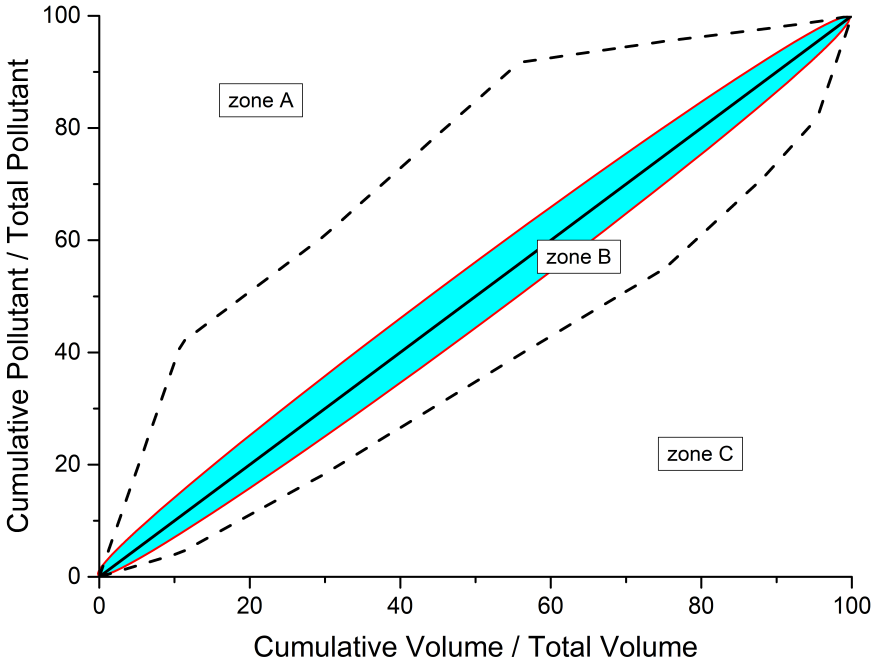

Figure 7 – EMC curve representation and zone identification

SOURCE: Adapted from (METADIER; BERTRAND-KRAJEWSKI, 2012)

The curves interpretation proposed by Metadier and Bertrand-Krajewski (2012) is:

- **Zone A:** It represents a fraction X of the total pollutant load transported in a fraction X-1 of the total volume. In other words, there is more pollutant load entering in the system than water volume transported along the rainfall episode. Curves will be above the bisector, and can indicate first flush occurrence.
- **Zone B:** It represent a fraction of X of the total pollutant load transported in a fraction X of the total volume, with not significantly difference. In other words, the pollutant load is equivalent to the same fractions of the water volume transported along the rainfall episode. Curves will be in the bisector, with maximum deviation of 5%.
- **Zone C:** It represents a fraction X of the total pollutant load transported in a fraction X+1 of the total volume. In other words, there is more water volume transporting the mass inputted into the system during the rainfall episode. Curves will be under the bisector, and can indicate pollutant dilution.

Moreover, it was observed changes in the concavity curves, for example, from zone C to A. The authors suggest a temporal delay of concentration compared to the flow measurements.

Mamoon et al. (2019) used EMC curves to assess first flush occurrence, in a controlled study in Doha (Qatar). For TSS, total Kjedahl nitrogen (TKN), and total organic carbon (TOC), EMC curves were above the bisector, indicating first flush occurrence in all the five sites monitored for the high and low intensity rainfalls. For TP and some metals measured, curves were varied, indicating a lower first flush effect and influence of the high intensity rainfall in the pollutant transport. Beside that, the authors evaluated first flush magnitude using the EMC ratio, between normalized pollutant load and normalized volume in a specific percentage of the rainfall episode. Results showed that in the first 40% of the runoff in the all monitored sites, around 50% of TSS, TKN, TP and TOC were flushed. In the same perspective, Alias et al. (2014) used an interval assessment of the EMC curves, every 10% of variation of mass and volume, to assess first-flush magnitude. Results indicate that the most pollutant loads were washed-off in the first 40% of the rainfall episode: 61.22% of TSS, 60.74% of TP, and 52.43% of TN.

The data analysis and interpretation by the EMC is useful, mainly in terms of planning actions to mitigate the diffuse polluting load. EMC value, being a flow-weighted average of the mass and volume transported during a rainfall episode, favors the comparison between different events in different watershed scales, and can also indicate how much mass is being introduced into the system during these periods. Additionally, based on the shape of the curves, it is possible to assess which is the most expressive moment of mass introduction during the rainfall episode and, which water quality parameters are most relevant. Thus, the association between these properties and hydrological characteristics can facilitate decision-making for the of water resources management.

2.2.3.3 Hysteresis

Another kind of interpretation is C/Q hysteresis. This analysis consist in to describe non-linear pollutant behavior during a rainfall episode, which lead different concentration changes on the rising limb compared to the falling limb of the pollutograph (BIEROZA; HEATHWAITE, 2015). As a result, it is possible to determine hysteresis loops, as presented in Figure 8. They are (i) clockwise loop: pollutant concentration that increase with increasing (Figure 8a); higher concentration in the rising limb than to the falling limb of the pollutograph; (ii) anticlockwise loop: pollutant concentration delayed from distant upstream tributaries (Figure 8b); (iii) figure-eight-shape loop: is a combination of clockwise and anticlockwise, where flow or pollutant concentration peaks first but without to form loop, going in opposite directions; concentration and/or discharge during the rising limb can be higher and lower values than those during the falling limb (Figure 8d); (iv) no hysteresis pattern: linear or unclear pattern (Figure 8c) (WILLIAMS, 1989; BIEROZA; HEATHWAITE, 2015).

Clockwise shape can be associated to the quickly wash-off in the begging of the event (rising limb) than close to the end (falling limb), whereas anticlockwise shape can be associated to large water discharges and small pollutant concentrations, thus the pollutant peak occurs later than the water peak, or dilution. And then, figure-8-shape is a combination of these two shapes, developing clockwise loop at high flows and an anti-clockwise loop at low flow (WILLIAMS, 1989).

Additionally, there are two semi quantitative descriptors to summarize pollutant fluctuations during the rainfall episodes, named as ΔC and ΔR. ΔC describes the pollutant concentration changes, calculated by Equation 2.2, and ΔR describes area and rotational hysteresis pattern, calculated by Equation 2.3 (BUTTURINI et al., 2008).

$$\Delta C = \frac{(C_s - C_b))}{C_{max}} * 100 \tag{2.2}$$

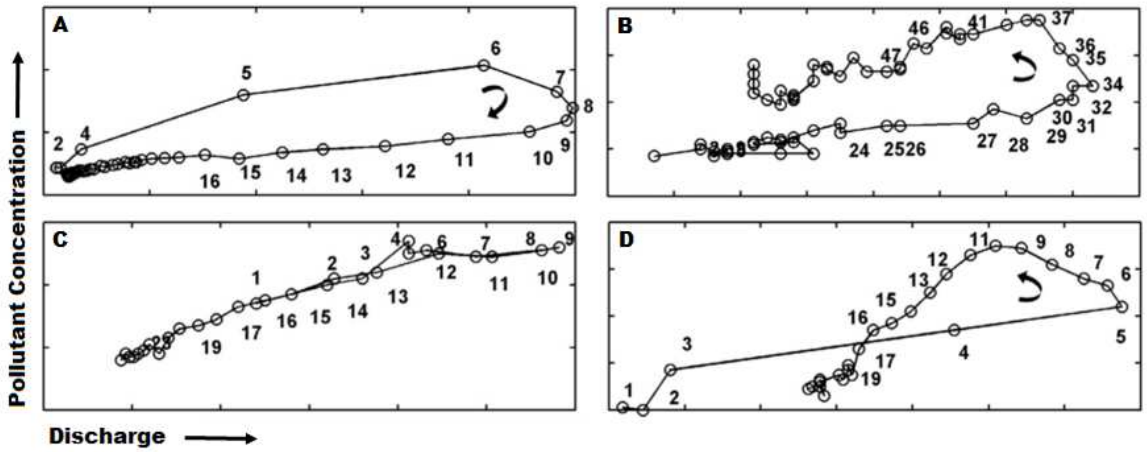

Figure 8 – Hysteresis patterns: (A) clockwise loop; (B) anticlockwise loop; (C) no hysteresis pattern; (D) figure-eight-shape loops

SOURCE: Adapted from Bieroza and Heathwaite (2015)

$$\Delta R = R * A_h * 100 \tag{2.3}$$

where C_s is the pollutant concentration in the peak flow (mg.L^{-1}), C_b is the pollutant concentration in the baseflow (mg.L^{-1}), C_{max} is the highest pollutant concentration observed (mg.L^{-1}), R is the rotational pattern, and A_h is hysteresis area estimated after standardising flow and concentration to unity scale. Both descriptors ranged between -100 to 100. Negative ΔC values suggest discharge trends, or pollutant dilution, whereas positive values means the opposite, or pollutant flushing. The term R, which indicate rotational pattern, is 1 if there is a clockwise loop; -1 if there is a anticlockwise loop; and 0 if there is unclear, linear pattern or figure-eight-shape. The variability of these descriptors can be evaluated in four categories (Figure 9), which are:

- ΔC $>$ 0, ΔR $>$ 0: clockwise pattern and general positive trend, which suggest pollutant flushing during discharge rising limb;
- ΔC $<$ 0, ΔR $>$ 0: clockwise pattern and general negative trend, which suggest pollutant dilution during discharge falling limb;
- ΔC $<$ 0, ΔR $<$ 0: anticlockwise pattern and general negative trend, which suggest pollutant dilution during discharge rising limb;
- ΔC $>$ 0, ΔR $<$ 0: anticlockwise pattern and general positive trend, which suggest pollutant flushing during discharge falling limb (BUTTURINI et al., 2006).

Therefore, hysteresis response indicates differences in the pollutant concentration during the flow discharge, lags between loads and flow, identifying flushing and dilution effects. All these information can clarify sources of pollutant and dissociation between different rainfall episodes (BUTTURINI et al., 2006; BUTTURINI et al., 2008; BIEROZA; HEATHWAITE, 2015; RAMOS et al., 2015). Ramos et al. (2015) studied twenty one rainfall episodes occurred in The Enxoé watershed (Portugal) with 60.8 km^2, using hysteresis. General results showed flushing behavior of the particulate parameters, such as TP and total particulate phosphorus (TPP), and dilution behavior of the dissolved parameters, such as N-NO_3^- and soluble reactive phosphorus (SRP). Furthermore, it were observed different pattern in rainfalls registered along the year. For example, autumn rainfall produces clockwise hysteresis for particulate parameters,

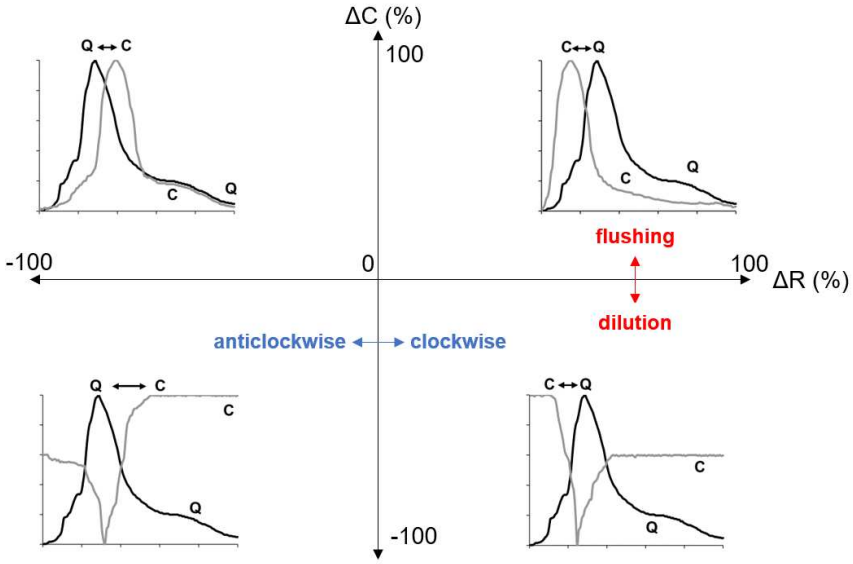

Figure 9 – Plot of ΔC vs. ΔR for hysteresis loop and pattern of flow and concentration

SOURCE: Adapted from Ramos et al. (2015)

and uncertainty hysteresis pattern for soluble parameters. During winter and early spring were registered unclear or figure-eight-shape hysteresis pattern for particulate and soluble parameters.

Lloyd et al. (2016) studied two small catchments (50.22 km^2 and 4.97 km^2) in Hampshire Avon, United Kingdom. From the sixty-four rainfalls event monitored nitrate response, sixty-one have clockwise loop observed. The loops from top-left to bottom-right indicates a dilution effect during the rising limb. However, for TP response anticlockwise loop was observed, in thirty-five rainfall episodes from forty-one observed. The events evaluated showed TP concentration increasing during the rising limb, which were significantly correlated to discharge. Moreover, for the sixty rainfalls event evaluated for turbidity response, hysteresis patterns were mixed: thirty-seven showed anti-clockwise shape, twenty-three showed clockwise shape, and twenty-five showed figure-of-eight shape, demonstrating more complex behavior than nutrient chemistry. The authors highlight hysteresis analysis relevance in to assess rainfall behavior, comparing distinct episodes between watershed, as well as different hydrological characteristics.

2.2.4 SUMMARY

The best strategy for assessing NPS contribution will be dependent on the available infrastructure. Every start should be based on the simplest and most objective strategy possible, according to the resources available. Gradually, the system will develop. So, first of all, it is necessary to define the main objective of the monitoring strategy and then make the necessary adjustments. Table 1 presents a simplified example of the logic evolution for diffuse pollution evaluation.

Therefore, for any NPS pollution study via runoff, rainy periods information is necessary. The greater the detail of the hydrograph, the more information can be related to the pollutant transport. Another important factor is the detailing of the land use and soil occupation of the watershed to be studied. Knowing all the processes that are developed in the area are fundamental to establish the potential sources of PS and NPS pollution, more appropriate and representative monitoring points, direction and form of transport and the potential cause-effect relationships between land use and water quality.

Table 1 – Logic evolution for diffuse pollution assessment

	Simple	Intermediate	Advanced
Objective	To assess rainy and wet seasons	To assess urbanization or agricultural areas effects into the water body	To assess daily water quality fluctuations during rainfall episodes
Strategy	Punctual sampling during wet and dry periods	First-flush sampling; To assess potential sources of pollution	To determine the contribution area; To define a safe monitoring site, with easy access
Infrastructure	Pluviometric station to collect rainfall data	Water level readings and flow; Sampling during rainfall episodes	High-frequency data sensors
Data Analysis	Box-plots and/or simples comparison	Pollutographs and EMC	Pollutographs and Hysteresis

SOURCE: The Author (2020)

Therefore, due to all the complexity and randomness that exist in the estimates of the diffuse contribution, greater detail of the processes is necessary. Brazilian water resources management does not yet consider this type of contribution, so any study on this subject is essential. The relationship between concentration and flow must always be consolidated and improved. Once the main contribution loads have been established, best management practices can be implemented to assess the mass input into the water body and, consequently, the long-term impacts on water quality.

2.3 WHAT ARE THE WATER QUALITY PARAMETERS NEEDED TO BE MEASURED?

To choose a set of water quality parameters is dependent of the monitoring program strategy and probable occurrence. For example, for water body classification in Brazil, there is a set of many water quality parameters based on visual, organic and inorganic parameters (CONAMA, 2005). The main parameter considered is biochemical oxygen demand (BOD), which indirectly can represent the amount of organic matter. However, for NPS assessment, this parameters is not reliable, due to its fragility and maximum period for analysis of 24h.

Therefore, for each monitoring objective, a set of parameters must be selected. In this section it will be presented four groups of water quality parameters able to be assessed NPS studies.

2.3.1 CONVENTIONAL WATER QUALITY PARAMETERS FOR NPS

Conventional water quality parameters are those associated to the land use and potential NPS dynamics, such as: total fractions of nutrients, as TN, TP, TSS, and turbidity (RANTAKARI et al., 2010; ALIAS et al., 2014; HALLIDAY et al., 2014; BIEROZA; HEATHWAITE, 2015; LLOYD et al., 2016; YU et al., 2016; ZHOU et al., 2016a; DING et al., 2016; KOZAK et al., 2019). According to Quigley Jane Clary and O'Brien (2009), TN and TP must be the minimum parameters to monitor in cases of diffuse pollution assessment. Both parameters are associated to eutrophication process, agricultural fertilizers, traffic emissions, soil erosion and detergents. TSS and turbidity are associated to soil erosion and pollutant accumulated in impervious area, which cause visual impacts, reduced light penetration, and can carry pollutant aggregated to the particles (NOVOTNY, 2003; SPERLING, 2017).

Dissolved fractions of nitrogen, such as nitrite (N-NO_2^-), nitrate (N-NO_3^-) and ammonia nitrogen (N-NH_4^+) (RANTAKARI et al., 2010; BU et al., 2014; BLAEN et al., 2016; KOZAK et al., 2019), and phosphorus, such as ortophosphate (PO_4^{3-}), and SRP (LEE et al., 2011; HALLIDAY et al., 2014; YU et al., 2016; ZHOU et al., 2016a; WANG et al., 2020) are also measured. Despite speciation of nitrogen (N) and P during rainfall episodes may be less important than post discharge and total fractions of them in water body (QUIGLEY JANE CLARY; O'BRIEN, 2009), it can provide information about the degree of pollution and possible sources. For example, N-NO_3^- is associated to distant pollution and/or fertilizers, whereas N-NH_4^+ is associated to recent pollution (BAUWE et al., 2015; SPERLING, 2017). In the same perspective, dissolved fraction of phosphorus can represent the reactive phosphorus, or PO_4^{3-}. They can be associated to fertilizers or wastewater inputs, and represent the phosphorus able to react.

Complementary water quality parameters are measured to better improve understanding of NPS sources, such as WaT, DO, EC, pH and turbidity (BRUNET et al., 2009; HALLIDAY et al., 2014; BIEROZA; HEATHWAITE, 2015; LLOYD et al., 2016; DING et al., 2016; WANG et al., 2017). These parameters, respectively, provide information about rates of physical, chemical and biological reactions, oxygen and ions dissolved availability in water, chemical reaction equilibrium, and suspended materials. For example, in Meyer et al. (2019) the impacts of combined sewer overflow on River Bist in Wadgassen (Germany) during rainfall episodes. Results showed TOC and N-NH_4^+ increasing while DO decreased, suggesting that the decomposition of these organic substances requires amounts of oxygen. Therefore, it is important highlight the usefulness water quality parameters assessment in an integrated routine, without strict separation in their various applications.

Additionally to these parameters, organic matter (OM) has been a parameter of interest in many studies (DELPLA et al., 2011; VISWANATHAN; MOLSON; SCHIRMER, 2015; FRANK; GOEPPERT; GOLDSCHEIDER, 2018; NÓBREGA et al., 2018), due to its presence in entire aquatic system and versatility to be use as a water quality indicator (CARSTEA, 2012; RUHALA; ZARNETSKE, 2017). The usual form to assess organic matter contribution is measuring organic carbon (OC), in both total and dissolved fraction. Dissolved organic carbon (DOC) is considered the doming form of OC in river system (FRIMMEL; ABBT-BRAUN, 2009; RUHALA; ZARNETSKE, 2017). DOC have significant influence in aquatic system, such as light attenuation, metals speciation, complexation, transport and bioavailability, agglomeration or dissolution, and regulates biogeochemical cycles (CORY; MCKNIGHT, 2005; FRIMMEL; ABBT-BRAUN, 2009; RUHALA; ZARNETSKE, 2017). The organic structure determine its quality, being dependent of the source. This can be classified in two main sources: (i) autochthonous (or aquagenic): generated inside the water ecosystem by bacterial action, such as microbial activity or algal productivity; and (ii) allochthonous (or pedogenic): generated outside of the water ecosystem and carried into through soil leaching, geological activities or degradation of terrestrial vegetation (FILELLA, 2009; CARSTEA, 2012). Human activities have influence in both fractions, for example, algae from eutrophication processes (autochthonous), animal and human waste, and land use changes (allochthonous) (CARSTEA, 2012).

Thus, considering the range of possibilities and feedback able to be assessed, the main water quality parameter to be measured is that one which provides the right information for the research question. McCarthy et al. (2018) aimed to develop a sampling strategy for measured the Site Mean Concentration in three different pollutant behavior: TSS to represent the particles and attached possible pollutant as metals, TN which is highly soluble and have distinct behavior of the TSS, and *E. coli* which is a microorganism and behaves differently than the other ones chosen. In Xie et al. (2019) the purpose was integrate monitoring, modeling and multivariate statistics to identify watershed responses during rainfall-runoff events. The water quality data used in calibration and validation of the model was TN, TP and suspended sediment concentration (SSC), mainly to improve the predictive ability of

the NPS modeling by incorporation the intra-rainfall-events variability in the model. These parameters were chosen due to agricultural activities developed in the watershed. In other perspective, in controlled runoff studies, such as Ali et al. (2017) and (MAMOON et al., 2019), which aimed, respectively, to study transport dynamic in paved zones of two distinct surfaces, and to investigate the relation among land use and urban runoff characteristics in distinct surface texture. In these cases, the main research question involved to understand the physical process of the pervious areas, thus, the main water quality parameters measured was TSS. Additionally, in Mamoon et al. (2019) more specific parameters, as trace metals and polyaromatic hydrocarbons (PAHs), were measured because they are generally associated to vehicle components, liquid fuel combustion, batteries, and plastic vehicle.

2.3.2 SPECTROSCOPY TECHNIQUES

Spectroscopy is a technique used to characterize a fraction of the dissolved organic matter (DOM) molecular structure (FRIMMEL; ABBT-BRAUN, 2009). There are many kinds of spectroscopic methods to measure DOM and humic substances (HS), for example, infrared spectroscopy (IR), nuclear magnetic resonance spectroscopy (NMR), mass spectrometry (MS), electron paramagnetic resonance (EPR) and Fourier transform ion cyclotron resonance mass spectrometer (FT-ICR MS) (SENESI; XING; HUANG, 2009; LI; HUR, 2017). However, just the spectral absorption and fluorescence in the ultraviolet (200 - 400 nm) and visible (400 - 750 nm) (UV-Vis) light will be considered in this topic.

UV-Vis absorbance and fluorescence are the most common and widely methods used to characterize qualitatively DOM in aquatic environments, due to easiness in use fast responses, low cost, and high sensitivity (LI; HUR, 2017). These techniques are used separately or combined in several kind of studies, such as: OM assessment in polluted river (CARSTEA, 2012; KNAPIK et al., 2014; LEITHOLD et al., 2017), rainfall events (CARSTEA et al., 2010; INAMDAR et al., 2011; TISSIER et al., 2013; YANG et al., 2015; FRANK; GOEPPERT; GOLDSCHEIDER, 2018; LEE et al., 2019)], seawater (HUGUET et al., 2009; MENDOZA; ZIKA, 2014; MAKAREWICZ et al., 2018) and lakes (ZHOU et al., 2016b; HU et al., 2017; ZHAO et al., 2017), organic characterization in soil and sediment (CLARET et al., 2003; DERRIEN et al., 2017; DERRIEN et al., 2018), wastewater characterization (NEALE et al., 2011; CARSTEA et al., 2016; BAETTKER et al., 2020) and others.

2.3.2.1 UV-Vis absorbances

The spectral absorption in the UV-Vis light range is the oldest characterization methods for DOM (FRIMMEL; ABBT-BRAUN, 2009). The energy involved in photon absorption is the electron transition from the ground state to the excited electronic energy state. There are two types of electron able to absorb UV-Vis light, that are: (i) shared electron one, which have directly participation in bond formation, therefore associated to more than one atom, and (ii) unshared outer electrons, which are located about such atoms as oxygen, halogens, sulfur and nitrogen. Therefore, molecule absorption depend upon how tightly its electrons are bound. Organic compounds, which contain double and triple bonds, generally exhibit absorption peaks in UV region because the electron in unsaturated bonds (easily excited), named as chromophores. So, the wavelength absorption and the intensity of light adsorbed represent a direct value of quantity and kind of organic molecule, which have π systems able to adsorb in UV-Vis region. For example, wavelength of 280 nm can be associated to -C=O structures, and wavelength of 214 nm to -CNO structure (MARTIN-NETO et al., 2009).

Considering low sensitivity of UV-Vis absorption spectra, this technique is able to estimate chromophoric DOM (CDOM) abundance and quality. CDOM is light-absorbing fraction of DOM, and determines optical properties of natural aquatic ecosystems. CDOM sources and chemical composition

can be assessed using absorption ratios, which is the ratio between two different wavelength from the UV-Vis absorbance spectra (LI; HUR, 2017). Furthermore, based on continuous decreasing of absorbance with increasing wavelength, additional information can be assessed. The wavelength 254 nm often used as characteristic information on DOM (FRIMMEL; ABBT-BRAUN, 2009), and 285 nm can detect phenolic compounds presence (BUFFLE et al., 1982; ROSTAN; CELLOT, 1995). Table 2 summarizes some of the ratios widely used in dissolved organic matter characterization.

Table 2 – UV-Vis absorbance ratios used for CDOM characterization

Ratio	Definition	Indication	Source
A_{285}/DOC [a]	$\frac{Abs\lambda 250nm}{Abs\lambda 365nm}$	Values ∼20 g L^{-1} indicate refractory pedogenic compounds (fulvic) Values ∼10 g L^{-1} indicate aquagenic compounds (aliphatic refractory)	(BUFFLE et al., 1982; ROSTAN; CELLOT, 1995)
$SUVA_{254}$ [b]	$\frac{Abs\lambda 254nm * DOC}{0.01}$	Values ∼4.4 L (mg m)$^{-1}$ indicate refractory characteristics Values ∼1.2 L (mg m)$^{-1}$ indicate labile characteristics	(WESTERHOFF; ANNING, 2000)
E_2/E_3	$\frac{Abs\lambda 250nm}{Abs\lambda 365nm}$	Both ratios are inversely proportional to aromaticity and molecular weight. (Range of values not defined)	(PEURAVUORI; PIHLAJA, 1997; LI; HUR, 2017)
E_3/E_4	$\frac{Abs\lambda 300nm}{Abs\lambda 400nm}$		(CLARET et al., 2003; LI; HUR, 2017)

NOTE: [a] DOC unit must be g/L; [b] DOC unit must be mg/L; 0.01 represent optical path correction

$SUVA_{254}$ allow DOM characterization according to its genesis, as for example, in allochthonous (plant and lignin origin) or autochthonous (algae - and aquatic microorganisms - derived), whereas A_{285}/DOC classify organic matter in pedogenic refractory with an aromatic functional groups (originate from soils) and in aquagenic refractory with an aliphatic chain (originate from aquatic biotia) (ROSTAN; CELLOT, 1995; FRIMMEL; ABBT-BRAUN, 2009). E_2/E_3 is generally used to indicate molecular size of CDOM, and E_3/E_4 is used to indicate the degree of humification. These both ratios have inversely correlation to molecular weight and aromaticity (PEURAVUORI; PIHLAJA, 1997; ERLANDSSON et al., 2012; LI; HUR, 2017). There are many other ratios that can be measured and used to characterize CDOM (LI; HUR, 2017), and choosing one or many depends on the type of characterization desired.

Knapik et al. (2014) and Leithold et al. (2017) used both ratios to characterize organic matter dynamics in Iguassu River (Brazil) with intense urbanization pressure. In Knapik et al. (2014) average of $SUVA_{254}$ (2.4 ± 0.9 - 3.0 ± 1.2 L (mg m)$^{-1}$) and A_{285}/DOC (16.9 ± 6.3 - 21.5 ± 7.6 L g^{-1}) suggest a mixture of autochthonous sources of biological activity and allochthonous sources of dissolved organic matter. The probable main source considered was domestic effluent, because DOC in this effluent have low absorption in UV region, and them diminishing both ratios. Leithold et al. (2017) used the ratios to identify predominant source of organic matter in the river. Results range between pedogenic sources and mixed sources. The monitoring site with less urbanization pressure it was measured high values of A_{285}/DOC and $SUVA_{254}$ (respectively 32.2 ± 20.1 L g^{-1} and 4.5 ± 2.7 L (mg m)$^{-1}$) indicating predominance of pedogenic organic matter, and in the monitoring site with more urbanization pressure it was measured low values (A_{285}/DOC = 16.1 ± 4.1 L g^{-1} and $SUVA_{254}$ = 2.4 ± 0.6 L (mg m)$^{-1}$) suggesting labile aquagenic organic matter or the contribution of anthropic allochthonous organic matter.

E_2/E_3 and E_3/E_4 ratios are usually used in DOM characterization in soils. For example, Claret et al. (2003) used E_3/E_4 to classify humic and fulvic acids in clay samples. The ratio for humic acid content ranged between 2.67 to 3.10, whereas for fulvic acid ranged between 5.14 to 7.03. No other characteristics

can be observed, however there is a pattern in the UV-Vis absorption spectrum of humic and fulvic acids where absorption increase with decreasing wavelength. However, Peuravuori and Pihlaja (1997) studied spectroscopic properties of DOM in waters of lake and river. They proposed the use of E_2/E_3 ratio in association to the aromaticity, wherein ratio increases with aromaticity and molecular weight decrease.

Stephens and Minor (2010) investigated differences in DOM composition between saltwater and freshwater using DOC concentration, UV-Vis spectroscopy, and other techniques. Samples were collected in Chesapeake Bay Estuary (saltwater - four sampling sites), and St. Louis River and Lake Superior (freshwater - seven sampling sites) located in Elizabeth River sub-watershed (area of 6.7 x 10^8 m^2). DOC concentration for freshwater ranged 34.5 $\pm$ 0.11 to 1.7 $\pm$ 0.03 mg L^{-1}, while for saltwater concentration were bigger, ranging between 141.6 $\pm$ 1.16 to 1.3 $\pm$ 0.07 mg L^{-1}. The E_2/E_3 ratio ranged from 5.40 to 15.29 for freshwater samples and from 4.42 to 10.28 for saltwater samples. Shifts in the values occurred in downstream direction of the sampling sites selected, suggesting low-molecular weight photoproducts DOM distribution. Furthermore, the authors conclude that basic processes, as microbial degradation and photochemistry, appear to mediate the pattern observed.

In the same perspective, (MA; LI, 2020) used UV–Visible spectroscopy and fluorescence to characterize DOM in temporal and spatial gradients and to explore land use effects in DOM composition on the Three Gorges Reservoir (China). Results showed similar E_2/E_3 ratio values between dry season (average of 6.51 $\pm$ 1.55) and wet season (with average of 6.00 $\pm$ 1.26), suggesting bigger molecular weight of DOM in wet season. The authors associated these results to the terrestrial DOM inputs by runoff and leaching induced during precipitation occurrence. Moreover, ratio E_2/E_3 in farmland-affected river were higher than in forest-affected river in dry season.

2.3.2.2 Fluorescence

There is a fraction of CDOM able to emit fluorescence when excited by photons with specific energy, called fluorescent DOM (FDOM) (LI; HUR, 2017). The photon, with appropriate energy, absorbed in UV-Vis spectra change their molecular electronic, causing transition in valence electrons. These transition are the excitation of electron from a occupied molecular orbital to the next more energetic orbital. This energy absorbed is dependent of the energy difference between the ground and excited state, and if it is not enough to molecule ionization or disassociation, it will remain at excited state a short lifetime (about 10^{-7} - 10^{-9} seconds). Afterward, a light will be re-emitted, being called as fluorescence (MARTIN-NETO et al., 2009). Therefore, the fluorescence spectroscopy technique is able to characterize DOM and to distinguish different sources of DOM due to numerous double bonds (π electrons) in the molecules (FRIMMEL; ABBT-BRAUN, 2009). The size of the π system determines energy of transition. For example, benzene rings in aromatic compounds will be observed at longer wavelengths, because in a large (or increasing size) conjugated bond chain, the transition energy decreases. The smaller the energy difference, the higher is the wavelength absorption, and therefore, fluorescence spectra shows maximum excitation and emission wavelength, which are dependent of the source (MARTIN-NETO et al., 2009).

Three dimensional excitation-emission matrix (EEM) is the fluorescence intensity from the combination of various pairs of λ excitation and pairs of λ emission (CARSTEA, 2012), which can identify specific DOM structures. The technique is non-destructive and requires little or no sample preparation (HUDSON; BAKER; REYNOLDS, 2007). There are two main pollutant groups generally detected in this approach: (i) protein-like substances, constitute by three aminoacids, which are tryptophan, tyrosine and phenylalanine; and (ii) humic-like substances, composed for humic and fulvic acid (HUDSON; BAKER; REYNOLDS, 2007). In general, protein-like have simpler organic structures than humic-like, being therefore, located in lower wavelenght, while humic-like are observed in higher emission wavelength. In order

to facilitate, Coble (1996) proposed a nomenclature to these substances and excitation/emission regions in EEM. Table 3 summarize the five main regions in EEM which contain humic-like and protein-like organic structures. For peak B, the region was adapted due to an observed emission shift.

Table 3 – Five main regions in the EEM for identification of the humic- and protein-like compounds

	Peaks name	Organic Compound	$\lambda_{excitation}$	$\lambda_{emission}$
Humic-like Substances	A	Humic acid	225 - 235	400 - 500
	C	Fulvic acid	300 - 350	400 - 500
Protein-like Substances	B	Tyrosine	215 - 245	265 - 315
	T_1	Tryptophan	285 - 295	345 - 355
	T_2	Tryptophan	225 - 235	345 - 355

SOURCE: Adapted from Coble (1996), Hudson, Baker and Reynolds (2007)

From fluorescence spectra is possible to calculated indices in order to improve DOM sources characterization. They are similar to those presented in UV-Vis section, and are calculated from fluorescence intensities ratio. There are three interesting ratios that reflects DOM composition and possible source, which are Fluorescence Index (FI), Biological Index (BIX) and Humification Index (HIX). Basically, they consist in slope of fluorescence spectra between different fluorescence intensities.

FI is used to indicate organic matter sources, where values greater than 1.8 indicate autochthonous origin (or microbially derived fulvic acids) and values less than 1.5 indicate allochthonous origin (or terrestrially derived fulvic acids) (WESTERHOFF; ANNING, 2000; MCKNIGHT et al., 2001).

BIX determine the presence of β fluorophore, which are characteristic of autochthonous biological activity in water samples. BIX values bigger than 1.0 indicate predominantly autochthonous origin of DOM, values between 0.8 - 1.0 indicate freshly DOM from biological or microbial origin, whereas values less than 0.7 indicate lower DOM production or little autochthonous OM (HUGUET et al., 2009; BIRDWELL; ENGEL, 2010).

HIX determine the degree of humification, being correlated to DOM aromaticity, due to the fluorescence intensity at long wavelength, which represent complex molecules, as high molecular weight aromatics. Values bigger than 16 indicate strong humic character (terrigeneous contribution), values between 4 - 10 indicate a transition in important and weak humic character, and values less than 4 indicate aquatic bacterial origin (biological) (HUGUET et al., 2009; BIRDWELL; ENGEL, 2010). Table 4 summarizes these three fluorescence indices, their calculation and indication.

Table 4 – Fluorescence indices for assessment of DOM sources and composition

Index	Definition	Indication	Source
FI	from $\lambda_{Ex}370nm$ $\frac{\lambda_{Em}450nm}{\lambda_{Em}500nm}$	>1.8 indicate autochthonous source <1.5 indicate allochthonous sources	(WESTERHOFF; ANNING, 2000; CORY; MCKNIGHT, 2005)
BIX	from $\lambda_{Ex}310nm$ $\frac{\lambda_{Em}380nm}{\lambda_{Em}430nm}$	Between 0.6-0.8 indicate low to intermediate autochthonous component Between 0.8-1.0 indicate strong autochthonous component >1.0 indicate aquatic bacterial origin	(HUGUET et al., 2009; BIRDWELL; ENGEL, 2010)
HIX	from $\lambda_{Ex}254nm$ $\frac{\sum\lambda_{Em}435-480}{\sum\lambda_{Em}300-345}$	>16 indicate strong humic character (terrigeneous contribution) 6-10 indicate important humic character 4-6 indicate weak humic character <4 indicate aquatic bacterial origin	(HUGUET et al., 2009; BIRDWELL; ENGEL, 2010)

NOTE: Ex - excitation; Em - emission

EEM peaks and these indexes have been used in recent studies about organic contribution (BIRDWELL; ENGEL, 2010; CARSTEA, 2012; GRAYSON; HOLDEN, 2016; HE et al., 2016; WANG et al., 2017; LEITHOLD et al., 2017; DERRIEN et al., 2018; XIAN et al., 2018; FRANK; GOEPPERT; GOLDSCHEIDER, 2018; LEE et al., 2019; MA; LI, 2020). Frank, Goeppert and Goldscheider (2018) used EEM to help characterization of the organic matter dynamic in three different spring water in Germany. The peaks regions observed was based on Coble (1996) classification. At the monitoring site of Marulbach Spring (MBQ), fluorescence peaks and TOC start to increase intensity and concentration about 6 hours after the beginning of the rainfall episode. The maximum values observed occurred 15 hours after the start of rainfall, reaching 2.05 $mg.L^{-1}$ of TOC, 2.47 r.u. of peak A, 1.23 r.u. of peak C, and 0.47 r.u. of peak T. These parameters showed high coefficients of determination, which was R^2 0.91 and 0.98. The authors highlighted the simultaneous river response to rainfall of TOC and fluorescence peaks, and suggest that the important amount of TOC is related to the FDOM, with humic-like and protein-like substances. Considering that, the probable organic matter sources is from decomposition of organic material from plant and animals, and land surface.

Wang et al. (2017) also used EEMs peak to identify DOM structures and, then, to estimate water pollution in surface water of the Ebinur Lake Watershed (50,621 km^2), which is a arid region from Central Asia. It were identified three peaks region in the EEM spectra, which correspond to tyrosine-like substances, as free aromatic amino acids (peak B - excitation/emission of 220/300 nm), and humic-like substances (peak A - excitation/emission of 250/400–450 nm; peak C excitation/emission of 280-340/350–450 nm) (Peak C). The author found these peak intensities increase with increase of conventional water quality parameters, as COD, TP, TN, N-NH_3 and BOD_5, suggesting serious water organic pollution. Moreover, the author used parallel factor analysis (PARAFAC) to model EEM components. The model identified the same fluorescence components, grouping as microbial humic-like (C1), terrestrial humic-like organic substances (C2 and C4) and protein-like organic substances (C3), corroborating the results of severe organic pollution from terrigenous and human sources.

Xian et al. (2018) verified the dynamic of soil DOM in rainfall events in controlled study. The study was conducted in 0.35 km^2 area, an agricultural head water catchment in Sichuan (China). It were simulated four rainfall condition, with rainfall amount and duration ranging, respectively from 39.4 to 110.8 mm, and 6 to 26.5 hours. In addition to EEMs and $SUVA_{254}$ analysis, the author used FI and HIX indices. The both indices ranged between 1.52–1.61 (FI) and 0.87–0.91 (HIX) without significant changes intra and inter events. These values indicate a mixture of microbial- and plant-derived DOM sources, with high humification degree from soil organic matter pool. $SUVA_{254}$ analysis was more sensitive to capture variations of DOM's aromaticity during rainfalls. Thus, from this set of DOM analysis, the authors highlighted an important pattern of DOM, where underground migration was the primary DOM export pathway during rainfall episodes. In the same aspect, (MA; LI, 2020) used FI, BIX and HIX indices, in addition to other ones, to investigate DOM properties in wet and dry season. Results showed FI and BIX values in dry season (1.84 and 1.02, respectively) higher than in wet season (1.63 and 0.89, respectively), while HIX had a reserved seasonal behavior. This suggest that during wet season there was a mixing of weak and strong microbial terrestrial and biologic/microbial sources of DOM with high degree of humification, regardless of changing in land use. Therefore, it was possible to conclude that monsoonal rainfall also controled DOM composition and sources.

Therefore, it was possible to observed that these spectroscopy techniques, ratios and indices can suggest sources, material composition and structure characteristic of DOM in water samples (WANG et al., 2017), as detecting different kind of compound, from protein- and humic-like substances (CARSTEA, 2012). Thus, remarkably, this technique has been shown to be a powerful way to look the organic contribution, easily applied in diffuse pollution studies.

2.3.3 EMERGING CONTAMINANTS

The definition of emerging contaminants (EmerC) or contaminant of emerging concern (CEC) is not well defined yet, due to conflicting perspective of interpretation. Sauvé and Desrosiers (2014) explain that EmerC can be related to that one which appeared only recently (more or less than two decades ago), and CEC can be related to that one which have been in the environment for a while but the concern have been raised recently. Moreover, the authors exemplified the context by analyzing that pharmaceuticals have emerged in the past decade due to increased consumption. Hormones and synthetic steroids have been studied frequently, whereas natural steroid hormones have been released into wastewater and rivers since the first colonizers humans (SAUVÉ; DESROSIERS, 2014). Therefore, it is a categorization issue.

Thus, EmerC definition considered will be the same used by UNESCO and the U.S. Geological Survey (USGS), which is: "Emerging pollutants can be understood as any synthetic or naturally-occurring chemical or any microorganism that is not commonly monitored or regulated in the environment with potentially known or suspected adverse ecological and/or human health effects" (KLAPER; WELCH, 2011; UNESCO, 2020).

"CEC" refers to different kinds of chemicals compounds used by human in our chemical-based modern lifestyle (USGS, 2020), but also used in veterinary science, livestock farming, agricultural products, industry, and others (REICHERT et al., 2019; USGS, 2020). They can be classified in groups as, for example, pharmaceutical, personal care products, hormones, endocrine disrupting compounds, synthetic musks, phthalates, brominated and fluorinated compounds (KLAPER; WELCH, 2011; REICHERT et al., 2019; WQA, 2020), and inside these groups there are further specific classifications, as for example, antipyretic and analgesic drugs, antibiotics, stimulant, beta-blockers, non-steroidal anti-inflammatory drugs, anti-depressives, UV filters, preservatives, antimicrobial agents, antisepctics, flame retardants, plasticizers and others (KLAPER; WELCH, 2011; REICHERT et al., 2019).

These compounds enter in the environment every day (USGS, 2020), and the risk for human health and environment is not fully understood (WQA, 2020). Figure 10 show a schematic representation of emerging contaminants interaction in the environment and potential human health risks. Lei et al. (2015) highlight that several interaction factors should be considered, and the effects of pollutant exposure must be improved, considering contaminant concentration, category, properties, scale, level and hazard of these pollutant. Thus, although there is no sufficient or large-scale evidence of the association between EmerC and adverse effect to humans and animals, experiments highlight these interactions and impacts, and they can not be ignored.

These contaminants are not contemplated as a priority pollutants or being considered in controlling (production and release) legal instruments in many countries of Latin America, as in Brazil and México (REICHERT et al., 2019). They are usually detected in low concentrations in the range of ng.L^{-1} or μg.L^{-1} (REICHERT et al., 2019). The main concern involving emerging contaminants are related to the ability to bioaccumulate (EBELE; ABDALLAH; HARRAD, 2017; USGS, 2020), mutagenicity (LEI et al., 2015), persistence and toxicity (EBELE; ABDALLAH; HARRAD, 2017). Moreover, there are not an efficient treatment processes capable of removing completely these compounds (USGS, 2020).

Considering that these products are generally consumed by human and/or animals and/or in theirs activities, the main source is sewage treatment plants, septic system, solids from waste treatment and livestock facilities, and landfill leachate (KLAPER; WELCH, 2011; EBELE; ABDALLAH; HARRAD, 2017). Figure 11 shows a schematic representation of the potential pollution sources of EmerC in the aquatic environment.

Generally, EmerC from industrial and agricultural activities are directly correlated to the human

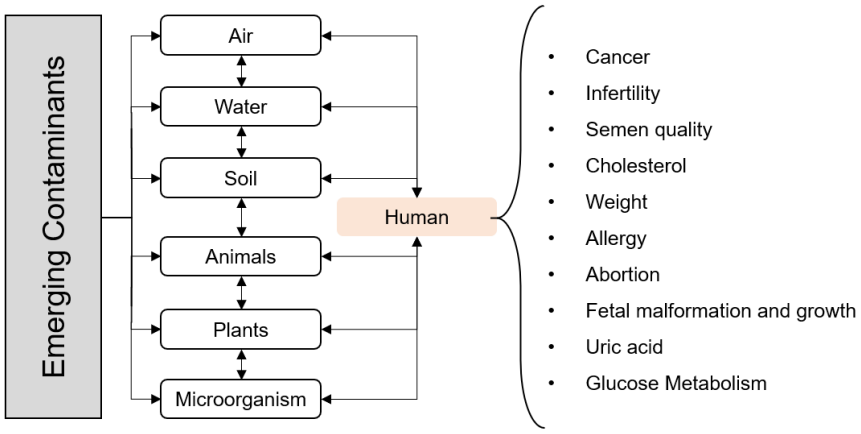

Figure 10 – Emerging contaminants interaction in the environment and potential human health risks

SOURCE: Adapted from (LEI et al., 2015)

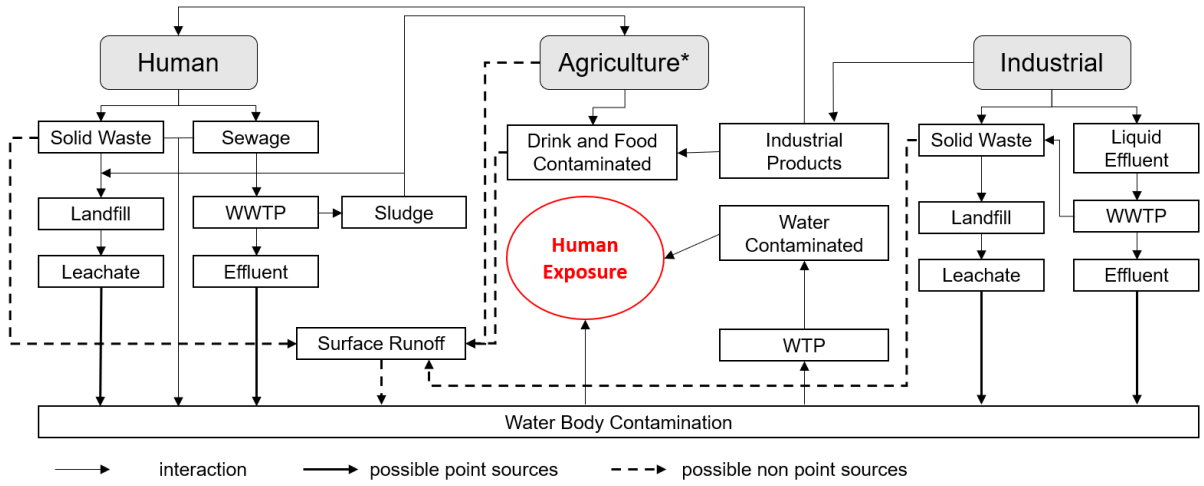

Figure 11 – Potential pollution sources of emerging contaminants into the water body and human exposure

SOURCE: Adapted from Aquino, Brandt and Chernicharo (2013)
NOTE: * agriculture represent agricultural and livestock activities
LEGEND: WWTP - wastewater treatment plant; WTP - water treatment plant

lifestyle, which use these elements as industry raw material to produce the products. These elements are consumed and/or absorbed by humans and animals, followed by excretion with their metabolite or even unchanged (EBELE; ABDALLAH; HARRAD, 2017). It is possible to anticipate that the main source of contamination the wastewater effluent (MONTAGNER; VIDAL; ACAYABA, 2017). Therefore, after they have been released in wastewater treatment plant (WWTP) or landfills, they can be classified as PS of pollution. However, NPS of these contaminants are related to urban and agricultural surface runoff, leaching to groundwater, and sewage overflow (EBELE; ABDALLAH; HARRAD, 2017). They can be favored by rainfall episodes or not.

Corada-Fernández et al. (2017) assessed the effect of extreme rainfall episodes in river and aquifers of Guadalete basin (Southern Spain). It was investigate a group of more than 180 emerging contaminants, including personal care products, surfactants and pharmaceuticals. The main problem observed in that area is combined sewer overflows (sewage from the city and from the WWTP) which increased organic contaminants concentration in surface water, mainly during rainfall. Three field campaigns were performed (one during dry season and two during raiy season), where twenty-nine sites from groundwater

and five sites from surface water were monitored. Surfactants were detected in all sampling points of the campaigns, with a frequency of detection ranging between 52% to 94% for linear alkylbenzene sulfonates (LAS), an surfactant used in detergents, shampoos and personal care products (PCP), and 1% to 3% for alcohol polyethoxylates (AEO), and surfactant used in domestic and industrial detergents, cleaners, emulsifiers, etc. In the campaign with heavy rainfall condition (water height of 4.5m, which causes important overland flow), the highest concentration of LAS (215 to 3996 $\mu g.L^{-1}$) and AEO (23 to 141 $\mu g.L^{-1}$) were found in surface samples in the two monitoring sites that received untreated (R7) and treated (R12) urban wastewater discharges. The authors highlighted that these concentration were similar to concentration in very heavily polluted areas. Additionally, in these two points, were detected caffeine (233 $\pm$ 67 $ng.L^{-1}$ (R7) and 26 $\pm$ 3 $ng.L^{-1}$ (R12)), and naproxen (289 $\pm$ 14 $ng.L^{-1}$ (R7) and 31 $\pm$ 3 $ng.L^{-1}$ (R12)) and ibuprofen (1747 $\pm$ 43 $ng.L^{-1}$ (R7)), strengthening the influence of point sources in water surface contamination.

Therefore, to monitor emerging contaminants is an important issue, mainly due to the few information and knowledge about these contaminants, processes, impact and effects. Thus, it will be presented an description for the three main groups of emerging contaminants, their basic characteristics and water surface interactions.

2.3.3.1 Pharmaceutical

Pharmaceutical is the general category of the EmerC which are the chemical products consumed by humans and used in animals with medicinal purpose. They can be classified according to their uses, as for example, anti-inflammatory, analgesic, metabolite, stimulant, beta-blocker and lipid regulator. According to Montagner, Vidal and Acayaba (2017), pharmaceutical is the EmerC group most studied in the world, and the second one in Brazil. Besides that, the authors highlight that there were a significative increase in medicine consumption worldwide, mainly that ones sold without medical prescription, as analgesic and/or continuous use medicines. Table 5 summarize some of the main characteristic of the pharmaceutical studied.

Paracetamol (PAR), Fenoprofen (FenP), Ibuprofen (IBU), Diclofenac (DIC), Naproxen (NAP), Acetylsalicylic Acid (ASS) and its metabolite Salicylic Acid (AS) are drugs used, basically as analgesics, antipyretics, anti-inflammatory, inhibitor and antifungal agent. They have ability to act on the central nervous system, cardiovascular system, dermatology, sensory organs, and others. After ingestion, they are eliminated in the urine and feces. In the soil, PAR and ASS have high mobility, however if released in water, adsorption on suspended solids and sediments is not expected to be an important fate process. The others ones have low to moderate mobility, but their adsorption in suspended solids and sediments is expected. None of these elements are expected to suffer volatilization from water, and their potential for bioconcentration is low (NIH, 2020).

Burns et al. (2018) studied an rapid determination method to assess pharmaceutical in aqueous matrix during a year over two rivers: River Ouse (urbanised and larger one), and River Foss (smaller and more rural one), in the city of York, UK. In the both sites, there is a WWTP. Of the thirty-three pharmaceuticals monitored, just twelve were detected along the year in River Foss, and ten pharmaceutical in River Ouse. Monthly summed concentration were higher in River Foss (above 2000 $ng.L^{-1}$) than in River Ouse (below 1000 $ng.L^{-1}$, respectively), due to the great dilution of discharged effects from the WWTP (flow ranged from 9.2 to 233 $m^3.s^{-1}$ in the Ouse, compared with 0.0096 to 1.68 $m^3.s^{-1}$ in the Foss). Metformin, a type II diabetes drug, had the highest annual median concentration (1117 and 237 $ng.L^{-1}$ in the Foss and Ouse, respectively), and PAR the thrid highest concentration (analgesic) (209 and 77.6 $ng.L^{-1}$, Foss and Ouse, respectively). The spatial trends showed that generally downstream of

the WWTP the concentration were higher, decreasing moving to downstream in the river; and, temporal trends showed the lowest concentration found in winter season, which had the highest average flow registered. Therefore, in this study area, the flow appears to be major driver in the pharmaceutical variability. The authors emphasize that there is a wide variation in relation to the drug with the highest annual concentration in several countries, and highlight that these variation are extremely regional, due to variability in prescribing practices, hydrology, wastewater management and degree of urbanisation. Another studies complement these ideas (GARRIDO et al., 2016; SANTOS et al., 2016; TALIB; RANDHIR, 2017; EBELE; ABDALLAH; HARRAD, 2017; EDWARDS et al., 2017; ZHANG et al., 2018b).

Another important category are β-blockers such as Metoprolol (MTL), Propranolol (PRL) and Nadolol (NAD). These drugs act directly on the cardiovascular system because they are used in the prevention of hypertension and arrhythmia, having the vasodilator capacity. They are excreted in the urine. In the soil, they have high mobility, but are not expected to adsorb to suspended solids and sediments. They also have low capacity for bioconcentration and, volatilization from water despite not expected to be an important fate process, they can be an interesting tracer to be considered (NIH, 2020). Osawa et al. (2015) assessed MTL, PRL and NAD in four rivers of the Curitiba city (Brazil) in order to evaluate temporal and spatial dynamics of these EmerC. Four field campaigns on fourteen monitoring sites were monitored. Results showed higher concentration in monitoring sites located in urban areas with WWTP influence (wastershed downstream) than in preserved area (watershed upstream). Among the sites monitored, maximum values ranged of 903.6 to 4658.5 ng.L^{-1} for MTL, 178.2 to 3,877.9 ng.L^{-1} for PRL, and $<$ LOQ to 123.8 ng.L^{-1} for NAD. Spatial dynamics were evaluated between campaigns performed during rainy and wet season, showing two behavior, which are: (i) lower concentration during periods with higher amount of precipitation, due dilution effects, in a more preserved monitoring site ($<$ LOQ in all β-blockers and P_{accum} of 53.6 mm at Palmital River), and (ii) high concentration during periods with high amount of precipitation in a monitoring site with high urban pressure, suggesting the increasing of the WWTP outflow and contributing to the higher concentration of PRL into the Atuba River (3,877.91 ng.L^{-1} and P_{accum} of 53.6 mm).

Finally, compounds such as Gemfibrozil (GemF) and Fenofibrate (FNF) are in the class of lipid regulators, acting on the cardiovascular system. They are used as hypolipidemic and lipid modifying agents, and are eliminated in the urine and feces. On the soil, they have moderate to low mobility, and it is expected suffer adsorption on suspended solids and sediments, but not volatilization from water. GemF has a low potential for bioaccumulation, while FNF has a high potential (NIH, 2020). Reichert et al. (2020) assessed these lipid regulators and some personal care products in the Tibagi River watershed (25,000 km^2), Southern Brazil. It were monitored three sub-basin, with a total of eleven river sites. Results indicate FNF above the limit of detection in all samples analyzed, probably due to the low water solubility, and GemF occurrence in 100% of the samples, reaching 2590.9 ng L^{-1} downstream of one WWTP. Additionally, the authors performed a risk assessment, where GemF was not relevant in terms of acute toxicity effect, however long-term exposures of higher concentration of GemF could mean a moderate risk to invertebrates (*V. fischeri*).

The occurrence of pharmaceutical in water is of great international relevance. According to Montagner, Vidal and Acayaba (2017) the main concern about pharmaceutical is the specific potential interference, as for examples, hormone pharmaceutical have endocrine interference, psychotherapy pharmaceutical acts directly on central nervous system, and antimicrobials increase the amount of resistant bacteria. Thus, it is increasingly important to monitor and assess properly these compounds, and to establish the better water resources and wastewater management to decrease their impacts in the environment and human health (REICHERT et al., 2019).

2.3.3.2 Caffeine (CAF)

CAF is a stimulant that acts mainly on the central nervous system. It can be found in various items such as food, energy drinks, medicines and cosmetics. Their route of elimination is through urine. In the soil, it has low or no mobility, however if released in water it is expected to be adsorbed on suspended solids and sediments. It is not expected that volatilization from water to be an important fate process for caffeine, and its potential for bioconcentration is low. Degradation in natural water can occur through photodegradation and biodegradation (NIH, 2020). Due to the CAF structure, similar to theophylline, it was concluded that CAF is readly biodegradable, with slow hydrolysis rate, in the atmosphere the photodegradation by reaction with hydroxyl radicals with a half-life of 19.8 hours (UNEP; OECD, 2003). Therefore, considering their characteristics, caffeine has been used as a chemical tracer, because its quantification is directly related to domestic wastewater discharges, since its presence in the environment is associated with humans lifestyle (MIZUKAWA et al., 2019).

In Mizukawa et al. (2019) study showed that caffeine anthropic tracer as an alternative tool for water quality monitoring in Alto Iguassu Watershed, an subtropical urban basin in Brazil. It were monitored three sub-basins of Alto Iguassu, in ten monitoring sites. Caffeine was detected in 98% of the samples, ranging concentrations 0.07 μg L^{-1} to 23.08 μg L^{-1}. Additionally, the authors compared caffeine occurrence with the traditional water quality parameters, as N-NH_4^+ and thermotolerant coliforms. It were observed similar behavior of these parameters and caffeine, suggesting the same source of contamination, and therefore, anthropic influence over aquatic environment. Thus, caffeine analysis showed an appropriate approach to environmental monitoring, enabling their use as a concise tool for environmental decision making.

2.3.3.3 Personal Care Products (PCPs)

Personal care products (PCPs) is the general category of the cosmetics, fragrances, antimicrobial compounds, antioxidant and preservative creams, insecticides and sunscreen, generally used by human. According to Montagner, Vidal and Acayaba (2017), PCP use has been increased exponentially worldwide over the last decade. They can be divided in two specific sub-grupos, which are preservative and agent bacteriostatic, summarized in Table 5. These emerging contaminants are used as antifungal, microbial and bacteriocide agent, cosmetics, pharmaceutical and food preservative. Therefore, are generally found in waste from domestic and industrial use.

Methyl- and ethylparaben have, respectively, high and moderate mobility in soil, however, if release in water, it is not expected they adsorbed in suspended solids and sediments. Both have low potential of bioconcentration and may be susceptible to photolysis by sunlight (chromophores that absorb at wavelengths > 290 nm). Besides biodegradation may be an important environmental fate process in water, it is not expected that volatilization from water to be an important fate process. Propylparaben has moderate mobility in soil, whereas butylparaben has low mobility, and it is expected that both, if release in water, can absorb in suspended solids and sediment. Besides that, it is not expected that volatilization from water to be an important fate process for them. Butylparaben has a high potential for bioconcentration, but biodegradation can be an important environmental fate process, whereas propylparaben has moderate potential for bioconcentration. At last, triclosan has slight or no mobility in soil, and low to moderate potential for bioconcentration. Although volatilization from water is not expected as a fate process, it is expected absorption in suspended solids and sediment if release in water (NIH, 2020).

Santos et al. (2016) determined parabens and triclosan presence in the aquatic environment in the Upper Iguassu Watershed, Southern Brazil. It were monitored Iguassu River (main river), and six

main tributaries, resulting in a total of twenty sampling sites, in four campaign performed in 2011 and 2012. Methyl-, ethyl-, propyl-, butylparaben and triclosan were detected in the surface waters monitored, with percentage of occurrence ranging between 10 to 90%. Just benzylparaben was not detected in any sample. The highest concentration measured was 2875 ng L^{-1} of methylparaben, followed by ethylparaben (1485 ng L^{-1}), propylparaben (486 ng L^{-1}), triclosan (415 ng L^{-1}), and buthylparaben (286 ng L^{-1}). The author highlight that parabens and triclosan were detected over the months, indicating intermitent consumption and release into the environment. Non-efficient wastewater treatment, discharge of sewage without any treatment and irregular occupation were some of the reason summarized for these high concentration of parabens and triclosan in river. Reichert et al. (2020) detected methyl- and propylparaben in 100% of the samples analyzed, and ethyl- and butylparabens were frequently detected, but not always quantified. The parabens concentration ranged from nd to 486,6 ng L^{-1} in the area. Triclosan were detected in all sampling points reaching a maximum of 788.8 ng L^{-1}. The risk assessment showed low risk for most of the species for parabens exposure, with exception for the fish *O. latipes*, which seems to be sensitive for propyl- and butylparabens. However, chronic exposure to triclosan can have high risk for many species, especially algae and fishes, and moderate risk for invertebrates.

2.3.3.4 Sterol

Sterol is the general category for the emerging contaminant which includes female sex hormones, phytoesterol, and fecal sterol derived from animals and human. According to Kramer (2016) these are the most studied sterols. Table 5 summarized some characteristics of the main sterol considered in this study.

Female sex hormones are chemical substances produced by endocrine glands, which are release directly in the blood. They are named as estrogens, and can be natural or synthetic. The hormones estradiol, estrone and estriol are the three main endogenous estrogens or natural produced, mainly, in the ovaries, being responsible for the development of female characteristics during the puberty and pregnancy periods (MONTAGNER; VIDAL; ACAYABA, 2017; MIZUKAWA, 2014). These hormones are naturally eliminated in the urine, therefore, they can be found in wastewater effluent. Estrone have moderate or no mobility in the soil, being able to absorb in suspendend solids and sedimentos if released in the water. 17β-estradiol have no mobility in the soil, and it is not expected absorption in suspended solids and sediments if release in water. For the both hormones volatilization from water is not expected as a fate process. Estrone had moderate potential for bioconcentration, whereas 17β-estradiol has high potential (NIH, 2020). The synthetic estrogens, as ethinyl estradiol, are used in contraceptive drugs, hormone replacement therapies and treatment of neoplasms. They acts directly on endocrine system, being high estrogenic potential. The route of elimination is in the urine, feces and bile (MONTAGNER; VIDAL; ACAYABA, 2017). The ethinyl estradiol has low mobility in the soil, and it is able to adsorb in suspended solids and sediment if release in water. This compound have high potential for bioconcentration, however volatilization from water is not expected as a fate process (NIH, 2020).

According to Raimundo (2007) the most portion of estrogens are metabolized and excreted in their inactive and conjugated form. However, bacterial activities in effluent discharge areas can easily biotransform these elements in active compounds, being able to produce adverse effect in the human health and biota. Therefore, considering severe influence in the environment caused by sex hormones, natural or synthetic, they are considered endocrine disruptors. Studies involving sex hormones normally considered their occurrence in the environment. For example, Ide et al. (2017) determined some emerging contaminants, such as pharmaceutical and female sex hormones, in the Iguassu River (Brazil), to assess the river quality and to evaluate the pollution status. Results showed that acetylsalicylic acid was detected in the highest concentration, gemfibrozil and naproxen was detected most frequently, and estradiol was

the most commonly detected. And, Edwards et al. (2017) determined if surface waters in Barbados were contamined with emerging contaminant from wastewater origin. They monitored pharmaceuticals, chemical tracers, fungicies and steroid hormones. Results showed that estrone was detected at trace concentration (< 10 ng L^{-1}) in surface water in rainy season campaign, and caffeine was detected in all samples in dry and rainy season campaing with high concentration (ranging between 56 ± 1.6 to 552 ± 16 ng L^{-1}).

Another sub-groups is the sterol from fecal and plant origin. Colesterol, coprostanol, epicoprostanol are exclusively of fecal origin from animals and human, and campesterol, stigmasterol and β-sitoesterol can be found in natural sources, as superior plants constituents. They have hydrophobic nature (elevated Kow values), being easily trapped by organic matter and found in sediments or particulate material (MACHADO et al., 2014).

Cholesterol is the main esterol from animal origin, the coprostanol is produced by microbial reduction of the cholesterol, and epicoprostanol is a coprostanol isomer (MIZUKAWA, 2014). There are many sterol ratios used to identify human fecal contamination or to discriminate types of human and animal fecal sources (MACHADO et al., 2014). In Machado et al. (2014), it was assessed historical fecal contamination in Barigui River (Southern Brazil), in the last 400 years, using fecal sterols and some ratios. The analysis were performed in a sediment sample with 100 cm of total depth. Coprostanol/(cholestanol + cholesterol) ratio (ratio 1) was used to indicate fecal human contamination, and (coprostanol + epicoprostanol)/cholesterol ratio (ratio 2) was used to indicate treat and untreat sewage influence. Results showed that a possible fecal contamination since 1820 (ratio 1 greater than 0.2), and increasing in human influence and untreated wastewater from 1930, with increases in the ratio 2 (greater than 0.5). More ratios examples are, coprostanol/cholesterol ratio proposed by Takada et al. (1994), to evaluate biogenic and sewage contributions, epicoprostanol/coprostanol proposed by Mudge and Seguel (1999) to assess level of treament or fecal material age, and coprostanol/(coprostanol + cholestanol) proposed by Grimalt et al. (1990) used to assess sewage contamination.

Therefore, these compounds are important elements to assess water quality dynamics and human activities impacts in the environment, due to singular and specific kind of information. Moreover, this indicators must be related to the population of the region and their lifestyle. Different regions have different development modes, and consequently, different sanitation infrastructure, socioeconomic level, social development, and different sewage coefficients. Therefore, all theses variable also should be considered together in the water quality assessment (LIN et al., 2019).

Table 5 – Emerging contaminants characteristics considered in this study

	Class	Compound	Molecular Formula	CAS Number	Molar Mass ($g.mol^{-1}$)	pKa	Log Kow	Solubility in water *	Koc ($ml.g^{-1}$)
Pharmaceutical	Analgesic; Anti-inflammatory	Paracetamol	$C_8H_9NO_2$	103-90-2	151.16	9.38	0.46	14,000	21
		Fenoprofen	$C_{15}H_{14}O_3$	29679-58-1	242.27	7.3	-	-	-
		Ibuprofen	$C_{13}H_{18}O_2$	15687-27-1	206.28	5.2	3.97	21	3400
		Diclofenac	$C_{14}H_{11}Cl_2NO_2$	15307-86-5	296.10	4.15	4.51	2.37	245
		Naproxen	$C_{14}H_{14}O_3$	22204-53-1	230.26	4.15	3.18	15.9	330
		Acetylsalicylic Acid	$C_9H_8O_4$	50-78-2	180.16	3.49	1.19	4,600	100
	Metabolite	Salicylic Acid	$C_7H_6O_3$	69-72-7	138.12	2.98	2.26	2,240	404
	β-blocking agents	Metoprolol	$C_{15}H_{25}NO_3$	51384-51-1	267.36	9.6	1.88	>1000	62
		Propanolol	$C_{16}H_{21}NO_2$	525-66-6	259.34	9.42		61.7	-
		Nadolol	$C_{27}H_{17}NO_4$	42200-33-9	309.40	9.67	0.71	8,330	60
	Lipid regulator	Gemfibrozil	$C_{15}H_{22}O_3$	25812-30-0	250.33	4.5	4.77	11	430
		Fenofibrate	$C_{20}H_{21}ClO_4$	49562-28-9	360.80	-	5.19	0.42	3800
	Stimulant	Caffeine	$C_8H_{10}N_4O_2$	58-08-2	194.19	14.0	-0.07	$2.16x10^4$	741 to 7762
PCPs	Preservative	Butylparaben	$C_{11}H_{14}O_3$	94-26-8	194.23	8.47	3.57	$2.07x10^2$ **	520
		Propylparaben	$C_{10}H_{12}O_3$	94-13-3	180.2	8.5	3.04	$5.00x10^2$	290
		Ethylparaben	$C_9H_{10}O_3$	120-47-8	166.17	8.34	2.47	$8.85x10^2$	119 to 209
		Methylparaben	$C_8H_8O_3$	99-76-3	152.15	8.5	1.96	$2.50x10^3$	87
		Benzylparaben	$C_{14}H_{12}O_3$	94-18-8	228.24	-	-	-	-
	Agent bacteriostatic	Irgasan/Triclosan	$C_{12}H_7Cl_3O_2$	3380-34-5	289.5	7.9	4.76	10.00 **	3500 to 20000
Sterol	Hormone/Contraceptive	Ethinyl Estradiol	$C_{20}H_{24}O_2$	57-63-6	296.4	-	3.67	11.3 ***	510
	Hormone	17-Estradiol	$C_{18}H_{24}O_2$	50-28-2	272.4	10.46	4.01	3.90 ***	30000
		Estrone	$C_{18}H_{22}O_2$	53-16-7	270.4	-	3.13	30	457 to 18,000
	Phytoesterol	Stigmasterol	$C_{29}H_{48}O$	83-48-7	412.7	-	9.43	$1.12x10^{-5}$	$5.4x10^5$
		β-Sitosterol	$C_{29}H_{50}O$	83-46-5	414.7	-	9.65	10	-
		Campesterol	$C_{28}H_{48}O$	474-62-4	400.7	-	9.16	-	-
	Fecal Sterol	Cholesterol	$C_{27}H_{46}O$	57-88-5	386.7	-	8.7	0.095 ****	16,000
		Coprostanol	$C_{27}H_{48}O$	360-68-9	388.7	-	8.82	-	-
		Epicoprostanol	$C_{27}H_{48}O$	516-95-0	388.7	-	8.82	-	-

SOURCE: https://pubchem.ncbi.nlm.nih.gov/

NOTE: - no information; * solubility in $mg.L^{-1}$ at 25°C; ** at 20°C; *** at 27°C; **** at 30°C

LEGEND: CAS - Chemical Abstracts Service; pka - coefficient of acid dissociation; Koc - partition coefficient between organic carbon and water; Kow - partition coefficient between octanol and water

2.3.4 INORGANIC ELEMENTS (IES) OR METALS

Inorganic elements are those that do not contain a carbon-to-carbon or carbon-to-hydrogen bond, and generally have mineral origin (VALLERO; LETCHER, 2012; SPEIGHT, 2017). Their structure is generally formed by ionic bond and do not contain carbon chemically bound to hydrogen, also being an essential component of life. In other words, they are not organic compounds and usually called as 'metals'. There are three main categories to arrange these elements, considering their physical and chemical properties, which are: (i) metals, (ii) metalloids, and (iii) non-metals (SPEIGHT, 2017).

Groups 1 and 2 of the periodic table are named, respectively, alkali metals and alkali earths, which includes, for example, sodium (Na), potassium (K), calcium (Ca) and magnesium (Mg). Groups 3 to 12 are the transition metals, which includes, for example, iron (Fe), zinc (Zn) and mercury (Hg), and in groups 13 to 15 there are other metals, such as aluminium (Al) and lead (Pb). Metals are good conductors with high density and melting point. In the same groups 13 to 15, there are elements named metalloids, as for examples boron (B), silicon (Si) and arsenic (As). This category represent semimetals that can not be well defined as either metal or non-mental. In groups 14 to 17 of the periodic table, there are non-metals, such as C, N, P, O and chlorine (Cl). Non-metals are poor conductors with low density and melting point. Finally, in the group 18 there are the noble gases, for example, helium (He) and argon (Ar).

Some of the metals are present in Earth´s crust in abundance, being considered major and/or essential elements. Oxygen and silicon are the two most common elements, however not considered as metal. Therefore, the six most common metals in the Earth's crust in order of abundance are Al, Fe, Ca, Mg, Na and K. Others elements can be considered as trace elements, because they are found naturally in very low concentrations. If the naturally concentration of some metals is exceeded, they can be extremely toxic to flora, fauna and human environment. For example, N - P - K - Mg - Ca - Na - Cl are essential elements necessary for life processes; Fe - copper (Cu) - Zn - manganese (Mn) are also necessary for life processes, but considered trace elements; Al - barium (Ba) are non essential elements for the life processes, and cadmium (Cd) - Pb - Hg are elements which produces disturb function, being considered toxic (SPEIGHT, 2017; ALVAREZ-CAMPOS; EVANYLO, 2020).

Trace elements, as mentioned, are elements found at very low concentration in soils, plant, and natural waters, lower than 1 $mg.L^{-1}$ (dissolved form), and lower than 100 $mg.kg^{-1}$ (solid form) (ALVAREZ-CAMPOS; EVANYLO, 2020; GAILLARDET; VIERS; DUPRÉ, 2003; ZULIANI et al., 2017). They can be naturally presented in the environment or can be introduced by human activities. In natural water system, trace elements can play a major role in hydro system, due to the potential for accumulation and toxicity. The natural occurrence of them in rivers is dependent of the abundance in the continental crust and capacity of mobilization (GAILLARDET; VIERS; DUPRÉ, 2003). Therefore, to determine trace elements behavior in the system it is fundamental to know geological processes.

According to Gaillardet, Viers and Dupré (2003), these elements are much more fractionated by weathering and transport processes than major elements, being very useful to understand nature and intensity of weathering plus transport processes. Besides that, human activities also contribute to increase of inorganic elements in the aquatic environment. Some examples are mining, industrial emission, urban runoff, waste, wastewater and leachate, vehicular particles and emission, co-products of the agriculture practices, deposition and others (ALVAREZ-CAMPOS; EVANYLO, 2020; HAYGARTH; JARVIS et al., 2002; ARAUJO; MAIA, 2008; ZULIANI et al., 2017).

Many of these elements exist in the environment in a valence state (VALLERO; LETCHER, 2012). The elements in groups 1 and 2 of the periodic table have tendency to form silicates or oxides. They include the macro-nutrients Ca and Mg, which have their sulfide and hydroxides with more soluble

capacity. Moreover, Ca and Mg, have highly mobility capacity in river waters. In other perspective, elements in groups 3 to 16 of the periodic table have with tendency to form silicates or oxides and sulfide minerals (if there is sulfur available). They include the micro-nutrients as Cu, Zn and Fe, which have their sulfides and hydroxides with less soluble capacity. In elements of this groups, capacity of mobilization in water rivers is reduced, for example: Cu and Ni have moderate mobility with, approximately, 10 times less than Ca and Mg; Zn and Pb have mobility 10 to 100 times less than Ca and Mg, being considered non-mobile in water rivers; and the most immobile elements have mobility more than 100 times lower than Ca and Mg (GAILLARDET; VIERS; DUPRÉ, 2003; SPEIGHT, 2017). pH and Eh are the most important factors which govern the metals mobility in solution, and must be considered (LICHT, 2001). Therefore, toxicity, persistence and fate are determined considering the equilibrium chemistry of each element (VALLERO; LETCHER, 2012).

In water, trace elements, in the ionic form, are rarely found in significant concentration, due to the transport with flow or water-sediments processes, which favor the decreasing of these dissolved elements in water (PITRAT, 2010). There are some physical-chemical transformation that these inorganic elements (or 'metals') can suffer (BAIRD; CANN, 2011; LANGMUIR, 2004), such as:

- **Complexation:** is the arrangement between cation and anion both in solution at the surface of minerals and/or organisms, making a complex. They can be colloidal or solids particles, generally insoluble and less bioavailable, which can remain suspended in water column or precipitated to the sediment. Moreover, pH have a important role in metal complexing, because favor complexation in pH above 6-8;
- **Adsorption:** is the free ion sorption onto the minerals´ surface or organic matter. In the porous media, the most important sorbent for metals are clay minerals, organic matter and oxyhydroxides of Fe and Mn. The adsorption is proportional to surface area, surface site density, and dependent of the pH;
- **Precipitation:** occurs when concentration of the element exceed the solubility products of their pure metal solids, and thus, to precipitate. After precipitation, further increase in concentration of the metals is limited;
- **Bioconcentration:** occurs when an organic specie lives in a water contaminated by dissolved elements, concentrating the element diffusion process. For example, a fish that lives in a river contaminated with metals, will be metals concentrated in their body. Bioconcentration affect all aquatic species, and depends on the animals' ability to metabolize a given substance;
- **Biomagnification:** it is the increase of a given substance along the food chain. This processes is a sequence of several steps of bioconcentration. Mercury is the best known example of biomagnification;

In general, trace elements are frequently adsorbed in the particles surface, mainly the organic which are dissolved in water as a free ion. Eventually, particles will sediment being deposit in the bottom of rivers bank or lakes, and covered by other sedimented particles. This effect represent an water purification stage, considering that toxic or potential toxic elements will be inert in the sediment. However, an resuspension of them or a more recently sediment deposited associated to some physical-chemical conditions can favor desorption process, making those elements available again. Therefore, to know the nature of the aquatic system, details of their condition and processes is important to understand how they work (BAIRD; CANN, 2011).

Some metals, such as Ca and Mg, may be present in water as Ca^{2+} and Mg^{2+} ions. These ions are the most commonly found in unpolluted natural waters that have limestone characteristics, along

with bicarbonates. The Mg^{2+} ion is derived from dissolution of $MgCO_3$, while the Ca^{2+} is derived from the dissolution of $CaCO_3$ rocks (BAIRD; CANN, 2011).

In environmental studies, metals are evaluated considering their occurrence in controlled storm urban runoff (LIU et al., 2018; JEONG et al., 2020), qualitative analyzed in sediments (ZULIANI et al., 2017; XIA et al., 2020) , lake (NICOLAU et al., 2012; GASIM et al., 2013) and rivers (SANTOS; LENZI; COELHO, 2008; CHIBA et al., 2011; HAZARIKA; KALITA, 2020). Moreover, there are some studies which observed metals behavior during rainfall episodes (PALLEIRO et al., 2012; YANG et al., 2013; MATSUNAGA et al., 2014; ZHANG et al., 2018a; GAO et al., 2019; LINDFORS et al., 2020) or in rainwater (FONTENELE; PEDROTTI; FORNARO, 2009). Generally, studies consider trace metals (recurrently named as heavy metals) in road surfaces.

In Liu et al. (2018) study, it was simulated an rainfall episodes with four different intensities (25 to 83 mm/h) combined with five rainfall duration (6 to 36 min), in order to identify and quantify wash-off contributions from road surfaces. The study also linked metal sources with rainfall characteristics and human health risk. The experiment was performed in two sites in Gold Cost (Australia), with residential and commercial land use, and high traffic volume, around 3000 vehicles per day. It were selected Na, Mg, Al, K, Ca, V, Mn, Fe, Ni, Cu, Zn, Mo, Cd and Sn for samples collected from commercial area, while just Na, Mg, Al, Ca, V, Fe, Cu and Zn were selected for residential area. Results showed three main sources of metals contribution, which were i) sea salt, related to metals Na, Mg, K and Ca, with 65% of apportionment in both sites, ii) soil, related to metals Al, Mn and Fe, with 23% and 18%, respectively for commercial and residential areas, and iii) traffic (tyre and brake wear), related to metals Ni, Zn, Mo and Cd with respectively 12% and 17%, respectively for commercial and residential areas. The authors highlights that sea salts provide the highest contribution during wash-off in the both sites, however these contribution decrease with the rainfall intensity increase, indicating that dilution effects took place in the process and sea salt was limiting sources. Therefore, the concentration of sea salts during rainfall episodes were dependent of the prior availability (or build-up period/antecedent dry periods) than transport capacity of runoff (or rainfall intensity). For the human health assessment, metals sources from soil (Fe, Al and Mn) and traffic (Ni, Cu, Zn, Cd, Pb and Cr) showed risks, with changing rainfall characteristics. Therefore, for the human health benefits, rainfall with longer duration are better to decrease risks, due to decrease of metals availability. The authors attributed this result to the first-flush phenomena, which is capable of wash-off the higher amount of pollutants at the beginning of the event (higher human risk), followed by dilution effects intensified during longer rainfall, reducing, therefore, human risks.

In similar perspective, but observing metals distribution in road surfaces considering natural rainfall episodes, Zhang et al. (2018a) study aims to characterize spatially and seasonally of heavy metals on Dakan River (China), in order to conduct quantitative sources apportionment using mass balance models, and to propose management strategies to control fluvial heavy metals pollution for aquatic environment protection. Samples were collected manually from the river (eight sites) and from runoff generation (five sites) during eight rainfall episodes. The metals analyzed were Mn, Cu, Zn, Ba, Pb, Cr, and Ni. Results showed a gradual increase of metals concentration as the river flowed through the urban area, indicating the influence of anthropogenic activities on river pollution. Moreover, the authors highlight that downstream river, heavy metals concentration had relatively high concentration which were associated to the heavy traffic activities and intense industrial production. Therefore, occurrence of heavy metals were significantly correlated to the land use of the study area. Mass balance model corroborate the results, showing that industrial runoff (industrial residues, roof erosion, and traffic activities) contributes with high proportion of heavy metals load (approximately 16% to 45%). The authors highlight that this industrial area of the study should be given special attention to reduce its contribution to the heavy metals load of the studied river. In comparison, residential runoff and municipal wastewater load were

relatively low. The proposed strategy to reduce fluvial metals loads in the river systems, the authors suggest coupling "sources elimination" and “transport barriers” to the source apportionment.

2.3.5 SUMMARY

In this section it was possible to identify many water quality parameters groups that can be analyzed in NPS studies. Each parameter or set of parameters provides specific information about the dynamics of pollutants during rainfall events. Therefore, the choice of the best set or the best parameter is extremely dependent on the purpose of the monitoring. Meyer et al. (2019) highlights that combined inspection of the water quality parameters can bring out duration, intensity and origin of the most pollution impacts in a river system (MEYER et al., 2019). Moreover, in rainfall studies it is essential the association with hydrological characteristics responsible to induce washing-off and transports.

In this thesis, it was chosen to study four distinct sets of parameters, based on the premise that the environment is not in itself described by a single variable, but for multiple integration of phenomena and elements, and to properly address the presented general goal and hypothesis. Thus, conventional parameters, such as nitrogen, phosphorus, carbon and solids, reflects the traditional understanding of the system, with the analysis of parameters usually used, better known and which are considered in the water resources legislation.

The organic matter evaluation is an evolution of the conventional parameters, where it is possible to investigate specific molecule behavior, pattern and dynamics. The occurrence of labile and/or refractory characteristics can be associated to the occurrence, affinity and availability of others elements, as well as, specific process in the water body (as erosion process). Emerging contaminant and metals are unconventional parameters to assess non point sources as proposed in this thesis. Therefore, these two set have opposite purpose, because emerging contaminant can help to understand the point sources of pollution with elements which are exclusively from human activities, while inorganic elements or metals can help to understand the non point sources and process of pollution with elements which are predominantly from the natural sources or geological formation.

2.4 WHERE ARE WE?

Facing to these three main conceptual aspects involving NPS studies, this study focus in integrating all considerations to a specific and unique discretization, that consists of collecting samples as the runoff hydrograph and performing their characterization with water quality data for two monitoring sites.

It was presented how hydrological process influenced water quality changes into the river system. Besides that, transport plume along the river can change as consequence of land use. Many studies mentioned distinct monitoring strategies, since high-frequency resolution ("movies") until ’snapshot’ traditional sampling ("photos"), and different approach to evaluate the process, spatially or temporally, considering seasonal variations, observing rainfall influences or just the relationships between land use and water quality. Therefore, it is known that each rainfall event with their specific conditions creates inimitable quali-quantity conditions into the river (BARBOSA; FERNANDES; DAVID, 2012), making right monitoring strategies essential.

Table 6 summarizes previously researches focused on strategies to monitoring water quality in rivers and proper assessment. The conventional strategy for assessment is based on spatial distribution, with many monitoring sites selected on the study area. Interestingly, this kind of strategy is performed,

generally, with manual or field campaign with low frequency, as for example: each 3 or 4 months, seasonal, just during rainy or dry season, or even isolated campaigns.

When this kind of strategy is improved, the use of sensors increases. However, it is necessary financial support to build structure and provide adequate maintenance for the equipment. In this scenario, generally, the quantity of monitoring sites decrease, being studies focused on specifics research questions, as for example: (i) to investigate how storm flow hydrochemical transport varies in relation to catchment hydrogeology, rainfall duration and extremes, antecedent conditions, land use or management and season (LLOYD et al., 2016); (ii) to understand the correlation between the variability of the pollutants concentrations and the number of events required to adequately estimate pollutant concentrations (MCCARTHY et al., 2018).

Also, it is possible to use both strategies, conventional and sensors. In this context, the number of monitoring sites is dependent of the monitoring purposes. Generally, the sensors or multi parameter probe are used to measure WQP, such as OD, EC, WaT, and pH, being chemical parameters, as TN, PT, and COD, assessed by conventional analytical procedures in the laboratory after manual water sampling, being possible to increase monitoring sites number. In some studies, as Bieroza and Heathwaite (2015), Bowes et al. (2015) it were used water quality high-frequency sensors to quantify, respectively, TP and TRP, and N-NO_3^- and TRP, and the manual sampling were performed weekly to guarantee and to check the analysers performance.

Finally, automatic samplers use has been increased along the years, mainly due to the technical advances on the equipment. Thus, it can be observed that studies which consider rainfall occurrence had less monitoring sites, but more temporal discretization on a single monitoring site (GOULART, 2017; GRUDZIEN, 2019; DRUMMOND, 2020), due to the high laboratory demands or to specific research questions, such as, to identify output fluxes in different land uses (NÓBREGA et al., 2018), or to determine temporal patterns of P dynamics (BENDER et al., 2018). Furthermore, there are few studies which consider multiples monitoring sites, rainfall episodes, and land use changes impacts in a integrative way, in order to estimate quali-quantitatively land use influence during rainfall episodes.

Then, considering this lack of information, monitoring program to assess NPS pollution based on rainfall episodes should be focused on integrating quality and quantity strategies. Barbosa, Fernandes and David (2012) affirms that for this kind of watershed management several samples need to be collected at different times in order to learn the changes along the event. Consequently, strategies must be considered at decisions levels, political and socially (BARBOSA; FERNANDES; DAVID, 2012), and a clear understanding will help to make decision on water resources management strategies. Therefore, it is important to contemplate these aspects together, in order to assess properly water quality and to determine NPS pollution, sources or pathways.

Shen et al. (2020) suggests a general NPS monitoring strategy in order to provide a bases for environmental management decisions. The authors highlight six main steps, which are: 1) research area investigation, to consider the multiples NPS pollution sources of the watershed; 2) geo-processing data, to understand pollution sources-transport pathways-receiving waters; 3) selection of monitoring points; 4) to establish conditions for monitoring purpose and objectives of the NPS assessment; 5) data collection and analysis; 6) NPS pollution assessment. Another specific recommendations are related to the monitoring sampling (manual or automatic ones) and monitoring point layout (input and output) which corroborate with the objectives proposed in this thesis.

Automatic samplers working with water level variation is able to estimate first-flush contribution and produces a hydrograph discretization, being possible to understand how rainfall characteristics influence on the pollutant carry, as observed in Bender et al. (2018), Kozak et al. (2019), Grudzien (2019),

Table 6 – Monitoring details from previously studies of water quality in rivers

Sources	Monitoring Strategy	Monitoring Sites	Frequency	Sampling
Zhou et al. (2016a)	Conventional	139	Dry season	Manual
Garrido et al. (2016)		6	Single	Manual
Ding et al. (2016)]		56	Baseflow	Manual
Zhou et al. (2017)		4	Rainfall	Manual
Wang et al. (2017)		29	Baseflow	Manual
GOULART (2017)		2	24hr in baseflow	Manual
Oliveira, Maillard and Pinto (2017)		17	Each 3 months	Manual
Ide et al. (2017)		16	Season	Manual
Zhang et al. (2018a)		13	Rainfall	Runoff
Mamoon et al. (2019)		6	-	Rainfall Simulator
Xie et al. (2019)		1	Rainfall	Manual
Wise et al. (2019)		1	Rainfall	Manual/Runoff
Shi et al. (2020)		32	Season	Manual
Reichert et al. (2020)		11	Season	Manual
Bowes et al. (2015)	Sensor	1	Weekly*	HF
Viswanathan, Molson and Schirmer (2015)		1	Season	24 hr
Lloyd et al. (2016)		2	n.m.	HF
Bauwe et al. (2015)		3	Rainfall	HF
McCarthy et al. (2018)		7	Rainfall	HF
Meyer et al. (2019)		8	Continuous	Trailer Multiparameters
Bieroza and Heathwaite (2015)	Conventional and sensor	1	weekly*	Manual and HF
Yu et al. (2016)		44	2 per year	Manual
Wang et al. (2017)		29	1 campaign	Manual
Corada-Fernández et al. (2017)		29	Dry and Rainy	Manual and HF
Barbosa et al. (2018)		38	Season	Manual
Frank, Goeppert and Goldscheider (2018)		3	6-10 days	Manual and HF
Ma and Li (2020)		63	Season	Manual
Yang et al. (2015)	Automatic Sampler	1	Rainfall	HF
Kozak (2016)		1	Rainfall	HF
Blaen et al. (2016)		4	Rainfall	HF
Bender et al. (2018)		1	Base and Rainfall	
Nóbrega et al. (2018)		4	Base and Rainfall	
Zhang et al. (2018b)		10	Continuous	Manual and HF
Grudzien (2019)		1	Base and Rainfall	HF
Drummond (2020)		1	Base and Rainfall	HF
Wang et al. (2020)		1	Rainfall	HF
Imfeld et al. (2020)		1	Rainfall	Runoff
Lindfors et al. (2020)		3	Rainfall	Runoff

Drummond (2020). Aspects as 'where the pollution comes from?", impact caused for changes in land use, river response, loads input and impacts, as well as other hydrological aspects on pollution carrying must be assessed in a integrative way. Moreover, the process inside control volume, such as pollutant plume transportation, advective and diffusive process are all influenced for the environment and watershed condition and it was not properly addressed.

In this sense, Table 7 presents the main characteristics of some state-of-art studies involving water quality in rivers during rainfall episodes. The characteristic includes study area and monitoring

strategy aspects, and WQP considered in each study. It can be observed that actual research involves study areas with high amplitude of areas and distinct land uses. There are many studies which use probes to collect water quality information, and less which use automatic sampling, being manual sampling the most common until nowadays. Thus, considering the WQP, it is defined a precise set of parameters associated to the research objectives, as for example, metals assessment in urban areas (ZHANG et al., 2018a; LINDFORS et al., 2020), and/or occurrence of emerging contaminants in water systems due to WWTP existence (ZHANG et al., 2018b; DONG et al., 2019).

Thus, observing the state-of-art literature, there is a lot of knowledge about standards related to the land use, association with dry and rainy season, technological improvements in sampling, data acquisition and analytical procedures. However, there is lack of understanding about incremental area, hydrological characteristics and a wide range of water quality parameters. Therefore, the main gap observed on NPS assessment is related to this comprehension about processes and behavior based on event driven influence. To know how is the water quality standards through out two monitoring points in the same river, consecutively is the basis for the novelty of this research, and the difference between these sites represent incremental area impacts on the water quality for potential influences from NPS. These differences can have important influence on water resources management improvement, mainly because these results serve for optimization and calibration of mathematical modeling. Additionally, identifying singularities based on different set of water quality parameters, beyond traditional WQ parameters, such as emerging components, inorganic elements and the molecule response to rainfall events, is few explored on the literature, and complement the contribution of this research.

Table 7 – Similar studies which evaluated organic matter contribution during rainfall episode

		Bauwe et al. (2015)	Yang et al. (2015)	Blaen et al. (2016)	GOULART (2017)	Frank, Goeppert and Goldscheider (2018)	Zhang et al. (2018a)	Zhang et al. (2018b)	Nóbrega et al. (2018)	Bender et al. (2018)	Kozak et al. (2019)	Grudzien (2019)	Dong et al. (2019)	Imfeld et al. (2020)	Ma and Li (2020)	Lindfors et al. (2020)	Drummond (2020)	Kozak (2020)
Study Area	Area (km^2)	15.5	0.23	3.5-1,008	260	n.m.	n.m.	n.m.	0.23-0.93	1.23	260	217	4,053	0.43	58,000	n.m.	217	260
	Predominant Land Use	A	F	n.m.	UA	P	A/UA	n.m.	R/P/C	A/F	A/F UA	R	F	A/F/P	Fa/F	UA	R	A/F UA
Monitoring Strategy	Monitoring Sites	3	1	4	3	3	8	10	4	1	1	1	8	1	64	3	1	2
	Are they consecutives	✗	-	✗	✓*	✗	✓*	✓*	✗	-	-	-	✓*	-	✓*	✗	-	✓ ✓
	Probes?	✓	✓	✓	✓	✓	✗	✓	✓	✓	✓	✓	✗	n.m.	✓	✗	✓	✓
	Automatic Sampler?	✓	✗	✗	✗	✗	✗	✗	✓	✓	✓	✓	✗	✓	✗	✓	✓	✓
	Rainfall Events Observed	212	2	6	✗	n.m.	7	n.m.	n.m.	8	5	9	3	78	n.m.	n.m.	10	8
	Hydrological Characteristics	✓	✓	n.m.	n.m.	n.m.	✓	✓	n.m.	✓	✓	✓	✓	✓	n.m.	✓	✓	✓
WQP	Conventional	✓		✓	✓	✓			✓	✓	✓						✓	✓
	Organic Matter		✓	✓	✓	✓			✓						✓			✓
	Emerging				✓			✓					✓					✓
	Metals						✓		✓			✓		✓		✓		✓

NOTE: * - consecutive monitoring sites with manual sampling and spatial assessment
LEGEND: n.m. - not mentioned; A - agriculture; C - cerrado; F - forest; Fa - Farmland; P - pasture; R - rural; UA - urban area

3 MATERIAL AND METHODS

> *"Engineering students undergo a much different form of training and education when compared with training to which the student of chemistry is subjected. The principles of chemistry can be used to develop how global sustainability can be supported and maintained. Also, it is important to increase awareness of the environmental impact of chemicals on the environment and develop an enhanced awareness of the importance of sustainable strategies in chemical research."*
>
> Speight (2017)

In this chapter will be presented tools and strategy used for the development of this thesis, as well as, study area and their characteristics. Moreover, will be present analytical procedures used to measure diverse types of water quality parameters. The sequence is: (i) Study Area; (ii) Hydrological Characteristics; (iii) Infrastructure; (iv) Control Volume and NPS Strategy; (v) Analytical Procedures.

3.1 THE BARIGUI WATERSHED

This study was developed at Barigui River Basin, which is a sub-basin located in the central of the Upper Iguaçu Watershed at Paraná State (southern Brazil), draining an area of approximately 260 km^2 and includes Almirante Tamandaré, Curitiba and Araucária municipalities (SUDERHSA, 2002). Barigui River has 67 km of extension (GONÇALVES, 2008)), crossing north to south until reaching the Iguaçu River at the right margin. Approximately, maximum altitude is 1,210m and the minimum is 864m above the sea level. It is located in Guabirotuba formation, at First Paraná Plateau. For this study, two monitoring sites along the Barigui River were defined, named as BA1 and BA2, as presented in Figure 12.

The monitoring site BA1 is located in Almirante Tamandaré city with UTM coordinates 671556 East and 7199322 North and drainage area of 58 km^2, representing 22% of the Barigui Watershed. At this monitoring site, river length is 14.8 km. The monitoring site BA2 is located downstream BA1, in the north of Curitiba city with UTM coordinates 670683 East - 7191046 North, drainage area in this point, considering BA1, is approximately 104 km^2. In BA2 river length is 32.8 km. Details of points and incremental area is presented in Table 8

Table 8 – Monitoring sites details: drainage area and river length

	BA1	Incremental Area	BA2
Drainage Area (km^2)	57.8	45.9	103.7
Proportion of the Basin (%)	22	18	40
River Length (km)	14.8	18.0	32.8

3.2 LAND USE

Land use classification was performed considering six main classes namely: (1) WATER - rivers and flood areas; (2) RESIDENTIAL URBAN AREA - high, intermediate and low urban condensation,

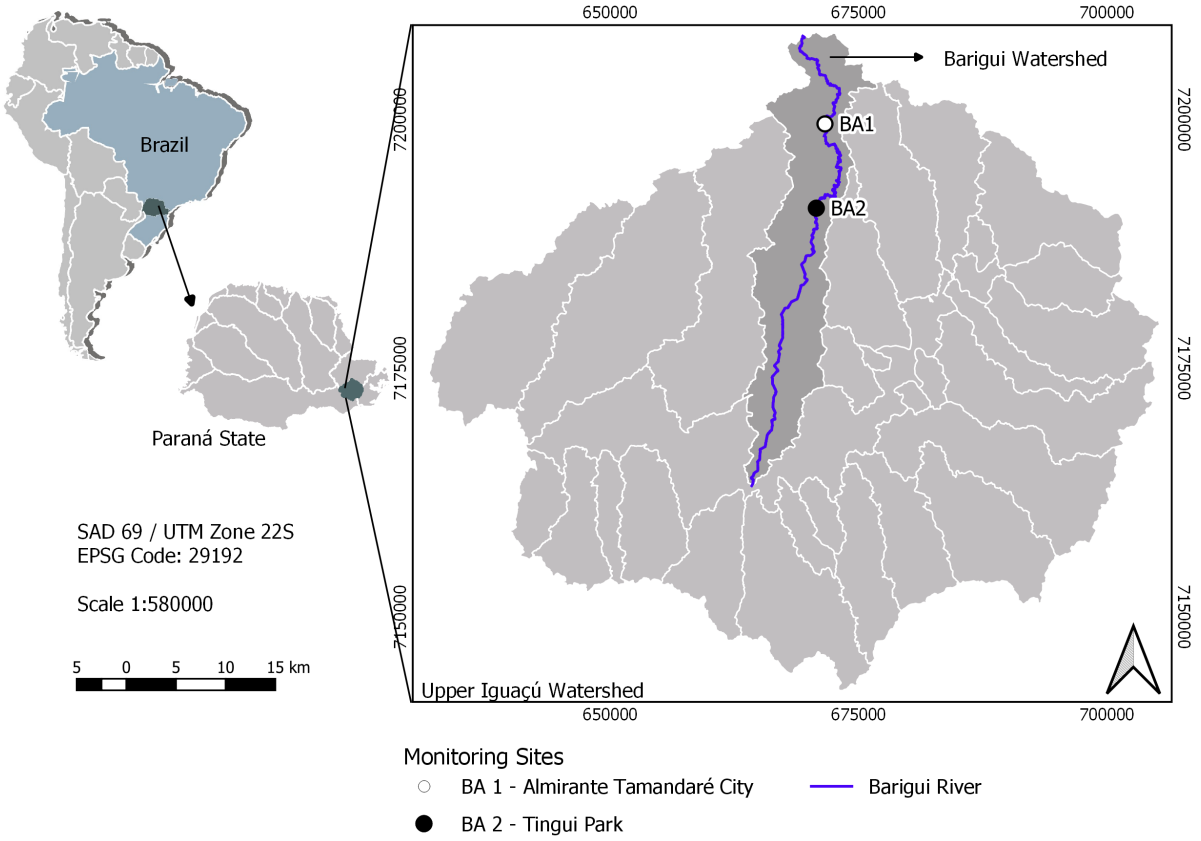

Figure 12 – Barigui Watershed and, BA1 and BA2 monitoring sites localization

allotment and villages; (3) INDUSTRIAL URBAN AREA - industrial area, landfill, warehouse and silos, farms and mining area; (4) PASTURE - fields and exposed soil; (5) AGRICULTURE - permanent and temporary cultures; (6) VEGETATION - natural and planted arboreal vegetation, and natural shrub vegetation. Figure 13 shows land use classification of Barigui Watershed.

Vegetation, residential urban area and pasture are the three main land use in this watershed, corresponding to 32.6%, 29.9% and 26.2% of the area, respectively. Industrial area and agriculture correspond to a smaller portion with 5.8% and 4.7% of the area (FERREIRA, 2016). These mixture of occupation has significant and distinct influences on the water quality dynamics of the river. At watershed downstream the level of water degradation is high (BRAGA, 2013), because of increasing urbanization pressure, as can be observed in Figure 13. However, BA1 and BA2 drainage areas represent the most preserved watershed portion. Figure 14 shows land use zoom for BA1 and BA2 sites. Table 9 summarize land use in BA1 and BA2, as well as, the incremental area between them, in terms of area and relative percentage.

Between BA1 and BA2 there is a WWTP, administered by SANEPAR. São Jorge WWTP has an grant of right to discharge 530 $m^3.h^{-1}$ - 24h (TAMANDARÉ, 2015). According to ANA (2017), São Jorge WWTP assisted approximately 34 thousand people in 2013, and works based on 85% of efficiency. Treatment process is anaerobic reactor type UASB followed by physic-chemical processes. The main affluent characteristics are: flow 48.3 $L.s^{-1}$, DBO load of 1,797.9 kg $DBO.dia^{-1}$ and discharged load of 269.7 kg $DBO.dia^{-1}$. The reference flow is 347.1 $L.s^{-1}$ (). This portion of Barigui River is classified as Class 3 (COLIAR, 2013)

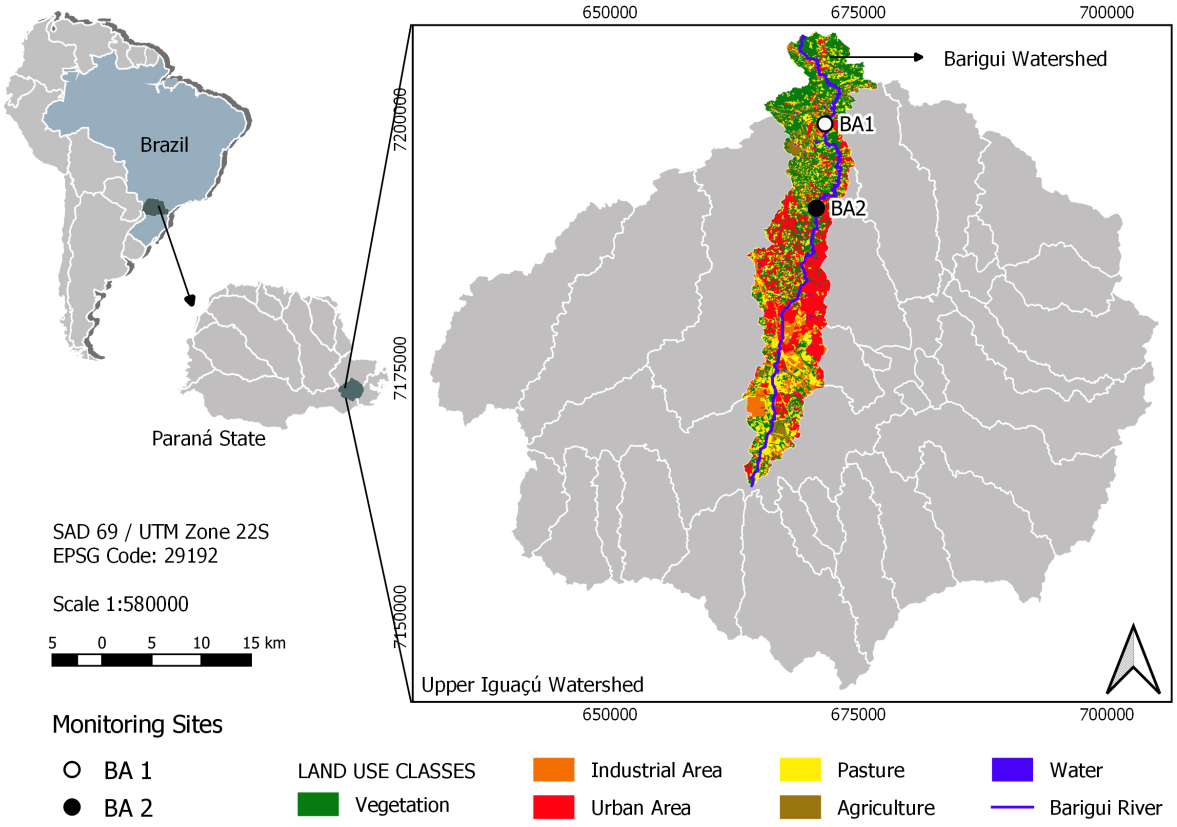

Figure 13 – Land use classification for Barigui Watershed

Table 9 – Land use and soil occupation in two monitoring sites in River Barigui

	BA1		Incremental		BA2		Changes
	Km^2	%	Km^2	%	Km^2	%	
Water	0.41	0.71	0.40	0.87	0.81	0.78	↑ 0.16
Residential Urban Area	3.44	5.94	10.60	23.10	14.03	13.54	↑ 17.16
Industrial Urban Area	0.84	1.45	0.59	1.28	1.43	1.37	↓ 0.16
Pasture	14.02	24.24	11.19	24.39	25.20	24.31	↑ 0.15
Agriculture	3.24	5.61	4.74	10.33	7.98	7.70	↑ 4.72
Vegetation	35.87	62.05	18.36	40.02	54.23	52.30	↓ 22.02
Total	**57.81**	**100.00**	**45.87**	**100.00**	**103.68**	**100.00**	

SOURCE: Adapted from (GONÇALVES, 2008; FERREIRA, 2016)

3.2.1 GEOLOGY

The geologic formation of the soil on the Curitiba region is composed by tertiary clastic sediments of the Guabirotuba formation, represented by gravel, sand, arches, silts and clays. The soil have a deep, mature and fertile profile. It can be found podzolic and red latosols soils, but also cambisols and litosols soils (MINEROPAR, 2005). According to MINEROPAR (2005), monitoring sites BA1 and BA2 have influence of North Argisol, South Latossol and Cambissol soils. Figure 15 shows geological formation of the soils under BA1 and BA2 monitoring sites.

Therefore, BA1 is located under *Cambissolo Háplico Tb distrófico típico* (CXbd) soil, receiving influence of the *Latossolo Bruno distrófico úmbrico* (LBd) soil, while BA2 is located under *Latossolo*

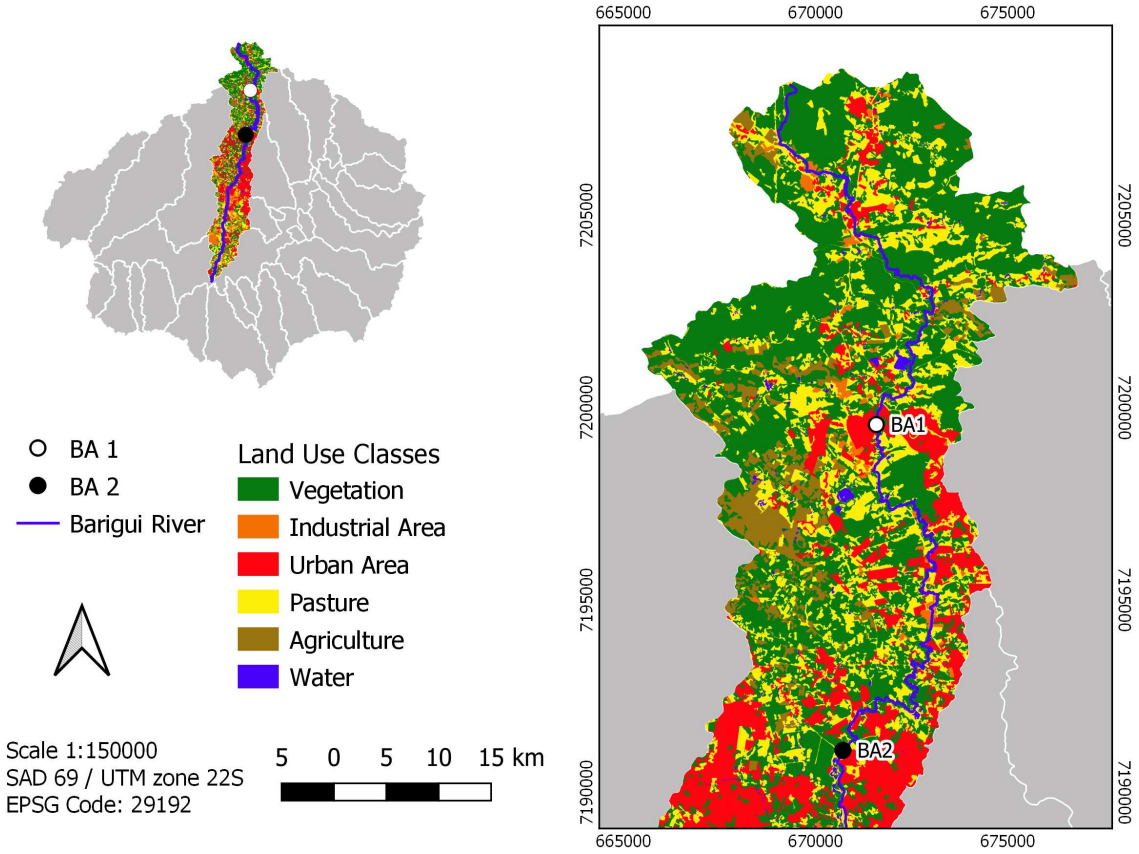

Figure 14 – Land use classification zoom for BA1 and BA2 drainage areas

Bruno distrófico cambissólico (LBdc) soil, receiving influence of the *Argisolo Vermelho-Amarelo distrófico úmbrico* (PVAd) (SANTOS et al., 2018). The main chemical characteristics of these kind of soils is summarized in Table 10

Table 10 – Main chemical characterization of Latossol, Cambisol and Argisol soils

	Higher Occurrence	Lower Occurrence
Latossol	$Al_2 2O_3$ - MgO - $Al_{exchangeable}$ - $Fe_{extractable}$ - $H^+ + Al^{3+}$	CaO - $Ca/Mg_{assimilable}$ - $Mn_{extractable}$ - Cu, Fe_2O_3, Mn, $Cu_{extractable}$
Argisol	Fe_2O_3 - Mn - $Al_{exchangeable}$ - $Mg_{assimilable}$ - CaO - Cu - MgO - $Ca_{assimilable}$ - $/Cu_{extractable}$ - $H^+ + Al^{3+}$	$Mn_{extractable}$ - $Al_2 2O_3$
Cambisol	$Mn_{extractable}$	CaO - Mn - $Al_{exchangeable}$ - $Mg/Ca_{assimilable}$ - $Al_2 2O_3$ - Cu - Fe_2O_3 - MgO - $/Fe_{extractable}$ - $H^+ + Al^{3+}$

SOURCE: Adapted from (MINEROPAR, 2005)

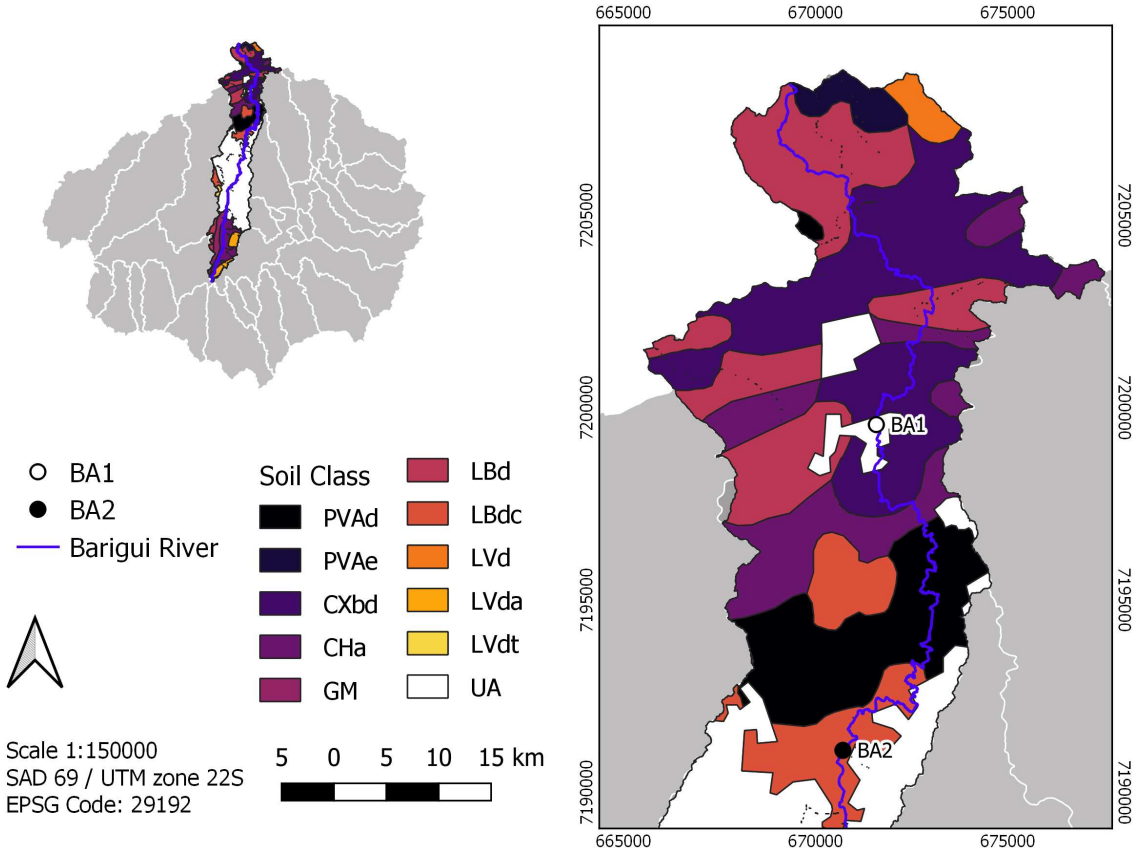

Figure 15 – Soil classification on the BA1 and BA2 monitoring sites

LEGEND: PVAd - Argissolo Vermelho-Amarelo Distrófico Úmbrico; PVAe - Argissolo Vermelho-Amarelo Eutrófico típico; CXbd - Cambissolo Háplico Tb distrófico típico; CHa - Cambissolo Húmico Alumínico típico; GM - Gleissolo Melânico Indiscriminado; LBd - Latossolo Bruno Distrófico Úmbrico; LBdc - Latossolo Bruno Distrófico cambissólico úmbrico; LVd - Latossolo Vermelho Distrófico Úmbrico; LVda - Latossolo Vermelho Distrófico argissólico; LVdt - Latossolo Vermelho Distrófico típico; UA - Urban Area

3.3 HYDROLOGICAL CHARACTERISTICS

The Barigui watershed is located in a sub-tropical region, with Cfb Köppen classification, indicating temperate weather, with mild summer. In general, rainfall are equally distributed, without defined dry station. Annual average temperature range between 16.1 to 18 °C, with maximum values between 23.1 to 24 °C, and minimum values between 12.1 to 14 °C. Moreover, this region receive an average annual solar radiation of 13.1 - 13.5 MJ $m^{-2}.d^{-1}$, which in terms of insolation (sunny days) represent 22% of the year (approximately 79 days). Along the year, relative humidity is 80.1 - 85% with average precipitation of 1400 - 1600 mm, and average evapotranspiration of 800 - 1000 mm. (NITSCHE et al., 2019).

Figures 16 and 17 shows 2018 hydrograph for BA1 and BA2, respectively, and Table 11 summarize the rainfall monthly distribution and flow behavior along the year. It was possible to observe some contradictions in relation to amount of rainfall along the year. BA2 rainfall station may had underestimated precipitation levels in the beginning of the year, due to rainfall gauge blocked (red values marked).

In order to fix this problem, rainfall data at BA1 were collected in upstream pluviometric station which contributes in Barigui Watershed. This pluviometric station is located in Colombo municipality, managed by *Companhia Paranaense de Energia* (COPEL) with code identification 02549090, collecting

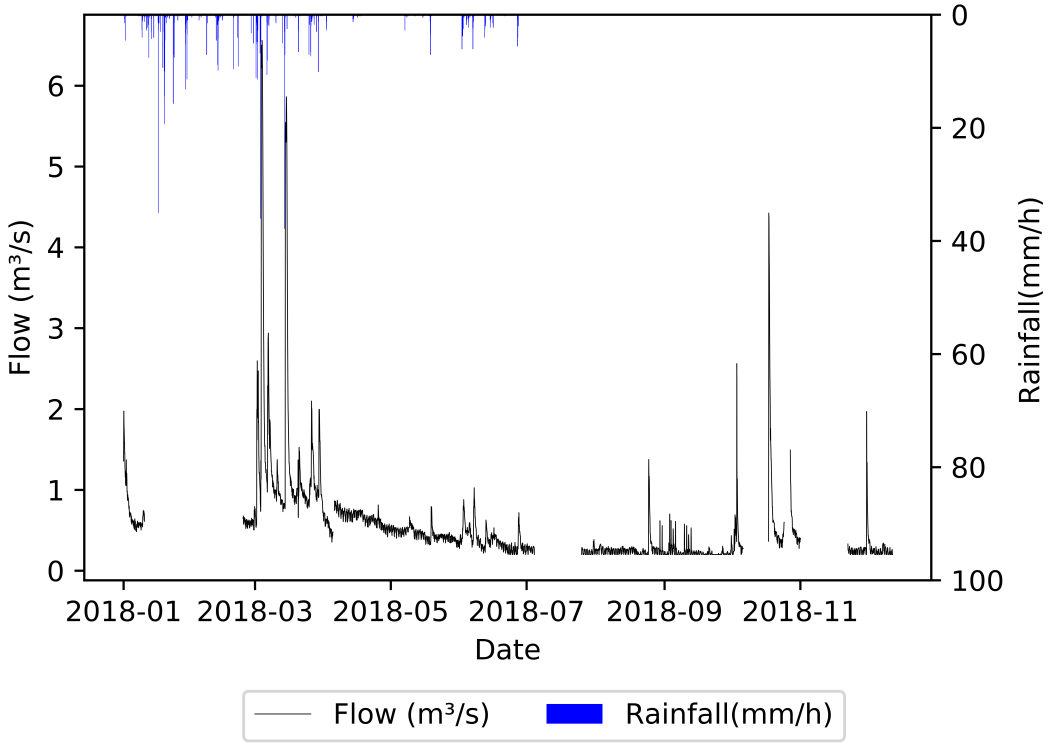

Figure 16 – BA1 hydrograph in 2018. Data used was collect from rainfall station located in BA1. White space represent lack of data

Table 11 – Total monthly precipitation and average monthly flow from BA1 and BA2 monitoring site during 2018.

	BA1		BA2	
	Rainfall (mm)	Flow (m^3 s^{-1})	Rainfall (mm)	Flow (m^3 s^{-1})
Jan	309.6	0.75	34.6	1.30
Fev	114.6	0.61	0.2	0.99
Mar	293.9	1.44	14.4	1.57
Apr	14.2	0.65	1.4	1.17
May	28.2	0.45	26.2	-
Jun	121.7	0.38	98.7	-
Jul	23.2	0.25	4.6	1.26
Aug	56.4	0.26	44.8	1.27
Sep	86.4	0.23	52.0	1.23
Oct	274.4	0.69	163.0	1.55
Nov	94.4	0.28	79.3	1.42
Dec	48.6	0.27	89.3	1.43
Total	1465.54		608.50	
Average		0.52		1.32

NOTE: The red rainfall values at BA2 corresponding to failed data due to gauge blocking during monitoring period. Missing flow data at BA2 during 2 months due to level sensor problems

rainfall data with a resolution of 15 minutes. The rainfall data at BA2 were collect from a metereological station located in Tingui Park (Curitiba municipality). The metereological station collect data of

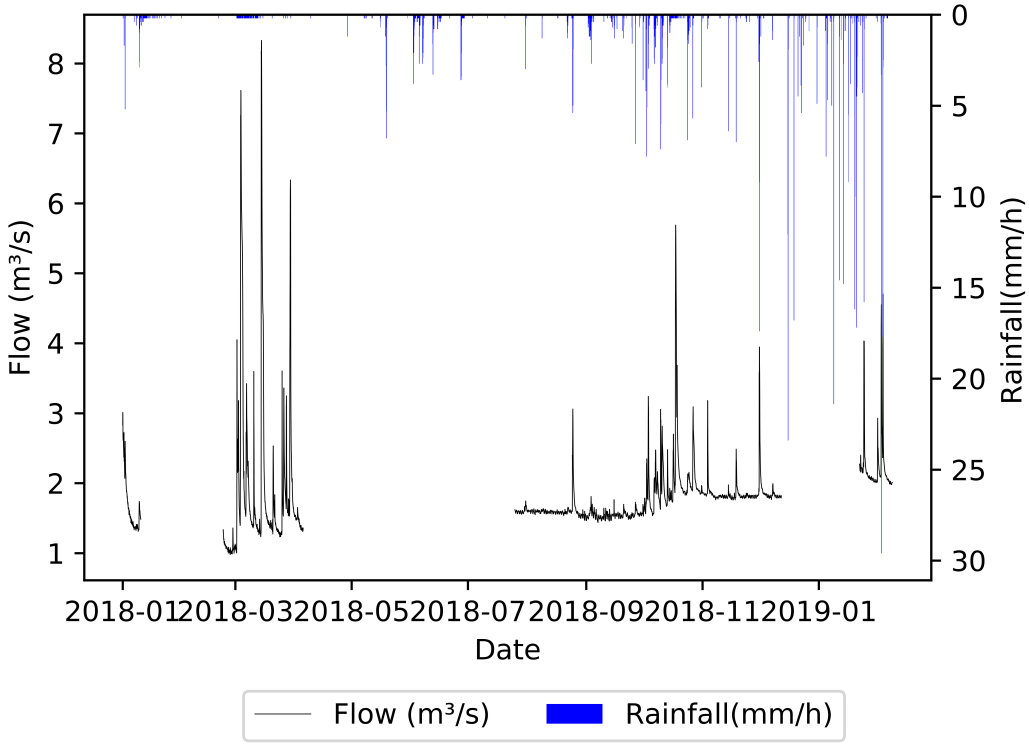

Figure 17 – BA2 hydrograph in 2018. Data used was collect from rainfall and meteorological station located in BA2. White space represent lack of data

air humidity and temperature, wind velocity and direction, solar radiation, atmospheric pressure, and precipitaion with a resolution of 15 minutes. Despite some operational issues during this research, it was possible to outline hydrological profile, which was very similar to the general determination above mentioned.

In general the summer season is the rainy period of the year, from October to March. In 2018, BA1 rainfall station registered 309.6 mm of rainfall in January, followed by 293.9 mm in March and 274.4 mm in October. BA2 also correspond to high amount of rainfall in 2018 October (163 mm). Furthermore, the intense rainfall occurred in 2018 March can be observed in maximum flow in BA2 (1.57 $m^3.s^{-1}$). Annual precipitation registered upstream Barigui watershed was 1465.54 mm which was dispersed downstream on Barigui river. Average flow observed was 0.52 $m^3.s^{-1}$ and 1.32 $m^3.s^{-1}$ respectively for BA1 and BA2. This distribution guarantee the representativeness of the hydrological regime, being possible identify diffuse pollution contribution in different conditions along the year.

Thus, hydrological characteristics are the hydrograph metrics, which indicate river´s response to the rainfall. These attributes can be divided in three main categories, based on the dominant hydrological factor, as (i) rainfall, such as amount, duration and intensity; (ii) flow, such as water level variations during a rainfall episode, flow variation and surface runoff; (iii) effects time metrics between the rainfall occurrence and river water level response. Besides that, antecedent dry periods also is an attribute associated to pollutant build- and wash-off in a watershed. All these characteristics are directly correlated to the land use. Figure 18 shows hydrological characteristics considered in this study.

According to the three proposed categories and additional attributes, hydrological characteristics can be summarized as:

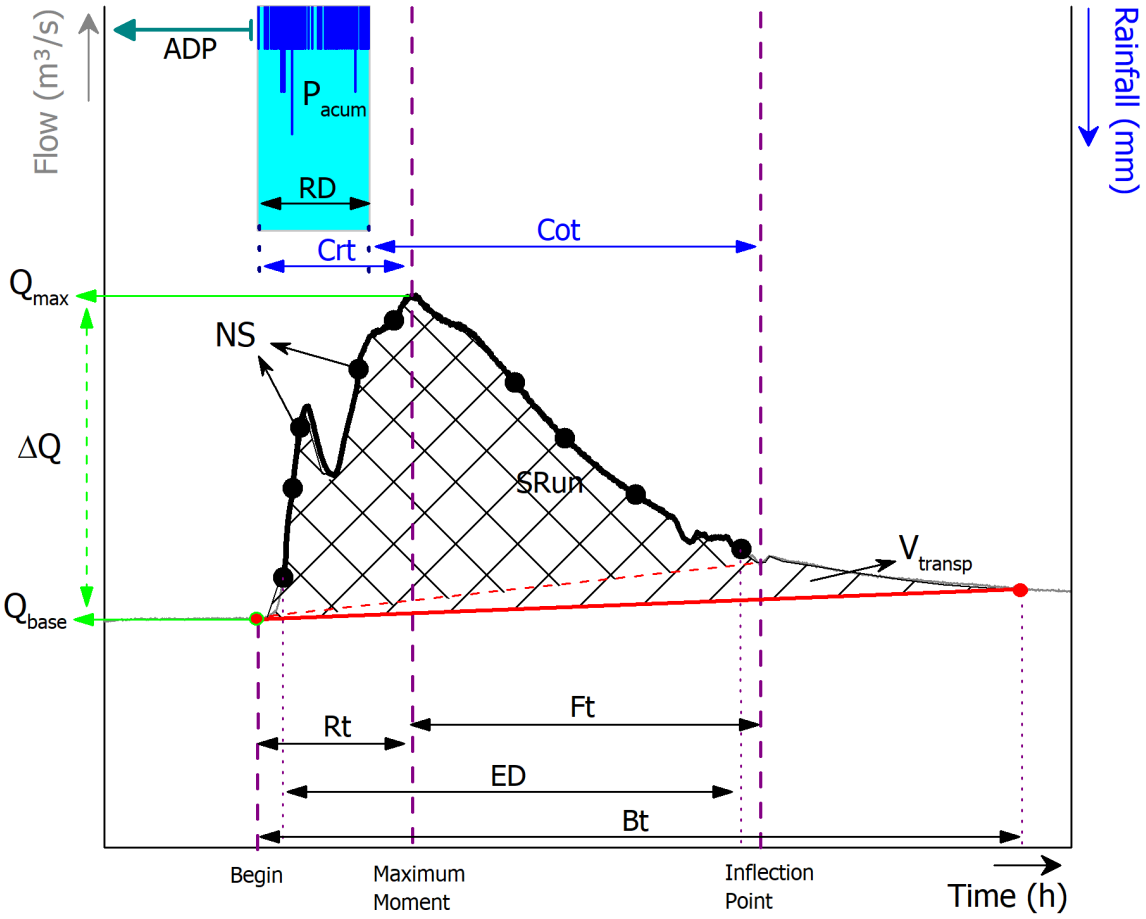

Figure 18 – Schematic representation of the hydrological characteristics calculated from hydrograph

1. **RAINFALL CATEGORY**

   - **Event Duration (ED)**: difference between the last and the first samples collected (hour);
   - **Rainfall Duration (RD)**: duration of the total precipitation observed (hour);
   - **Accumulated Precipitation (P_{acum})**: quantity of rainfall (mm);
   - **Rainfall Intensity (RI)**: ratio between P_{acum} and RD (mm hour^{-1});
   - **Rainfall classification (RClass)**: classification of the rainfall according to (WHO, 2008)

2. **FLOW CATEGORY**

   - **Transported Water Volume (V_{transp})**: amount of water transported during the rainfall event; area under flow curve, starting in the base flow condition before rainfall, and ending in the return to the base flow condition after the rainfall (m^3);
   - **Surface Runoff (SRun)**: amount of water transported during surface runoff condition, that is, when the infiltration capacity of the soil is reached; area under the flow curve, starting in the beginning at the flow rise and ending in the inflection point of the hydrograph (m^3);
   - **Base Flow (Q_{base})**: flow in the baseline condition before river response to the rainfall (m^3 s^{-1});

- **Maximum Flow (Q_{max})**: maximum flow measured during the rainfall episode ($m^3\ s^{-1}$);
- **Variation Flow (ΔQ)**: difference between Q_{max} and Q_{base} ($m^3\ s^{-1}$);

3. **EFFECTS**

- **Rising Time (Rt)**: time to the maximum flow observation, that is, difference between the moment of the Q_{max} and the moment of the Q_{base} (hour);
- **Falling Time (Ft)**: time to the inflection point, that is, difference between inflection point moment and the Q_{max} (hour);
- **Rising/Falling time (Rt/Ft)**: ratio between Rt and Ft;
- **Critical Time (Crt)**: time between the maximum flow observed and the beginning of the rainfall (hour);
- **Concentration Time (Cot)**: time between the hydrograph inflection point and end of the rainfall (hour);
- **Base Time (Bt)**: time to restore the usual base flow, that is, difference between base flow condition after the rainfall and Q_{base} (day);

4. **ADDITIONAL**

- **Number of Samples (NS)**: number of samples collected during the rainfall episode monitored;
- **Antecedent Dry Periods (ADP)**: quantity of days without an rainfall which causes water level variation (day);

The monitoring period for this study was between 2017 and 2019, with sample collection during rainfall episodes in August and October 2018 and April 2019. These data are presented in detail in the section 4.1.

3.3.1 RAINFALL EPISODES CLASSIFICATION - RECLASS

In order to facilitate the comparison between rainfall episodes monitored, an classification was proposed using three hydrological characteristics which are: 1) RI; 2)RD, and 3)ΔQ.

The values were parameterized adjusting proportionally all values considering the highest one measured. After this, weights of 1, 2, and 3, were attributed considering an division in three categories, respectively as low (0-33), medium (34-66), and high (67-100). The classification ranged between 3 to 9, where 3 was attributed to rainfalls with low RI, RD and ΔQ, and 9 was attribute to rainfalls with high RI, RD and ΔQ. The score classification is presented in the Table 12.

Table 12 – Rainfall episode classification according to RI, RD and ΔQ

Scores	3	4	5	6	7	8	9
RD	low	medium-to-low		medium	medium-to-high		high
RI	low	medium-to-low		medium	medium-to-high		high
ΔQ	low	medium-to-low		medium	medium-to-high		high

Thus, rainfall episodes could be interpreted with the same magnitude of impacts or occurrence.

3.4 MONITORING STRATEGY FOR NPS CONDITIONS

3.4.1 INFRASTRUCTURE

In BA1, there is a high-frequency pluviometric station. Level and precipitation data are collected at 1 minute intervals. These data is stored in SBn command control unit. Similarly, in BA2 there is the same infrastructure to collect water level variations with high-frequency. However, rainfall data for BA2 is collect by meteorological station some meters ahead, including: air temperature, wind velocity and direction, precipitation, solar radiation and atmospheric pressure at 10 minutes intervals.

Sampling strategy adopted to monitor NPS contribution is based on AMS, as defined by Blaen et al. (2016), Krause et al. (2015), using an automatic sampler (SBn), developed by Braga (2013). There is one equipment in each monitoring site. Each SBn has capacity to collect 24 sample bottles with one liter volume. SBn was build on Electronic Monitoring Lab (LME) at Federal University of Paraná. Figures 19 and 20 shows all infrastructure adapted to proceed this kind of monitoring strategy.

Figure 19 – Almirante Tamandaré monitoring point. (a) improvement in structures to collect samples; (b) ruler to read water level; (c) SBn automatic sampler; (d) SBn storage/ (e) Monitoring site

SOURCE: The Author (2020)

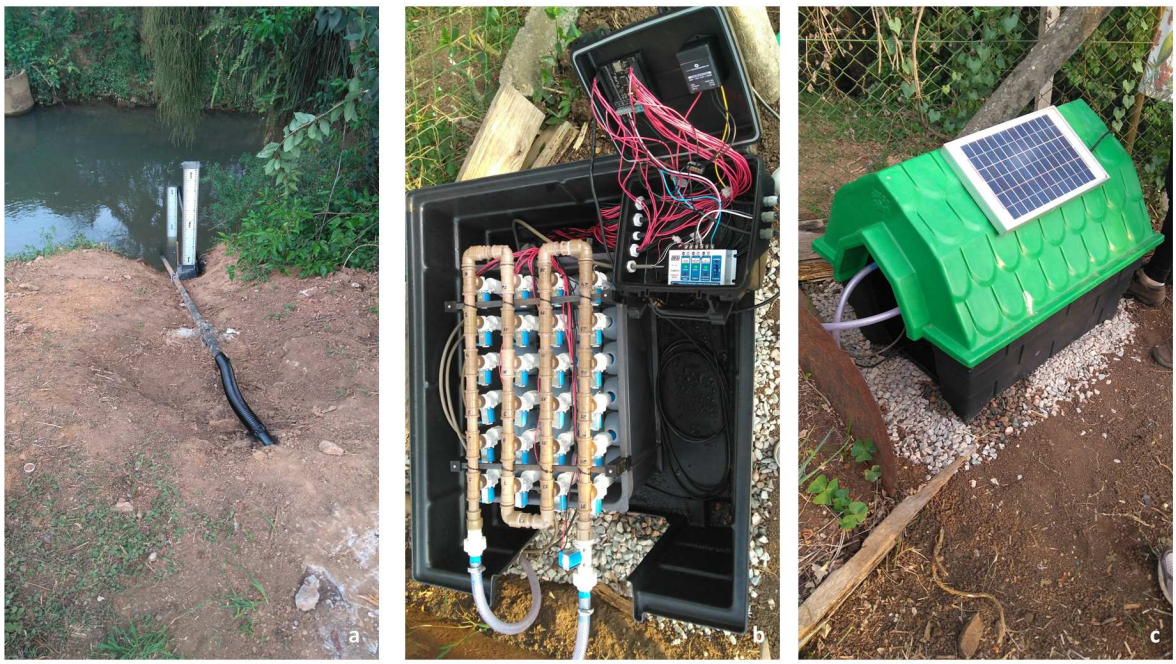

Figure 20 – Tingui monitoring point. (a) ruler to read water level; (b) SBn automatic sampler; (c) SBn storage

SOURCE: The Author (2020)

3.4.2 AUTOMATIC SAMPLER - SBN

From a printed circuit with the microprocessor, the main function is to distribute water samples to bottle through valves. The best advantage to use SBn is the versatility. Thus, it is important highlight the possibility to use appropriate batteries and bombs at any point where it is desired to monitor. For this study case, structure in the field is composed for:

- SBn automatic sampler;
- Battery (12V - 18 Ah) which is recharged constantly with a solar panel;
- Pump, which execute clean and collect routines;
- Level sensor (also developed at LME), reading water level at 1 minute intervals;
- Pluviometric station, which collect rainfall data;

The SBn schedule was developed in C language, programmed on the microprocessor (MSP430F5529) in the Texas Instruments software, called "Code Composer Studio". This interface can work in (i) time mode: samples are collect according to fixed times; (ii) schedule mode: samples are collect in defined dates; (iii) flow rate: samples are collect with water level variations (BRAGA, 2013; KOZAK et al., 2019; GRUDZIEN, 2019; DRUMMOND, 2020)

In this study, it was used flow rate programming summarized in Figure 21. General features considered in this routine are volume sample collecting always 1 liter, 10 cm of sampling step rising or falling water level and stop trigger with 5% of initial water level to end an event. Specific features are considered based on differences in cross section area, as: BA1 cleaning time is 20 seconds, pump flow rate of 180 $mL.s^{-1}$ and initial trigger is 10 centimeters of water level variation in maximum 5 minutes to

start an event, and BA2 cleaning time is 40 seconds, pump flow rate of 60 $mL.s^{-1}$ with initial trigger in 6 centimeters of water level variation in maximum 8 minutes.

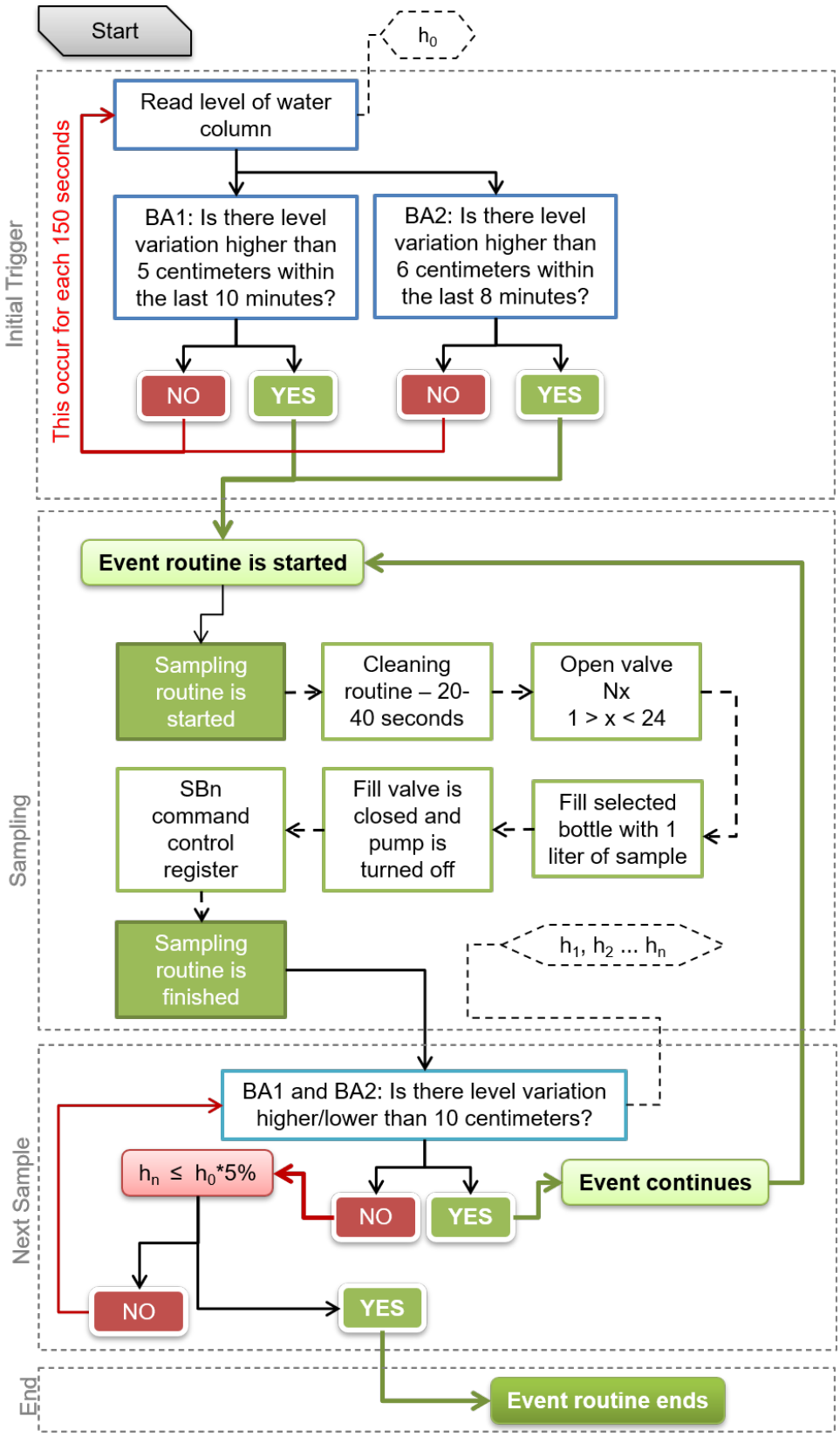

Figure 21 – Programming logistical of SBn sampling based on flow rate schedule

SOURCE: The Author (2020)

3.4.3 BASELINE CONDITIONS

It was performed a baseline campaign in order to assess river quantity and quality without rainfall influence. This campaign were performed on July 2019 (drier season) after about 15 days without rainfall registered in the watershed. Thus, for this profile, Barigui River was monitored during 24 hours, in three monitoring site: (i) BA1 and (ii) BA2, the traditional sites presented in section 3.2, and (iii) BA1-2 that is a intermediate site between BA1 and BA2 (coordinates 672963E, 7194773N). This site was located downstream the treatment station São Jorge WWTP outflow. The distance of BA1-2 to BA2, in river length, is 9 km. Considering the velocity calculated, this distance represent transport time of, approximately, 1 hour between points. Figure 22 located the intermediate sampling site, monitored for the baseline profile

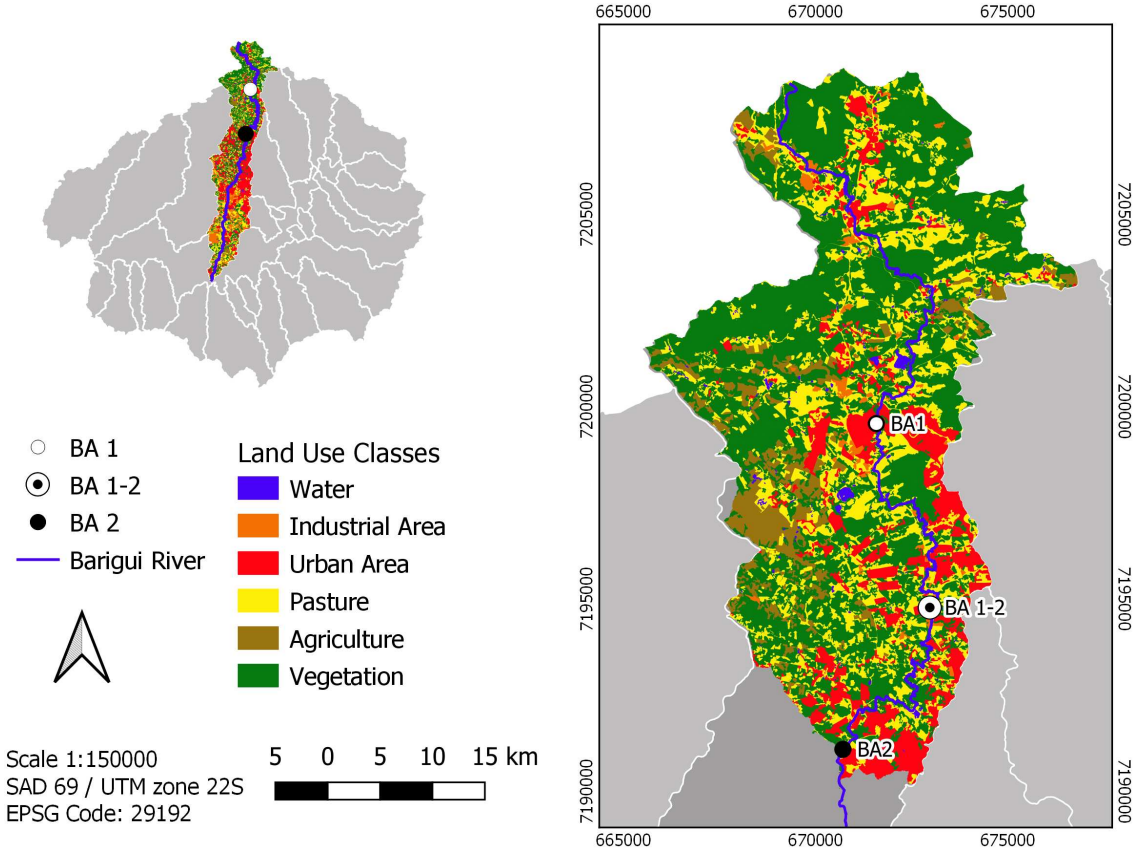

Figure 22 – BA1-2 intermediate monitoring site localization

Sampling routine was conducted each hour using automatic sampler, simultaneously in the three points. All samplers were programmed to collect samples at the same time. The programming schedule and logistic was prior and exhaustively tested. On BA1 and BA2 was used automatic sampler presented in the section 3.4.2, and on BA1-2 was used a ISCO 6712C (Teledyne ISCO) sampler.

The campaign was performed in July 10^{th} 2019 (Wednesday). This day of the week represent an neutral period to monitor baseline condition due to the less influence of the weekend. The first sample was collected at 6 p.m. and the last sample was at 5 p.m. of the next day (July 11^{th} 2019 (Thursday). To ensure data quality and to reduce lag time between sampling and analysis, a first set of 12 samples in each monitoring site was collected and transported to the laboratory to water measurements. The remaining 12 samples were transported to the lab at the end of the campaign.

For the 72 samples collected, it were measured the conventional water quality parameters (TN, N-NH_3, TP, TDP, PO_4^{3-}, TSS, COD, COD_d and DOC), inorganic elements, and spectroscopy analysis. Emerging compounds and PAHs it were analyzed just in 4 samples in each point: 10 p.m. - 3 a.m. - 9 a.m. and 3 p.m. The details of analytical processes are presented in section 3.5.

3.4.4 CONTROL VOLUME

A control volume is defined as a arbitrary volume where some fluid can flow. Here, this concept it is applied considering BA1 as initial observation point and BA2 as final observation point, and distances between them as controlled volume. Figure 23 shows Barigui watershed slope. BA1 is located at 1,050 m above the sea and BA2 is located at 936.4 m above the sea.

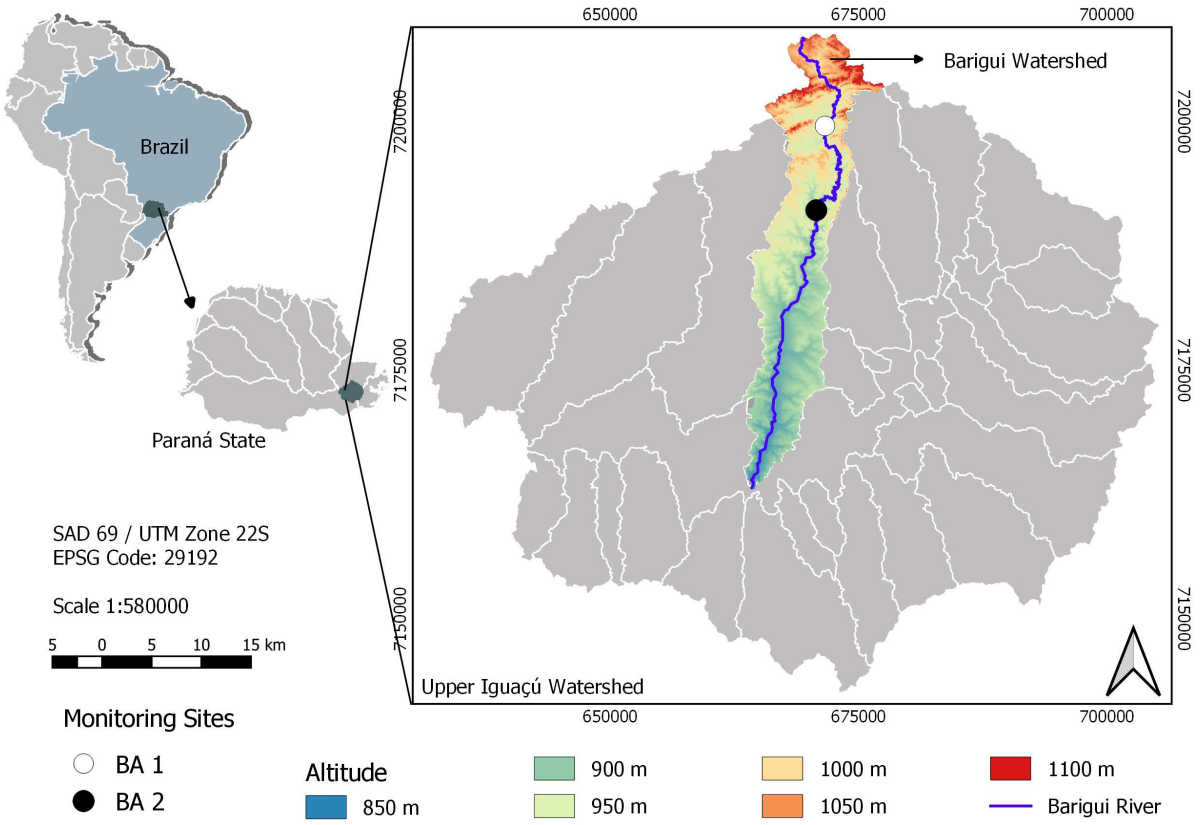

Figure 23 – Barigui Watershed slope, ranging between 1,100 m (hot colors) and 850 meters (cold colors)

BA1 have cross section area is narrower than BA2 cross section, as can be showed in Figure 47. Channel velocity was calculated using Manning equation, considering a roughness of 0.025 (rock channel), annual average water level in BA1 ($\approx$ 11 cm), inclination of 0.00631 m m^{-1} between 18 km of river length. Therefore, velocity is 2.36 m s^{-1}, which correspond an 2.11 hours of distance between BA1 and BA2.

Water level registered is converted in flow (m^3 s^{-1}) according to respective rating curve. BA1 rating curve was developed by FILL et al. (2005) (Equation 3.1. BA2 rating curve was developed during this study from flow and water level measurements along 2017 to 2019. It was adjusted an exponential function (R^2 = 0.917) in the data collected, producing the Equation 3.2. In both equation h is required in meters.

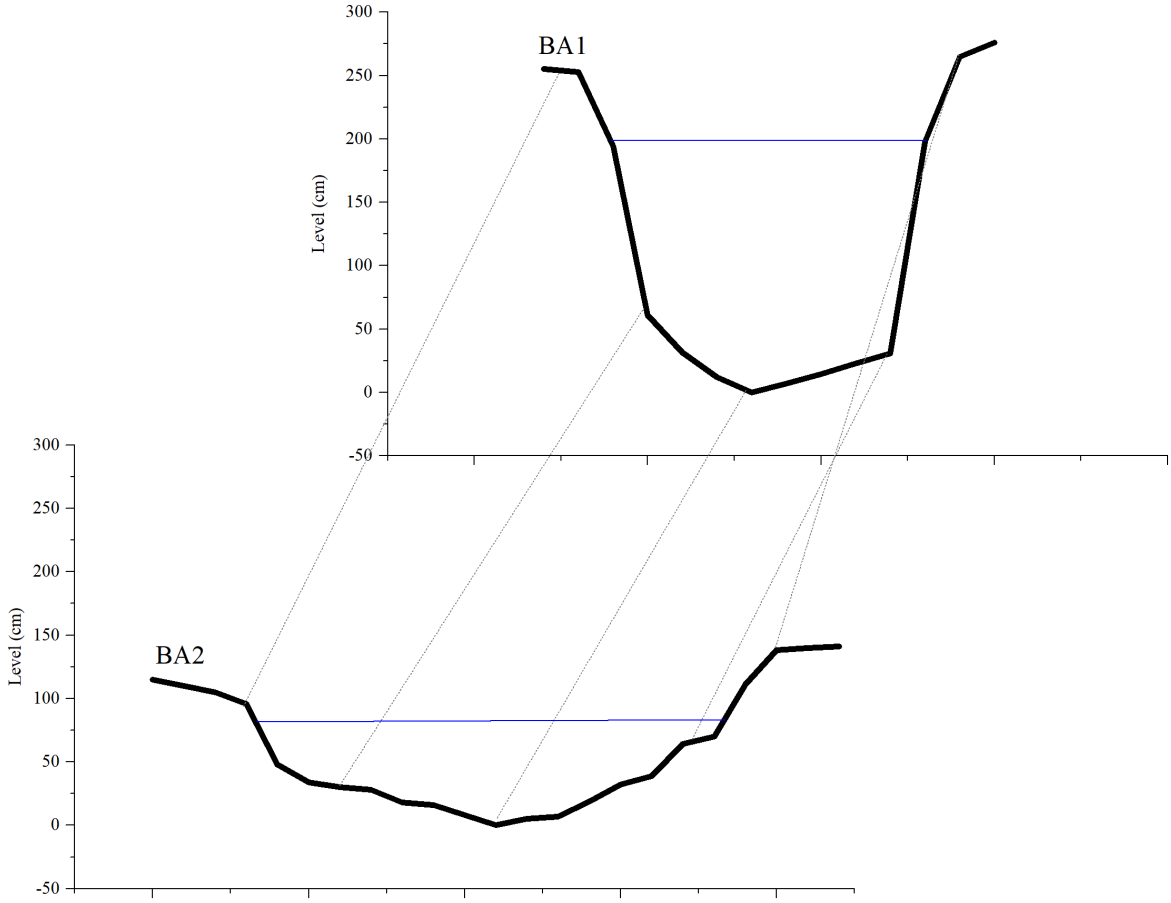

Figure 24 – Schematic representation of the cross section area in BA1 (up) and BA2 (down)

$$Q = 3.1517 * (h + 0.07941)^{1.0907} \tag{3.1}$$

SOURCE: FILL et al. (2005)

$$Q = 0.619 * e^{1.554*h} \tag{3.2}$$

SOURCE: The Author (2020)

3.5 WATER QUALITY PARAMETERS

In this section the analytical procedure used to determine water quality parameters measured in this study is presented. They were divided in main four groups, as: (1) Conventional Parameters, (2) Dissolved Organic Matter, (3) Emerging compounds, and (4) Inorganic Elements.

3.5.1 CONVENTIONAL WATER QUALITY PARAMETERS

Conventional water quality parameters are those generally used to characterize qualitatively water bodies in monitoring programs. It was measured TN, N-NH_3, PO_4^{3-}, TP TDP, TSS, COD, CODd, COD. Table 13 summarize the analytical procedures used (APHA, 2012).

Table 13 – Analytical procedures used to determine conventional water quality parameters

Parameter	Analytical Procedure
TN	4500-N. C: persufalte method 4500-NO_3^-. E: cadmium reduction method 4500-NO_2^-. B: colorimetric method
N-NH_3	4500 – NH3 F: phenate method
TP	Acid digestion method 4500-P. E: ascorbic acid method
TDP	Acid digestion method 4500-P. E: ascorbic acid method
PO_4^{3-}	4500-P. E: ascorbic acid method
TSS	2540 B: total solids dried at 103∘C-105∘C
COD CODd	5220 D: closed reflux, titrimetric method
DOC	5310 B: high-temperature combustion method

SOURCE: APHA (2012)

For TDP, CODd and DOC analysis samples were pre-filtered with acetate cellulose membrane, with 0.45 μm porosity. Membranes were soaked in distillate water to eliminate impurities. DOC sample were acidified with H_2SO_4 (p.a.) until pH < 2. Concentration was measured using TOC-VCPH analyzer (Shimadzu), pre-purged with oxygen gas to eliminate inorganic carbon. For TSS procedure it was used an glass fiber membrane, with 0.7 μm porosity. These membranes were heated in furnace at 400 ° C during 4 hours to eliminate organic contamination.

Samples collected in BA1 and BA2 have high pH and alkalinity, due to karst geologic formation of the region, which affect some analytical process efficiency, as phosphorus. Therefore, it was establish an acid digestion (Prado, 2015) to guarantee phosphorus availability in solution. The procedure consist in 25 mL of samples, add 5 mL of chloride acid (HCl) 1 mol L^{-1} and 0.8 mL of persulfate solution. This solution must be prepared add 2.5 mL of sulfiric acid (H_2SO_4 p.a.) and 2.5 g of potassium persulfate into a volumetric flask of 50 mL. The samples prepared must be placed in warming plate for 2 hours or until evaporate to 5 mL approximately. After that, to transfer remaining volume into a volumetric flask of 25 mL and to wash with distillate water the glass where occurred the digestion and transfer the residual to the volumetric flask too. Correct the pH of the samples: add phenolphthalein and then sodium hydroxide (NaCl 1N) until the pink color completely develop in sample. After add sulfuric acid (H_2SO_4 5N) until the pink color disappear. Filled the volumetric flaks (25 mL) until meniscus. Always homogenize the sample. Remove a 5mL aliquot and add mix reactive. Wait for 10 minutes (but no more than 30 minutes) and procedure the reading in spectroscopy ($\lambda = 880$nm)

3.5.2 DISSOLVED ORGANIC MATTER (DOM)

DOM was evaluated using spectroscopy techniques of UV-Vis absorbance and fluorescence. The samples for these analysis were filtered in acetate cellulose membrane, with 0.45 μm porosity, soaked in distillate water. Aliquots (10 mL) were stored in ambar glasses <4°C until further analysis. Ambar glasses were heated in furnace at 400°C during 4 hours to eliminate any organic contamination.

UV-Vis absorbance were measured using a UV-1601 PC spectrometer (Shimadzu), with a 1 cm quartz cells. Scan ranged between 200 to 600 nm, with 1 nm interval. It was used distilled water as blank. From this spectra were calculated A_{285}/DOC, $SUVA_{254}$, E_3/E_4, and E_2/E_3 indices, detailed in Table 2. Figure 25 shows UV-Vis scan from 200 to 600 nm with specific absorbance's location of the ratios presented.

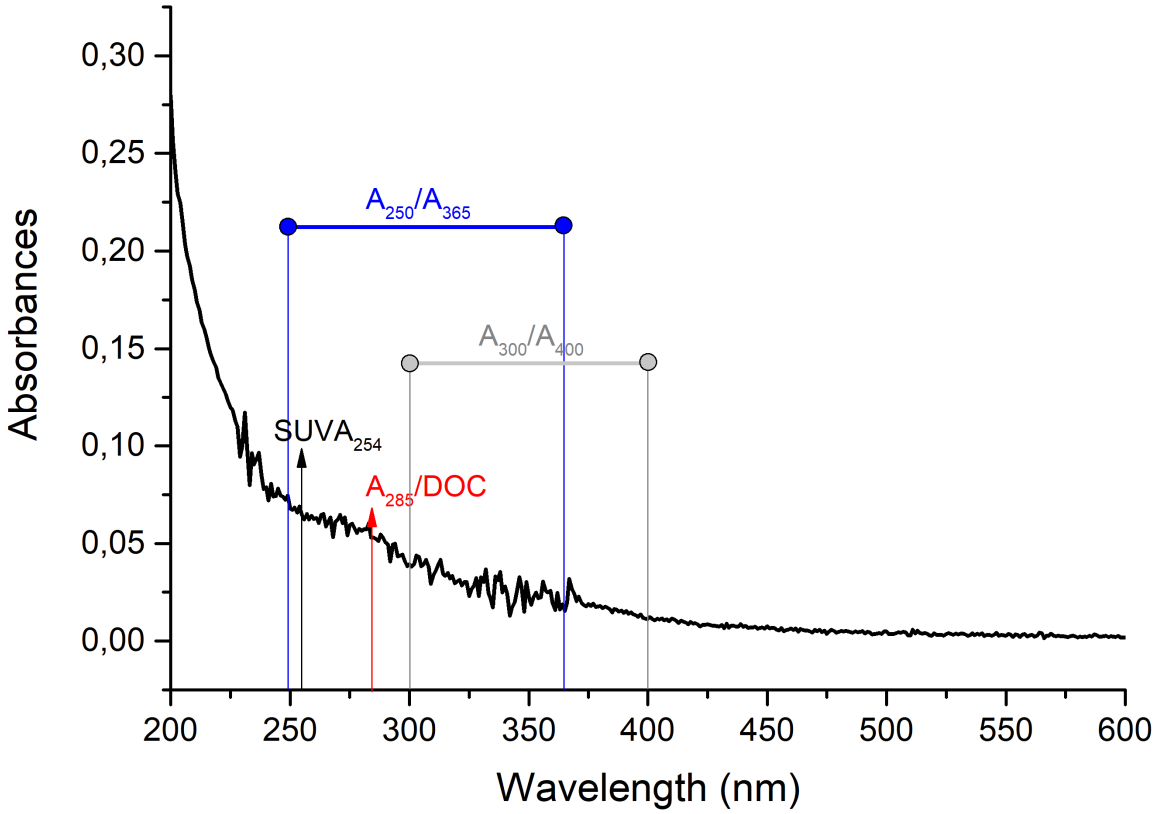

Figure 25 – UV-Vis scan from 200 to 600 nm with specific absorbance's location of the $SUVA_{254}$, A_{285}/DOC, E_2/E_3 and E_3/E_4 . Black arrow indicates absorbance in 254 nm for the $SUVA_{254}$ calculation; Red arrow indicates absorbances in 285 nm for the A_{285}/DOC calculation; Grey lines indicate absorbances in 300 nm and 400 nm for the ratio A_{300}/A_{400} (E_3/E_4) calculation; Blue lines indicate absorbances in 250 nm and 365 nm for the ratio A_{250}/A_{365} (E_2/E_3) calculation

SOURCE: The Author (2020)

Fluorescence measurements were performed in a fluorescence spectrophotometer Cary Eclipse (Varian Inc.) with a 1 cm quartz cells. Excitation wavelength ranged between 200 – 600 nm, in 5 nm intervals and emission wavelength ranged between 200 - 600 nm in 5 nm intervals, resulting in matrices with 81 lines and 81 columns. It was used Mili-Q water as blank. It is important to highlight that all measurements performed in the spectrophotometer was done on PMT voltage of 900 V, velocity of 8000 nm per minute (0.0375 s), to guarantee molecules excitation. From this data was generated the Excitation-Emission Matrices (EEMs), using a Fluorescence Excitation-Emission Matrix Code (FEEMC) developed

in python language. This mathematical routine process corrections of inner-filter effects (CARSTEA, 2012; MCKNIGHT et al., 2001), Raman Units (r.u.) normalization and day interference as air humidity, temperature, equipment resolution, light, others. Moreover, it was evaluated EEMs peaks (A, B, C, T_1 and T_2), and FI, BIX and HIX indices, as detailed in Table 3 and Table 4, respectively. Additionally, Figure 26 show fluorescence peaks and indices location in the EEM.

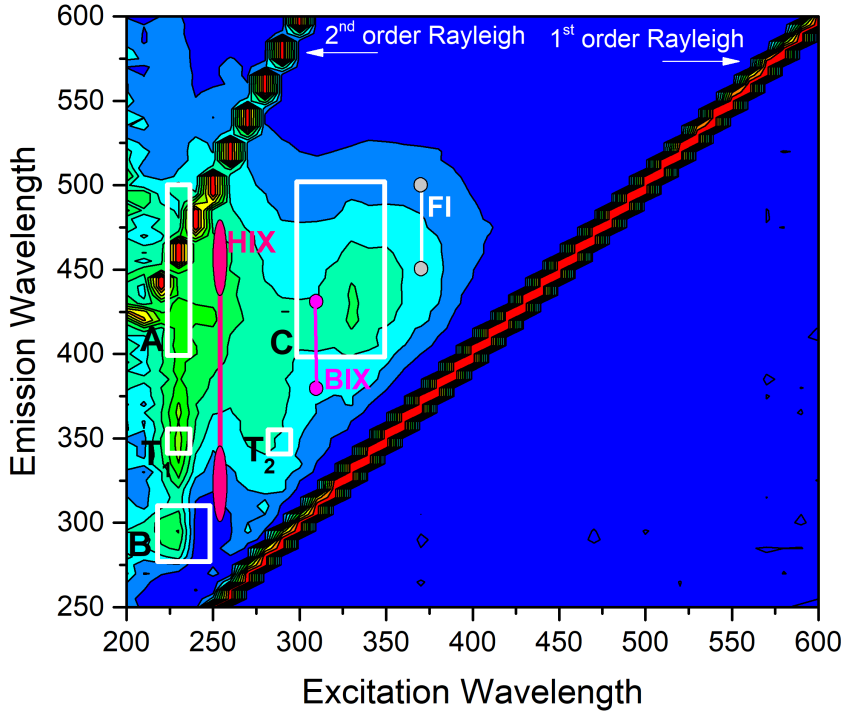

Figure 26 – Peak and indices identification on EEM representation. White rectangles represent the specific region where peak A, C, T_1, T_2 and B are measured. A peak is identified as the highest intensity value, measured in Raman Units (r.u.). Locations of emission intensities used to calculate HIX (pink circles, λ_{Ex} 254 nm), BIX (cian points, λ_{Ex} 310 nm) and FI (light gray points, λ_{Ex} 370 nm) are indicated

SOURCE: The Author (2020)
NOTE: Ex - excitation; Em - emission

For this data processing, an mathematical code was developed, named FEEMC, and presented in Appendix 6.1.3

3.5.3 INORGANIC ELEMENTS (IES)

It was determined Al, Ca, Cd, Cu, chromium (Cr), cobalt (Co), Fe, Mg, Mn, nickel (Ni), Pb and Zn elements in total recoverable and dissolved fraction from water samples. Measurements were performed in inductively coupled plasma optical emission spectrometry (ICP-OES) in opened water samples (APHA, 2012).

For dissolved fraction, samples were filtered in acetate cellulose membrane (0.45 μm) and stored 20 mL in sterile flask. To preserve and make metals available in solution it was added 2 mL of nitric acid (HNO_3 p.a.).

For total recoverable fraction samples were submitted to digestion step. In 25 mL of sample was added 5 mL of HNO_3 p.a., homogenized and placed in a hot plate at 150 °C, for 2 hours or until to reduce volume to 5 mL. After that, remained volume was transferred to a volumetric flask and filled with distilled water until meniscus. Before final storage, samples were centrifuged during 10 minutes in 3400 rpm to deposit solid in the bottom. Just supernatant was storage <4°C until further analysis.

A blank sample control, with distillate water, was performed equally to eliminate process interference. Difference between total fraction and dissolved fraction represent the amount of heavy metal in particulate fraction. Additional quality control information, as element identification, correspondent wavelength, calibration curve, correlation coefficient, LOD, LOQ, is presented in Appendix Section on Table 37 and Table 38.

3.5.4 EMERGING CONTAMINANTS (EMERC)

In order to evaluated EmerC, all analytical standards, BSTFA derivatizing and solvents used were obtained from Sigma Aldrich. It was used Chromabond ő C_{18} SPE cartridges (6 mL/1000 mg). Solvents used to prepare samples and to chromatography analyses were HPLC degree. Ultrapure water was obtained with Milipore ő equipment (KRAMER, 2016; FILIPPE, 2018).

The calibration curve was used 9 standard with distinct concentration (0.1 - 0.2 - 0.4 - 0.6 - 0.8 - 1 - 2 - 3 - and 5 ppm) and a free standard sample (blank). Blank sample was processed in triplicate, another standards and samples were processed in simple replicate. Quantification and detection limits (LOQ and LOD, respectively) were calculated according to ANVISA (2004), Amarante et al. (2001)

It was utilized 400 mL of sample filtered in acetate cellulose membrane (0.45 μm) and acidified with HCl (6 mol.L^{-1} until pH $\approx$ 3. For solid phase extraction it was used C_{18} cartridges. They were previously conditioned with 6mL of hexane, 6 mL of ethyl acetate, 6 mL of methanol and 6 mL of acidified ultrapure water (pH = 3). Then, sample was passed throughout with a velocity of 6 a 8 mL.min^{-1}, cartridges were vacuum dried. After that, 12 mL of acetonitrile was used to elution cartridges. Extracts were route evaporated at 40°C. Reconstitution occurred with 0.4 mL of acetonitrile in ultra-sonic equipment, which represent 1000 times concentration. 100 μL of this final extract was transferred to a 1 mL inserts and dried in a heating chamber at 40°C. After evaporation, it was added 20μL of derivatizing (BSTFA + 1% TMCS) at 60°C during 30 minutes to guarantee total reaction. Then, it was added 80μL of ethyl acetate to the sample reconstitution. After all these processes, samples were analyzed in gas chromatography (GC/MS-MS). Table 14 summarize the emerging contaminants analyzed in this study considering this method of extraction, and Figures 27, 28, and 29 presented theirs molecular structure.

Chromatography analyze was performed in GS/MS-MS (gas chromatography coupled to a quadruped triple mass detector - Agilent Technologies 7890 and 7000, respectively). The equipment is equipped with an automatic sampler (Agilent Technologies 80), capillary column HP-5Msi (30m x 0.25mm x 0.25 μm). The method used was determined by Kramer (2016), which are: initial oven temperature was 100°C during 2 minutes; then, temperature was reaching at 15°C.min^{-1} rate until 180°C, 6°C.min^{-1} rate until 270°C and 5°C.min^{-1} rate until 310°C keeping at this temperature for 3 minutes. Analyze total time was 33.3 minutes. Injector and transfer line temperature was programmed to 280°C. Chromatographic column pressure was 12.93 psi, with continuous helium flux of 1.2 mL.min^{-1} and samples injection of 1μL. Ionization method used was by Electrons Impact (EI) with energy of 70eV and source temperature of 250°C in Multiple Reactions Mode (MRM)

The assessment of the analytical data quality was performed by Kramer (2016). Pollutant selectivity was evaluated, defining the fragmentation to be monitored for each compound, energy of collision

Table 14 – EmerC categorization and classification, nomenclature and abbreviations used in this thesis

Category	Class	Compound	Abbr.
Pharmaceutical	Analgesic/Anti-inflammatory	Fenoprofen	FenP
		Ibuprofen	IBU
		Naproxen	NAP
		Acetylsalicylic Acid	AAS
	Metabolite	Salicylic Acid	AS
	Stimulant	Caffeine	CAF
	Beta blocking agents	Metoprolol	MTL
		Propanolol	PRL
		Nadolol	NAD
	Lipid regulator	Fenofibrate	FNF
PCPs	Preservative	Butylparaben	BuP
		Propylparaben	PrP
		Ethylparaben	EtP
		Methylparaben	MeP
		Benzylparaben	BeP
	Agent bacteriostatic	Irgasan/Triclosan	TCS
Sterol	Hormone/Contraceptive	Ethinyl Estradiol	EE2
	Hormone	17-Estradiol	E2
		Estrone	E1
	Phytoesterol	Stigmasterol	STI
		B-Sitosterol	Bsi
	Fecal Sterol	Cholesterol	CLT
		Colestanona	CLN
		Coprostanol	CPL
		Epicoprostanol	EPL

SOURCE: The Author (2020)

and retention time. These data are presented in Appendix Section (Table 34). Results confirm the analytical signal determined.

Linearity and sensitivity were analyzed, respectively, by correlation coefficient (r) and slope of the analytical curve. These data are presented in Appendix Section (Table 35). All correlation coefficient were above 0.98, confirming the linearity of the method. Angular coefficients from calibration curve had different values for each compound. The higher its value, the better the sensitivity of the method.

The limits of detection (LOD) and quantification (LOQ) were calculated from equations 3.3 and 3.4, where, σ is the standard deviation of the black measures, and S is the sensitivity of the compound (angular coefficient). They are used, respectively, to verify analytical parameters that express the lowest detectable and the lowest quantifiable value of a sample. These results are presented in Appendix Section (Table 36). The calculated values indicate good ability to determine compounds at very low concentrations. Likewise, the working range was between 10 and 1000 μg L^{-1} for all compounds, with the exception of ibuprofen, which was 2500 to 10000 μg L^{-1}. It is worth mentioning that these values were obtained for the analysis in the liquid samples.

$$LOD = \frac{3 * \sigma}{S} \tag{3.3}$$

$$LOQ = \frac{10 * \sigma}{S} \tag{3.4}$$

Figure 27 – Molecular structures of the pharmaceutical emerging contaminants considered in this study

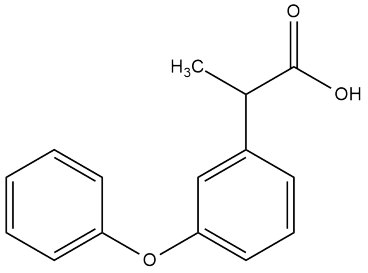

(a) Fenoprofen (FenP)

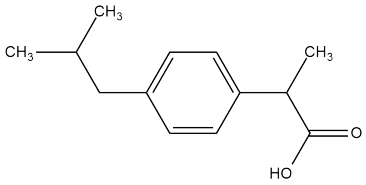

(b) Ibuprofen (IBU)

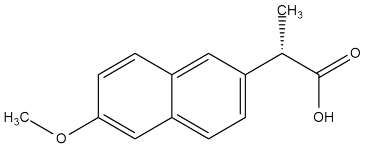

(c) Naproxen (NAP)

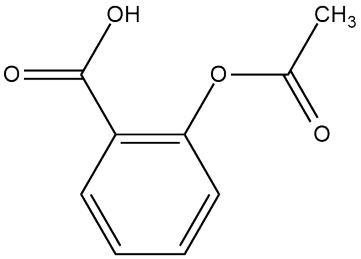

(d) Acetylsalicylic Acid (AAS)

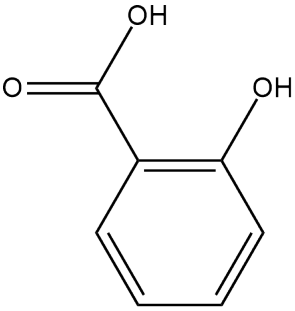

(e) Salicylic Acid (AS)

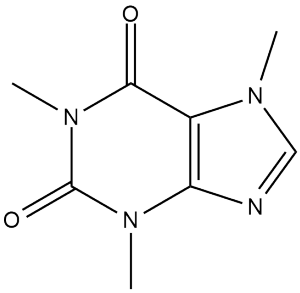

(f) Caffeine (CAF)

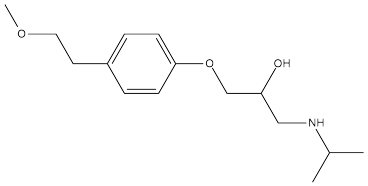

(g) Metoprolol (MTL)

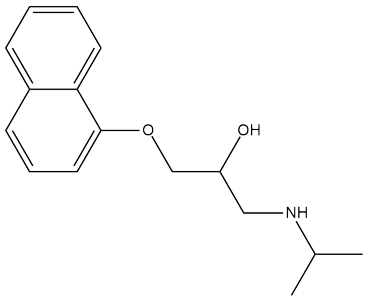

(h) Propanolol (PRL)

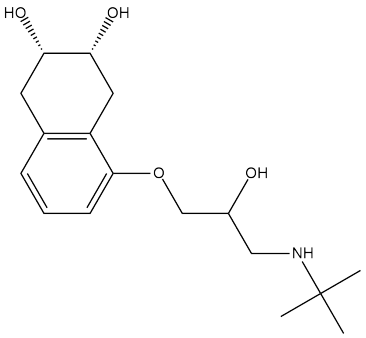

(i) Nadolol (NAD)

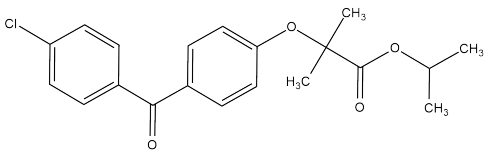

(j) Fenofibrate (FNF)

SOURCE: (NIH, 2020)

Figure 28 – Molecular structures of the PCPs emerging contaminants considered in this study

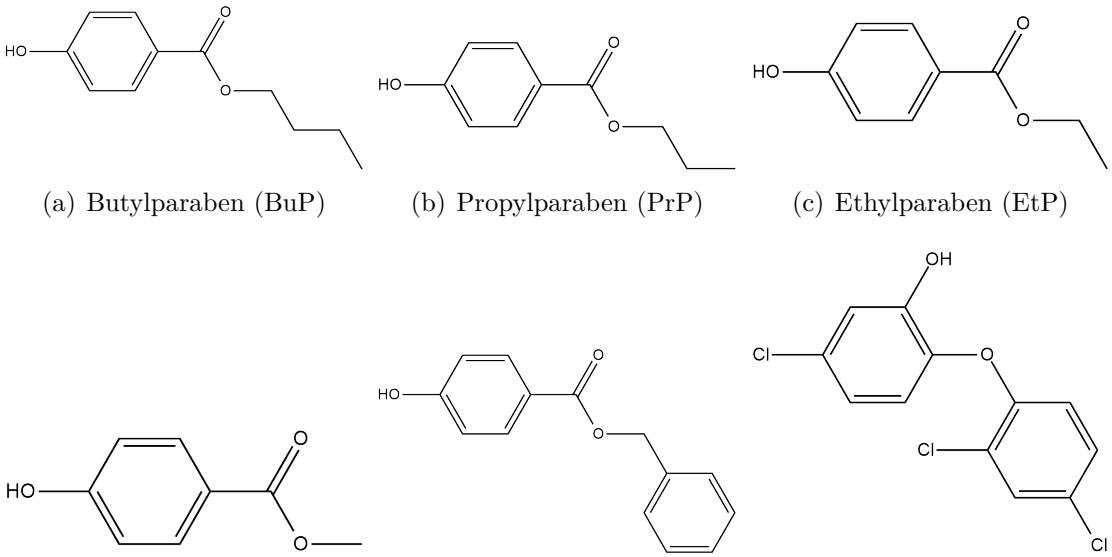

(a) Butylparaben (BuP) (b) Propylparaben (PrP) (c) Ethylparaben (EtP)

(d) Methylparaben (MeP) (e) Benzylparaben (BeP) (f) Triclosan (TCS)

SOURCE: (NIH, 2020)

Figure 29 – Molecular structures of the sterol emerging contaminants considered in this study

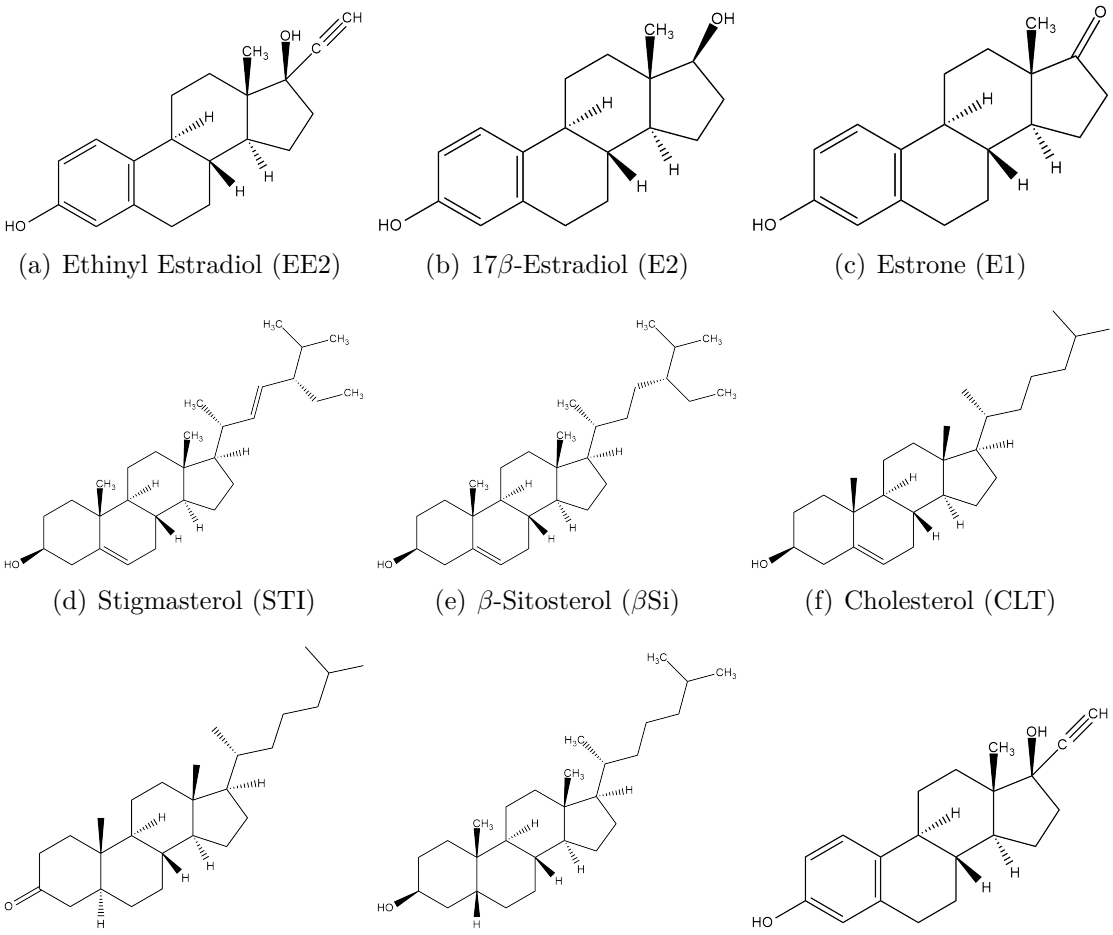

(a) Ethinyl Estradiol (EE2) (b) 17β-Estradiol (E2) (c) Estrone (E1)

(d) Stigmasterol (STI) (e) β-Sitosterol (βSi) (f) Cholesterol (CLT)

(g) Colestanona (CLN) (h) Coprostanol (CPL) (i) Epicoprostanol (EPL)

SOURCE: (NIH, 2020)

4 RESULTS AND DISCUSSION

"There exist complicated relationships between event-based non-point sources pollution patterns and hydroclimatological characteristics, making identifying controlling factors more complicated or even impossible. (...) Considering different event types could give more insights into the key drivers and lead to mechanistic understanding and informed decision makings on planning water management measures." Xie et al. (2019)

In this chapter, we will discuss the main results form the strategy herein presented. This strategy allows that each data set to provide different information and responses for the NPS effects. In order to provide a meaningful analysis, a baseline campaign was carried out. Thus the results chapters will first have the profile of the Barigui River during its baseline stage followed by the analysis of rainfall episodes. There will be 5 different chapters of results, according to the following strategy and schematized in the Figure 30:

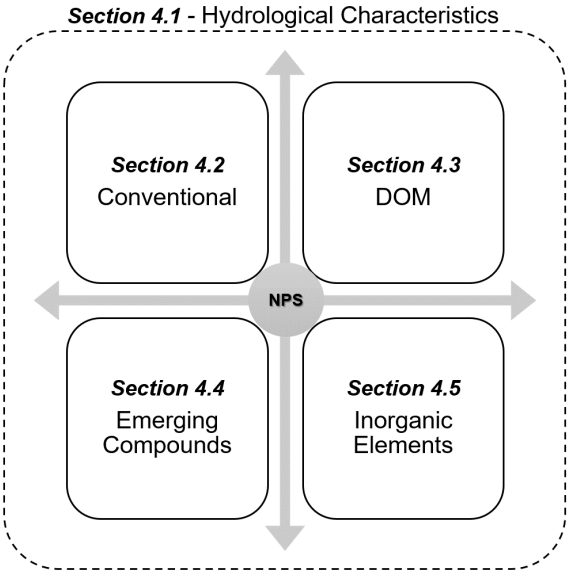

Figure 30 – Graphical Abstract of the results subdivision, considering hydrological characteristics and water quality parameters

1. Section 4.1 - **Hydrological Characteristics**: considering the relevance that the rainfall parameters have on the pollution transport profile, a discussion on these indicators will be presented. Each aspect of the hydrograph of the 8 rainfall events monitored in this work was analyzed. Thus, the main contribution to be explored is associated to defining the most relevant hydrological characteristic(s)
2. Section 4.2 - **Conventional Water Quality Parameters**: observing the basic (more common) water quality parameters, the Barigui River baseline of these parameters will be presented followed by an analysis of the pollutographs and EMCs of the conventional water quality parameters, in order to assess effects of land use and diffuse pollution. In this item discussion will be addressed as: pollutant transport pattern, most relevant rainfall moment and control volume analysis.

3. Section 4.3 - **Dissolved Organic Matter**: considering the influence of the organic matter in the aquatic system, an assessment of the composition of dissolved organic matter during the rainfall episode and in its baseline state will be performed. It will be used indicators of dissolved organic matter by techniques spectroscopy and DOC polutographs.
4. Section 4.4 - **Emerging Compounds**: the emerging compounds assessment during rainfall episodes will be carried out in relation to the baseline period, in order to identify pollution transport pathways and sources, since the elements measured in this category are directly related to point and/or anthropogenic pollution source.
5. Section 4.5 - **Inorganic Elements**: with this set of parameters it can be possible to evaluate possible sources and transport routes of diffuse pollution, using them in association with conventional parameters, as for example, DOC.

All the analysis will be based on 8 rainfall episodes monitored: 3 in BA1 monitoring site, and 5 in BA2 monitoring site.

4.1 RAINFALL EPISODES ASSESSMENT

"What are the most important hydrological characteristics?"

This section will present the rainfall episodes assessment, in order to (i) identify hydrological characteristics based on hydrographs, (ii) establish proper classification, and (iii) determine the main influences on hydrological parameters.

4.1.1 RAINFALL EPISODES

In this research, the monitoring period was between 2017 and 2019 in both monitoring sites at Barigui river. In total, were detected and collected samples during 8 rainfall episodes that happened in August 2018 (Event 1 - E1), in October 2018 (Event 2 - E2; Event 3 - E3; and Event 4 - E4), and in April 2019 (Event 5 - E5).

From these events, 3 rainfall episodes occurred in BA1 (E1, E2 and E4), and other 5 rainfall episodes occurred in BA2 (E1, E2, E3, E4, and E5). Therefore, E1, E2 and E4 potentially represent the input and output of pollution in the control volume (BA1-BA2), as consequence of the simultaneous sampling in both sites, whereas E3 and E5 represent pollution impacts from diffuse and punctual sources of pollution in a mixed land use drainage area.

Table 15 summarizes the rainfall events monitored, with the respective period of the year and number of samples collected. Figure 31 shows hydrographs for the rainfall events performed in BA1 and BA2 monitoring sites. Moreover, it is important to highlight that events E2, E3 and E4 occurred in October 2018 characterising these episodes as consecutive ones. Events E3 and E5 have proper sampling only for BA2, due to technical problems with the automatic sampler at BA1.

Table 15 – Detailing of the rainfall episodes monitored: number of samples collected in each monitoring site, and period of the year which occurred the sampling

	E1	E2	E3	E4	E5
Input (BA1)	7	15	n.c.	9	n.c.
Output (BA2)	8	13	15	16	13
Period	Aug/2018	Oct/2018	Oct/2018	Oct/2018	Apr/2019

NOTE: ***Highlighting****: Events E1, E2 and E4 represents control volume monitoring as a consequence of the simultaneous sampling in BA1 and BA2; Events E3 and E5 represent diffuse and punctual dynamics from a mixed land use drainage area*
LEGEND: E1: Event 1; E2 - Event 2; E3 - Event 3; E4 - Event 4; E5 - Event 5; n.c. - not collected

Table 16 summarizes hydrological parameters calculated for each rainfall episode collected. Parameters can be classified in three main groups which correspond to rainfall aspects, flow response and effects to the rainfall. Rainfall category is rainfall volume, duration and intensity. Flow category is river response to the rainfall, increase in flow, amount of water transported during unsteady state and surface runoff. Effects category is physical response in the water body corresponding to the hydrograph times. This last category can be extremely associated to the land use and soil occupation of the drainage area.

The rainfall classification of episodes E1 (sites BA1 and BA2), and E2 (site BA1) were classified as moderate, because rainfall intensity "i" ($2.5 \leq i \leq 10.0$ mm.h^{-1}). Other rainfall episodes were classified as light ($i < 2.5$ mm.h^{-1}), as consequence of long duration and low intensity well distributed over time (WHO, 2008). However, as observed, just the rainfall intensity was not enough to proper classify the events. Long rainfall duration also produced high flow variations (ΔQ), regardless the intensity, due to the amount of rainfall and water transported on the river. Therefore, rainfall episodes classification

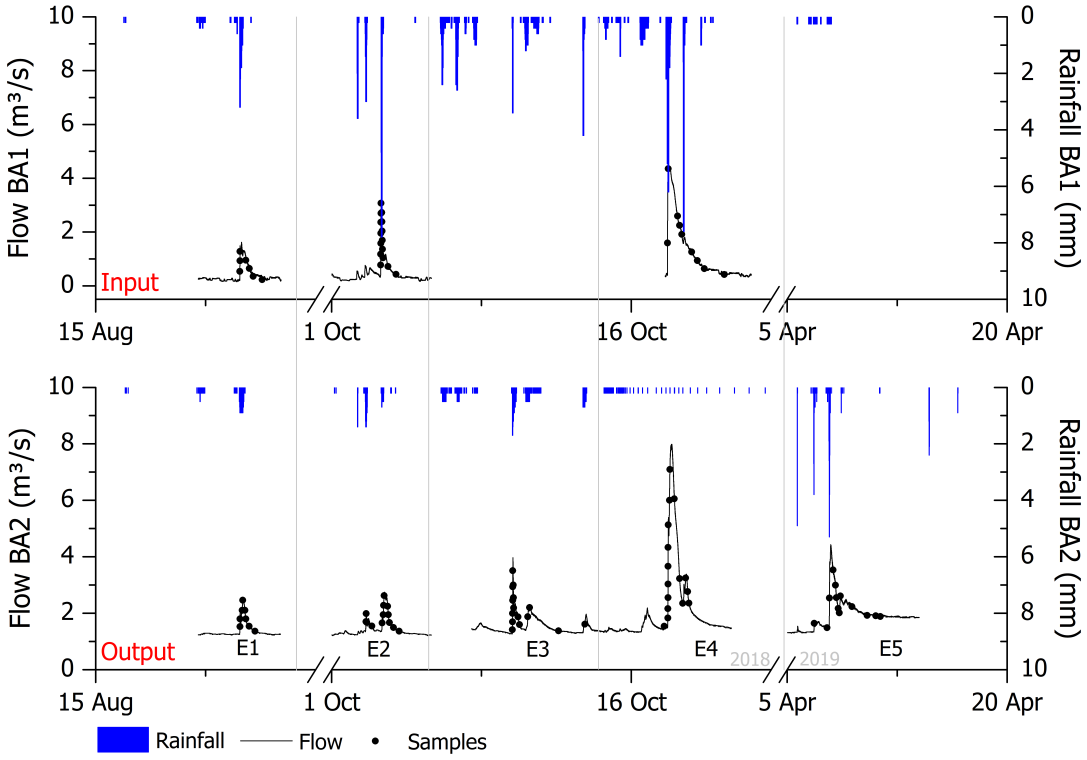

Figure 31 – Hydrographs for rainfall events collected in BA1 and BA2 monitoring sites

NOTE: Input: represent upstream monitoring site; Output: represent dowstream monitoring site
LEGEND: E1: Event 1; E2 - Event 2; E3 - Event 3; E4 - Event 4; E5 - Event 5

(REClass) proposed using RI, RD and ΔQ, in order to facilitate adequate rainfall interpretation and pattern is presented in Table 17.

According to the proposed classification summarized in Table 17, E4 in BA2 was classified as medium-to-high rainfall episode monitored, with high RD (62.5 hours) and ΔQ (6.43 $m^3.s^{-1}$), and low RI (1.58 $mm.h^{-1}$), being considered the most significant event. Interestingly, E4 in BA1, was classified as a medium rainfall episode, with medium RD (24 hours), RI (1.91 $mm.h^{-1}$), and ΔQ (4.16 $m^3.s^{-1}$). E2 in BA1 and E5 in BA2 had the same classification of medium rainfall episode, but with distinct weight for their parameters. E1 in both sites and E3 in BA2 were classified as medium-to-low rainfall episodes. The lowest one observed was E2 in BA2, with medium RD (24 hours) and low RI (0.98 $mm.h^{-1}$) and ΔQ (1.52 $m^3.s^{-1}$). High and medium RD with low RI can be considered an spaced rainfall event, slowly over time, which contribute to significant amount of accumulated water in the soil.

E1 had the same REClass in both sites related to the rainfall shape, low RD (4.75 and 9.33 hours, for BA1 and BA2) and ΔQ (1.36 and 1.26 $m^3.s^{-1}$, for BA1 and BA2), and high RI (4.97 and 3.65 $mm.h^{-1}$, for BA1 and BA2). This event was influenced by small precedent rainfall before the main episode detected in SBn. In BA1 occurred two light rainfall episodes with intensities of 0.8 $mm.h^{-1}$ and 0.35 $mm.h^{-1}$, respectively 15 hours and 4.5 hours before SBn start the triggering system. Then, fifteen samples were collected seven in BA1, where three were during rising-limb and four during the falling-limb of the hydrograph, and eight in BA2, where four samples were collected during rising-limb and four during falling limb of the hydrograph. ΔQ was similar, but bigger in BA1, probably due to river cross section. For the same reason, Crt was faster in BA1 (2.40 hours) than in BA2 (6.03 hours). V_{transp} in BA2 was

Table 16 – Hydrological characteristics for the rainfall events analyzed in this study in BA1 and BA2 monitoring site

		E1		E2		E3	E4		E5
		BA1	BA2	BA1	BA2	BA2	BA1	BA2	BA2
	NS	7	8	15	13	16	10	22	13
Rainfall	ED	36.57	24.65	18.38	39.80	86.97	68.04	79.98	108.28
	RD	4.75	9.33	3.00	24.00	35.17	24.00	62.50	53.83
	P_{acum}	23.60	34.10	15.40	23.60	41.60	45.80	98.90	48.40
	RI	4.97	3.65	5.13	0.98	1.18	1.91	1.58	0.90
	RClass	moderate	moderate	moderate	light	light	light	light	light
Flow	V_{transp}	1.19	2.41	0.83	3.63	5.44	4.48	10.70	11.16
	SRun	0.87	1.62	0.71	2.72	3.75	3.74	7.66	9.14
	Q_{base}	0.26	1.26	0.36	1.23	1.41	0.41	1.55	1.36
	Q_{max}	1.62	2.52	3.20	2.75	3.96	4.57	7.98	4.43
	ΔQ	1.36	1.26	2.84	1.52	2.55	4.16	6.43	3.07
Effects	Rt	2.63	5.10	0.83	22.30	0.68	1.13	9.25	2.82
	Ft	19.37	21.80	16.50	7.18	50.15	44.18	28.75	53.23
	Rt/Ft	0.14	0.23	0.05	3.10	0.01	0.03	0.32	0.05
	Crt	2.40	6.03	0.63	24.87	1.77	2.55	39.78	32.35
	Cot	17.02	18.50	14.13	8.05	16.75	22.73	6.03	31.75
	Bt	1.84	1.76	1.05	1.97	3.42	3.34	2.86	4.60
	ADP	2.39	2.36	1.47	1.81	1.70	0.91	0.00	7.62

NOTE: More detail is presented in Figure 18

LEGEND: E1: Event 1; E2 - Event 2; E3 - Event 3; E4 - Event 4; E5 - Event 5; NS - Number of samples; ED - Event duration (h); RD - Rainfall duration (h); P_{accum} - Accumulated precipitation (mm); RI - Rainfall intensity (mm.h^{-1}); RClass - Rainfall classification according to WHO (2008); V_{transp} - Volume of water transported (m^3); SRun - Surface runoff (m^3); Q_{base} - Base flow (m^3.s^{-1}); Q_{max} - Maximum flow (m^3.s^{-1}); ΔQ - Difference between Q_{max} and Q_{base} (m^3.s^{-1}); Rt - Rise time (h); Ft - Falling time (h); Crt - Critical time; Cot - Concentration time; Bt - Base time (h); ADP - Antecedent Dry Periods (day)

Table 17 – Rainfall episodes parameterization and classification (REClass) proposed, according to RI, RD and ΔQ measured from the hydrograph

	E1		E2		E3	E4		E5
	BA1	BA2	BA1	BA2	BA2	BA1	BA2	BA2
RD	low (1)	low (1)	low (1)	medium (2)	medium (2)	medium (2)	high (3)	high (3)
RI	high (3)	high (3)	high (3)	low (1)	low (1)	medium (2)	low (1)	low (1)
ΔQ	low (1)	low (1)	medium (2)	low (1)	medium (2)	medium (2)	high (3)	medium (2)
Sum	5	5	6	4	5	6	7	6
REClass	medium-to-low		medium	low	medium-to-low	medium	medium-to-high	medium

LEGEND: E1: Event 1; E2 - Event 2; E3 - Event 3; E4 - Event 4; E5 - Event 5; RI - Rainfall intensity (mm h^{-1}); RD - Rainfall duration (h); ΔQ - Difference between Q_{max} and Q_{base} (m^3 s^{-1})

double of V_{transp} in BA1, and considering the incremental area between both sites, about 49% of the water volume received in BA2 is from BA1. Bt for E1 was, in average, 1.80 days.

E2 had REClass of medium in BA1 and low in BA2. The main difference is in RI, with high intensity in BA1 (5.13 mm.h^{-1}) and low intensity in BA2 (0.98 mm.h^{-1}), and low RD in BA1 (3 hours) and medium RD in BA2 (24 hours). This wide contrast on RD values is related to the three precipitation of the event, where the precedent rainfall had greater influence than the main rainfall. In BA1, the two precedent rainfall had moderate intensity, with 4.8 and 3.7 mm.h^{-1}00, respectively. The first one contributed exclusively to the soil saturation, and the second, there was a small water level variation without SBn triggering, justifying the lowest RD. In BA2, precedent rainfall was very similar. There was one moderate rainfall with intensity of 8.4 mm.h^{-1} which contribute to the soil saturation. The second

rainfall observed in BA2 produced enough water level variation to SBn trigger.

These differences can also be associated to the amount of water received in BA2 from BA1, about 23%, which contribute to the low REClass of this event in BA2 site. Furthermore, these precedent rainfall could contribute for the wide difference in the hydrological characteristics measured in this event, as for example, Crt of 0.63 hours in BA1 and 24.87 hours in BA2, and V_{transp} of 0.83 m^3 in BA1 and 3.63 m^3 in BA2. The main rainfall considered was more pronounced in BA1, with Q_{max} of 3.20 $m^3.s^{-1}$ and ΔQ of 2.84 $m^3.s^{-1}$, than in BA2 with Q_{max} of 2.75 $m^3.s^{-1}$ and ΔQ of 1.52 $m^3.s^{-1}$, also associated to the cross section of the river. Twenty-eight samples were collected, where fifteen in BA1 with seven samples during rising-limb and eight samples during falling-limb of the hydrograph, and thirteen in BA2, where, and samples eight samples were collected during rising-limb and five during falling-limb of the hydrograph. Additionally, BA1 assimilated rainfall faster than BA2, with difference of 1 day in Bt, which can be related to the land use of BA1 drainage area.

E4 was the biggest event measured, with REClass of medium in BA1 and medium-to-high in BA2. The rainfall observed had high duration and precipitated volume, almost reaching 100 mm during three days. Thus, there was the highest ΔQ observed, 4.16 $m^3.s^{-1}$ in BA1 and 6.43 $m^3.s^{-1}$ in BA2. V_{transp} in BA2 was 2.4 times bigger than BA1 (10.70 m^3 and 4.48 m^3), suggesting that 42% of the water received in BA2 is from BA1. Rt had low values, which correspond to the fast increase in the water level, probably due to two consecutive rainfall episodes precedent (E2 and E3). However, the assimilation along the time was slow, with high Ft, in average 36 hours to reach inflection point of the hydrograph. Beside the low ADP in this event, Bt was about 3 days. It were collected nine samples in BA1, where just two were collected during rising-limb and seven during falling-limb of the hydrograph, and sixteen samples in BA2, where ten samples were collected during rising-limb, and six during falling-limb of the hydrograph.

E3 and E5 are rainfall episode with observation just in BA2. E3 had REClass as medium-to-low, due to medium RD (35.17 hours) and ΔQ (2.55 $m^3.s^{-1}$), and low RI (1.18 $mm.h^{-1}$) observed. E5 was classified as medium rainfall episode, with high RD (53.83 hours), low RI (0.90 $mm.h^{-1}$) and medium ΔQ (3.07 $m^3.s^{-1}$) observed. The long duration of these events contribute to the elevated volume transported (5.44 m^3 in E3 and 11.16 m^3 in E5), and slow assimilation, with the highest Ft values, 50.15 hours and 53.23 hours, respectively for E3 and E5. Also, these events had the highest Bt times, which, in average, was 4 days. There is a wide difference in Crt of these event, which is related to the precedent rainfall observed before the main rainfall.

E3 had not precedent rainfall, therefore rainfall measured was concentrated in that period, while E5 had a precedent rainfall and behavior similar to occurred in E2-BA2. There was a strong rainfall with intensity of 16.4 $mm.h^{-1}$ about 27 hours before the main rainfall, which can contribute to the soil saturation. Then, E5 is characterized by three main rainfall: the first was light rainfall, with intensity of 1.66 $mm.h^{-1}$, which contribute to the soil saturation and to the SBn trigger; the second one was a moderate rainfall, with intensity of 3.22 $mm.h^{-1}$, which produced wide water level variation; and the third one, which occurred during the falling time, with intensity of 0.58 $mm.h^{-1}$ producing a light increase in the water level. It were collected fifteen samples in E3, where six during rising-limb and nine during falling-limb of the hydrograph, and in E5 thirteen samples were collected, where three during rising-limb and ten during falling-limb of the hydrograph.

Therefore, considering that rainfall episodes can be similar, Figure 32 shows scores and loadings from PCA to the rainfall episodes and hydrological characteristics. Two components explain 76.54% of the rainfall episodes distribution, where component 1 represent 53.51% and component 2 represent 23.03%. It is possible to observe four group of similarity. Two of them are isolated rainfall episodes: (i) E2-BA2 which is separated for the effects parameters, Ft and Rt/Ft parameters, and (ii) E4-BA2 which is

separated for the flow parameters, as Q_{base}, Q_{max}, ΔQ, and P_{acum}. Both event correspond, respectively, to the lowest and highest rainfall episode observed: E2-BA2 have the opposite values of Ft and Rt/Ft, suggesting that rising limb was faster than falling limb, probably due to the precedent rainfall observed and above mentioned; and E4-BA2 had the highest Q_{max} (7.98 $m^3.s^{-1}$), ΔQ (6.43 $m^3.s^{-1}$), and P_{acum} (98.90 mm) observed.

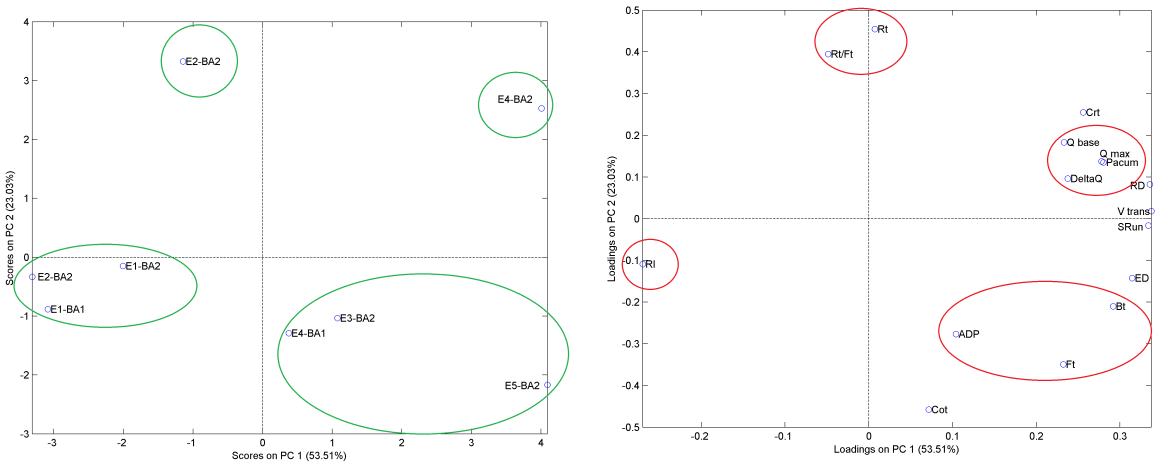

(a) Scores (b) Loadings

Figure 32 – Scores and loadings from PCA of rainfall episodes and hydrological characteristics

Another group formed are events E1-BA1, E1-BA2, and E2-BA2, which were influenced by RI. This suggest that rainfall episode without precedent rainfall to saturate the soil have similar behavior. These events have the most intense rainfall observed, respectively 4.97, 3.65 and 5.13 $mm.h^{-1}$, low RD and high P_{acum}. The last group is formed by E3-BA2 and E5-BA2 (singles site episodes), and E4-BA1, which were influenced by ADP, Bt and Ft. These events grouped had the highest Bt observed, which can be related to the consecutive rainfall occurrence during E3 and E4, and the highest ADP observed in E5.

Bauwe et al. (2015) observed 72 rainfall episodes considering 21 hydrological characteristics. Furthermore, to a better understanding of the dominant hydrological characteristics, the author performed assessment considering rainfall episode division considering summer event, snow events, event controlled by RD (longer ones), by P_{acum} (high volume), by ADP and antecedent wet conditions. Xie et al. (2019) used a mathematical model to predict intra and inter-events patterns. The authors classified the rainfall episodes (medium, heavy, very heavy and extremely-heavy) using P_{acum}, RD and maximum RI. Furthermore, the author also divided 10 hydrological characteristics in three categories, which are antecedent conditions, rainfall event and discharge. Pérez-Gutiérrez et al. (2020) observed 46 rainfall episodes considering 9 hydrological characteristics based on duration, intensity, total precipitated and time between rainfall episodes. Moreover, considering frequency and P_{acum}, authors divided rainfalls in classes, which are (I) moderately frequent with moderate rainfall, (II) less frequent with very high rainfall, (III) highly frequent with moderate rainfall, and (IV) infrequent with low rainfall.

Pollutant concentration depend of the wash-off and dilution effect, being related with the flow-concentration, that is, rainfall (LIAO et al., 2019). Therefore, dividing rainfall episodes into categories considering their own characteristics can help to understand river response and further water quality assessment. For example, intense rainfall could contribute to the fast first-flush, with low Rt value, transporting the pollution accumulated along the previous days. As well as, a longer rainfall could favor dilution of the pollutant transported, smoothing the impacts in the water body. Furthermore, rainfall

classification can help NPS mathematical modelling estimation . Rainfall classification associated with the correspondent frequency (%) can estimate the amount of pollutants transported into the river, and in parallel, to develop scenarios with best management practices to reduce load received.

4.1.2 INFLUENCE OF THE HYDROLOGICAL CHARACTERISTICS ON DISCHARGE BEHAVIOR

The hydrological characteristics must be associated in groups because they are complementary and dependent. The same rainfall event will have distinct impacts in a different watershed, and consequently with potential differences in terms of the spatial and temporal distribution of pollutants. The kind of rainfall occurrence has influence on the transport and preferential pathways, while watershed land use has influence on the kind of pollutant available to be transported.

Magnitude of E2, E3, and E4 increased due to their consecutive occurrence, with ADP lower than 2 days. V_{trans}, P_{acum} and RD, in average, doubled between E2 to E3 and E3 to E4. According to Hernández-Crespo et al. (2019), frequent rainfall does not favour the water retention. Considering all water volume transported during the rainfall episode, about 75% could be related to the SRun, as can be observed in Figure 33. Therefore, an slight estimation indicate that about 25% of the initial rainfall can be infiltrate in the soil, and therefore, the other 75% contribute to the water level variations.

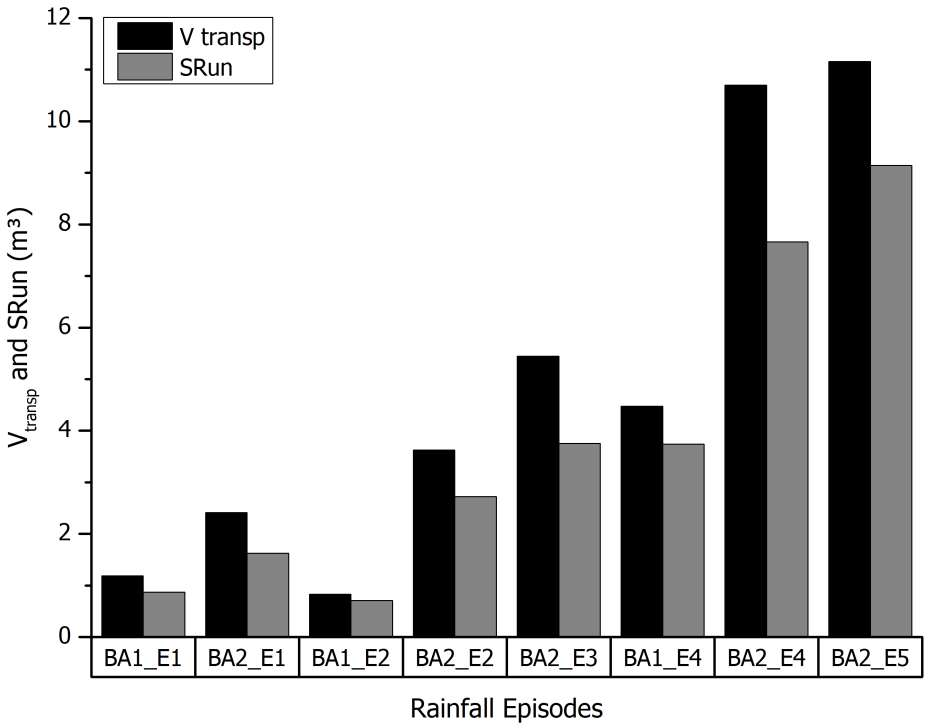

Figure 33 – Water volume transported (V_{transp}) (black bar) and surface runoff (SRun) (grey bar) proportions during the rainfall episode monitored in BA1 and BA2

In this sense, Table 18 shows the rainfall proportions of 25% and the time to achieve that quantity. As a result, low proportions of rainfall in BA1 can be sufficient to saturate the soil, probably associated to more permeable area in BA1 drainage area and narrow cross section. In BA2, the river response to the rainfall is longer than 2 hours, which can be associated to the precedent rainfall or spaced rainfall

occurred. Also, 2 hours is the estimated travel time between BA1 and BA2, and therefore, the initial contribution in BA2 can be is highly influenced by the incremental areas and can reflect the water quality consequences more precisely.

Table 18 – V_{transp}, SRun and P_{acum} considering the proportions of water volume precipitated and transported

	E1		E2		E3	E4		E5
	BA1	BA2	BA1	BA2	BA2	BA1	BA2	BA2
V_{transp}	1.19	2.41	0.83	3.63	5.44	4.48	10.70	11.16
SRun	0.87	1.62	0.71	2.72	3.75	3.74	7.66	9.14
Proportion	73.3	67.3	84.9	75.0	69.0	83.5	71.6	81.9
P_{acum}	23.60	34.10	15.40	23.60	41.60	45.80	98.90	48.40
P_{acum} 25%	5.90	8.53	3.85	5.90	10.40	11.45	24.73	12.10
RD 25%	30 min	2 h	15 min	1 h	2 h	2 h	*	6 h

NOTE: RD 25% represent RD until achieve 25% of the total precipitated
LEGEND: V_{transp} - volume of water transported (m^3); SRun - Surface runoff (m^3); P_{accum} - accumulated precipitation (mm); P_{accum} 25% - accumulated precipitation (mm) until achieve the first 25% of the total rainfall amount

Beside rainy months observed, Q_{base} have always been restored between events, with Q_{base} average of 0.34 $m^3.s^{-1}$ for BA1 and 1.36 $m^3.s^{-1}$ for BA2. Rt/Ft showed low values, which indicate that Rt was faster than Ft. In other words, there was fast response to the rainfall episode and a slow soil assimilation over time. BA1 have lower values than BA2, which can be related to the sub-superficial contribution in the water system. Event time of the Barigui River can be considered fast associated to the land use and soil occupation of these drainage area, which is more vegetated and less urbanized, in comparison to the downstream land use.

To understand hydrological characteristics without a specific event, Pearson correlation with 95% confident limit was performed. Table 19. The significant correlation observed are:

- HIGH RD: correlated to high P_{acum} (0.85, p-value < 0.05), which produced more V_{transp} (0.98, p-value < 0.05), in episodes with low RI (-0.79, p-value < 0.05), which suggest that longer rainfall episode transported more water, however, more intense rainfall transported less water.
- HIGH RI: produce less Crt (-0.60, p-value $= 0.11$) during few time (-0.77, p-value < 0.05) which suggest fast water level increase in intense rainfall, and intense rainfall represent short rainfall episode. Intense rainfall produces clearly peak flow, whereas low intense rainfall produces less peak flow, due to the longer duration (HERNÁNDEZ-CRESPO et al., 2019)
- HIGH Ft: produced in event with high ED (0.85, p-value < 0.05), suggesting that long rainfall episodes generated a lot of water transported will be difficult to be assimilated by the system, with high Cot (0.69, p-value $= 0.06$), that is, long time to Q_{base} get back to usual, being indirectly related to RD (0.56, p-value $= 0.15$) and V_{transp} (0.60, p-value $= 0.11$).
- HIGH ADP: produce high Cot (0.79, p-value < 0.05), suggesting that longer periods without rainfall reflects in a bigger time to river assimilation.
- HIGH Bt: extremely associated to high ED (0.97, p-value < 0.05) and RD (0.77, p-value < 0.05) with low RI (-0.76, p-value < 0.05), producing high amount of V_{transp} (0.81, p-value < 0.05) and SRun (0.84, p-value < 0.05) during slow assimilation by the river system, high Ft (0.89, p-value < 0.05).

Table 19 – Pearson correlation for the hydrological characteristics measured in the five rainfall episode

		ED	RD	Pacum	RI	Vtrans	Runoff	Qbase	Qmax	Q	Rt	Ft	Rt/Ft	Crt	ADP	Cot	Bt
ED	Pearson's	-															
	p-value	-															
RD	Pearson's	**0.87**	-														
	p-value	<0.05	-														
Pacum	Pearson's	0.61	**0.85**	-													
	p-value	0.10	<0.05	-													
RI	Pearson's	**-0.77**	**-0.79**	-0.50	-												
	p-value	<0.05	<0.05	0.21	-												
Vtrans	Pearson's	**0.88**	**0.98**	**0.81**	**-0.74**	-											
	p-value	<0.05	<0.05	<0.05	<0.05	-											
Runoff	Pearson's	**0.89**	**0.96**	**0.75**	**-0.73**	**0.99**	-										
	p-value	<0.05	<0.05	<0.05	<0.05	<0.05	-										
Qbase	Pearson's	0.53	**0.73**	0.57	**-0.72**	0.69	0.63	-									
	p-value	0.18	<0.05	0.14	<0.05	0.06	0.09	-									
Qmax	Pearson's	0.61	**0.84**	**0.94**	-0.51	**0.79**	**0.75**	0.49	-								
	p-value	0.11	<0.05	<0.05	0.19	<0.05	<0.05	0.22	-								
Q	Pearson's	0.51	**0.71**	**0.87**	-0.35	0.67	0.64	0.24	**0.96**	-							
	p-value	0.19	<0.05	<0.05	0.40	0.07	0.09	0.57	<0.05	-							
Rt	Pearson's	-0.17	0.15	0.04	-0.39	0.07	0.04	0.38	0.02	-0.10	-						
	p-value	0.69	0.73	0.93	0.34	0.88	0.93	0.35	0.97	0.82	-						
Ft	Pearson's	**0.85**	0.56	0.38	-0.51	0.60	0.63	0.26	0.39	0.35	-0.59	-					
	p-value	<0.05	0.15	0.36	0.20	0.11	0.09	0.53	0.34	0.40	0.13	-					
Rt/Ft	Pearson's	-0.24	-0.03	-0.22	-0.34	-0.11	-0.12	0.23	-0.19	-0.29	**0.95**	-0.58	-				
	p-value	0.57	0.94	0.61	0.40	0.79	0.77	0.59	0.65	0.49	<0.05	0.13	-				
Crt	Pearson's	0.51	**0.82**	0.68	-0.60	**0.82**	**0.81**	0.67	0.65	0.52	0.54	0.06	0.33	-			
	p-value	0.19	<0.05	0.06	0.11	<0.05	<0.05	0.07	0.08	0.19	0.17	0.89	0.42	-			
ADP	Pearson's	0.43	0.22	-0.17	-0.21	0.37	0.45	0.18	-0.21	-0.30	-0.16	0.42	-0.12	0.26	-		
	p-value	0.29	0.60	0.68	0.62	0.37	0.26	0.66	0.61	0.48	0.71	0.30	0.78	0.54	-		
Cot	Pearson's	0.42	0.04	-0.19	-0.09	0.20	0.29	-0.13	-0.21	-0.19	-0.58	0.69	-0.49	-0.16	**0.79**	-	
	p-value	0.30	0.92	0.65	0.84	0.63	0.48	0.75	0.62	0.65	0.13	0.06	0.22	0.70	<0.05	-	
Bt	Pearson's	**0.97**	**0.77**	0.49	**-0.76**	**0.81**	**0.84**	0.45	0.47	0.38	-0.21	**0.89**	-0.25	0.42	0.54	0.60	-
	p-value	<0.05	<0.05	0.22	<0.05	<0.05	<0.05	0.26	0.24	0.35	0.62	<0.05	0.55	0.30	0.17	0.11	-

NOTE: **Bold** values represent significant correlation at the 0.05 level

LEGEND: NS - Number of samples; ED - Event duration (h); RD - Rainfall duration (h); P_{accum} - Accumulated precipitation (mm); RI - Rainfall intensity ($mm.h^{-1}$); RClass - Rainfall classification according to WHO (2008); V_{transp} - Volume of water transported (m^3); SRun - Surface runoff (m^3); Q_{base} - Base flow ($m^3.s^{-1}$); Q_{max} - Maximum flow ($m^3.s^{-1}$); ΔQ - Difference between Q_{max} and Q_{base} ($m^3.s^{-1}$); Rt - Rise time (h); Ft - Falling time (h); Crt - Critical time; Cot - Concentration time; Bt - Base time (h); ADP - Antecedent Dry Periods (day)

Then, in order to assess the most relevant hydrological characteristics, Cluster analysis was performed by method of nearest neighbor. Figure 34 shows dendrogram performed for the hydrological characteristics. It can be observed that four main groups are formed: (I) SRun and V_{transp}, (II) ΔQ and Q_{max}, (III) Rt/Ft and Q_{base} and (IV) Bt and ADP, which are grouped with RI afterward, forming the main hydrological characteristics. Effects category, RD, ED and P_{acum} had weak association.

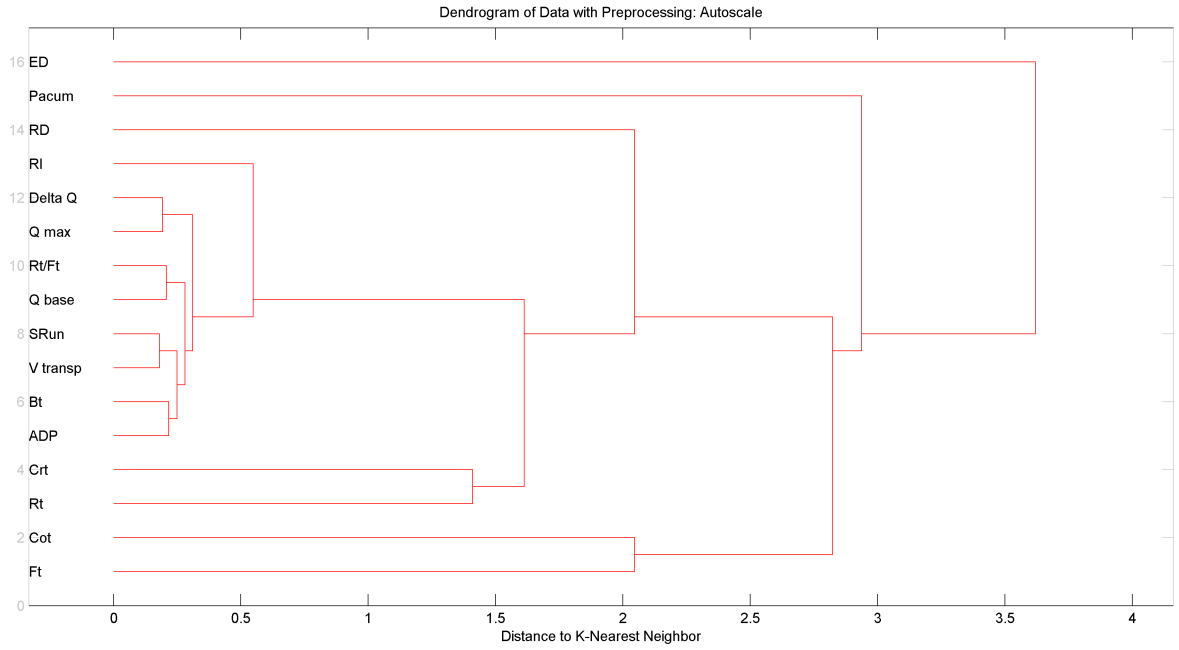

Figure 34 – Dendrogram of the hydrological characteristics measured in the rainfall episodes

LEGEND: ED - Event duration (h); RD - Rainfall duration (h); P_{accum} - Accumulated precipitation (mm); RI - Rainfall intensity ($mm.h^{-1}$); RClass - Rainfall classification according to WHO (2008); V_{transp} - Volume of water transported (m^3); SRun - Surface runoff (m^3); Q_{base} - Base flow ($m^3.s^{-1}$); Q_{max} - Maximum flow ($m^3.s^{-1}$); ΔQ - Difference between Q_{max} and Q_{base} ($m^3.s^{-1}$); Rt - Rise time (h); Ft - Falling time (h); Crt - Critical time; Cot - Concentration time; Bt - Base time (h); ADP - Antecedent Dry Periods (day)

Groups I and II present expected correlations because they are dependent. SRun is a part of V_{tranps} (Figure 35a), as well as, Q_{max} is a variable of ΔQ (Figure 35b). Group III present a relation between the flow category (Q_{base}) and effects (Rt/Ft) (Figure 35c). However Rt/Ft value vary in function of the rainfall. The rapid changes in the flow (or hydrographs times, in this case) can be explained by the small size of the drainage area (XIE et al., 2019), or even, due to narrow cross section areas. Finally, group IV present relation between ADP and Bt (Figure 35d), which can represent rainfall effects in the river system, favoured for the non occurrence of the rainfall. This group have positive correlation, suggesting that long periods without rainfall represent long Bt, that is, long time to river restore Q_{base}.

After that, these four groups formed an group with RI. Rainfall intensity indirectly represent the amount of water precipitated and duration. This parameter have negative significant correlation with Bt (-0.76, p-value < 0.05) and V_{tranps} (-0.74, p-value < 0.05), suggesting that intense rainfall will have short Bt and low V_{tranps}, in the other words, fast rainfall episodes. Therefore, the amount of pollution inputted into the river during rainfall episode can be will be dependent to the RI associated to the ADP in specific land use and soil occupation. For example, Xie et al. (2019) observed TP concentration lower than the standard limit in event with long ADP, suggesting that infiltration was favoured and, then, decreasing surface runoff to carry particulates.

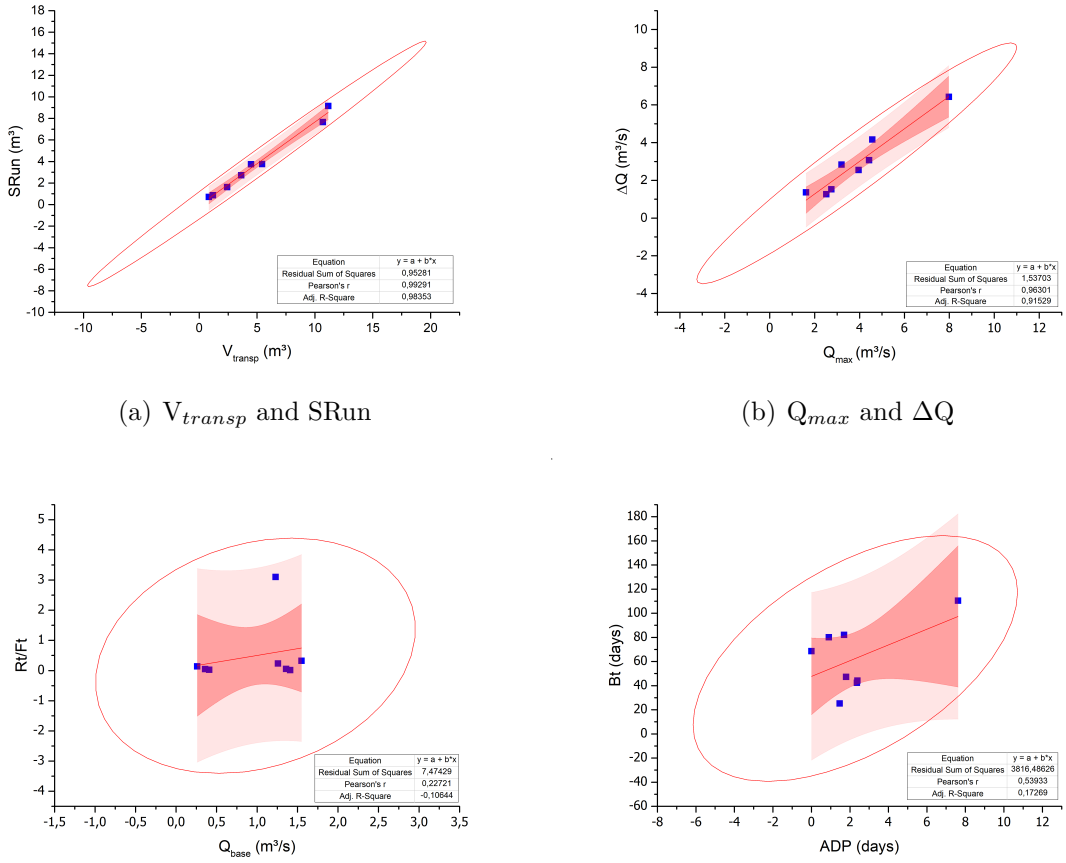

(a) V_{transp} and SRun

(b) Q_{max} and ΔQ

(c) Q_{base} and Rt/Ft

(d) ADP and Bt

Figure 35 – Linear Fit of the groups identified in the Cluster analysis

4.1.3 SUMMARY

In this section the hydrological characteristics influenced by the 5 rainfall monitored episodes were presented. The events E1, E2 and E4 allowed explore input and output of flow and pollution, for a proper assessment from diffuse and point sources. Rainfall classification using just intensity had moderate and light stages. However, hydrological characteristics showed big differences between rainfall episodes. Thus, using RD, RI and ΔQ, REClass proposed showed different types of rainfall, ranging from medium-to-high (E4-BA2) to medium (E2-BA1, E4-BA1, E5-BA2) to medium-to-low (E1-BA1, E1-BA2, E3-BA2) until low (E2-BA2).

PCA analysis showed rainfall episodes divided in four groups. They are formed under influence of the parameters of hydrological effect (Ft and Rt/Bt - E2-BA2), flow variations (Q_{base}, Q_{max}, ΔQ and P_{acumm} - E4-BA2), rainfall occurrence (RI - E1-BA1, E1-BA2, and E2-BA2) and external plus river effects (ADP, Bt and Ft - E3-BA2 and E5-BA2). These division highlight how much and potentially significant can different types of rainfall episodes result in significant impacts on the flow regime of a water body. Each isolated rainfall event is extremely dependent on the conditions that characterize it, but similar rainfalls tend to have the same response. Pollution transport will be dependent of the land use and soil occupation.

Furthermore, it was determined that 75% of the amount of water transported during a rainfall episode is from surface runoff. In this sense, about 25% of the initial rainfall can be infiltrate into the

soil, and remaining of the rainfall have influence on the water level variations. Thus, few proportions of rainfall amount and duration are enough to saturate the soil in BA1 (3.85-5.90 mm and 15-30 min) probably associated to the more percentage of permeable area and narrow cross section. Whereas, in BA2 big proportions of rainfall amount and duration are required, associated to the less percentage of the permeable area, favouring surface runoff.

Lastly, observing just hydrological characteristics other four groups were formed. Groups of SRun and V_{transp}, and ΔQ and Q_{max} have expected correlation because they are dependent variables. Group of Q_{base} and Rt/Bt indicate fast flow variations during the rainfall episode, which can be associated to the narrow cross section. And, the group of ADP and Bt indicate that long periods without rainfall represent long Bt or, in other words, long time to river restore the Q_{base}. Afterwards, all these parameters are grouped for the RI, which indirectly represent the amount and duration of the rainfall. Thus, intense rainfall produce fast rainfall episodes, with short Bt and low V_{transp}.

Therefore, the amount of pollution added to the river system during rainfall episode is dependent to the RI associated to the ADP associated to the in specific land use, being these hydrological parameters the most relevant characteristics to assess the pollution process of transport. Longer ADP can facilitate to the build-up pollution as more pollutant will be accumulated in surfaces and intense rainfalls can introduce this pollution into the river fastly, thus, the initial portion of the rainfall event is the crucial to the pollutant inputs from diffuse sources. This hypothesis must be evaluated considering pollutographs and EMC.

4.2 CONVENTIONAL WATER QUALITY PARAMETERS

"How much pollution is carried into the rivers during rainfall episodes?"

This section contains the assessment of the pollution quantity as consequence of the rainfall episodes, observing conventional water quality parameters. Firstly, river baseline will be presented in order to evaluate the river condition without rainfall influences. After that, water quality analysis will be performed considering four aspects: (i) pollutographs generated for each rainfall episodes for the traditional water quality parameters; (ii) EMC curves to identify the most relevant moment of the rainfall episode; (iii) the EMC values, observing baseflow and rainfall conditions; (iv) the control volume analysis.

4.2.1 BASELINE

The baseline campaign occurred without rainfall influence, with 6 days of ADP before campaign. The average flow in BA1 was 0.39 ± 0.02 $m^3.s^{-1}$, and in BA2 was 1.35 ± 0.02 $m^3.s^{-1}$, ensuring the representativeness of the base flow. Samples were numbered in a row according to the sampling time, as presented in Table 20.

Table 20 – Sample identification (ID) and sampling schedule in the baseline campaign

Sample ID	Date and Hour	Sample ID	Date and Hour
1	10/07/2019 18:00	13	11/07/2019 06:00
2	10/07/2019 19:00	14	11/07/2019 07:00
3	10/07/2019 20:00	15	11/07/2019 08:00
4	10/07/2019 21:00	16	11/07/2019 09:00
5	10/07/2019 22:00	17	11/07/2019 10:00
6	10/07/2019 23:00	18	11/07/2019 11:00
7	11/07/2019 00:01	19	11/07/2019 12:00
8	11/07/2019 01:00	20	11/07/2019 13:00
9	11/07/2019 02:00	21	11/07/2019 14:00
10	11/07/2019 03:00	22	11/07/2019 15:00
11	11/07/2019 04:00	23	11/07/2019 16:00
12	11/07/2019 05:00	24	11/07/2019 17:00

Baseline profile showed that concentration increase from BA1 to BA1-2 and BA2. BA1 had the lowest average values, whereas at BA2 these increased under WWTP outflow influence in BA1-2, as can be observed in Figure 36. This influence can be observed at the maximum average values of TN, N-NH_4^+, TP and PO_4^{3-} measured at BA1-2, typical residual of wastewater discharge. Thus, advection processes and self-cleaning capacity of the river probably allowed N and P concentration decrease until BA2. At BA2, DOC, COD, SS and turbidity showed the maximum average concentration, which is associated to complex degradation process of these parameters, being accumulated downstream the river. Dissolved fraction had lower concentration than total fraction, as expected. Table 21 summarize average (± standard deviation), maximum and minimum concentration (- with respective sample and sampling hour) in baseline campaign for conventional water quality parameters.

Thus, it is possible to assume that BA1 reflects potential water quality changes from NPS, whereas BA2 is strongly influenced by PS and the effects of the incremental area and flow. This pollution source introduce high amount of pollutant into the river. In the WWTP outflow, there was increase in the average concentration of 49%, 82%, 96%, and 99% respectively for turbidity, DOC, COD and SS, in relation to BA1. And, for TP, PO_4^{3-}, TN and N-NH_4^+ concentration increase in the order of 420%, 300%, 200% and 8033%, respectively, in relation to BA1. Therefore, although small WWTP located in BA1-2, the impact in the river is high.

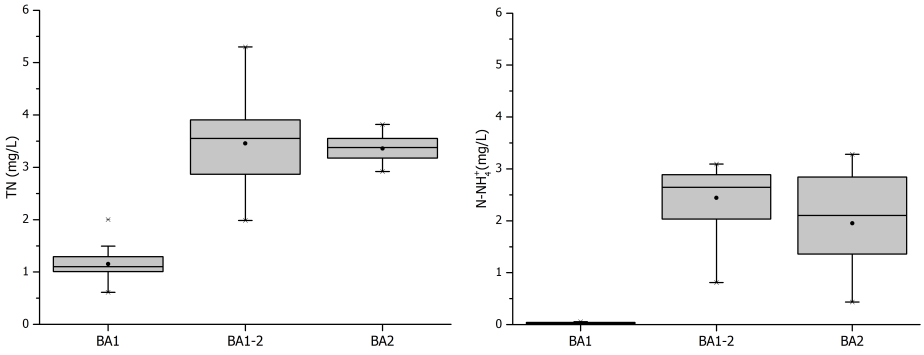

(a) TN box plot

(b) NH_4^+ box plot

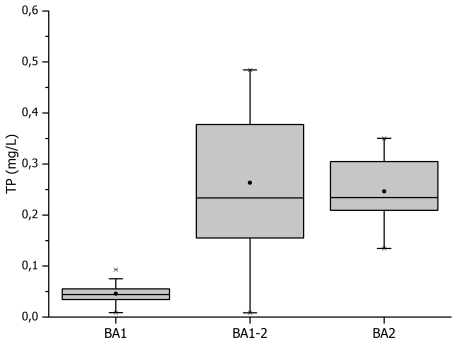

(c) TP box plot

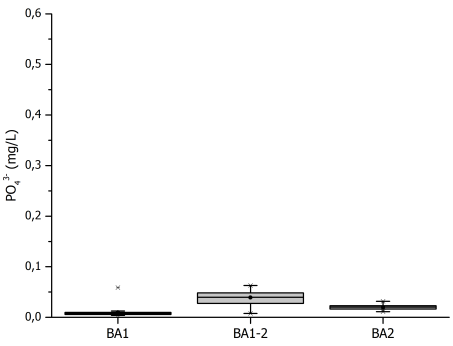

(d) PO_4^{3-} box plot

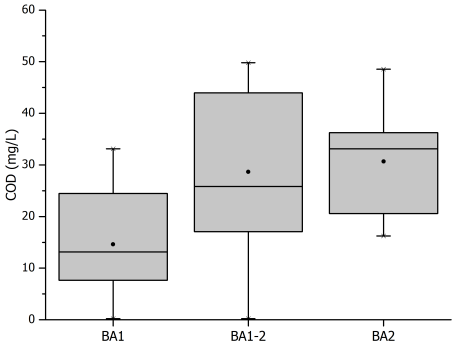

(e) COD box plot

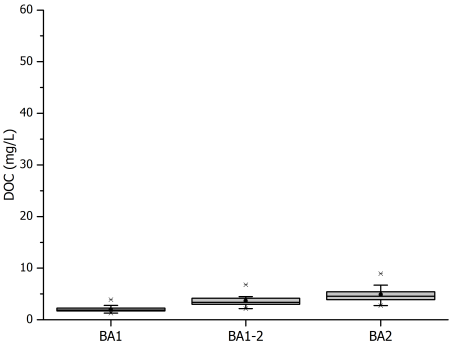

(f) DOC box plot

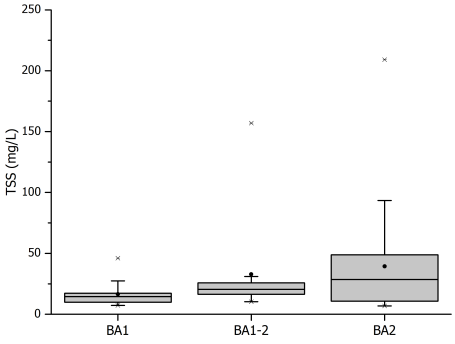

(g) SS box plot

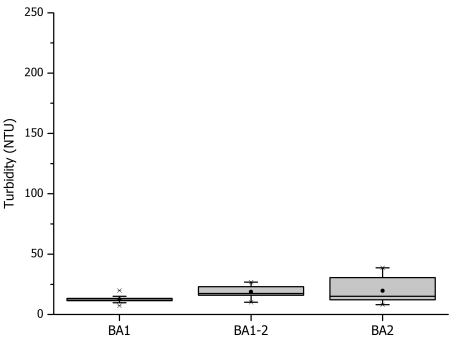

(h) Turbidity box plot

Figure 36 – Box plot of the conventional water quality parameters for baseline campaign

In detail, water quality variation along 24 hours observed were:

Table 21 – Average ($\overline{x}$) (± standard deviation (σ)), maximum (max) and minimum (min) concentration of the water quality parameters (WQP) in baseline campaign

WQP	Statistic	BA 1	BA 1-2	BA 2
TN ($mg.L^{-1}$)	$\overline{x} \pm \sigma$	1.15 ± 0.33	3.45 ± 0.79	3.36 ± 0.23
	max (S)	2.00 (S16 - 09h)	5.30 (S1 - 18h)	3.82 (S15 - 8h)
	min (S)	0.61 (S3 - 20h)	1.98 (S16 - 09h)	2.92 (S22 - 15h)
$N\text{-}NH_4^+$ ($mg.L^{-1}$)	$\overline{x} \pm \sigma$	0.03 ± 0.01	2.44 ± 0.57	1.95 ± 0.89
	max (S)	0.06 (S21 - 14h)	3.09 (S7 - 00h)	3.28 (S17 - 10h)
	min (S)	0.01 (S10 - 03h)	0.81 (S24 - 17h)	0.44 (S1 - 18h)
TP ($mg.L^{-1}$)	$\overline{x} \pm \sigma$	0.05 ± 0.02	0.26 ± 0.14	0.25 ± 0.06
	max (S)	0.09 (S12 - 05h)	0.48 (S6 - 23h)	0.35 (S17 - 10h)
	min (S)	0.01 (S6 - 23h)	0.01 (S16 - 09h)	0.13 (S24 - 17h)
PO_4^{3-} ($mg.L^{-1}$)	$\overline{x} \pm \sigma$	0.01 ± 0.01	0.04 ± 0.01	0.02 ± 0.01
	max (S)	0.06 (S5 - 22h)	0.06 (S7 - 00h)	0.03 (S16 - 09h)
	min (S)	0.004 (S21 - 14h)	0.01 (S24 - 17h)	0.01 (S23 - 16h)
COD ($mg.L^{-1}$)	$\overline{x} \pm \sigma$	14.61 ± 9.30	28.67 ± 15.71	30.67 ± 8.96
	max (S)	33.13 (S14 - 07h)	49.79 (S12 - 05h)	48.54 (S6 - 23h)
	min (S)	0.21 (S2 - 02h)	0.21 (S16 - 09h)	16.25 (S21 - 14h)
DOC ($mg.L^{-1}$)	$\overline{x} \pm \sigma$	2.01 ± 0.56	3.66 ± 1.06	4.90 ± 1.45
	max (S)	3.89 (S10 - 03h)	6.79 (S12 - 05h)	8.94 (S23 - 16h)
	min (S)	1.29 (S4 - 21h)	2.17 (S16 - 09h)	2.77 (S5 - 22h)
SS ($mg.L^{-1}$)	$\overline{x} \pm \sigma$	16.47 ± 9.18	32.84 ± 35.26	39.34 ± 45.83
	max (S)	46.00 (S7 - 00h)	157.00 (S1 - 18h)	209.00 (S7 - 00h)
	min (S)	7.25 (S24 - 17h)	10.25 (S24 - 17h)	6.80 (20 - 13h)
Turbidity (NTU)	$\overline{x} \pm \sigma$	12.67 ± 2.73	18.83 ± 4.41	19.70 ± 9.88
	max (S)	19.9 (S7 - 00h)	26.8 (S6 - 23h)	38.7 (S2 - 19h)
	min (S)	7.22 (S1 - 18h)	10.2 (S24 - 17h)	8.1 (S23 - 16h)

NOTE: S is the respective sample (- and sampling hour) where maximum or minimum concentration was measured

1. TN and $N\text{-}NH_4^+$ (Figure 37):
   - TN concentration in BA1 can be associated to nitrate present, due to low concentration of $N\text{-}NH_4^+$ measured.
   - Lower concentration of $N\text{-}NH_4^+$ measured in BA1 indicate absence of organic pollution in this site, and possibly a good water quality.
   - $N\text{-}NH_4^+$ concentration in BA1-2 increase during the night period of observation, from 20h until 06h with average of 2.87 ± 0.17 $mg.L^{-1}$; after that, at 07h, concentration decrease to 1.67 $mg.L^{-1}$.
   - At BA2, $N\text{-}NH_4^+$ behavior was opposite of BA1-2, which can be associated to advection process which spread pollution downstream plus self-cleaning capacity of the river and degradation process between two points.
   - TN had low concentration variation throughout campaign in BA1 and BA2. At BA1-2, TN behavior was similar to $N\text{-}NH_4^+$ behavior in the same site.
2. TP and PO_4^{3-} (Figure 38):
   - TP concentration were about 6 times lower than TN concentration.
   - TP and PO_4^{3-} behavior along 24 hours of monitoring was similar to TN: BA1 and BA2 had low concentration variation measured, and at BA1-2 during the night concentration were higher than during the day.

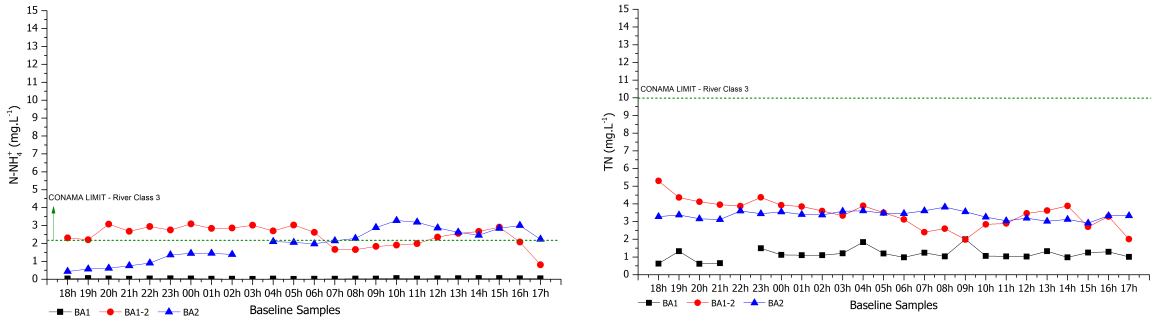

(a) $N\text{-}NH_4^+$ (b) TN

Figure 37 – $N\text{-}NH_4^+$ and TN concentration along baseline campaign

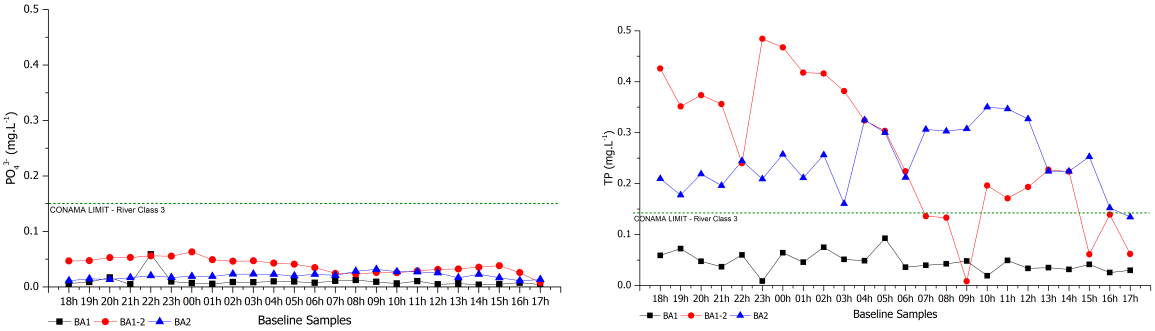

(a) PO_4^{3-} (b) TP

Figure 38 – PO_4^{3-} and TP concentration along baseline campaign

- TP and PO_4^{3-} concentration in BA2 were bigger than BA1 but lower than BA1-2, which can be associated to steady-state of pollutant receiving of the WWTP.
- PO_4^{3-} concentration represent about 20% of TP concentration measured.

3. COD and DOC (Figure 39):
   - DOC concentration represent about 15% of COD concentration measured.
   - COD showed wide variation during the monitoring campaign, without a clear pattern.
   - COD and DOC concentration were BA1 < BA1-2 < BA2 (Table 21), indicating pollutant accumulation in BA2 from the upstream sites.
   - As observed in the other parameters, COD and DOC concentration during the night were bigger than during the day at BA1-2, associated to WWTP outflow.
   - DOC had low concentration variation during all monitoring period in the three monitoring sites.
4. SS and Turbidity (Figure 40):
   - SS and turbidity had low values observed in the three monitoring sites, due to non occurrence of rainfall, and consequently not re-suspension of the particles.
   - For both parameters, concentration were BA1 < BA1-2 < BA2 (Table 21) without high variation in concentration during monitoring campaign.

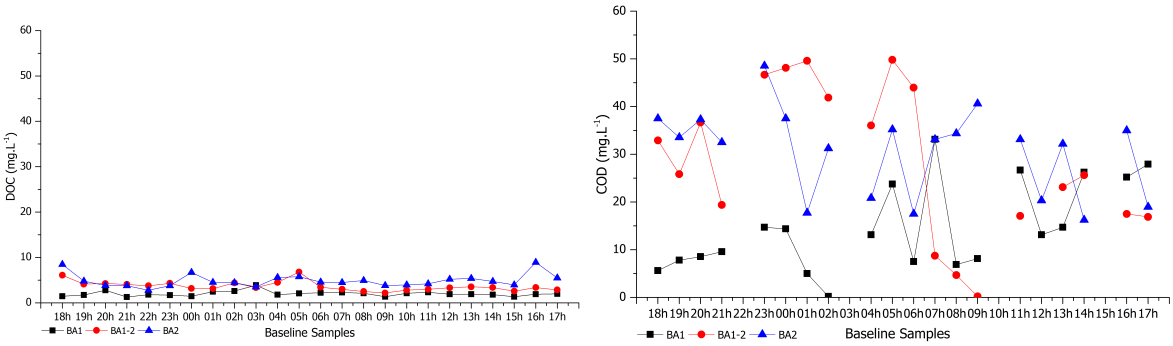

(a) DOC (b) COD

Figure 39 – DOC and COD concentration along baseline campaign

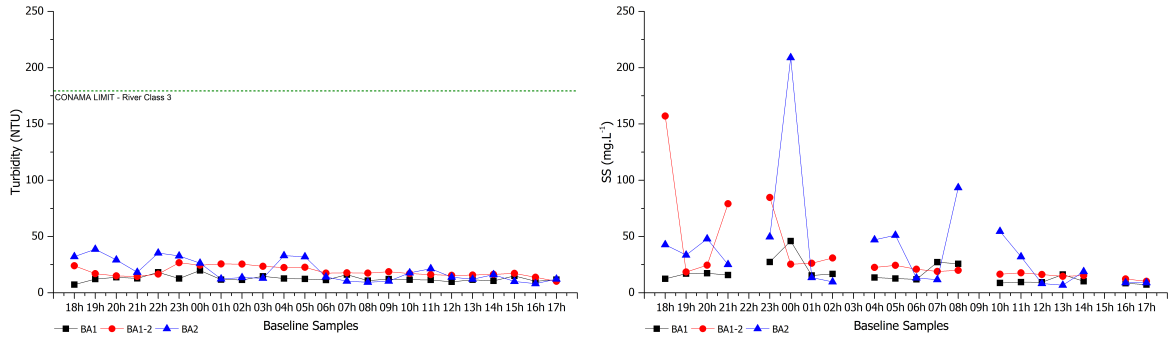

(a) Turbidity (b) SS

Figure 40 – Turbidity and SS concentration along baseline campaign

Therefore, it was possible to verify the WWTP influence on the water quality of the Barigui River at point BA1-2, under base flow conditions, where the concentrations of the key parameters had a considerable increase, suggestion water quality degradation. These impacts are carried naturally downstream of the river. A fraction of this pollution is susceptible to degradation, however another fraction is amplified, with the introduction of other point sources of pollution.

The river profile without rainfall influence can be considered constant over the 24 hours of observation. In addition, although the concentrations of TN and TP are higher than N-NH_4^+ and PO_4^{3-}, the dissolved fractions are more relevant to assess the level of pollution of the water bodies and, possibly, to support NPS identification than the total fractions, since the dissolved portion is the first fraction to be biodegraded (e.g. N-NH_4^+) and/or to react (e.g. PO_4^{3-}).

Thus, with baseline profile determined, in this research, the impacts of rainfall episodes into the river system can be properly addressed, specially to characterize NOS sources and diffuse pollution. More specifically, the dilution of these compounds, due to the greater introduction of water into the system than the pollutant, or the concentration increase of these pollutant by input of the diffuse source of pollution.

4.2.2 POLLUTOGRAPHS

For the 5 rainfall episodes monitored at BA1 and BA2, the conventional parameters of DOC, COD, TN, N-NH_4^+, TP, PO_4^{3-}, Turbidity and SS were analyzed. In BA1, there are three pollutographs

referring to E1, E2 and E4 (Figure 41), and for BA2, five referring to E1, E2, E3, E4 and E5 (Figure 42). In order to better analyze these results , it was establish an standard behavior considering hydrograph and flow. Table 22 summarizes patterns observed at each monitoring point for each measured water quality parameter, considering: [↗↘] pollutant pattern according to hydrograph pattern, that is increase and decrease with the flow; [↔] pollutant did not follow any pattern; [↘↔] initial high pollutant concentration, decreasing soon after and stabilized in low concentration; [↘↔↗] high concentration, decreasing soon after along the event, and increasing again in the end; [↗↔] initial low concentration, increasing soon after and remained high until the end; [↗↘↔] increase and decrease fastly in the beginning of the event, and stabilized in low concentration along the event; [↘↗] reverse pattern, that is concentration decrease during flow increasing, and concentration increase during flow decreasing.

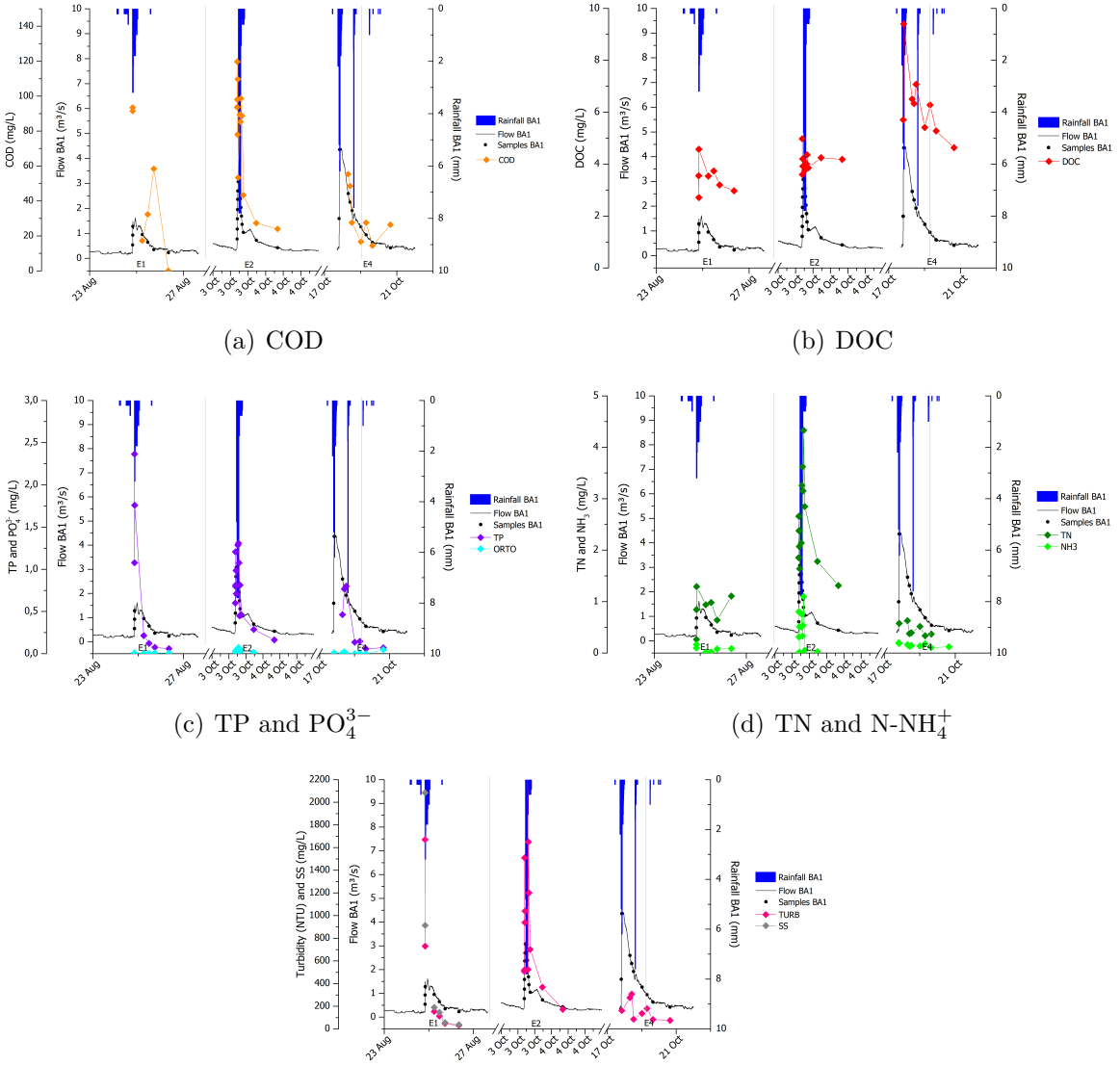

(a) COD

(b) DOC

(c) TP and PO_4^{3-}

(d) TN and N-NH_4^+

(e) SS and turbidity

Figure 41 – Pollutographs from BA1 monitoring site in E1, E2 and E4, respectively along the horizontal axis

According to Table 22, TP, PO_4^{3-}, turbidity and SS had a well-defined and direct pattern, being found in all observed events as function of increasing or decreasing flow conditions, as, for example TP [↗↘]. The same pattern was observed for turbidity and SS, with the exception of E1 at BA1. This may be related to the transport of particulate during rainfall events, and phosphorus affinity to the

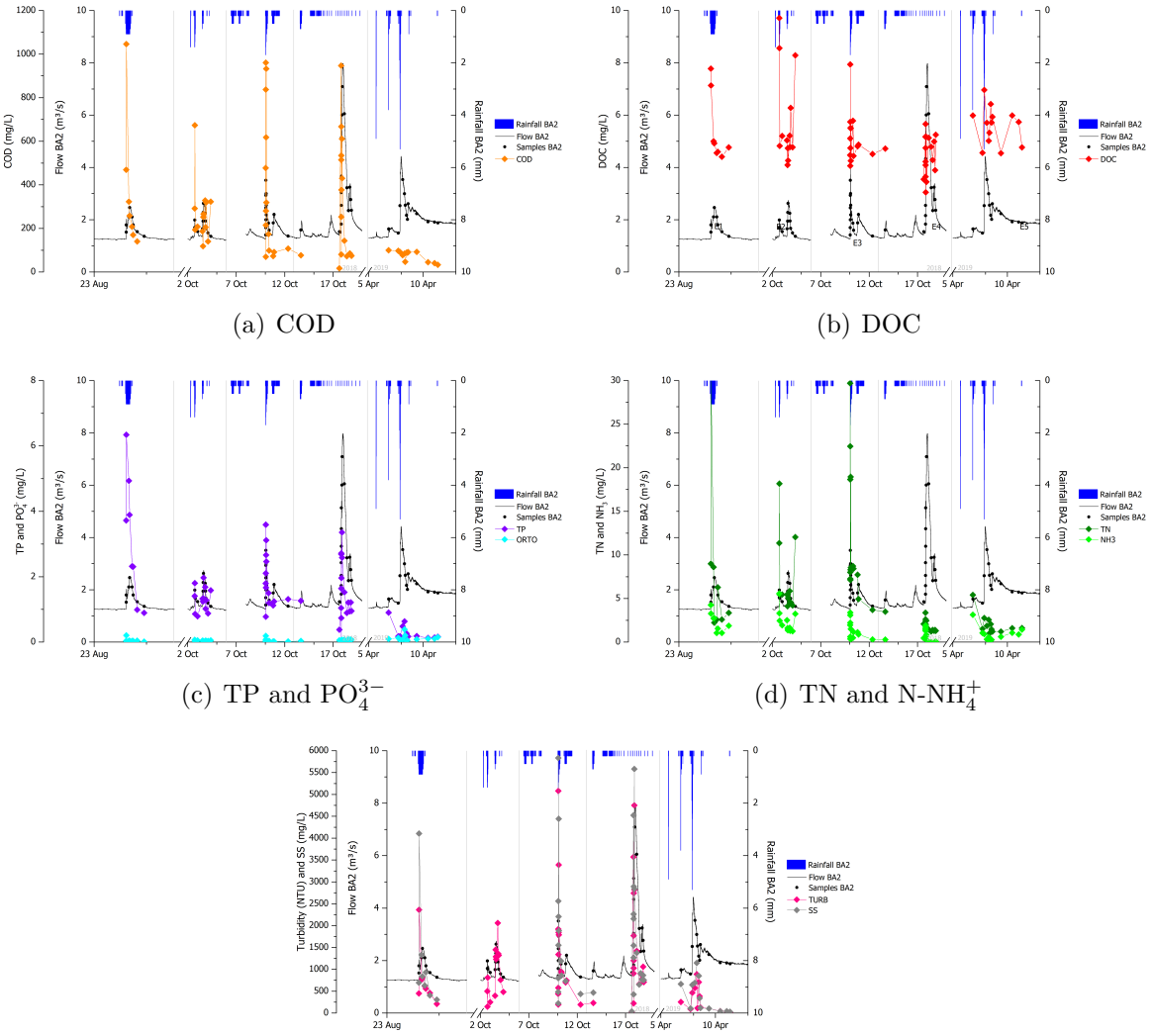

(a) COD

(b) DOC

(c) TP and PO_4^{3-}

(d) TN and N-NH_4^+

(e) SS and turbidity

Figure 42 – Pollutographs from BA2 monitoring site in E1, E2, E3, E4 and E5, respectively along the horizontal axis

Table 22 – Pollutographs pattern observed for the traditional water quality parameters during rainfall episodes monitored

		DOC (mg/L)	COD (mg/L)	TP (mg/L)	PO43- (mg/L)	TN (mg/L))	NH3 (mg/L)	Turbidity (NTU)	SS (mg/L)
E1	BA1	[↗↘]	[↘↔]	[↗↘]	[↔]	[↗↘]	[↔]	[↘↔]	[↘↔]
	BA2	[↘↔]	[↘↔]	[↗↘]	[↔]	[↗↘↔]	[↘↔]	[↗↘]	[↗↘]
E2	BA1	[↔]	[↔]	[↗↘]	[↔]	[↘↗]	[↔]	[↗↘]	
	BA2	[↘↔↗]	[↘↔]	[↗↘]	[↔]	[↘↔↗]	[↘↔↗]	[↗↘]	
E3	BA2	[↗↘]	[↗↘]	[↗↘]	[↔]	[↔]	[↗↘↔]	[↗↘]	[↗↘]
E4	BA1	[↗↘]	[↘↔]	[↗↘]	[↔]	[↔]	[↔]	[↗↘]	
	BA2	[↔]	[↗↘]	[↗↘]	[↔]	[↔]	[↗↘]	[↗↘]	[↗↘]
E5	BA2	[↗↔]	[↔]	[↗↘]	[↔]	[↔]	[↘↔]	[↗↘]	[↗↘]

particles. Mean TP values were higher in BA2 than in BA1, as expected. E1 at BA2 had a higher mean concentration of TP among events, with 3.17 ± 1.90 mg.L^{-1}. In this same event (E1), the highest concentration was measured in sample 2 (6.34 mg.L^{-1}), and the lowest in sample 8 (0.89 mg.L^{-1}). This was the highest measured concentration of P within all samples, probably associated with the rainfall

characteristic, classified as medium-to-low with low duration and high intensity, carrying pollutants into the water body. The lowest concentration measured was in sample 6 of E4 at point BA2, with 0.01 $mg.L^{-1}$. In this case, the sequence of events may have favored dilution effects.

The turbidity and SS followed the hydrograph pattern [↗↘]. Due to the large concentration changes, the standard deviation were high (Table 23). Unlike TP, there were not necessarily higher concentrations in BA2 than in BA1, as for example in E2. The highest average concentration measured for turbidity and SS was during E4, at BA2, with, respectively, 1,535.61 ± 1,291.97 NTU and 1,803.56 ± 1,527.52 $mg.L^{-1}$. The highest concentrations were measured always close to the peak of the event (Q_{max}). Although the highest averages were observed in E4, it was E3 that obtained the highest concentration of turbidity and SS, reaching 5,080 NTU and 5,835.38 $mg.L^{-1}$ of SS, both in sample 5. This may be associated with the magnitude of this rainfall episode, which had medium duration and light intensity, introducing constant mass into the system.

The PO_4^{3-}, the dissolved fraction of P, do not present any pattern [↔], remained stable (low standard deviation) at low concentrations of all rainfall episodes. This behavior may have been influenced by the high presence of particulate material in the system. The highest average concentration observed was in E5, with 0.12 ± 0.09 $mg.L^{-1}$. It was also in this event that the highest concentration was measured, in sample 5 with 0.39 $mg.L^{-1}$.

The TN showed an inverse pattern in E1 and E2. At point BA1 during E1 the concentrations followed the behavior of the hydrograph [↗↘], while during E2 the behavior was the opposite [↘↗], where the concentrations decreased with increasing flow and increased with decreasing flow. The highest concentration measured at this point was in sample 12 (4.33 $mg.L^{-1}$). This reverse pattern was observed only in this case and E2 showed higher average concentrations of TN than E1.

For point BA2 in E1, the TN concentration increased and decreased rapidly at the beginning of the event, like a pulse, and then remained stable throughout the rest of the event [↗↘↔]. The highest concentration was measured in sample 2 (30.58 $mg.L^{-1}$). During E2, at BA2, concentrations were high only at the beginning and at the end of the event (highest concentration measured in sample 2: 18.18 $mg.L^{-1}$), remaining low and constant throughout the entire event ↘↔↗ (lower concentration measured in sample 6: 4.12 $mg.L^{-1}$). For events E3 and E4, which were consecutive rain episodes, TN concentrations did not have any established pattern [↔].

Despite no predefined pattern, E3 also had high TN concentration and wide variation, with an average concentration of 11.07 ± 7.67 $mg.L^{-1}$, which may indicate that this event received great influence from the effects of upstream, such as effects of land use with higher concentration observed in sample 1 (29.71 $mg.L^{-1}$) and its mild occurrence. E4 had low concentrations throughout event and without great variations, with an average concentration of 0.46 ± 0.12 $mg.L^{-1}$ at point BA1 and 1.85 ± 0.61 $mg.L^{-1}$ at point BA2. For the E5, there was also no recognized pattern [↔], which may be associated with the long duration of the event, where the dilution effects are favored.

N-NH_4^+ at point BA1 did not show any pattern [↔] in any observed event. The average concentrations were the smallest measures with low standard deviation, indicating little variability during the events. Such behavior may be associated with the land use characteristics of the drainage area at point BA1, which indicate the absence of any point source of pollution that could favor the introduction of this compound directly to the water body. For point BA2, after the point of discharge from a sewage treatment plant, variations occur, however, without a single pattern for all rain episodes.

Only the E4 distribution of N-NH_4^+ followed the hydrograph pattern [↗↘]. For E1 and E5, concentrations were high at the beginning of the event and decreased, remaining constant until the end [↘↔], where both had their highest concentrations measured in sample 1 (4.26 $mg.L^{-1}$ in E1 and 3.14

mg.L^{-1} on E5). At E3, concentration increased and decreased rapidly at the beginning of the event and remained constant until the end in low concentrations [↗↘↔]. And the behavior of N-NH_4^+ in E2 was the same observed for TN, with high concentrations at the beginning and in the end of the rainfall episode, with low concentrations during the whole event [↘↔↗]. For this parameter, the average concentrations were higher at point BA2 than at point BA1, due to the influence of the discharge from the sewage treatment plant. However, these concentrations decrease throughout the consecutive event, with 2.23 ± 1.23 mg.L^{-1} in E2 (low rainfall), decreasing to 1.20 ± 1.03 in E3 (medium-to-low rainfall) and 0.81 ± 0.69 mg.L^{-1} in E4 (medium-to-high), which may indicate dilution effects.

The COD showed 3 types of behavior, where the most relevant was high concentrations at the beginning of the event, decreasing and remaining constant until the end of the event [↘↔]. This pattern was observed at E1 at both monitoring points, at E2 at point BA2, and at E4 at point BA1, where the highest concentrations were measured in the first samples collected. The highest concentration measured was 1,046 mg.L^{-1} at E1 point BA2, values similar to domestic sewage. E3 and E4 for point BA2 had a COD distribution following the pattern of the hydrograph [↗↘], probably associated with the amount of water volume transported during these consecutive events and the significant influence of the sewage treatment plant .

For these events (E3 and E4) the maximum measured concentrations are also close to those of domestic sewage, with 960.44 mg.L^{-1} in sample 5, and 947.11 mg.L^{-1} in sample 2, respectively. The station may have been compromised due to the excess volume of water caused by the rains. In this situation, generally the system can be operating through the by-pass mode, influencing the large contributions received in the water bodies, as observed. E2 at point BA1, and E5 at point BA2 has not been established any pattern [↔]. However, in these episodes, it was possible to observe a wide range of concentrations throughout the event, not following hydrograph pattern, but at high concentrations. The average concentrations for E2 at point BA1 were 78.43 ± 29.77 mg.L^{-1} and 75.18 ± 24.20 mg.L^{-1} during E5 at point BA2.

DOC also did not show a standard behavior, varying in each observed rainfall episode. The concentration followed the hydrograph pattern [↗↘] in E1 point BA1, E3 point BA2 and E4 point BA1. At the point BA2 during E5, concentrations increased during the rain event and remained constant [↗↔], where the highest concentration was measured in the sample 3, with 6.96 mg.L^{-1}. However, at the same point, during E1, concentration decreased and remained stable until the end of the event [↘↔], with the highest concentration measured in sample 1 (7.78 mg.L^{-1}) and lower in sample 7 (4.41 mg.L^{-1}).

The distribution of DOC concentration during E2 at point BA2 were the same as those observed for TN [↘↔↗], with an average of 5.83 ± 1.83 mg.L^{-1}, and the highest concentration of DOC measured between samples of 9.71 mg.L^{-1} in sample 1 of this event. During E2, at point BA1 was a constant behavior throughout the event [↔], average concentration of 4.09 ± 0.35 mg.L^{-1}. And, during E5, at point BA2, no defined pattern [↔] was also established, but the concentrations suffered great variations throughout the rain event, presenting an average concentration of 5.59 ± 0.72 mg.L^{-1}.

Table 23 summarizes the average concentrations (± standard deviation) of traditional water quality parameters measured in this work, for each observed event and monitoring point. In addition, the maximum and minimum values measured at the event are presented, and the respective sample in which that value was determined.

Table 23 – Average (± standard deviation), maximum (max) and minimum (min) concentration of the conventional water quality parameters for rainfall episodes monitored

	E1		E2		E3	E4		E5
	BA1	BA2	BA1	BA2	BA2	BA1	BA2	BA2
Flow ($m^3.s^{-1}$)	0.70 ± 0.37	1.84 ± 0.37	1.73 ± 0.81	1.86 ± 0.36	2.15 ± 0.63	1.77 ± 1.21	3.58 ± 1.67	2.20 ± 0.64
Max	1.28 (3)	2.46 (4)	3.07 (7)	2.63 (8)	3.51 (6)	4.36 (2)	7.09 (10)	3.53 (4)
Min	0.23 (7)	1.36 (8)	0.43 (15)	1.37 (13)	1.38 (14)	0.42 (9)	1.54 (1)	1.43 (11)
Turbidity (NTU)	457.68 ± 648.84	778.88 ± 666.92	1213.31 ± 1035.62	927.08 ± 569.64	1355.00 ± 1344.32	163.39 ± 88.12	1535.61 ± 1291.97	293.92 ± 286.07
Max	1670 (1)	2360 (2)	3540 (8)	2060 (9)	5080 (5)	307.00 (4)	4750 (9)	889 (5)
Min	30.60 (7)	209 (8)	172 (15)	146 (2)	194 (2)	76.00 (9)	32.70 (1)	22.60 (13)
DOC ($mg.L^{-1}$)	3.47 ± 0.60	5.39 ± 1.30	4.09 ± 0.35	5.83 ± 1.83	5.10 ± 0.95	6.29 ± 1.38	4.44 ± 0.78	5.59 ± 0.72
Max	4.57 (3)	7.78 (1)	4.98 (2)	9.71 (1)	7.94 (4)	9.39 (2)	5.66 (4)	6.96 (3)
Min	2.71 (2)	4.41 (7)	3.60 (3)	4.09 (6)	4.06 (2)	4.63 (9)	3.05 (8)	4.54 (10)
COD ($mg.L^{-1}$)	48.83 ± 38.84	373.62 ± 316.27	78.43 ± 29.77	269.85 ± 139.29	355.40 ± 328.52	30.94 ± 15.41	325.84 ± 282.50	75.18 ± 24.20
Max	93.42 (2)	1046 (2)	119.67 (2)	673.78 (2)	960.44 (5)	55.35 (3)	947.11 (2)	99.82 (1)
Min	0.08 (7)	140.44 (7)	24.00 (15)	118.22 (6)	69.67 (2)	14.43 (8)	16.90 (1)	33.24 (13)
TP ($mg.L^{-1}$)	0.81 ± 0.94	3.17 ± 1.90	0.78 ± 0.36	1.32 ± 0.37	1.96 ± 0.92	0.35 ± 0.33	1.49 ± 0.94	0.29 ± 0.24
Max	2.36 (1)	6.34 (2)	1.31 (9)	1.97 (8)	3.59 (5)	0.80 (5)	3.36 (9)	0.90 (1)
Min	0.06 (7)	0.89 (8)	0.16 (15)	0.79 (4)	0.78 (2)	0.06 (8)	0.01 (6)	0.13 (11)
PO_4^{3-} ($mg.L^{-1}$)	0.007 ± 0.002	0.05 ± 0.06	0.03 ± 0.02	0.04 ± 0.01	0.04 ± 0.05	0.01 ± 0.015	0.05 ± 0.02	0.12 ± 0.09
Max	0.01 (6)	0.203 (2)	0.074 (9)	0.065 (1)	0.186 (4)	0.05 (9)	0.081 (13)	0.39 (5)
Min	0.003 (5)	0.013 (8)	0.012 (10)	0.019 (3)	0.001 (7)	0.001 (6)	0.012 (2)	0.03 (7)
TN ($mg.L^{-1}$)	0.87 ± 0.33	8.15 ± 9.47	2.53 ± 0.84	7.06 ± 4.20	11.07 ± 7.67	0.46 ± 0.12	1.85 ± 0.61	2.02 ± 1.19
Max	1.29 (3)	30.58 (2)	4.33 (12)	18.18 (2)	29.71 (1)	0.63 (3)	3.37 (2)	5.41 (1)
Min	0.26 (1)	2.24 (4)	1.31 (15)	4.12 (6)	3.49 (15)	0.34 (7)	1.22 (12)	1.00 (6)
NH_4^+ ($mg.L^{-1}$)	0.08 ± 0.06	2.32 ± 1.14	0.45 ± 0.35	2.23 ± 1.23	1.20 ± 1.03	0.15 ± 0.03	0.81 ± 0.69	0.90 ± 0.80
Max	0.17 (1)	4.26 (1)	1.10 (12)	5.56 (1)	3.38 (4)	0.20 (1)	1.90 (7)	3.14 (1)
Min	0.01 (4)	1.05 (5)	0.01 (5)	1.25 (12)	0.29 (15)	0.11 (8)	0.003 (12)	0.17 (6)
SS ($mg.L^{-1}$)	571.01 ± 810.42	1156.44 ± 1233.37			1690.93 ± 1644.60		1803.56 ± 1527.52	397.82 ± 385.19
Max	2084 (1)	4105 (2)			5835.38 (5)		5581.50 (9)	1146.67 (5)
Min	37.50 (7)	306.98 (8)			222.50 (2)		38.50 (1)	27.63 (13)

4.2.3 EMC

The EMC assessment is very a versatile information, considering that represents a weighted average of the received pollutant concentration during a rainfall episode, and therefore, can be used to to estimate the total amount of pollutant (ton.day^{-1}) introduced into the water body. The EMC curve, on the other hand, is a way to represent graphically the behavior of the introduction of these pollutants into the river during rainfall event, being possible to estimate rainfall moment that the greatest supply of pollutant occurs, and to detect the temporal addition of these pollutants.

Table 24 summarizes the EMC values calculated for WQP during the rainfall events. As expected, at point BA1 the input of pollutants was less than point BA2, as consequence of land use differences.

Table 24 – EMC values for the rainfall episodes monitored in BA1 and BA2

EMC		DOC	COD	TP	PO_4^{3-}	TN	NH_4^+	Turbidity	SS
E1	BA1	3.63	39.38	0.98	0.00	1.03	0.05	369.70	461.62
	BA2	5.34	331.59	3.32	0.06	8.87	2.32	805.65	1181.95
E2	BA1	3.14	77.15	0.83	0.02	2.37	0.35	1230.96	
	BA2	5.71	274.19	1.36	0.04	6.97	2.16	1094.45	
E3	BA2	5.09	342.04	1.95	0.03	10.23	1.02	1445.72	1655.88
E4	BA1	7.06	23.36	0.30	0.01	0.44	0.16	169.36	
	BA2	4.40	327.14	1.75	0.05	1.82	0.67	1855.28	2115.96
E5	BA2	5.62	76.77	0.30	0.12	1.85	0.71	342.08	420.41

NOTE: Turbidity (NTU); Other parameters have unit of mg.L^{-1}

Among rainfall events monitored in BA1, E2 had the highest EMC values, with the exception of DOC in E4. E2 had low ADP, classified as an medium event, but producing high EMC values of COD (274.19 mg.L^{-1}) and turbidity (1,230.96 NTU). DOC, TP and TN that had an EMC of 5.71 mg.L^{-1}, 1.36 mg.L^{-1}, and 6.97 mg.L^{-1} represent a contribution of approximately, 2.500, 670 and 1.900 ton.year^{-1} of C, N and P, respectively. The measured values increase about 1,800% from point BA1 to point BA2, indicating that the change in land use between points have a great influence on this increasing, via superficial runoff.

At point BA2, E3 had the highest EMC values, despite being consecutive event (ADP of 1.7 d). However, as point BA2 is influenced by a WWTP, the high EMC values on consecutive rainfall episodes can be associated to the overflow during these events. C, N, and P contribution in this event, corresponds to about 9,000, 18,000 and 3,500 ton.year^{-1}. These pollutants were inserted into the system during rainfall events, and it will remain there, being possibly slowly assimilated by the aquatic system. The impact of these pollutants introduction exists, but it is not immediate, because dilution process is favoured during rainfall episode. However, in long-term effects, downstream of BA2, these pollutants remains in the system, which can cause relevant impacts further. Therefore, it is important to determine the period of greatest pollutant input in the river, in order to be reduced, using for example BMPs.

Figure 43 shows the EMC curves of points BA1 and BA2 for the conventional WQP measured. The curves were classified into three zones, according to Metadier and Bertrand-Krajewski (2012) and schematized in Figure 7. Curve located at zone A indicates concentration of the pollutant observed (more mass in less volume), while the curve located at zone C indicates dilution of the observed pollutant (less mass in more transported volume). Curve that is located at zone B indicates that concentration distribution was proportional to the water transport during the rain event. It is also possible that, there is inversion on the curvature curve, indicating changing in the input of pollutant along rainfall events.

It is possible to observe that there was no establish pattern observed in curves distribution, as observed in the pollutographs analysis of the polygraphs (Table 22). Only E1-BA1 (medium-to-low events)

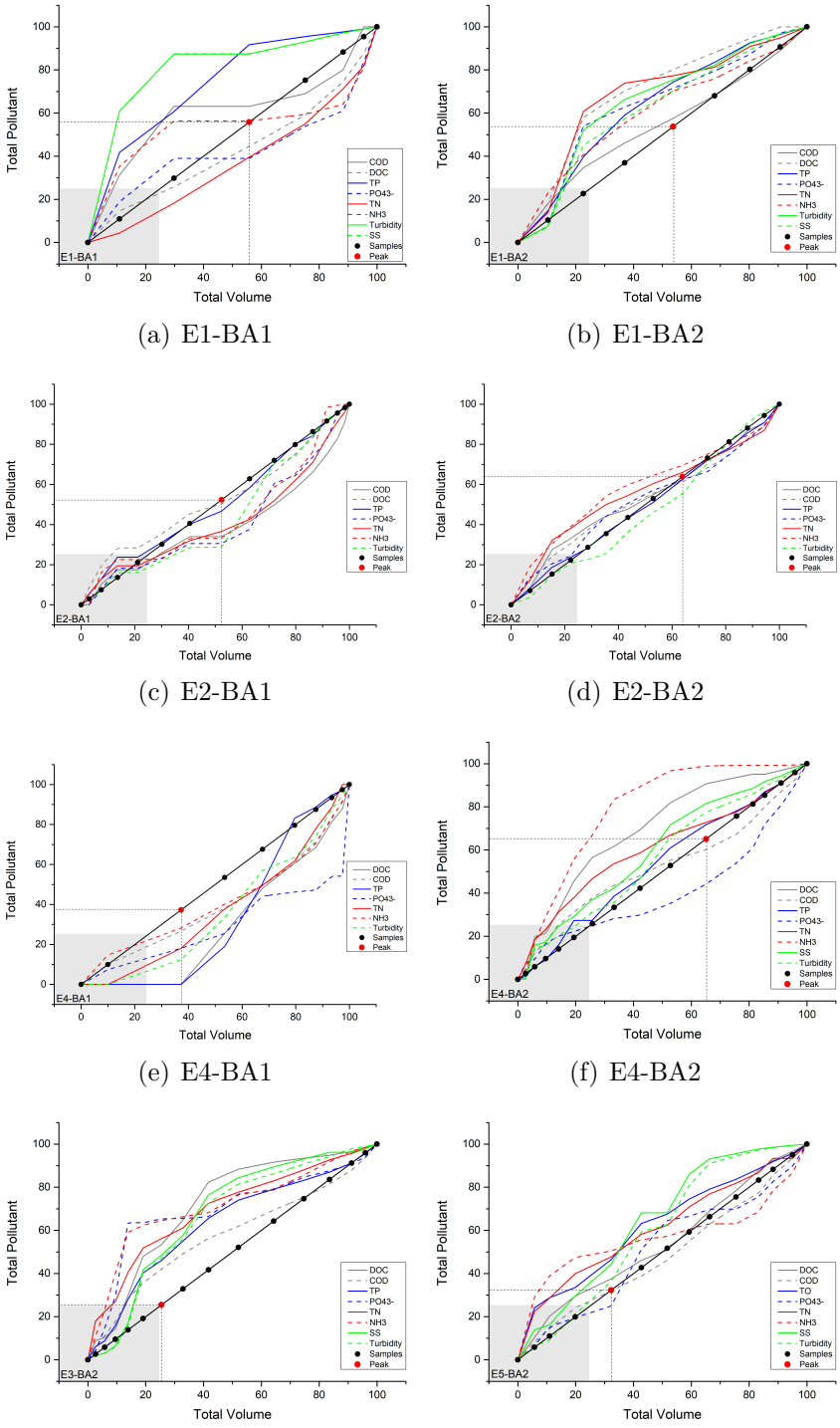

(a) E1-BA1 (b) E1-BA2

(c) E2-BA1 (d) E2-BA2

(e) E4-BA1 (f) E4-BA2

(g) E3-BA2 (h) E5-BA2

Figure 43 – EMC curves during rainfall episodes in BA1 and BA2

has some curves located in zone A, while in events E2-BA1 and E4-BA1 (both medium events), curves are located in zone C. This indicates that at point BA1, with greater influence of vegetated area than urbanization, pollutants inserted in the system during rainfall events, in general, are diluted. However, for events analyzed in point BA2, curves were usually located in zone A, indicating greater mass input into the system during rain events, that is, additional pollutant concentration. The events E1 and E3, classified as medium-to-low, have the distribution of similar curves, with all located in zone A. E2 and

E5, classified as low and medium events, have a variable distribution, with curves very close to the zone B and changes in concavity. E4 (medium-to-high), which was the largest monitored event, has curves in zone A with wide concavity, and two curves in zone C (PO_4^{3-} and COD).

Moreover, it is possible to observe that the peak of the event was identified in red point on the line that represents samples. Just, events E3-BA2, E4-BA1 and E5-BA2 have their maximum before 40% of the event. Table 25 summarizes the proportion of the pollution input up to maximum peak of the rainfall event.

Table 25 – EMC values in the peak of each rainfall episode, in BA1 and BA2

Proportional EMC		Peak Sample	DOC	COD	TP	PO43-	TN	NH4+	Turbidez	SS
E1	BA1	3	44.59	63.10	91.65	38.96	39.51	56.35	87.40	87.51
	BA2	4	80.19	57.59	74.42	71.50	77.32	70.25	75.43	70.48
E2	BA1	7	51.08	34.70	47.79	31.25	37.21	34.19	30.78	
	BA2	8	62.40	61.24	62.40	62.33	65.94	69.45	55.18	
E3	BA2	6	53.26	41.93	45.99	65.34	56.14	64.51	46.98	48.37
E4	BA1	2	0.00	26.66	0.00	18.05	18.05	28.53	12.39	
	BA2	10	90.72	60.16	71.79	44.25	72.82	98.95	81.58	77.53
E5	BA2	4	37.48	31.94	46.37	24.94	47.65	50.45	44.15	36.22

Pollutant peak occurred almost in the middle of the rainfall events. About 50% of the WQP were transported until the peak of events, and with exception of E2-BA1, E4-BA1 and E5-BA2. Other rainfall events had, on average, more than 50% of all pollutants carried along with. E1-BA2 (medium-to-low) and E4-BA2 (medium-to-high) had, approximately, 72% and 74% of the pollutant transported until the peak sample

It was possible to observed that EMC values helps to compare distinct rainfall episodes between them, simplifying land use association with pollutant occurrence. However, the periods of rainfall are essential to determine the most important moment which in this case represent the first 50% of the rainfall episodes, mainly in BA2 than in BA1. Thus, BMPs can be addressed to reduce this initial contribution, specifically in areas more urbanized. Occurrence of consecutive rainfall (less ADP) smooth this contribution, favoring dilution effects.

4.2.4 BASELINE AND RAINFALL EPISODES

In the five NPS events collected were observed the conventional WQP. They can be divided in physical and chemical categories: (i) physical: SS and Turbidity, and (ii) chemical: COD, TN and TP, which represents total fractions, and DOC, N-NH_4^+ and PO_4^{3-} which representing dissolved fractions. To identify the amount of pollutant transported during rainfall episodes EMCs values were compared to the EMC from baseline conditions, and to evaluate potential differences between rainfall episodes, load values were compared with baseline load, as well. Figure 44 shows the overall EMC and load values for the WQP measure in the rainfall episodes and baseline.

It can be observed baseline concentration and load were low for all WQP, as expected, indicating that rainfall episodes introduces high quantity of pollutants into the rivers. Turbidity and SS have the highest EMC and load in both monitoring sites, followed by COD. For these physical parameters, both EMC and load indicates the increased contribution through events E2, E3 and E4, being these parameters clearly associated to the NPS processes. Distinctly, COD EMC values indicate similar values along rainfall episodes on BA2, while COD loads indicate that E3 and E4 had higher magnitude in comparison to other

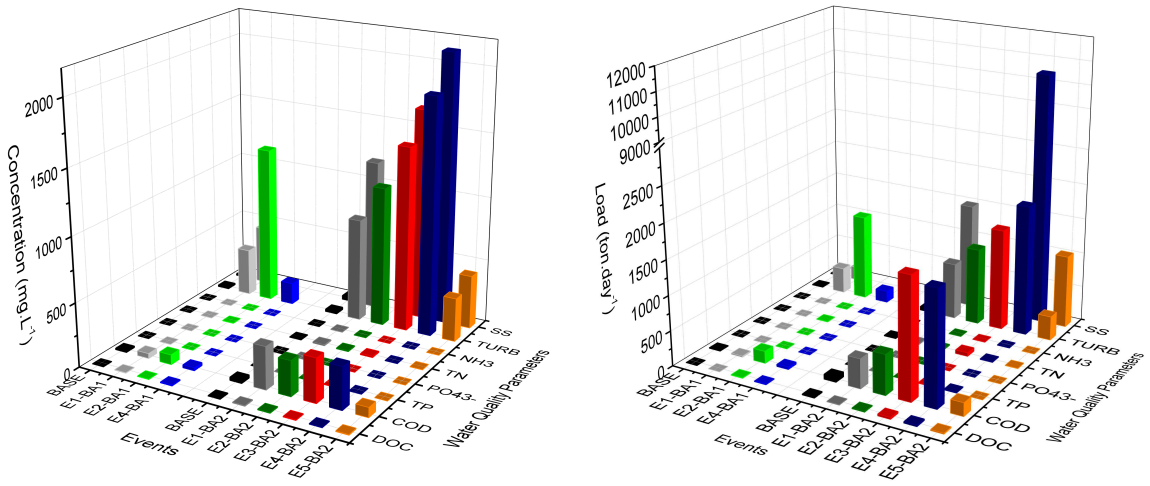

(a) EMC (mg.L^{-1}) (b) Load (ton.day^{-1})

Figure 44 – Overall EMC and load values for the WQP measured in the five diffuse pollution events and baseline

events, suggesting that consecutive rainfall induced more input of COD into the river system. This can be related to the WWTP before BA2, which suffers overflow with many rainfall episodes occurrence.

For the other chemical WQP, both EMC and load had lower values, indicating that pollutant inputs during rainfall episodes is more related to SS and COD . Overall, EMC values and loads were bigger in BA2 than BA1, as expected. The differences between rainfall episodes are associated to specific hydrological characteristics of each event. These details will be explored forward.

4.2.4.1 BA1

BA1 represent an drainage area of 57.8 km^2, where the biggest proportion is covered by vegetated area (35.9 km^2). The second most relevant land use is pasture (14.0 km^2), followed by residential urban area (3.4 km^2) and agriculture (3.2 km^2). This composition characterize the area as preserved drainage area, without significative urban influence. Baseline measurements corroborate to that, as:

- Low concentration of N-NH_4^+ (0.03 $\pm$ 0.01 mg.L^{-1}), which represent the recent organic content and/or inputs into the system
- Low concentration of SS (16.47 $\pm$ 9.18 mg.L^{-1}) and Turbidity (12.67 $\pm$ 2.73 NTU), which indicate the baseline condition of the system
- Low concentration of COD (14.61 $\pm$ 9.30 mg.L^{-1}) and DOC (2.01 $\pm$ 0.56 mg.L^{-1}), which suggest low present of organic content
- Concentrations as required by (CONAMA, 2005) for river class 3.

However, during the rainfall episodes, some changes can be observed. Figure 45 shows the differences between EMC rainfall and baseline, respectively. Each color bar represent a rainfall episode monitored in BA1. The main introduction are observed in turbidity and COD. Almost all WQP increased during rainfall, with exception in E1 for PO_4^{3-} and TN.

The event E1 represent a medium-to-low episode, which in comparison to the baseline, had increase in WQP concentration. The exception were PO_4^{3-} and TN, where negative values indicate that

dilution effects were more pronounced than mass introduction. TP had the highest input observed, probably due to land use associated to the ADP of 2.39 days.

The event E2 is a medium episode, bigger than E1, driven by high RI and medium ΔQ. This event produced positive input of mass into the system for all WQP. The high introduction observed is related to the intense rainfall observed, which contribute to the fastly input of mass accumulated. Also, land use had influence in the mass transport into the system, considering that are more permeable portion of land able to be transported by erosion processes.

The event E4 also is a medium episode, however classified as medium in all hydrological characteristics. With exception of TN, all WQP were input into the system. The differences between baseline and rainfall episodes were smaller than E2, which is related to the set of samples analyzed, which correspond the hydrograph recession. Moreover, E4 was a third consecutive rainfall occurred in October 2018. Rainfall episode with low ADP can transport less pollutant mass, due to the low time to accumulate pollution to be washed-off.

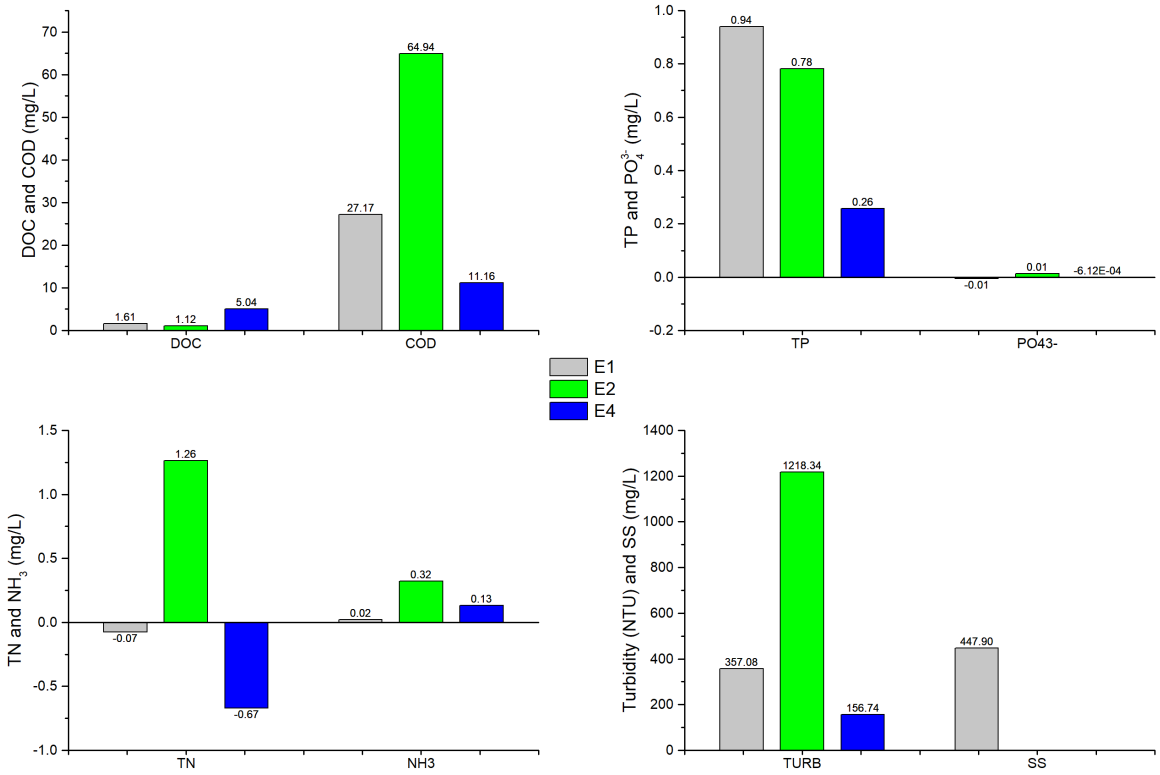

Figure 45 – EMC changes in BA1 during rainfall episodes. Positive values indicates input mass and negative values indicate dilution effects.

NOTE: Gray bars represent E1, green bars represent E2, and blue bars represent E4. E3 and E5 did not have collect in this site.

Overall, it can be observed that rainfall episodes monitored in BA1 introduced mass pollutant into the river. These variation showed that during rainfall episodes, river classification according to (CONAMA, 2005) was not attended. The total fraction were more pronounced than dissolved one, probably due to physical transport of particulate and pollution from upstream. However, the concentration magnitude suggests land use influence in BA1 drainage area: high TN and TP input associated to agriculture effects, turbidity associated to vegetated area sensitive to erosion, and low NH_4^+ associated to the low impact of the urban area.

4.2.4.2 BA2

BA2 have an incremental area of 45.9 km^2. The predominant land use are vegetation area (18.4 km^2), pasture (11.2 km^2), as similarly observed in BA1, followed by residential area (10.6 km^2) and agriculture (4.7 km^2). These values represent an increase of 0.2% in pasture areas, 4.7% in agriculture areas and 17.2% in the residential urban areas, with decrease of 22.0% in vegetation areas. The observed differences can reflect decrease in the water quality, mainly during rainfall episodes, due to more potential PS pollution on the incremental area.

Furthermore, BA2 received influence of the one wastewater treatment plant (São Jorge WWTP) operated by Sanepar. During the baseline event, WWTP outflow was monitored along 24 hours of measurements. The WQP measured showed:

- three times more input of N and five times more input of P than BA1, with average of 3.45 ± 0.79 $mg.L^{-1}$ and 0.26 ± 0.14 $mg.L^{-1}$, respectively for TN and TP.
- 81 times more input of N-NH_4^+ than BA1, with average of 2.44 ± 0.57 $mg.L^{-1}$.
- almost double increase in the organic contents, with average of 25.71 ± 20.21 $mg.L^{-1}$ of COD and 3.66 ± 1.06 $mg.L^{-1}$ of DOC
- higher suspended solids input, with more volatile fractions

These values indicate the WWTP influence in the river system. However, river classification remains in accordance to the establish in the (CONAMA, 2005) for River Class 3. As observed in BA1, during rainfall episodes there were changes in river water quality in BA2 too. Figure 46 shows the differences between EMC rainfall and EMC baseline measured in BA2. Each color bar represent a rainfall episode monitored in BA2. E1, E2 and E4 also were measured in BA1.

It can be observed that, concentration measured in BA2 are bigger than in BA1, as expected. BA2 received influence of BA1 drainage area, incremental drainage area with distinct land uses, and WWTP outflow. The most visible inputs are related to turbidity, SS and COD. Dissolved water quality parameters has difference kind behavior, that can be related to the rainfall characteristics such as ΔQ and ADP, because they are not associated to a particle, but available in the river systems in their ionic state.

The event E1 was a medium-to-low rainfall episodes, driven by high RI. COD and TP EMC had the biggest inputs into the system. This can be associated to ADP and land use composition, with enough time to accumulate pollutant in impervious surface.

Events E2, E3 and E4 were consecutive rainfall episodes, which justify increases in TP, COD, turbidity and SS. E2 was a low rainfall episode, driven by low RI and medium RD, introducing pollutant slowly over time. E3 was a medium-to-low rainfall episode, driven by medium RD and low RI, also introducing mass slowly over time, also receiving influence from BA1. E4 was a medium-to-high rainfall episode, driven by high RD and low RI. This third episode occurred in a watershed saturated of water along time, therefore rainfall impact with high duration produce high water transport, being dilution effects favored, such as in PO_4^{3-}, N-NH_4^+, DOC and TN EMC. The amount of TP, COD, turbidity and SS continue being input in the system, probably associated to the land use characteristics. Some samples collected in BA2 had black coloration, with oil aspect and sewage smell.

E5 was a medium rainfall episode, driven by high RD and low RI, that is, a rainfall distributed along the time. This episode had the highest ADP, indicating potential for pollutant accumulation, and at the same time, the highest V_{transp}, favoring dilution, and consequently, low EMC values observed.

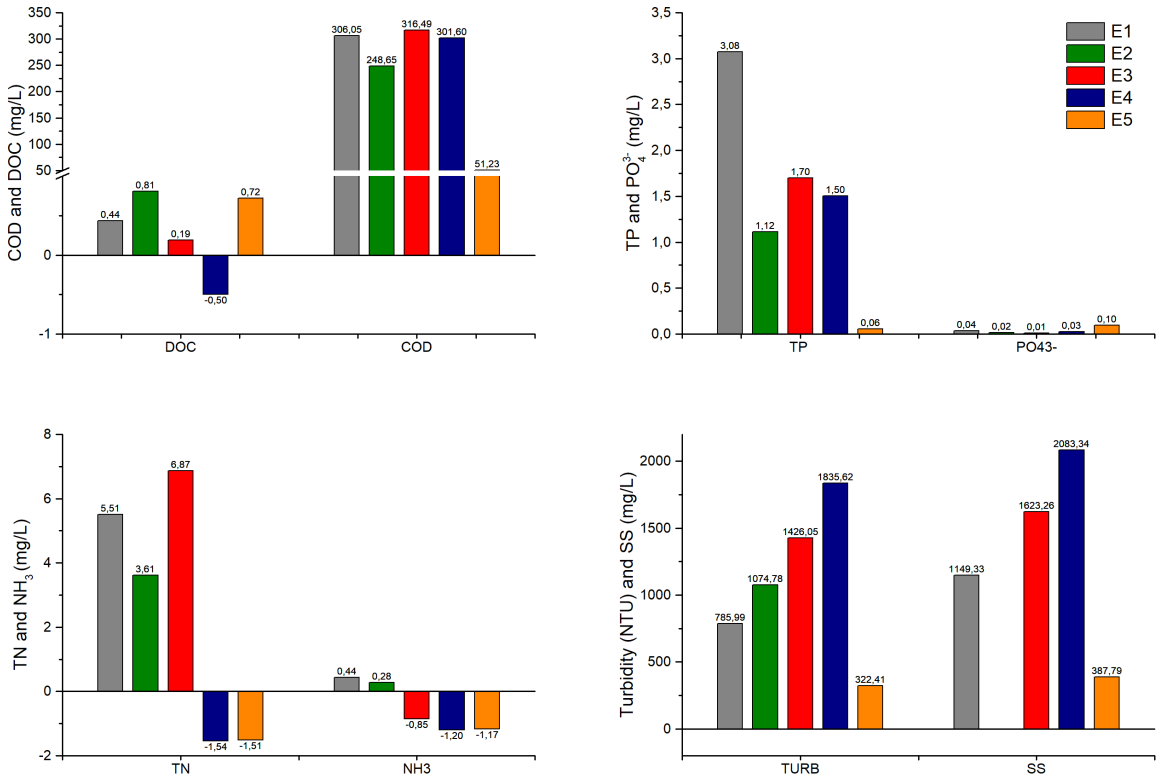

Figure 46 – EMC changes in BA2 during rainfall episodes monitored. Positive values indicate input mass and negative values indicate dilution effects

NOTE: Dark grey bar represents E1, dark green bar represents E2, red bar represents E3, dark blue bar represents E4 and orange bar represents E5.

Only TN and NH_4^+ EMC had negative values, while other WQP were positive, suggesting that mass were introduced into the river system despite the long rainfall characteristics.

Overall, during all these rainfall episodes measured in BA2, river classification is practically not attended. The exception are dissolved fractions (PO_4^{3-} and NH_4^+), TP on E5, and TN on E4 and E5. It is important to highlight that COD had high concentration in all rainfall events monitored, indicating urbanization influence. TP showed higher values suggesting effects from upstream land use of vegetated areas or agriculture practices. Therefore, changes between BA1 and BA2 probably contribute to the differences in the input. The slight increase of urbanization areas had influence in SS, COD and DOC increases

4.2.5 CONTROL VOLUME: BA2 - BA1

In order to understand how incremental area contribute to the pollution input into the system during rainfall events, will be considered difference between BA2 and BA1 EMCs. Figure 47 shows pollutant increment between BA1 and BA2 per event for the traditional WQP measured.

For all WQP monitored in input and output, negative values indicate more influence from BA1 drainage area than incremental one, as well as, positive values indicate more influence of incremental area than from BA1. Only, DOC in E4 and turbidity on E2 had negative values, indicating that BA1 contribute with more turbidity than BA2 incremental area. This can be related to the more vegetated land use, promoting erosion process. DOC negative value can be associated to the consecutive occurrence

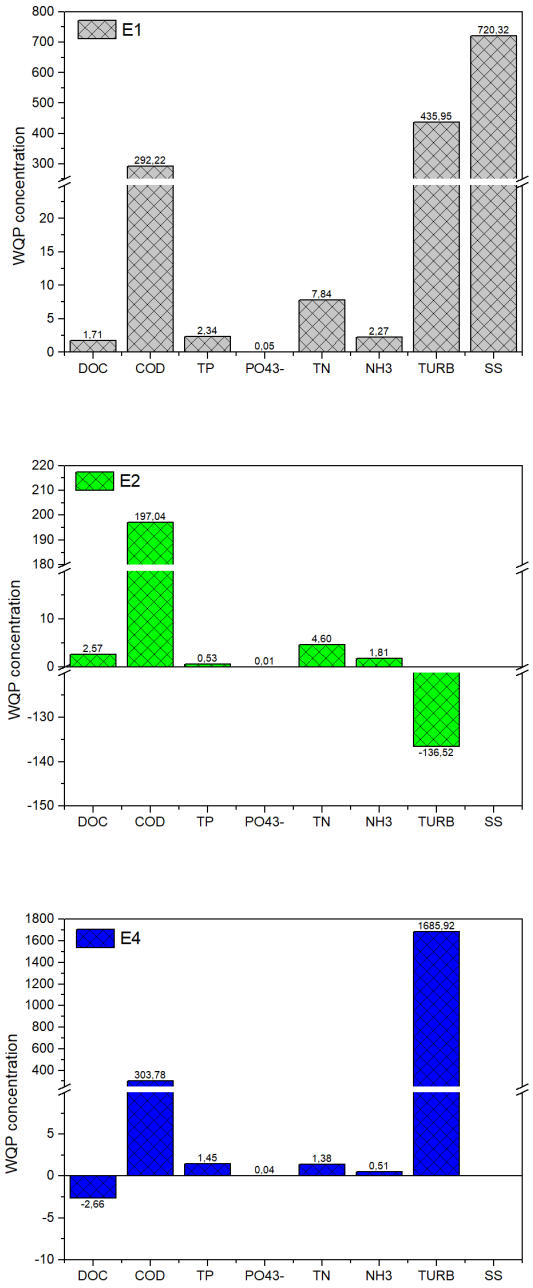

Figure 47 – WQP increment between control volume (BA2-BA1) during E1 (grey), E2 (green) and E4 (blue).

of rainfall, where dilution effects and low time to pollutant build-up between rainfall episodes contribute to these negative value.

The different types of rainfall observed contributed with mass input into the system, in association to the high RI observed during E1, or high RI and spaced rainfall observed during E2, or consecutive and the biggest rainfall measured in E4. High increment concentration of TN, TP, DOC and COD indicate incremental area contribution, indicating that distinct land use produce significant impacts on pollutant input during rainfall episodes. Figure 48 shows drainage areas contribution in the WQP introduction into

the river system.

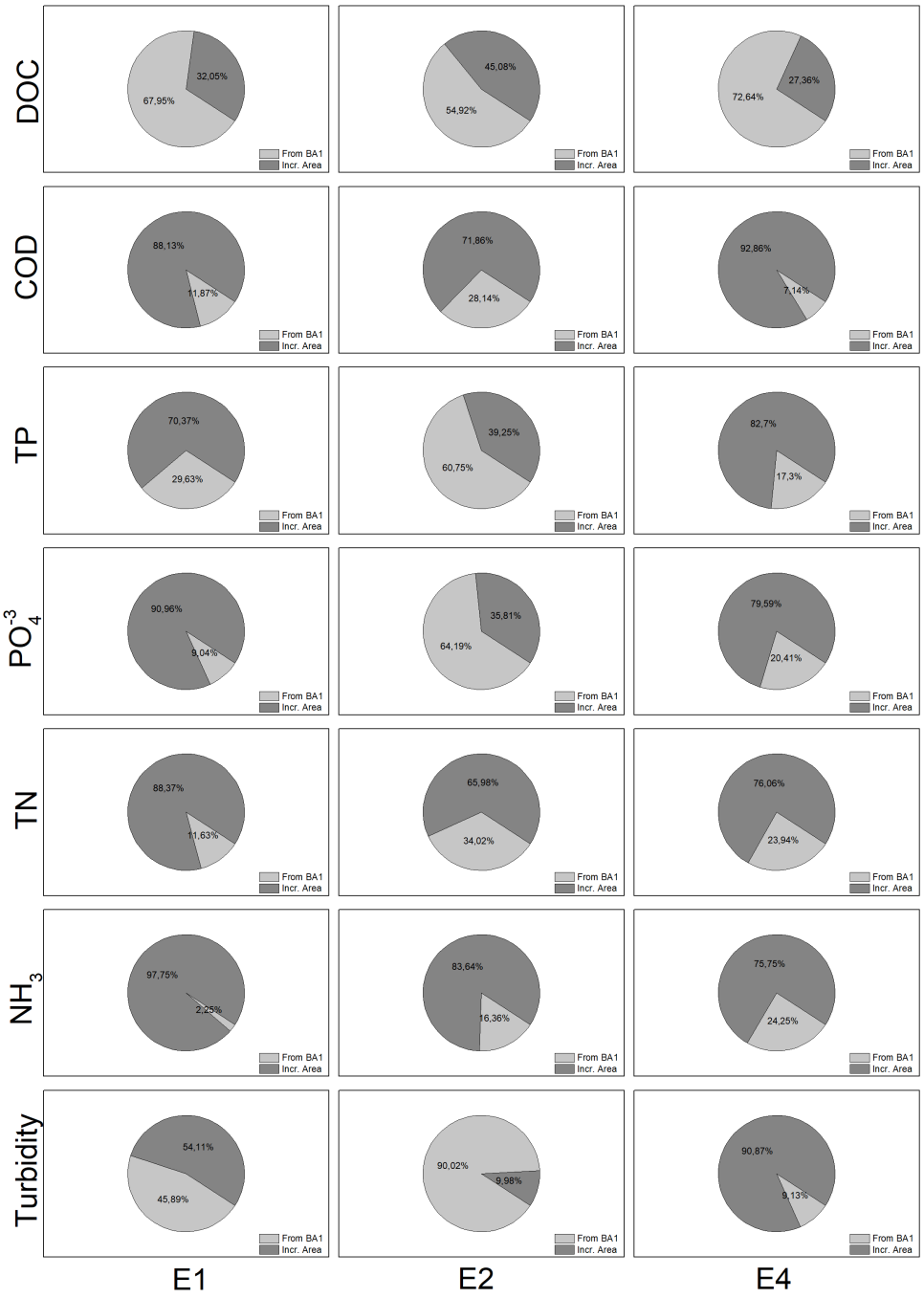

Figure 48 – WQP proportion of contribution from each drainage area

SOURCE:)
NOTE: Light grey represent pollutant from BA1 and dark grey represent pollutant from incremental area (BA2-BA1)

E1 and E4 had higher proportions of pollutant inputted in rivers from incremental area than E2. This can be associated to the specific rainfall characteristics, which are high ADP before event E1, facilitating pollutant build-up, and high RD observed in E4, producing more pollutant transport into the

system, mainly with WWTP influence. E2 had an intermediate contribution (50-50 % on average), which can be associated with the balance between the most intense rain in BA1 and the mildest rain in BA2.

The PS sources in the incremental area are WWTP outflow, drainage galleries, unknown PS contribution, urbanization activities as car traffic, solid waste and pollutant from impermeable surfaces. As a consequence, COD, TP, TN and NH_4^+ were the WQP more pronounced from incremental area in all rainfall episodes monitored.

4.2.6 SUMMARY

In this section were presented rainfall episodes monitored, in terms of pollutographs, EMC values, EMC curves and loads. Moreover, it was presented the baseline profile in BA1 and BA2 monitoring sites, allowing a proper assessment of rainfall impacts and magnitudes.

Such comparison indicated how much a rainfall event can contribute to the variation on rivers water quality and pollutant introduction. Incremental area evaluation showed, clearly, the impact on water quality with land use changes between BA1 and BA2, where had decrease in vegetation and increase in urbanization. This analysis confirm the hypothesis establish in terms of conventional WQP. Therefore, NPS processes, which favor pollutant introduction into a water body is relevant water resources issue to be improved, in order to control potential sources of pollution, and preserved water quality.

4.3 DOM DYNAMICS

"What are the potential sources of organic pollution during a rainfall episode?"

This section contains the assessment of DOM through spectroscopy techniques of UV-Vis and fluorescence. Firstly, the river baseline will be presented in order to evaluate the predominant DOM source without rainfall influences. After that, DOM dynamic during rainfall influence is presented to assess main DOM source and pathways.

4.3.1 BASELINE

The EEM peak intensities were BA1 < BA1-2 < BA2 for all peak, with exception peak B, which had more intensity in BA1-2 (Figure 49). Fluorescence intensities did not have wide variation along 24 hours of monitoring observation, with exception for peak T_2. Overall distribution of the intensities were similar, where peak A was higher than peak C, and both were higher than peaks B and T_1, suggesting a mixture of refractory and labile compounds during baseline period. The predominance was of organic compounds with simpler structures, which is labile or protein-like. The intensities increase about 200% between BA1 and BA1-2, reflecting labile organic material input into the river by the WWTP. Table 26 summarizes peak intensities measured (-respective sample and sampling hour) in the three monitoring sites in baseline.

Table 26 – Average ($\overline{x}$)(± standard deviation (σ)), maximum (max) and minimum (min) peak intensity of the EEMs in baseline campaign

EEM region	Statistic	BA1	BA1-2	BA2
A	$\overline{x}\pm\sigma$	0.34 ± 0.07	0.76 ± 0.06	0.87 ± 0.14
	max	0.54 (S24 - 17h)	0.87 (S20 - 13h)	1.20 (S23 - 16h)
	min	0.25 (S20 - 13h)	0.65 (S14 - 07h)	0.66 (S20 - 13h)
B	$\overline{x}\pm\sigma$	0.32 ± 0.09	1.01 ± 0.26	0.88 ± 0.18
	max	0.49 (S15 - 08h)	1.50 (S7 - 00h)	1.53 (S16 - 09h)
	min	0.16 (S23 - 16h)	0.57 (S24 - 17h)	0.62 (S06 - 23h)
C	$\overline{x}\pm\sigma$	0.18 ± 0.01	0.50 ± 0.06	0.59 ± 0.07
	max	0.20 (S21 - 14h)	0.64 (S7 - 00h)	0.71 (S14 - 07h)
	min	0.15 (S20 - 13h)	0.39 (S24 - 17h)	0.42 (S20 - 13h)
T_1	$\overline{x}\pm\sigma$	0.14 ± 0.04	0.46 ± 0.12	0.52 ± 0.12
	max	0.22 (S5 - 22h)	0.64 (S7 - 00h)	0.80 (S23 - 16h)
	min	0.07 (S15 - 08h)	0.25 (S17 - 10h)	0.35 (S20 - 13h)
T_2	$\overline{x}\pm\sigma$	0.81 ± 0.32	1.81 ± 0.47	1.85 ± 0.51
	max	1.51 (S11 - 04h)	2.58 (S3- 20h)	3.01 (S11 - 04h)
	min	0.34 (S18 - 11h)	1.11 (S19 - 12h)	1.24 (S24 - 17h)

The highest intensity peak measured was peak T_2 in all monitoring sites, suggesting presence of organic compounds similar to the protein, specifically tryptophan. Peak T_2 intensities reached 1.51 r.u. in BA1 at 04h (Figure 50(a)), 2.58 r.u. in BA1-2 at 20h (Figure 50(b)), and 3.01 r.u. in BA2 at 04h (Figure 50(c)). The occurrence of peak T_2 at BA1-2 and BA2 is related to WWTP outflow, where there were higher N-NH_4^+ concentration measured in these both site than in BA1. In this case, labile compounds input have anthropogenic allochthonous source from WWTP (BA1-2), which was transported downstream in river until BA2 with significantly intensity. However, at BA1, peak T_2 occurrence suggest that the organic compounds have simplified structures probably derived from primary production (aquagenic allochthonous source), due to non known of point sources of pollution and low concentration of N-NH_4^+.

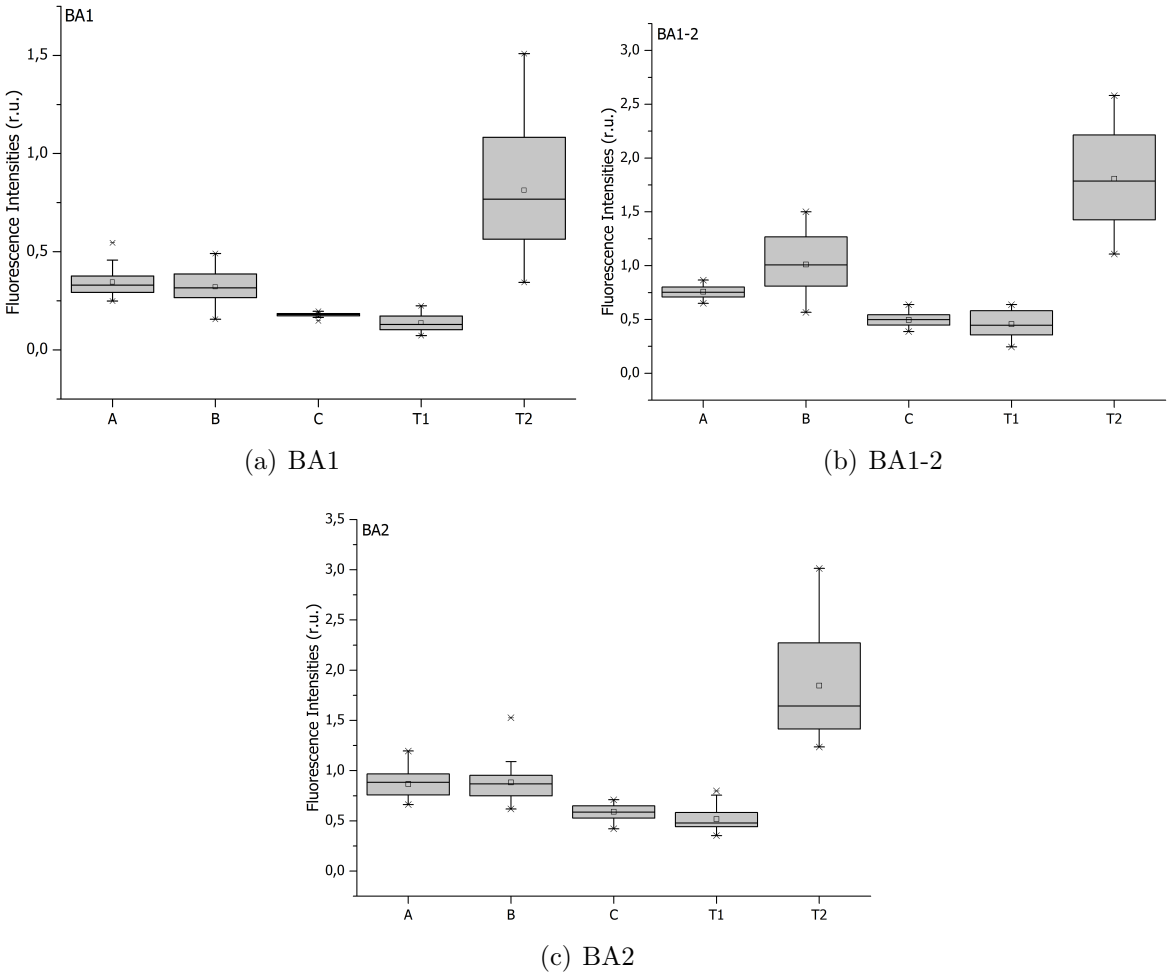

(a) BA1

(b) BA1-2

(c) BA2

Figure 49 – Box plot of EEMs peaks for BA1, BA1-2 and BA2 monitoring sites during baseline campaign

Moreover, peak T_2 were more pronounced during the night than during the day in the three monitoring sites, while others peak had low variation of intensities. This behavior in BA1-2 is related to the WWTP outflow, following conventional water quality parameter distribution. In BA1 and BA2, higher intensity during the night than during the day can be associated to the non biodegradability of this organic fraction during during the absence of light and due to persistence downstream in the river.

To verify these occurrences, UV-Vis ratio and fluorescence indices assessment are applied. A_{285}/DOC value in BA1 (11.53 ± 3.54 L.g^{-1}) were bigger than in BA1-2 (7.30 ± 1.91 L.g^{-1}) and BA2 (7.11 ± 2.01 L.g^{-1}), suggesting mixture of allochthonous and autochthonous sources in BA1, while in other ones had more labile compounds. $SUVA_{254}$ values had same pattern that A_{285}/DOC, indicating that in all monitoring site there was DOM with simplified structures, more labile in BA1-2 (1.01 ± 0.23 L.(mg.m)$^{-1}$) and BA2 (1.01 ± 0.28 L.(mg.m)$^{-1}$) than in BA1 (1.58 ± 0.41 L.(mg.m)$^{-1}$). This classification corroborate with EEMs previously observed. Figure 51 shows A_{285}/DOC and $SUVA_{254}$ biplot for the monitoring sites during baseline campaign.

FI also indicated a mixture of allochthonous and autochthonous sources of DOM in the three monitoring sites. The average values of FI suggest that BA1 (1.52 ± 0.60) have more allochthonous sources influence than BA1-2 (1.59 ± 0.38) and BA2 (1.68 ± 0.36), which are in transition to the bigger influence of autochothonous (anthropic) source of DOM. This one is related to the WWTP outflow. BIX index complements, indicating that samples of BA1 (0.69 ± 0.24) and BA2 (0.74 ± 0.12) had low

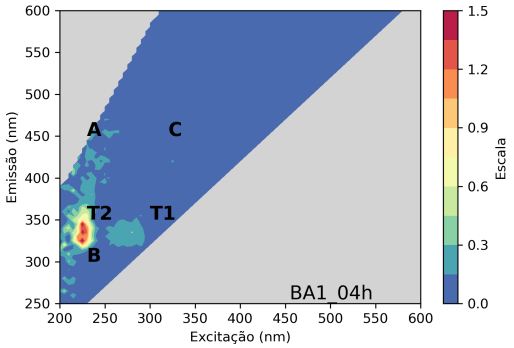

(a) BA1 - 04h

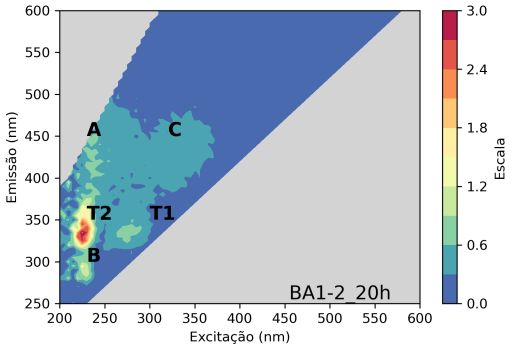

(b) BA1-2 - 20h

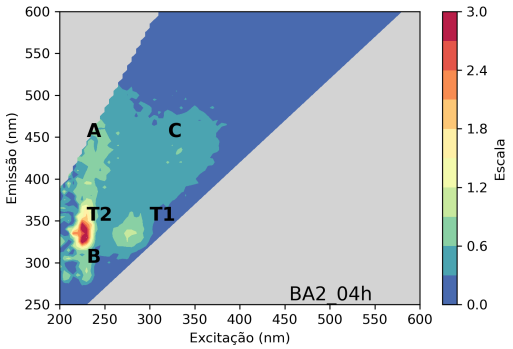

(c) BA2 - 04h

Figure 50 – EEMs with the highest peak T_2 intensity measured during baseline campaign

biological component, while BA1-2 (0.77 ± 0.16) samples had intermediate biological component, as can be observed in Figure 52. Lastly, HIX which expresses how humic the samples are, indicate biological or aquatic bacterial origin for all samples in the three monitoring sites, with average of 2.14 ± 0.74 in BA1, 1.69 ± 0.31 in BA1-2, and 1.82 ± 0.31 in BA2 (Figure 53).

Overall, analysis suggest that samples have a mixture of distinct DOM sources mainly in BA1, probably with simple humic/fulvic structures (quality) or less refractory compounds (quantity) than labile one. However, downstream in river with changes in land use and existence of point source of pollution between sites, BA1-2 and BA2 present anthropic/aquagenic sources of DOM. Moreover, without rainfall influence river showed absence of humic characteristics.

4.3.2 RAINFALL

Rainfall assessment for DOM dynamics have the same strategy presented, where BA1 has 3 rainfall episodes, and BA2 has 5 rainfall episodes. Events 1, 2 and 4 represent control volume approach, with input and output assessment, whereas events 3 and 5 represent an monitoring site with influence of point and non-point sources of pollution.

Different from baseline profile, DOM dynamic during rainfall episodes had more refractory characteristics than labile in BA1, and a mixture of the both sources in BA2. Figure 54 shows EEMs peaks distribution along rainfall episodes monitored in BA1, without time scale approach.

In E1-BA1 it was possible to observed that, peak A was more intense than others. Peaks B

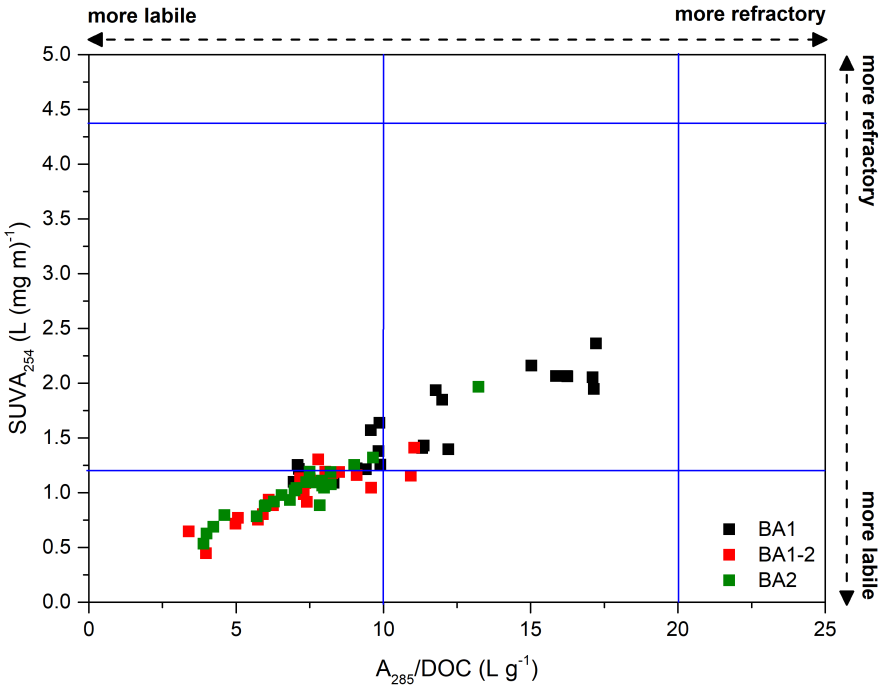

Figure 51 – Biplot of A_{285}/DOC and $SUVA_{254}$ values between BA1, BA1-2 and BA2 during baseline campaign

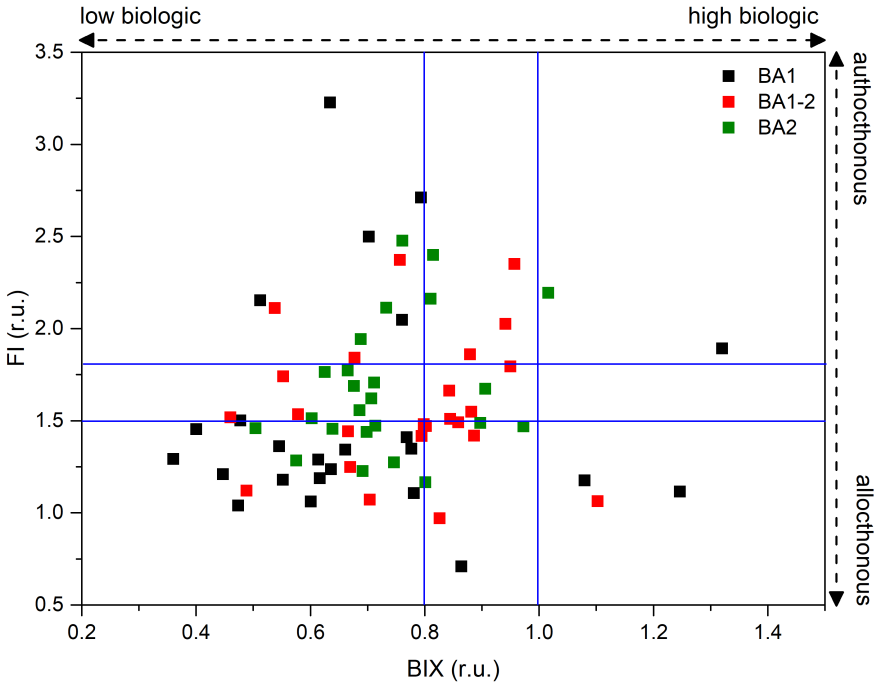

Figure 52 – Biplot of FI and BIX values between BA1, BA1-2 and BA2 during baseline campaign

and T2 had higher values in the beginning of the event, decreasing afterwards. Peak C intensities were bigger than peaks T1 intensities, and both had constant values during the events. In general, no peak followed DOC or flow pattern. However, in sample 3, which represents the peak flow (1.28 $m^3.s^{-1}$) and

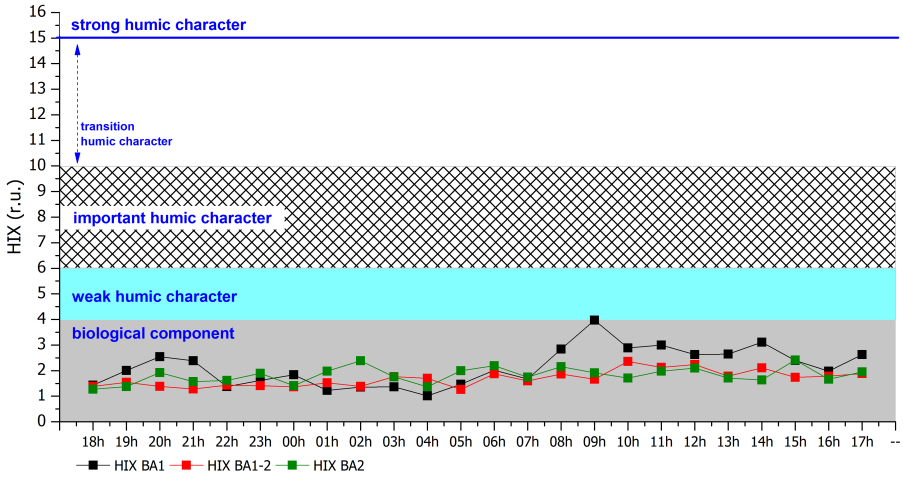

Figure 53 – HIX values distribution in BA1, BA1-2 and BA2 during baseline campaign

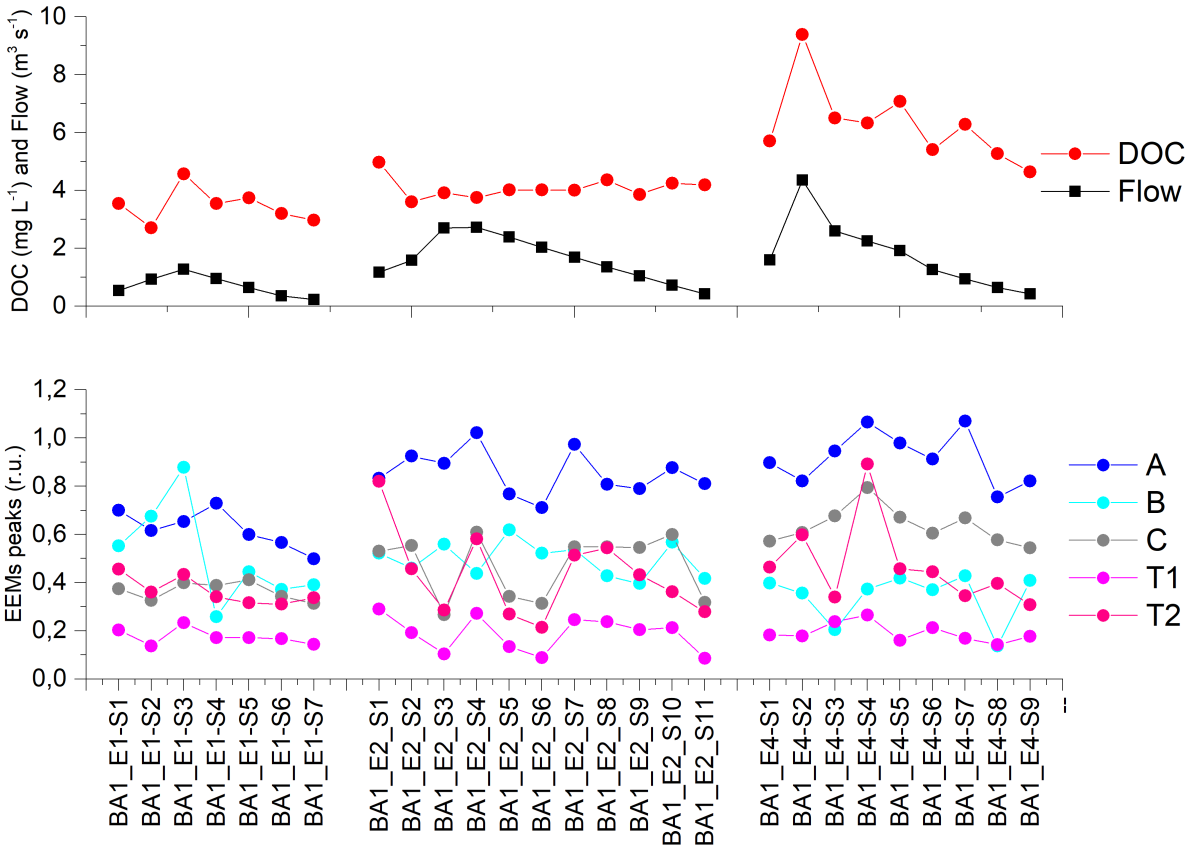

Figure 54 – EEMs peaks distribution along the three rainfall episodes monitored in BA1

the highest DOC concentration (4.57 mg.L^{-1}) in this event, there was the highest peak B intensity (0.88 r.u.) measured, as well. All distribution suggest that there was a fast labile input in the beginning of the event, although refractory material predominated.

In E2-BA1, also peak A had the highest intensity throughout the event. Peaks C, T1, and T2 had a similar behavior with greater intensities in the beginning (sample 1), middle (sample 4) and end

of the event (samples 7 to 10). Peak B had opposite behavior that peak A, when A increased B decrease, e.g. sample 4 and 5. No peak followed DOC concentration or flow pattern. However, peak T2 had the highest intensity (0.82 r.u.) in the sample 1 which had the biggest DOC concentration (4.98 $mg.L^{-1}$) in the event. Before peak flow in sample 7, all peaks had intensities decreasing, which can be a result of the amount of water transported.

And, in E4-BA1, DOC concentration were bigger than other events and followed the pattern of the flow. However, no peak followed DOC or flow patterns during the episode. As in the other events monitored in BA1, peak A was the predominant one throughout the event, followed by peak C, indicating that this event carried more refractory components. However, in samples 4 there was an increase in the T2 peak (and highest intensity measured - 0.89 r.u.) suggesting labile material input into the system. Peaks B and T1 had the lowest intensities recorded. In sample 7 there was an increase in band A, suggesting a input of refractory material in the end of the event.

At BA2, five rainfall episodes were monitored, and peaks distribution are presented in Figure 55, without time scale approach. In general, the behavior were different from BA1, with presence of labile and refractory DOM and more pattern trending with DOC concentration.

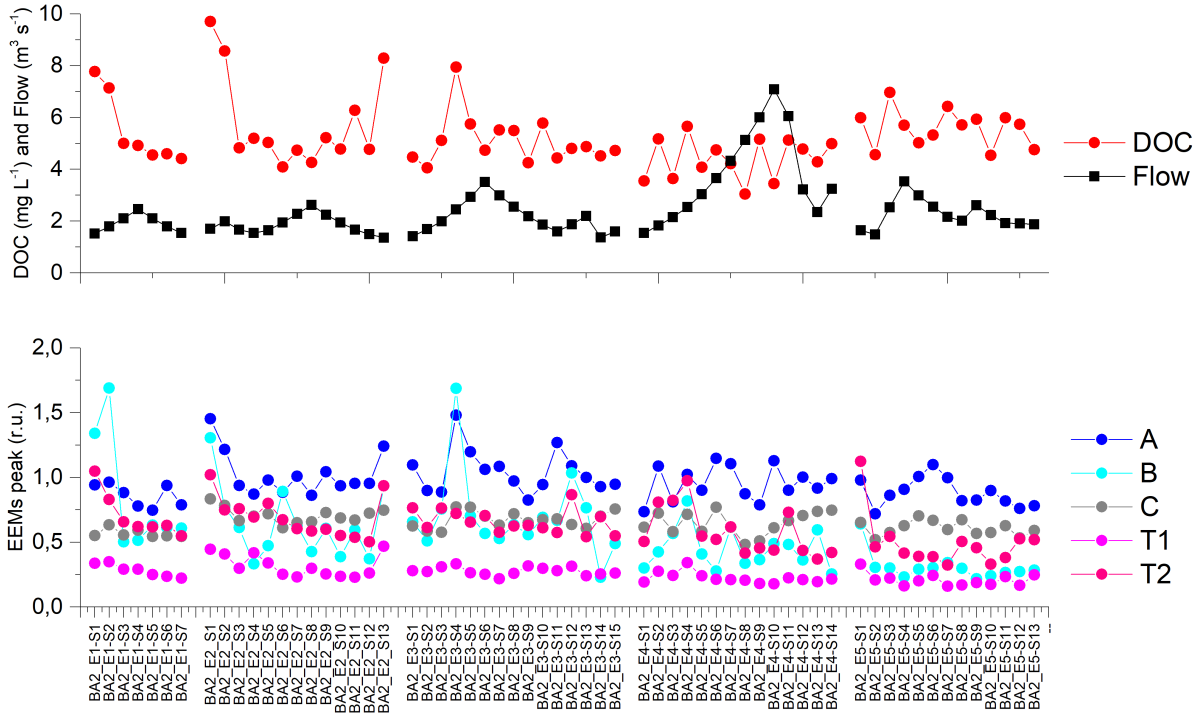

Figure 55 – EEMs peaks distribution along the five rainfall episodes monitored in BA2

At E1-BA2, peak B had a higher intensity at the beginning of the event, then decreased until the end of the event, as DOC concentration behavior. Peak T2 had the same behavior as B, but at a lower intensity. Peaks A, C and T1 had relatively constant intensities throughout the event, where peak A > peak C > peak T1. It is suggested that there was a greater supply of organic material with a more labile characteristic, probably associated with ADD (2.36 days) and the presence of a WWTP.

In E2-BA2, peak A was the most intense observed, mainly in samples 1 and 13. These samples had peculiar characteristics, which were black color and with a very strong asphalt aspect, justifying the increase of refractory peaks in EEMs. With the exception of peak C, the other peaks also had higher values in these samples (1 and 13). All of them, followed DOC concentration pattern and did not follow

flow variations pattern. In the consecutive rainfall monitored just in BA2, E3-BA2 (ADD of 1.70 days), peak A had the biggest intensities measured, except for sample 4. Sample 4 had the highest intensities of bands A (1.48 r.u.) and B (1.69 r.u.). The peak flow occurred in samples 6, suggesting that there was mixed organic material inputted into the river system along the event, although with low dry condition period. This can be observed in the two pulses registered in the end of the event: peak A in sample 11 (1.27 r.u.), and peak B (1.04 r.u.) and T2 (0.87 r.u.) in sample 12.

At event E4-BA2, there was predominance of peak A. At the beginning of the event peak T2 had greater intensities, decreasing until the end of the event. There was no defined pattern, with wide variation, as DOC concentration, and mixing of fluorescence intensities throughout the event. At the end of the event, peak C has increased intensity, which may be related to the second recorded flow increase, from BA1. And, in E5-BA2, as similar to the others events, peak A was the most evident during the whole event, except for the first sample that had peak T2 with the highest intensity (1.12 r.u.). Peak flow occurred in sample 4, and intensities were increased from sample 2 until 6, mainly in bands A and C, probably due to the dragging of material with refractory characteristics (the highest ADD - 7.62 days).

Therefore, rainfall episodes showed more refractory characteristics than labile, mainly in BA1. In BA2, there is a mixture of both characteristics, as a result of the WWTP and BA1 influence. Table 27 summarize peaks intensities measured in the rainfall episodes at BA1 and BA2.

Table 27 – Average (± standard deviation) of peaks A, B, C, T1 and T2 measured in EEMs for all rainfall episodes monitored in BA1 and BA2

		A	B	C	T1	T2
BA1	E1	0.62 ± 0.08	0.51 ± 0.21	0.37 ± 0.04	0.18 ± 0.03	0.36 ± 0.06
	E2	0.86 ± 0.09	0.50 ± 0.07	0.47 ± 0.13	0.19 ± 0.07	0.43 ± 0.18
	E4	0.92 ± 0.10	0.36 ± 0.11	0.64 ± 0.08	0.20 ± 0.05	0.52 ± 0.23
BA2	E1	0.86 ± 0.09	0.84 ± 0.47	0.57 ± 0.03	0.28 ± 0.05	0.71 ± 0.17
	E2	1.03 ± 0.17	0.64 ± 0.28	0.71 ± 0.06	0.32 ± 0.09	0.69 ± 0.16
	E3	1.05 ± 0.17	0.70 ± 0.32	0.67 ± 0.06	0.28 ± 0.03	0.66 ± 0.09
	E4	0.96 ± 0.13	0.45 ± 0.16	0.65 ± 0.09	0.22 ± 0.04	0.58 ± 0.19
	E5	0.88 ± 0.11	0.31 ± 0.11	0.61 ± 0.06	0.21 ± 0.05	0.49 ± 0.20

To complement EEMs peaks, indices from UV-Vis indicate a mixture of labile and refractory characteristics and sources during all rainfall episodes. Figure 56 shows A_{285}/DOC and $SUVA_{254}$ distribution along rainfall monitored, in BA1 (three rainfall) and BA2 (five rainfall).

For all events in BA1 and BA2, A_{285}/DOC and $SUVA_{254}$ had average values which indicated, respectively, a mix of allochthonous and pedogenic sources of DOM (ranging from 10.26 ± 1.91 to 19.57 ± 6.17 $L.g^{-1}$), with labile and refractory characteristics (ranging between 1.49 ± 0.28 and 3.75 ± 2.17 $L.(mg.m)^{-1}$). Just E4-BA2 A_{285}/DOC had bigger average value (28.20 ± 18.50 $L.g^{-1}$), suggesting that this event had predominant pedogenic sources of DOM.

In the rainfall episodes monitored in BA1, all of them had some samples with allochthonous sources characteristics in the beginning of the event, as a first flush of labile compounds. Then, along the episode samples had mix characteristics of allochthonous and pedogenic sources. Considering BA1 characteristics, without influence of a point source of pollution, but with the presence of labile material during the base flow, the first flush of the flow continued to bring labile material into the river, probably from an upstream point closer to the BA1. However, along with the rainfall episode occurrence and increased flow rates, material arrived from distant upstream locations from BA1, with a predominantly more refractory component, such as more decomposed material and suspended solids from erosion. Such conditions are typical of diffuse pollution transport routes.

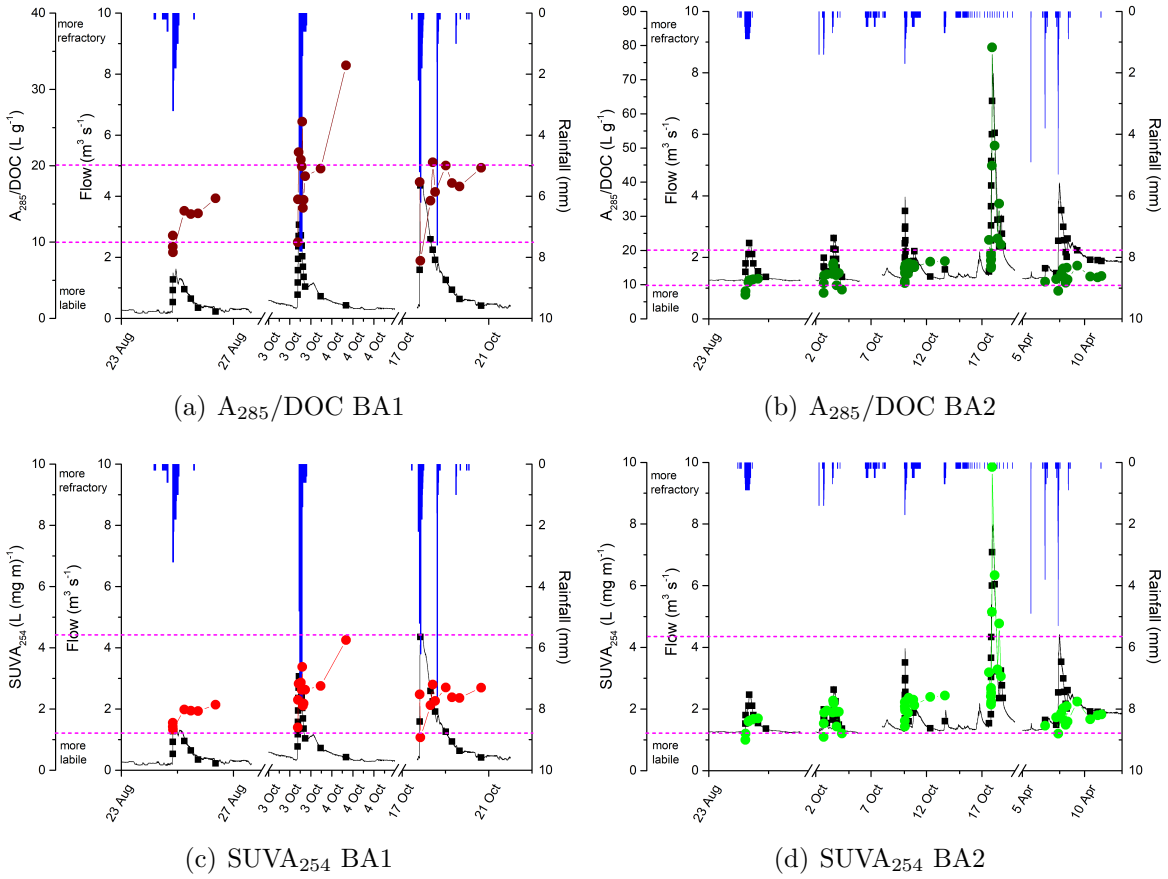

(a) A_{285}/DOC BA1 (b) A_{285}/DOC BA2

(c) $SUVA_{254}$ BA1 (d) $SUVA_{254}$ BA2

Figure 56 – A_{285}/DOC and $SUVA_{254}$ distribution during rainfall episodes monitored in BA1 and BA2.

At BA2, classification was very similar, with singular samples in the beginning of the event with labile characteristic. Moreover, beside mix classification of the indices, the values were mix close to allochthonous antropic sources ($\sim$ 10 L.g^{-1}) with labile characteristics ($\sim$ 1.2 L.(mg.m)$^{-1}$). The distinct behavior was E4. E4-BA2 was a consecutive event (ADD of $<$ 1 day), with the longest duration (62.5 hours) and the biggest rainfall amount precipitated (98.9 mm), reaching the maximum flow at 7.98 m^3.s^{-1}. A_{285}/DOC and $SUVA_{254}$ indicated pedogenic sources of DOM with refractory characteristics along rainfall episode, increasing values with flow increase. This can indicate wash-off produced contributed to input of more refractory organic material into the river. The occurrence of massive and consecutive rainfall reduce infiltration process and favour runoff transport, therefore facilitating erosion process and surface wash-off.

In this sense, the indices FI, BIX and HIX give complementary information, respectively, about potential DOM source, biologic and humic component. Figure 57 highlights a biplot of FI and BIX calculated from EEMs spectra with respective indication, and HIX distribution along pollutographs for the rainfall monitored in BA1 and BA2.

It is possible to observe that in BA1, all samples had BIX classification as low biologic component, with FI classification in transition between allochthonous sources and mixture. Only two samples had characteristics authocthonous. This distribution corroborate to other indices, suggesting that DOM input in BA1 had more refractory characteristics than labile, probably due to the land use of upstream drainage area. Moreover, HIX distribution along the event showed a transition between weak to important and strong humic character. E1-BA1 had sample 3 with biologic character (HIX of 3.82), changing for weak and important humic character until the end. E2-BA1 had humic character during all event, ranging

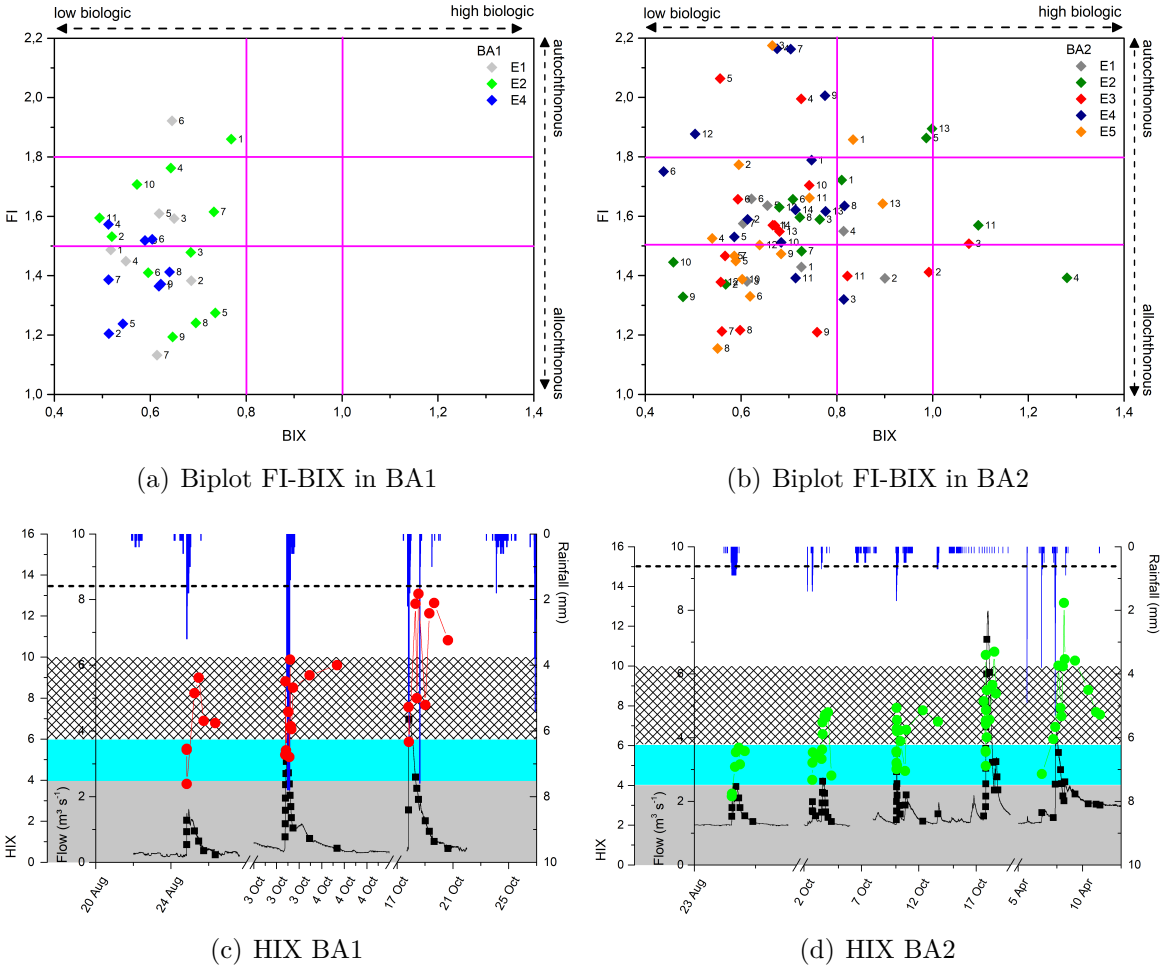

(a) Biplot FI-BIX in BA1

(b) Biplot FI-BIX in BA2

(c) HIX BA1

(d) HIX BA2

Figure 57 – Biplot FI-BIX and HIX distribution along rainfall episodes monitored in BA1 and BA2.

between weak and important humic classification (HIX Of 5.24 to 9.87). E4-BA1 had HIX with more humic characteristics than other events, and increasing along with, reaching HIX > 10 in the end of the event.

For BA2, classification was similar to BA1. Samples had low biologic classification for the most samples measured, with few samples with BIX more than 1.0. FI values were distributed between allochthonous and authocthonous, suggesting that DOM sources have antropic labile and refractory pedogenic characteristics, associating point and diffuse sources. HIX values indicate weak to important humic character along rainfall episodes. E1-BA2 had biologic classification in the beginning of the event, increase value and changing the classification for weak humic character. E2-BA2 and E3-BA2 had entire humic character, ranging between weak and important. In the same perspective, E4-BA2 and E5-BA2 had more humic character than other events, with values ranging between important to strong humic characters. These classification indicates that the rainfall episodes contribute to the input of refractory material in the rivers, probably from surface wash-off, associated to the WWTP residuals and erosion processes of the river channel. The labile characteristics are decreased or diluted during the rainfall episode.

4.3.3 DOM DYNAMICS IN THE CONTROL VOLUME DEFINED

A possible assessment is the estimate of protein- and humic-like content. Protein-like corresponds to sum of peak B, T1 and T2 from EEMs, which are related to labile organic compounds, as for example,

proteins, carbohydrates, and lipids. Thus, humic-like corresponds to the sum of peak A and C from EEMs, which are related to the refractory organic compounds, as for example, humic and fulvic acids. Table 28 summarize the average values of the EEMs peaks, and humic- and protein-like content.

Table 28 – Average values of peaks A, B, C, T1 and T2, and humic- and protein-like sum for baseline and rainfall episodes monitored in BA1 and BA2

		A	B	C	T1	T2	humic-like	protein-like
BA1	Baseline	0.34	0.32	0.18	0.14	0.81	0.52	**1.27**
	E1	0.62	0.51	0.37	0.18	0.36	0.99	**1.05**
	E2	0.86	0.50	0.47	0.19	0.43	**1.33**	1.12
	E4	0.92	0.36	0.64	0.20	0.52	**1.57**	1.09
BA2	Baseline	0.87	0.88	0.59	0.52	1.85	1.46	**3.25**
	E1	0.86	0.84	0.57	0.28	0.71	1.43	**1.83**
	E2	1.03	0.64	0.71	0.32	0.69	**1.73**	1.65
	E3	1.05	0.70	0.67	0.28	0.66	**1.72**	1.64
	E4	0.96	0.45	0.65	0.22	0.58	**1.61**	1.25
	E5	0.88	0.31	0.61	0.21	0.49	**1.49**	1.01

Considering the differences between baseline profile and rainfall episodes, it was possible to observe that both baseline profiles in BA1 and BA2 have more predominant labile characteristics, with protein-like > humic-like, respectively 1.27 r.u. and 0.52 r.u. for BA1, and 3.25 r.u. and 1.46 r.u. for BA2. At point BA1, with low N-NH_4^+ concentration measured, the probable source is allochthonous aquagenic, in other words, labile material from primary productivity. However, in BA2, due to the existence of WWTP and the higher N-NH_4^+ concentration, the probable source of labile DOM is allochthonous antropic.

Under rainfall influence, only E1, at both monitoring points, had the predominant composition of protein-like > humic-like. This may be associated with the type of event (medium-to-low, with low RD) and ADD time ($\sim$ 2.4 days), providing a smaller input of refractory material from upstream from monitoring site, and favouring input from available material closer to point BA1 effectively. However, for the other events, at both monitoring points, the predominant DOM profile changes, in which humic-like > protein-like. This can be related to the rainfall shape, which had RD, P_{acum} and runoff increased. In the case of events 2, 3 and 4, which were consecutive, it favors the effects of surface washing and soil transport from erosion, increasing therefore, the allochthonous pedogenic material carried into the river. Associated with this, the labile material available may have already been degraded or carried downstream, making labile DOM fraction negligible compared to the DOM refractory fraction.

In this sense, observing average peaks from EEMs of rainfall episodes with baseline profile, at point BA1, only peak T_2 had a decrease in its intensity, in the three monitored events. This suggests that rain events contribute to the dilution of the labile material available and favor the introduction of refractory material in the system. At point BA2, the condition was similar, where peaks B, T_1 and T_2, suffered a decrease in their average intensities when compared to baseline profile. E1-BA2 had also peaks A and C reduced, and for the other events there was no reduction, however the increase in humic compounds intensity was small. This suggests that the effects of rain to the point BA2 have distinct impacts on water quality, where volume of water transported favors dilution DOM available than to carry additional DOM inside the system. Figure 58 shows boxplots for EEMs peak in baseline and rainfall episodes for BA1 and BA2.

Thus, considering the difference between BA2 and BA1, it is possible to estimate that larger events have less influence downstream than smaller events, probably associated with the volume of water transported and its speed. In event 4 (medium in BA1 and medium-to-high in BA2), about 2% of humic-

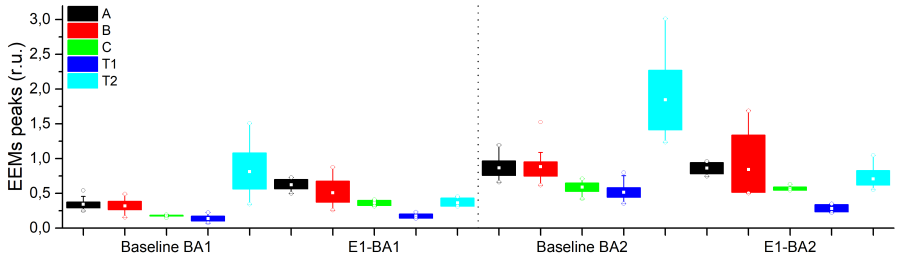

(a) Baseline and E1

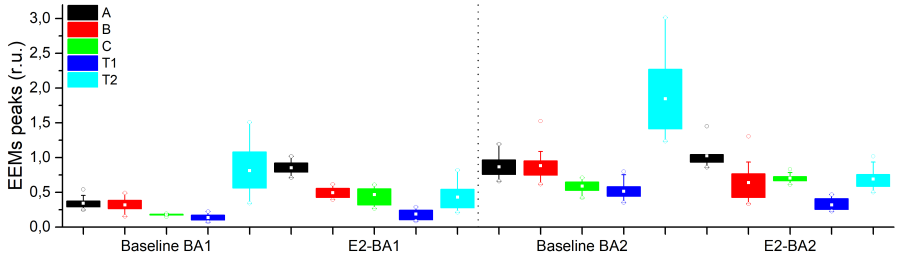

(b) Baseline and E2

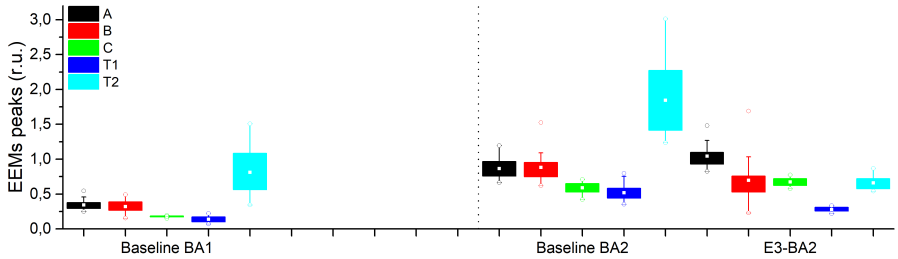

(c) Baseline and E3

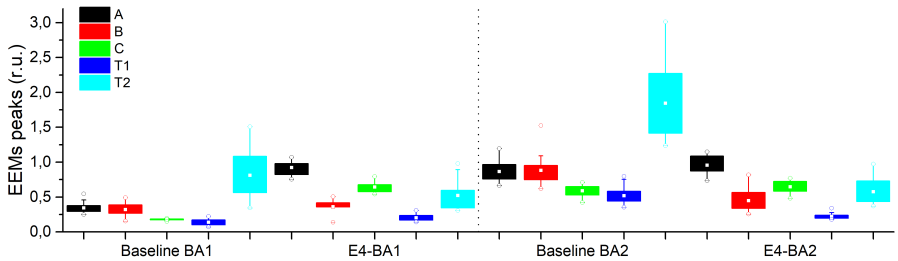

(d) Baseline and E4

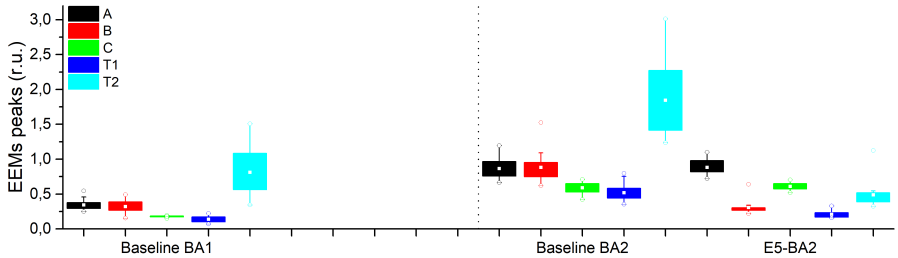

(e) Baseline and E5

Figure 58 – Box plot of EEMs peaks from baseline profile and events monitored in BA1 and BA2

like DOM and 10% protein-like DOM protein may have come from BA1, while events 1 (medium-to-low) and 2 (medium and low), respectively 30% and 25% for protein-like and humic-like, arrived in BA2 may have come from BA1.

In general, RD had a positive correlation with peaks A (Pearson = 0.52) and C (Pearson = 0.62), indicating that the longer the event is, the greater is refractory material presence. However, the same peaks have a negative correlation with RI (-0.77 for peak A and -0.91 for peak C, both with p-value <0.05), suggesting that less intense events contribute more refractory material inputs. Finally, to complement and corroborate, A_{285} and $SUVA_{254}$ had a positive correlation with Q_{max} and ΔQ and P_{acum}, suggesting that the more rainfall precipitated, the more flow is transported, the higher the index values will be. If the indices are higher, it indicates that they have more refractory characteristics.

4.3.4 SUMMARY

In this section, it was possible to observe DOM variations during rainfall episodes, and the baseline campaign (this one without rainfall). The analysis were based on EEMs peaks and indices.

DOM profile without rainfall showed a predominance of more labile material, due peak T_2 highlight, in all samples from the three monitored points. Complementary, $SUVA_{254}$ and A_{285}/DOC indices also classify samples as having more labile characteristics than refractory. FI and BIX indicated DOM from mixed allochthonous and authocthonous sources with weak biological characteristic, corroborated by HIX with biological component constant throughout the entire monitored period. At BA1, labile component can have autochthonous aquagenic source, derived from primary decomposition and associated with low N-NH_4^+ concentration, whereas at BA2, labile component can have allochthonous anthropic sources, derived from domestic effluent (mainly at BA1-2) and associated with higher N-NH_4^+ concentration.

During rainfall, behavior is reversed. The predominant labile material is diluted, with peak T_2 intensity reduced, and the humic components enhanced (peak A and C). $SUVA_{254}$ and A_{285}/DOC indices classified samples mixed allochthonous and authocthonous sources, being possible to verify transition from more labile to more refractory characteristics along the rainfall episodes. For FI and BIX indices, the classification remained mixed, still indicating a weak biological component. Thus, HIX presented a labile component just at the beginning (initial washing-off) and then switching to humic characteristics along the rainfall episodes. There were increasing in HIX values, varying from weak to important humic character.

Finally, baseline profile had predominantly protein-like characteristic, exchange during the rainfall, becoming predominantly humic-like characteristic, both for BA1 and BA2. This indicates that labile material input during rainfall episode may be less than runoff contribution, undergoing dilution or being carried downstream. Thus, refractory components remained more accentuated during rainfall events, which may come from, for example, runoff washing, dry decomposed material and eroded soil transported on the riverbed. Such sources of this refractory material indicate the relevance of the diffuse transport of substances.

4.4 EMERGING CONTAMINANTS

"How is the influence of point sources of pollution during non-point transport?"

In this section, the Emerc analysis is presented based upon the same monitoring strategy: the baseline campaign and the rainfall episodes, despite some differences from what has been presented previously. Results will be presented considering their occurrence and behavior along the rainfall episodes.

In the baseline, 4 from 24 samples were analyzed in each monitoring site (BA1, BA1-2 and BA2). Samples 5 (22h p.m.), 10 (03h a.m.), 16 (09h a.m.) and 22 (15h p.m.) as presented in Table 14 in the Section 3.5.4. They were chosen in order to detect variation in specific moment, which can represent the most influence of urban activities without rainfall occurrence, in a similar way as presented in GOULART (2017).

In order to process the analysis for the influence of the rainfall episodes, it were chosen samples with bigger volumes of water collected among all samples, due to the minimal water volume required to performed the analytical procedure with the best representativeness and conditions (KRAMER, 2016; FILIPPE, 2018).

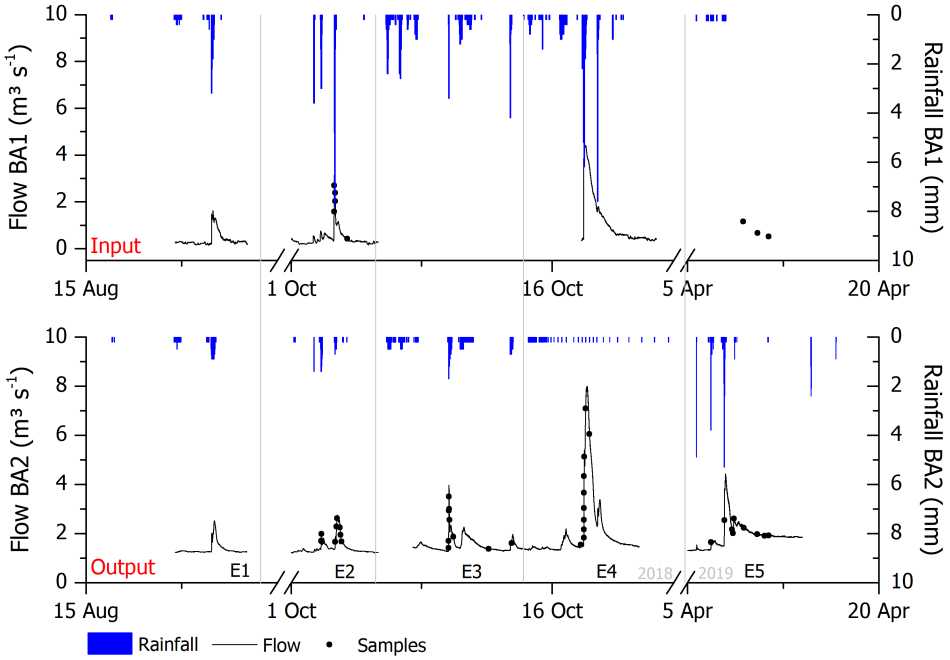

Figure 59 – Samples collected during rainfall episodes and assessed for emerging contaminants at BA1 and BA2 monitoring sites

NOTE: E1 was not monitored for these compounds. E2 had 14 samples considered, of which 5 were in BA1 and 9 in BA2. E3 and E4 had, respectively, 9 and 10 samples considered, just in BA2. E5 had 12 samples considered, if which 3 were in BA1 and 9 in BA2

4.4.1 OCCURRENCE

The analytical procedure used allows determination of 25 emerging contaminants, which are ten pharmaceuticals, six PCPs, and nine sterols. From them, MTL, NAD, Es2 and βSi had concentration below the limit of detection (LOD), in any campaign (baseline and rainfall episodes). FenP, AAS, AS, EE2, Es1, STI and EPL were detected just in event 2, with respectively percentage of occurrence on

the samples analyzed of 21%, 64%, 64%, 7%, 93%, 79% and 29% considering the both sites. FenP were detected just in one sample in BA1 (43.36 μg.L^{-1}), and AAS, AS and EE2 were detected below the limit of quantification (LOQ). Es1, STI and EPI had concentration ranging between < LOQ - 0.23 μg.L^{-1}, < LOQ - 497.47 μg.L^{-1}, and < LOQ - 149.77 μg.L^{-1} respectively. Therefore, considering the low occurrence of theses elements, they will not be discussed further. Table 29 summarized % of occurrence of the others emerging contaminants determined in the baseline and rainfall episodes at BA1 and BA2.

CLT and CLN were detected just in baseline campaign, which can indicate more marked fecal contamination than in rainfall episode. Water transported during rainfall can contribute to dilution of these compounds. It is important to highlight that CLT were detected just in two samples (one in BA1-2 and one in BA2), with concentration < LOQ, whereas CLN were detected in all samples of BA1-2 and BA2, with values ranging from < LOQ to 34.6 μg.L^{-1}.

Moreover, other contaminants as IBU, EtP and CPL were detected just in BA1-2 and BA2, indicating the influence of the WWTP. However, contaminants as NAP and CAF were detected in 100% of the samples performed in baseline, which suggest inadequate inputs of sewage before the WWTP, persisting and being carried downstream, with concentration ranged between < LOQ - 0.23 μg.L^{-1} for NAP and 0.14 - 1.65 μg.L^{-1} for CAF. Although PRL had a high percentage of occurrence, its presence was only determined < LOQ.

Thus, considering emerging contaminants just in rainfall episodes, the occurrence of parabens, TCS and some sterols (mainly in event 2) increased. Parabens had an increase from, in average, 13% from baseline, which detected two parabens (EtP and MeP), to 8%-100% in the rainfall episodes, where had detection of, practically, all parabens and TCS. Therefore, rainfall episodes contributed to the carrying and input of these kind of compounds into the river. The probable and expected source is the WWTP, reflecting in BA2 concentrations.

However, at BA1 without point sources influence, there were occurrence of these compounds, suggesting diffuse transport of pollution into the river. The specifics sources can be raw sewage (septic tanks or irregular discharges) and surface wash-off, reflecting human activities. For sterol fecals, it was detected just in event 2 probably due to the higher ADD period than other rainfall events, and occurrence were more frequently in BA2 than in BA1 due to WWTP influence. CPL detected in BA2 event 4 was < LOQ.

Additionally, pharmaceutical compounds had persistence occurrence in all samples analyzed. NAP and CAF had 100% of occurrence, IBU increased their occurrence during rainfall episodes. This indicates how persistent the effects of human activities are for the aquatic environment, even in different flow regimes, and suggest that rainfall episode can contribute with pharmaceutical transport into river through diffuse pathways.

Table 29 – Percentage of occurrence of the emerging contaminants in the baseline and rainfall episodes monitored in BA1 and BA2

	BA1 (N = 4)	BA1-2 (N = 4)	BA2 (N = 4)	BASELINE (N = 12)	BA1 (N = 5)	BA2 (N = 9)	E2 (N = 14)	BA2 - E3 (N = 9)	BA2 - E4 (N = 10)	BA1 (N = 3)	BA2 (N = 9)	E5 (N = 12)
IBU	0	75	50	42	80	100	93	100	70	0	89	67
NAP	100	100	100	100	100	100	100	100	100	100	100	100
CAF	100	100	100	100	100	100	100	100	100	100	100	100
PRL	100	50	25	58	-	-	-	11	-	-	-	-
FNF	0	25	25	17	-	-	-	-	-	0	33	25
BuP	-	-	-	-	-	-	-	11	-	0	11	8
PrP	-	-	-	-	100	89	93	100	100	100	100	100
EtP	0	25	0	8	80	44	57	78	80	33	89	75
MeP	25	25	0	17	80	56	64	-	-	0	11	8
BeP	-	-	-	-	100	100	100	44	50	33	44	42
TCS	-	-	-	-	100	100	100	100	100	33	67	58
CLT	0	25	25	17	-	-	-	-	-	-	-	-
CLN	0	100	100	67	-	-	-	-	-	-	-	-
CPL	0	50	25	25	0	89	57	-	10	-	-	-

NOTE: "-" represents concentrations < LOD

LEGEND: N - number of samples analyzed; IBU - Ibuprofen; NAP - Naproxen; CAF = Caffeine; PRL - Propanolol; FNF - Fenofibrate; BuP - Buthylparaben; PrP - propylparaben; EtP - Ethylparaben; MeP = Methylparaben; BeP - Benzylparaben; TCS - Triclosan; CLT - Cholesterol; CLN - Colestanona; CPL - Coprostanol

4.4.2 CAF, NAP AND TCS BEHAVIOR

Considering NAP, CAF and TCS most frequent occurrence in rainfall episodes,their significance and potential adverse impacts into the aquatic environment, behavior of these compounds will be assessed in the pollutographs analysis. Table 30 summarized range concentration of them in the events monitored. As mentioned, CAF and NAP had 100% of occurrence in baseline and rainfall episodes, while TCS was not detected in baseline, but with occurrence of 100% in events 2, 3 and 4, and 58% in event 5.

Table 30 – CAF, NAP and TCS average ($\overline{x}$)± standard deviation σ, max and min concentration (μg.L^{-1}) in baseline and rainfall episodes monitored

		CAF			NAP			TCS		
		max	min	$\overline{x}\pm\ \sigma$	max	min	$\overline{x}\pm\ \sigma$	max	min	$\overline{x}\pm\ \sigma$
BA1	Base	0.49	0.14	0.24 ± 0.17		<LOQ			<LOD	
	Event 2	5.63	1.55	3.25 ± 1.76	1.09	0.21	0.50 ± 0.35	0.24	0.16	0.21 ± 0.03
	Event 5	0.52	0.29	0.43 ± 0.13		<LOQ		0.09	<LOD	-
BA1-2	Base	1.65	0.36	0.90 ± 0.56	0.23	<LOQ	0.15 ± 0.07		<LOD	
BA2	Base	1.61	0.52	0.98 ± 0.49	0.19	0.08	0.11 ± 0.05		<LOD	
	Event 2	5.40	0.59	2.99 ± 1.64	4.84	0.39	1.92 ± 1.36	0.62	0.22	0.38 ± 0.11
	Event 3	1.23	0.21	0.54 ± 0.33	0.15	<LOQ	0.09 ± 0.03	0.12	0.09	0.10 ± 0.01
	Event 4	1.29	<LOQ	0.60 ± 0.34	0.16	<LOQ	0.11 ± 0.03	0.12	0.09	0.10 ± 0.01
	Event 5	4.50	0.18	1.77 ± 1.33	0.28	<LOQ	0.15 ± 0.09	0.1	<LOD	0.09 ± 0.01

For the baseline campaign, it was not expected to quantify these emerging contaminants at point BA1, as there is no known point source upstream of it. TCS was not detected, but NAP was detected < LOQ indicating its occurrence, but not its quantity, and CAF was detected in all samples, with an average concentration of 0.24 ± 0.17 μg.L^{-1}. In BA1-2 and BA2, emerging contaminants quantification was already expected as they are downstream from WWTP, however TCS was not detected in any monitored sample. NAP and CAF had an increase in concentration between BA1 and BA1-2, indicating the impact of the WWTP discharge, remaining until BA2 (on average), demonstrating their impacts downstream of WWTP point.

However, during rainfall episodes it was possible to observe some changes. At BA1 point, only in event 2, it was possible to quantify CAF, NAP and TCS. In event 5, only CAF had quantifiable concentrations. From baseline for event 5, the average concentration increased about 1.8 times. For NAP and TCS in event 5 remained as observed in baseline. Additionally, from baseline to event 2, there was NAP and TCS occurrence, which suggests that there was a diffuse carrying of these pollutants into the river, increasing their concentrations only during the rainfall event. CAF, on the other hand, was detected in both monitored campaigns, indicating that there is a supply of this material during periods with and without rainfall. CAF concentrations increased, from baseline to event 2, of approximately 13 times.

At point BA2, which already receives the influence of WWTP, TCS was detected in rainfall events, indicating that these contaminants were introduced only during rainy moments. This can be be associated with WWTP overflow, since this pollutant was not quantified during the baseline. NAP average concentration, from baseline to rainfall events, had an increase only in event 2 and, for the other events, average concentration was similar to baseline.

For CAF, it was observed a concentration increase in events 2 and 5, relatively to the baseline, which can be associated to longer ADD time of these events (1.8 and 7.6 hours), allowing a greater accumulation of these pollutants. In events 3 and 4, average concentration are lower than baseline concentration, suggesting dilution effects. Figure 60 indicates the CAF, NAP and TCS dynamics as consequence of the rainfall events monitored in BA1 and BA2.

In event 5 at BA1, samples were collected manually, during three days in a row, after the peak

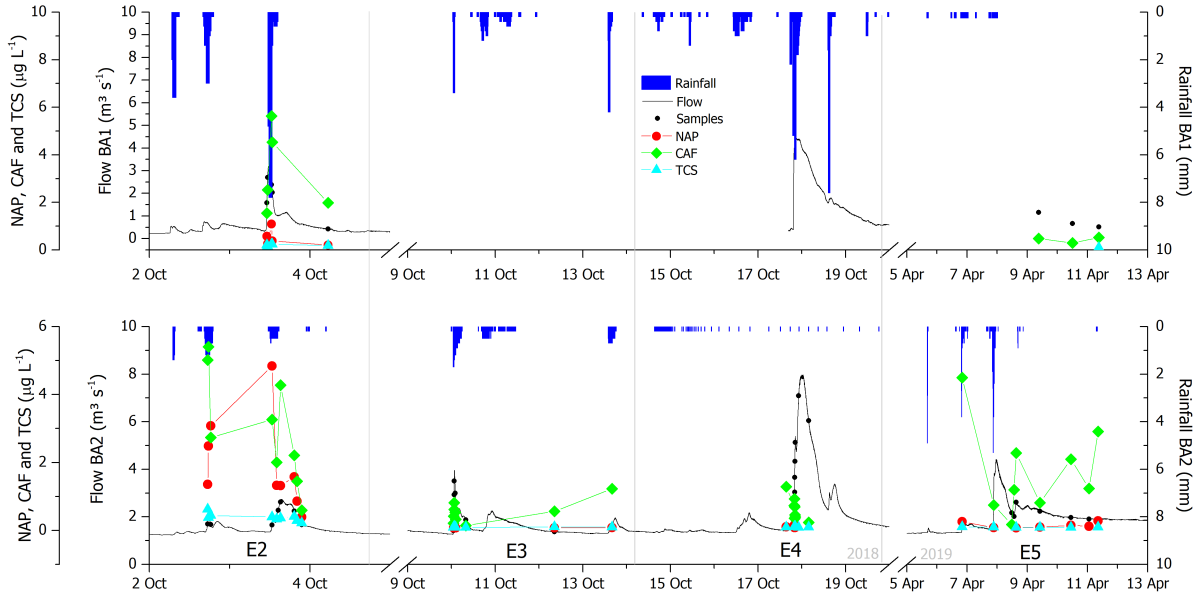

Figure 60 – CAF, NAP and TCS behavior along rainfall episodes monitored in BA1 and BA2 sites

of the rainfall. In general, only CAF was quantified in these 3 samples collected, where its concentrations decreased with decreasing flow. NAP had < LOQ concentrations in all samples and TCS had < LOD concentrations for samples 1 and 2 and 0.09 μg.L^{-1} in sample 3. However, in event 2, the three compounds were detected in all samples collected. NAP and CAF followed the pattern of the hydrograph, with increasing concentrations along with an increase in flow. The TCS had constant concentrations over time.

At point BA2, the three compounds were detected in all samples from events 2, 3, 4 and 5, with some exceptions. Thus, as observed in point BA1, TCS concentration in BA2 did not change over time along with the flow, in any observed event. The average concentrations were 0.38 ± 0.11 μg.L^{-1} in event 2, 0.10 ± 0.01 μg.L^{-1} in events 3 and 4, and 0.09 ± 0.01 μg.L^{-1} in event 5. This indicates that there are constant introduction of this type of compound in the water body, probably from WWTP. These point inputs are favored by rainfall events, since baseline concentrations were < LOD.

Similarly, NAP has only concentration changes with flow in event E2. For the other events, NAP did not have any variation, as well as the TCS, which may be associated with the particular characteristics of these three events. Event E2 has a longer ADD time, and events E3 and E4 were consecutive to event E2. Therefore, after initial washing off, these pollutants occurred in event E2, via diffuse paths. The contribution measured in events E3 and E4 had low variation in the EmerC concentration and flow, which can be associated to the WWTP influence. Then, events 3 and 4 favor dilution effects, considering average decreasing concentration observed from events 2 to 3 and from 3 to 4. Moreover, probably had the decreasing of diffuse carrying of these pollutants and remaining only the influence of WWTP, since there is no disappearance of these concentrations, but the occurrence of a steady-state scenario.

CAF, in general, followed the pattern of the hydrograph, with an increasing /decreasing concentrations along with the flow changes. It is possible to observe such variation in events 2, 3 and 5. The samples from event 4 represent only hydrograph rising, and due to its extreme characteristics (the largest measured event - med-to-high -, and the lowest ADD - third consecutive rainfall measured-), favored dilution effects of this compound from diffuse pathways, but continue to emphasize constant point influence of the WWTP. This similar pattern observed on CAF occurrence during rainfall events, suggests

that human activities developed in the incremantal drainage area have a great impact on water quality, considering both PS and NPS routes.

Thus, observing that, event 2 was the one that induced the greatest contribution via diffuse routes, without great dilution effects. Figure 61 shows in detail, the pharmaceuticals NAP and IBU, stimulant CAF and the personal care product TCS behavior in event 2.

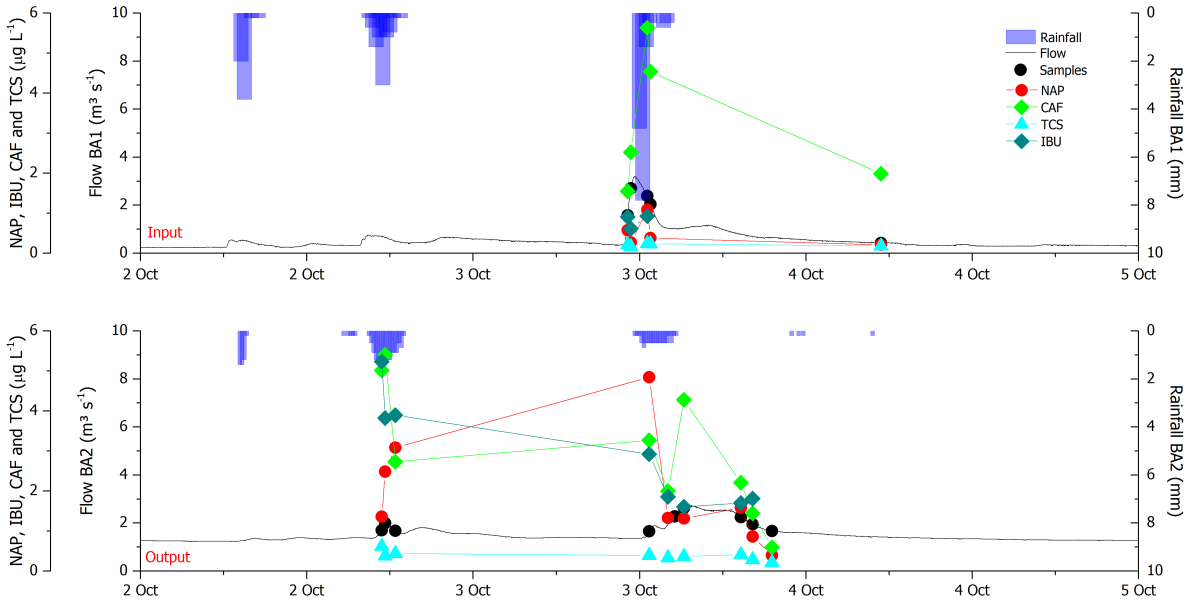

Figure 61 – NAP, CAF and TCS behavior in rainfall event 2 monitored in BA1 and BA2

It is possible to observe that TCS did not have variation following flow, in BA1 and BA2 sites, while NAP and CAF had variation with the flow, and IBU followed the flow in BA1 and had opposite behavior in BA2.

The highest NAP concentration were measured in the rising limb of the hydrograph in the both monitoring sites (sample 3 in BA1 - 1.09 $\mu g.L^{-1}$, and sample 4 in BA2 - 4.84 $\mu g.L^{-1}$), suggesting input through diffuse pathways. CAF had similar behavior, with higher values during higher flows. In BA1, the highest concentration of CAF was after the peak flow (sample 3 - 5.63 $\mu g.L^{-1}$), suggesting carrying from upstream, whereas in BA2, the highest concentration were measured in samples 3 and 6, which correspond to the both peak flow observed in BA2 (respectively, of 5.40 and 4.28 $\mu g.L^{-1}$). This suggests that CAF input was favored by rainfall episodes where there was wash-off from diffuse and point sources of pollution.

IBU in BA1 had the same pattern observed for NAP, following the flow, with higher concentration in sample 3 (0.93 $\mu g.L^{-1}$). For BA2, IBU concentration were decreasing with the flow, where the highest and lowest concentration were measured in the first sample (5.24 $\mu g.L^{-1}$) and last (< LOQ) samples, respectively.

To corroborate to pollutograph analysis, EMC curves showed these same pattern, as can be observed in Figure 62. In BA1, IBU indicate slight concentration, concave down above central line, during rainfall episode. NAP and TCS had initial concentration with changing in their concavity, suggesting dilution. Interestingly, CAF had concave up under central line during all event, indicating dilution, whereas concentration followed the hydrograph pattern. In BA2, all emerging contaminates had EMC curves above the central line, with concavity down, suggesting concentration during rainfall event 2. This

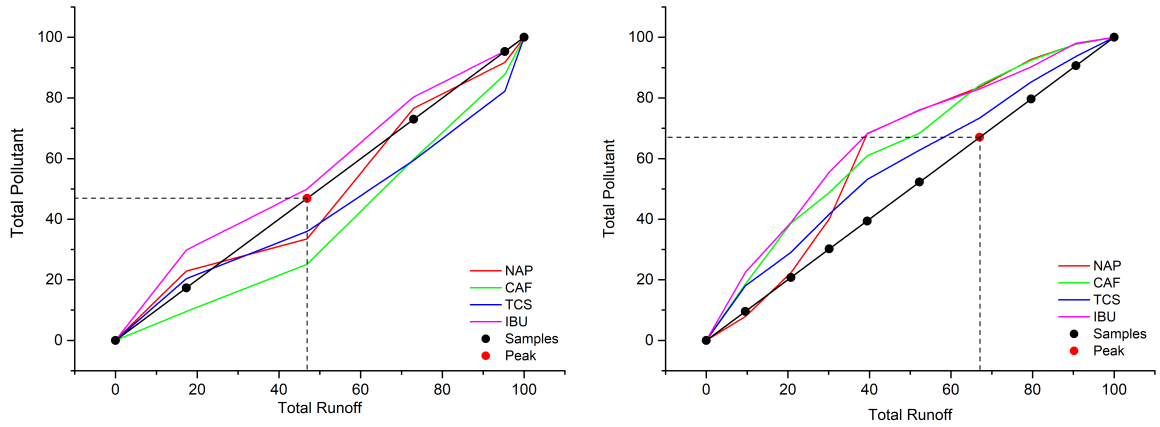

(a) EMC curve BA1 (b) EMC curve BA2

Figure 62 – EMC curves of emerging contaminants during event 2

behavior may have been favoured by WWTP point contribution, which does not stop during high flow periods.

For BA1, the peak of the event occurred on the second samples measured, which correspond to 47% of the total volume and pollutant transported during event 2. In that moment of the rainfall episode, approximately 50% of the IBU, 36% of TCS, 33% of NAP, and 25% of the CAF were transported. For BA2, the peak of the event occurred on the sixth sample measured, which correspond to 67% of the total volume transported during event 2. However, different from BA1, in BA2 the amount of emerging contaminant carried were above 73% in the peak of the event, indicating the relevance of the first flush in this kind of drainage area, with more urbanization and more potential pollution source.

The load analysis of these pollutants indicates that the amount in BA1 is lower than in BA2, as expected. From BA1 to BA2, there were an increase of, approximately, 7 times of NAP and IBU, 4 times of TCS and 2 times of CAF. This can indicate that the point sources (WWTP) have great influence in emerging contaminants input into the river, mainly pharmaceuticals. However, the unexpected contribution from BA1 also is important, because this diffuse contribution correspond, in average, to 30% of the emerging contaminants measured in the river during rainfall episodes. Figure 63 presents load value for these four emerging contaminants during event 2.

Thus, to check the influence of each drainage area on the input of these pollutants, the difference between BA2 and BA1 was made. The results showed that the largest proportions are NAP and IBU, with approximately 85% of their load, and the TCS, with 72% of their load measured just from point BA2, which may be associated with the influence of WWTP. However, CAF has a divergent behavior, in which 39% of its load corresponds only to point BA2, while 61% corresponds to point BA1, suggesting that the greatest contributions of CAF during rain events come from the monitored area upstream of the WWTP discharge. In addition, the CAF load during the baseline corresponds to 1 and 10% of the CAF load during event 2, respectively in BA1 and BA2, indicating that the greatest contribution of this compound was via diffuse routes. During the baseline, CAF from the point source corresponds to 52% of the CAF measured in BA2.

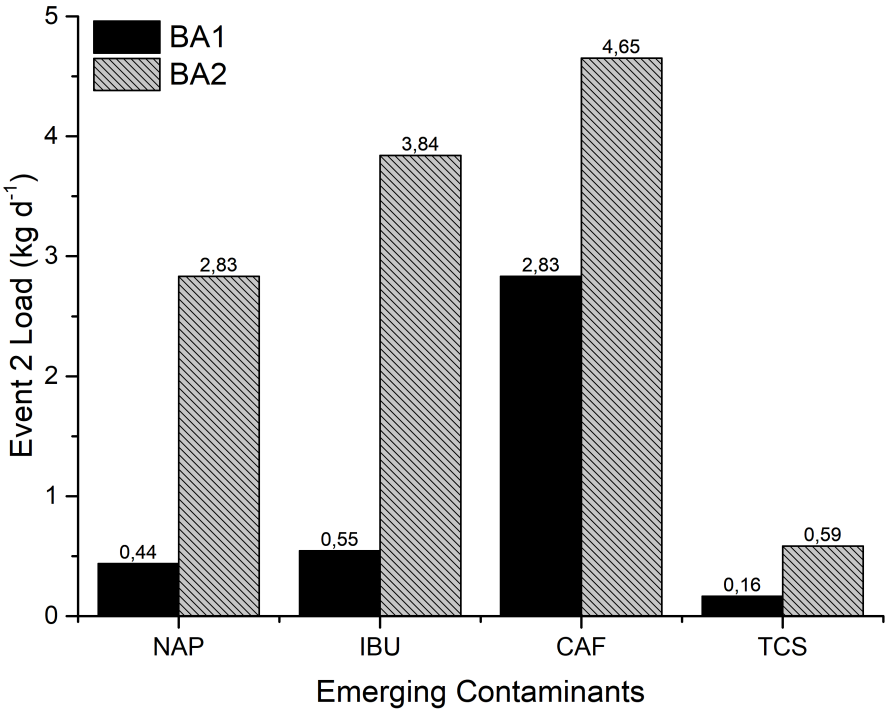

Figure 63 – Load of emerging contaminants during event 2 in BA1 and BA2

4.4.3 SUMMARY

In this section was possible to observe the occurrence of emerging contaminants and their behavior during rainfall episodes. The analyses were based on pharmaceutical, personal care products, and sterol determination.

Baseline campaign showed occurrence of sterol which did not occurred during rainfall episodes, probably due to dilution. In other perspective, some elements just occurred during rainfall episodes, as for example, PCPs, which can indicate the transport of them trought diffuse pathways. Pharmaceuticals were the emerging contaminants presented during baseline and rainfall episodes, which reflect human lifestyle of the population: high consume of caffeine, and medication with naproxen and ibupofren and use of agent bacteriostatic.

Moreover, CAF was the most consistent emerging contaminant monitored during the campaign. This compound followed the hydrograph pattern, increase and decrease with the flow, suggesting that their introduction into the system was favored by diffuse pathways. The estimate input of CAF during rainfall episode was 2.83 kg per day in BA1 and 4.65 kg per day in BA2. From these values, 39% correspond to BA2 and 61% to BA1, indicating the higher influence of the monitoring site upstream WWTP than downstream.

4.5 METALS

"How is the behavior of natural elements during non-point transport?"

In this section, will be presented the result of metals measured during baseline and rainfall episodes. There were analyzed both dissolved and total fraction. Similar to the other water quality parameters presented, events 3 and 5 were measured just in BA2, and events 2 and 4 were measured in BA1 and BA2, also the respective baseline profile. Event 1 was not monitored for metals category. Figure 64 shows hydrograms and exemplify metals samples at BA1 and BA2.

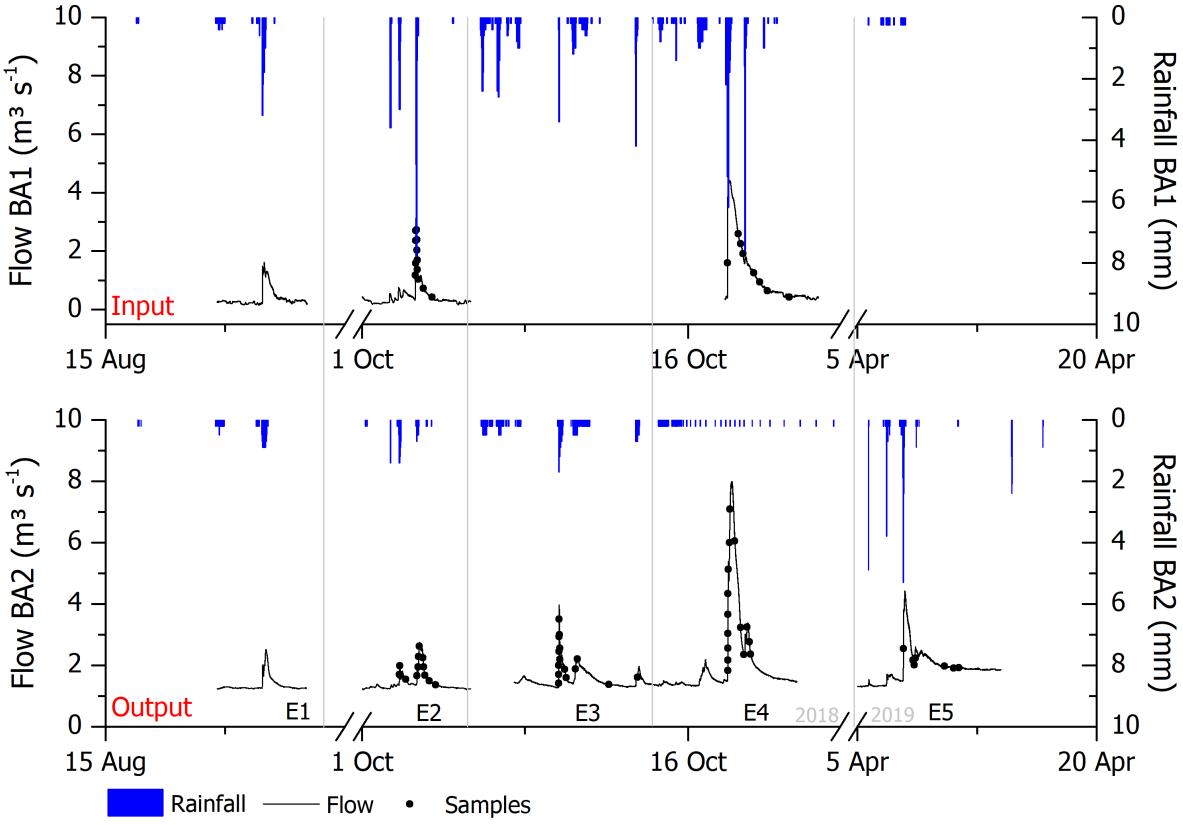

Figure 64 – Samples collected and analyzed for metals in BA1 and BA2

From the eight elements analyzed by the method presented in 3.5.3, elements Pb and Cd, which are considered toxic, had concentrations < LOD, and the other metals, which are considered non-toxic (Al, Ca, Cu, Fe, Mg and Mn), in general, showed concentration. Table 31 summarized the average concentration (± standard deviation) of the metals measured for baseline and rainfall episode, for the both sites in the both fractions.

Considering the average concentration measured, two important observation must be highlighted, such as: (i) Dissolved Ca and Mg had the highest concentration measured in the baseline and rainfall episodes, where Ca > Mg. These concentration were bigger in BA1 than in BA2, and higher during baseline than during rainfall episodes, which reflects geological composition of the region, where these elements are predominant in soil formation and have constant influence in the river system; (ii) Total Al and Fe had higher concentration measured in BA2 than in BA1, which can be associated to the WWTP discharge. Moreover, these concentration were bigger during rainfall episodes than during baseline, sug-

gesting the overflow influence of the WWTP. The main coagulants used in sewage treatment processes are aluminum sulfate and ferric chloride (SPERLING, 2017). Therefore, some residual of these elements may be discharged into the river and favoring the great increase of these concentrations principally during the rainfall episodes.

Therefore, considering the great differences between fraction and to ensure a clear presentation of these results, dissolved and total fraction will be, firstly, explained separately using hydrographs and EMC values. After that, will be presented the control volume perspective and EMC curves.

4.5.1 DISSOLVED FRACTION

At BA1, dissolved Fe, Mn and Cu had concentration just during baseline, and Al had concentration in the baseline and events 2 and 4. At BA2, dissolved Fe and Cu had concentration < LOD just in events 2, 3 and 4, while the others elements presented had concentration in the campaigns performed. Ca and Mg had the highest concentration measured in the both monitoring sites. Figure 65 shows the dissolved metals variation during rainfall episodes. Table 31 summarized the average concentration (± standard deviation) of the metals measured for baseline and rainfall episode, for the both sites in the both fractions.

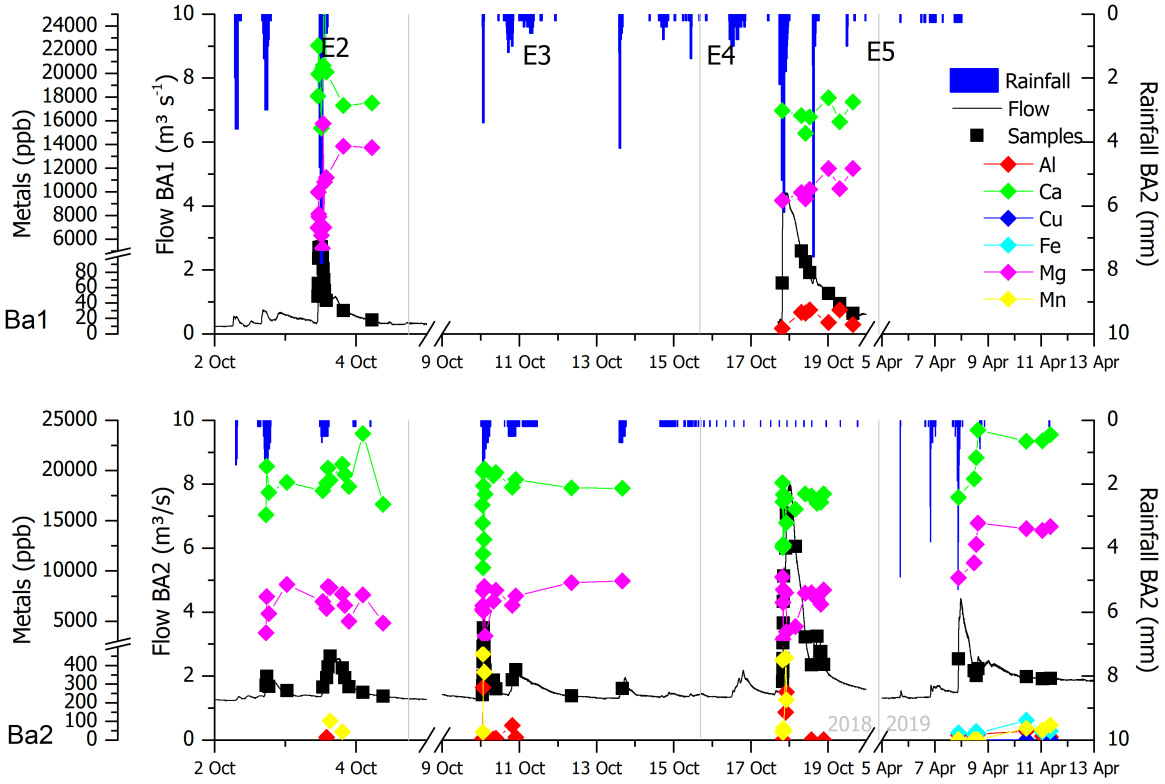

Figure 65 – Pollutographs of dissolved metals monitored in BA1 and BA2 during rainfall episodes

It was possible to observed that just Ca and Mg were measured in all rainfall episodes, with high concentrations. In BA2, more trace elements had concentration than in BA1, which can be associated to dilution effects in BA1 and/or WWTP influence in BA2. The highest values of Ca and Mg measured at BA1 and were in event 2, reaching 29670 ppb and 15760 ppb, respectively. At BA2, the highest Ca and Mg values measured were in event 5, reaching 24033 ppb and 14768 ppb, respectively.

For this fraction, Ca and Mg elements did not have an observed pattern following the flow. While flow increase and decrease, the concentration were constant overtime, suggesting the influence of the geological formation in the area. This behavior is corroborate with Pearson's correlation, where: (i) Ca and flow had Pearson of -0.27 (p-value < 0.05), (ii) Mg and flow had Pearson of -0.42 (p-value < 0.05), and (iii) Ca and Mg had Pearson of 0.54 (p-value < 0.05). Therefore, with increase of the flow, dissolved elements have tendency to decrease, whereas Ca and Mg increase and decrease together, suggesting the same input source.

Moreover, dissolved fraction had bigger concentration during baseline than during rainfall, suggesting the high and constant influence of these fraction into the river system without rainfall influence. Thus, Figure 66 shows EMC values during baseline and rainfall episodes for the dissolved metals measured.

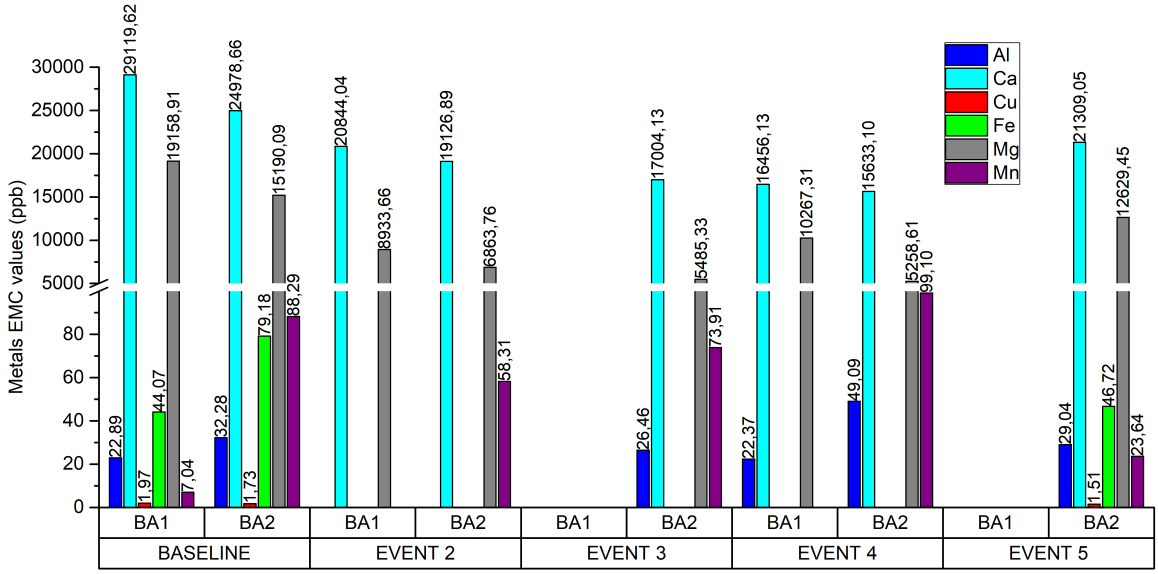

Figure 66 – EMC for dissolved metals analyzed during baseline and rainfall episodes at BA1 and BA2

It is possible to observe the same in concentration and pollutographs for EMC values. Ca and Mg were the highest elements measured. Dissolved Cu EMC had the lowest values and did not have variation between the campaigns. Dissolved Mn EMC had the lowest values in BA1 baseline, increasing in BA2 baseline. During the rainfall episodes, the values were higher than baseline. Dissolved Al EMC had similar values during baseline and rainfall episodes in the both monitoring sites, whereas dissolved Fe EMC had values just in baseline and event 5.

Table 31 – Average concentration (± standard deviation) (ppb) of the metals analyzed in BA1 and BA2 during baseline and rainfall episodes

Dissolved fraction		Al	Ca	Cu	Fe	Mg	Mn
BASELINE	BA1	23 ± 19	29106 ± 812	2 ± 1	44 ± 19	19150 ± 423	7 ± 6
	BA2	34 ± 50	26058 ± 1155	2 ± 1	83 ± 54	15847 ± 579	92 ± 10
EVENT 2	BA1	<LD	20778 ± 3906	<LD	<LD	9747 ± 3375	<LD
	BA2	<LD	19045 ± 2006	<LD	<LD	6727 ± 1519	223 ± 261
EVENT 3	BA1	not measured					
	BA2	47 ± 91	17057 ± 3123	<LD	<LD	8487 ± 2241	289 ± 219
EVENT 4	BA1	22 ± 10	16850 ± 1228	<LD	<LD	10786 ± 1436	<LD
	BA2	82 ± 117	15854 ± 2260	<LD	<LD	6109 ± 2460	206 ± 189
EVENT 5	BA1	not measured					
	BA2	29 ± 10	21609 ± 2498	2 ± 1	50 ± 26	12889 ± 2085	29 ± 35

Total fraction		Al	Ca	Cu	Fe	Mg	Mn
BASELINE	BA1	518 ± 304	32269 ± 1599	15 ± 33	1966 ± 3827	20310 ± 591	44 ± 77
	BA2	100 ± 92	26566 ± 858	4 ± 4	742 ± 796	16083 ± 465	23 ± 16
EVENT 2	BA1	20037 ± 11603	104857 ± 54121	44 ± 22	39782 ± 23327	64684 ± 26756	621 ± 482
	BA2	22474 ± 17879	50486 ± 28447	81 ± 57	48788 ± 33395	34997 ± 21703	790 ± 757
EVENT 3	BA1	not measured					
	BA2	21509 ± 22402	38359 ± 9968	65 ± 84	40592 ± 41148	26433 ± 8003	581 ± 609
EVENT 4	BA1	2963 ± 1091	29612 ± 4593	21 ± 15	4109 ± 1022	22555 ± 3638	<LOD
	BA2	30940 ± 34023	45660 ± 30401	104 ± 133	58169 ± 62767	31758 ± 22144	1005 ± 1337
EVENT 5	BA1	not measured					
	BA2	14692 ± 11736	33539 ± 8265	25 ± 17	17667 ± 12606	18366 ± 3642	385 ± 240

SOURCE: The Author (2020)

4.5.2 TOTAL FRACTION

For this fractions, all elements had concentration measured, with exception Mn in BA1 during event 4. Difference from dissolved fraction, total fraction had bigger concentration during rainfall episodes than during baseline. Moreover, there was not observed an clear pattern of BA2 concentration > BA1 concentration, which can be related to the good affinity between metals and suspended solids. Thus, total fraction had wide variation along the rainfall episodes, as can be observed in Figure 67. Table 31 summarized the average concentration (± standard deviation) of the metals measured for baseline and rainfall episode, for the both sites in the both fractions.

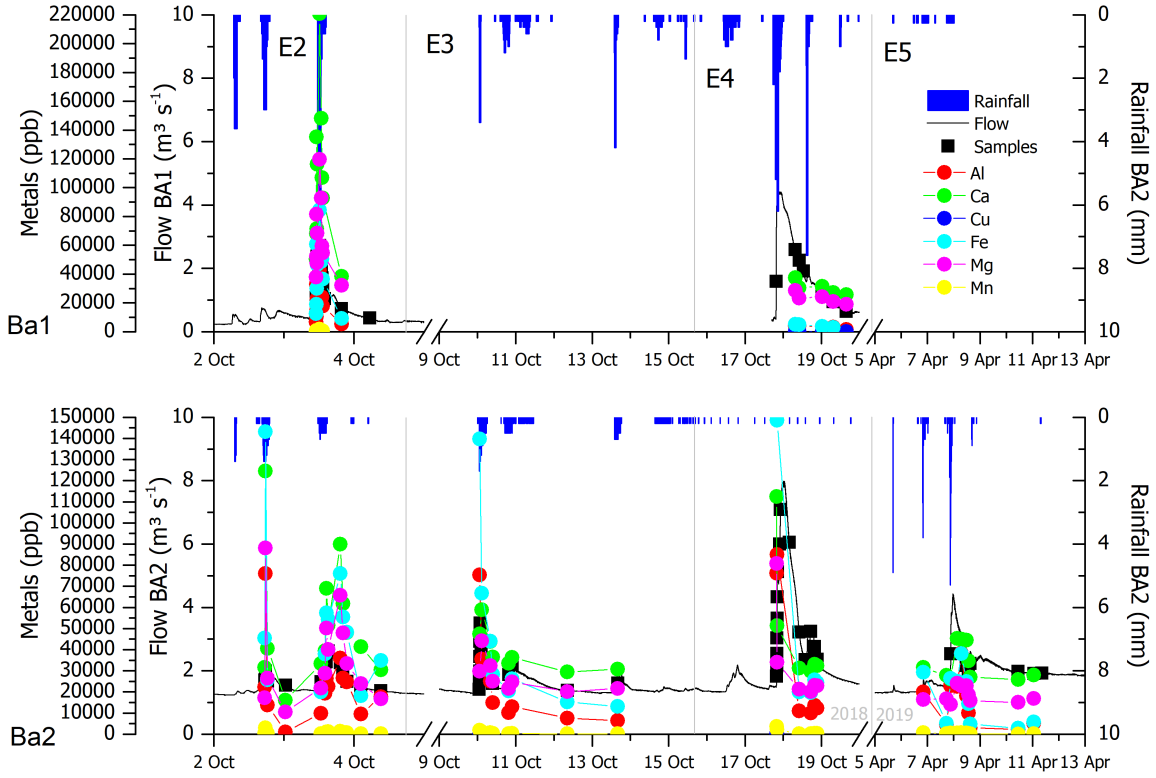

Figure 67 – Pollutographs of total metals monitored in BA1 and BA2 during rainfall episodes

It can be observed that Ca and Mg, considered macro elements, and Al, Fe, Cu and Mn, which are considered trace elements, had higher concentration on the total fraction. This occurred due to the high affinity that metals have to the particles. Therefore, in the total fraction there was not an predominant elements in all rainfall episodes. Ca and Mg still had high concentration in the rainfall episode, however with high concentration of Fe and Al.

There is not a predominant bigger concentration in BA2 than in BA1, but a variation. While BA2 have the influence of pervious surface which accumulate particles and the WWTP outflow, BA1 have more impervious surface favouring river bed erosion and particles from the soil.

Events 2 and 4 had the highest amount of metals. In event 2, in BA1, were measured the highest values of Al (42567 ppb), Ca (220800 ppb), Fe (84440 ppb) and Mg (119600 ppb). These values of Ca and Mg were the highest concentration measured among all samples analyzed. For BA2, event had higher concentration for Ca (124600 ppb) and Mg (88190 ppb), while event 4 had higher values

for Al (84960 ppb), Cu (258 ppb), Fe (151400 ppb), and Mn (3594 ppb). Samples that had the highest concentration of metals did not, necessarily, have the highest turbidity values. However, as can be observed in pollutographs, these inorganic elements in total fraction followed the flow behavior during rainfall episodes.

Pearson's correlation showed a slight positive correlation between flow and elements, where just Al and flow had p-value < 0.05, with Pearson of 0.27. However, turbidity and Al (0.53, p-value <0.05), Ca (0.67, p-value <0.05), Fe (0.59 , p-value <0.05) and Mg (0.67 , p-value <0.05) had stronger positive correlation, suggesting that occurrence of total inorganic elements can be related to the turbidity occurrence, or, suspended particles. Between these four elements, all have positive and strong correlation, in which, Fe and Al had Pearson of 0.98 (p-value < 0.05), and Ca and Mg had Pearson of 0.97 (p-value <0.05), suggesting that these elements probably have the same sources of contribution.

In absolute values, EMC values were higher concentration during rainfall episode than during baseline campaign, indicating that transport of metals was favoured during rainfall, and were associated to the particles. Figure 68 shows EMC values for baseline and rainfall episodes of the total fraction of the metals analyzed in BA1 and BA2.

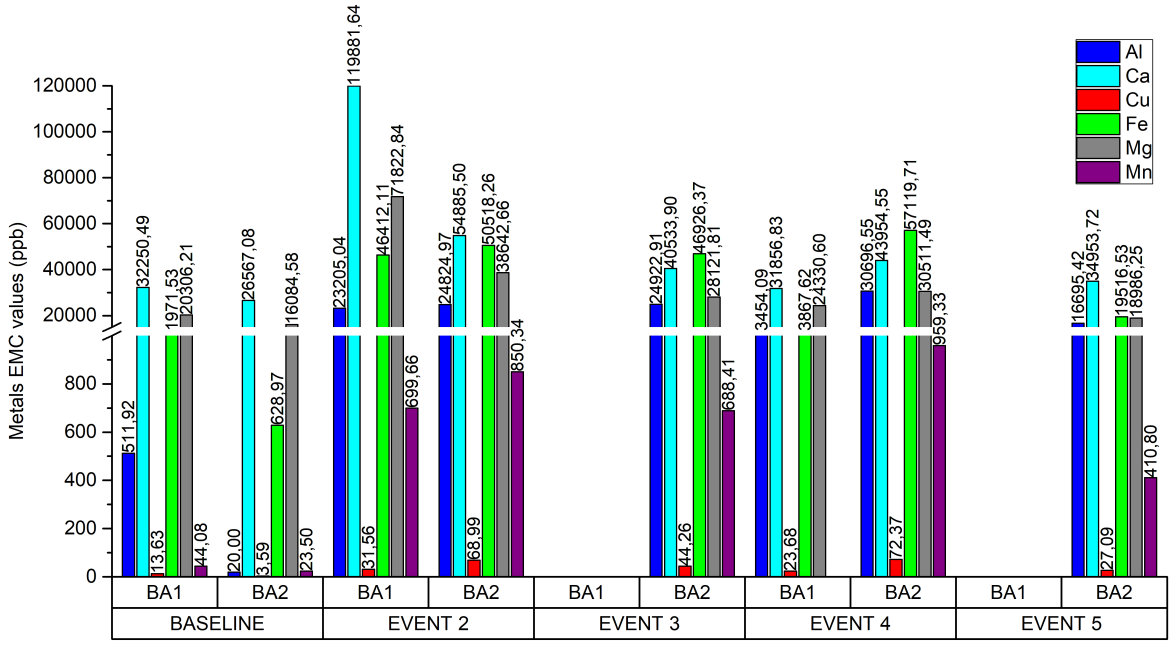

Figure 68 – EMC for total metals analyzed during baseline and rainfall episodes at BA1 and BA2

It is possible to observe that, for total fraction, there is not a clear pattern as occurred in dissolved fraction. As mentioned, EMC values increased from baseline but did not have differences between rainfall episodes, which can suggest that the transport of metals and particles occurs similarly during all rainfalls. At the same time, there is not a predominance of higher concentration in BA2 than in BA1, probably due to the influence of difference sources of contribution in each monitoring site.

Cu EMC had the lowest value, which increase during rainfall episodes, with higher values in BA2 than in BA1. Mn EMC had lower values in baseline, increasing about 10 times during rainfall episodes. EMC of Al and Fe were close to EMC of Ca and Mg, suggesting the relevance of particles carrying and input during rainfall episodes.

4.5.3 METALS DYNAMICS

Considering there is not high differences between rainfall episodes in the EMC values for total metals, event 2 will be detailed in this section. The main purpose is to highlight metals behavior during rainfall episodes, and the control volume perspective.

Figure 69 shows pollutographs of the event 2, where it is possible to observe increase and decrease of the concentration following the flow. In BA1, sample 6, which represent peak flow (2.72 $m^3.s^{-1}$), had the highest concentration of Al, Ca, Fe, Mg and Mn. At this point, concentration had the first increase of concentration in sample 3, decreasing in sequence, and then increasing again until the peak flow in sample 6. This first input in sample 3, can be associated with the first-flush occurrence, introducing pollutants from the nearest drainage area. In BA1, the concentration order were Ca > Mg > Fe > Al > Mn > Cu.

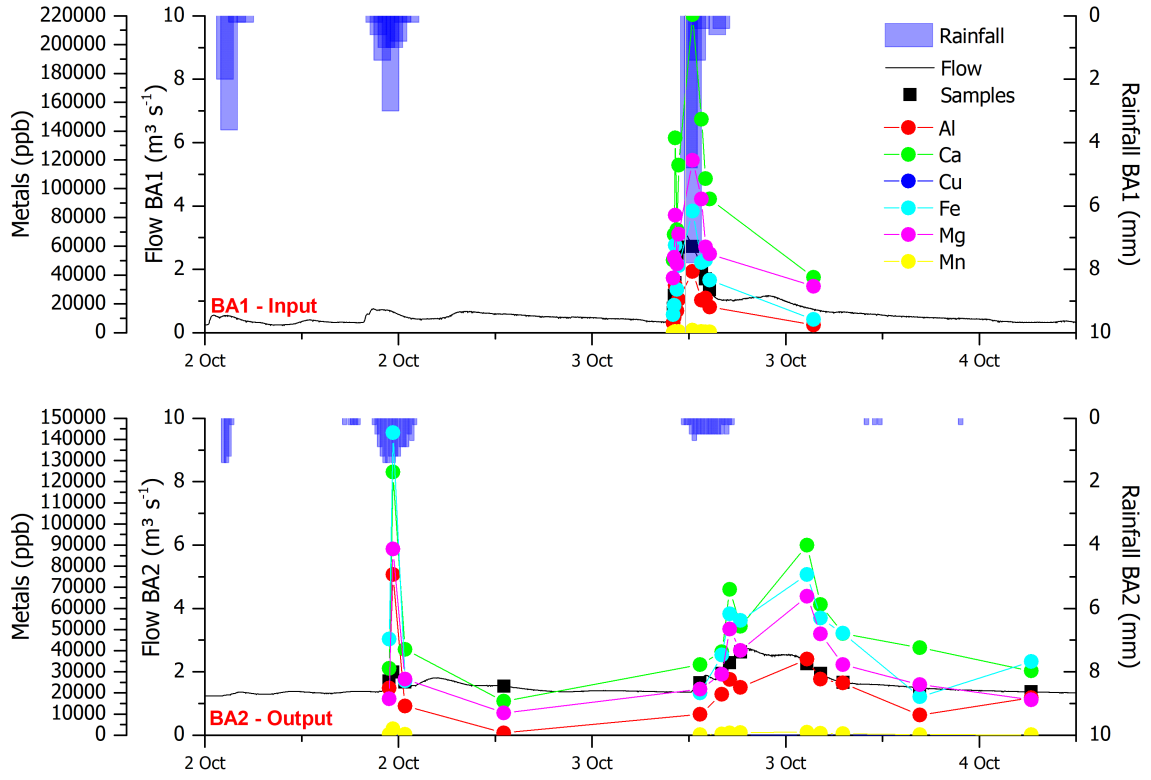

Figure 69 – Pollutograph of total metals in event 2 at BA1 and BA2

At point BA2, there are two peak flow, induced by two isolated rainfalls. In the both peaks, metals concentration increase following the flow, with the highest concentration in samples 2 and 9. Sample 2 represent the peak flow in the first set of samples (1.99 $m^3.s^{-1}$), and sample 9 is the sample after the peak flow in the second set of samples (2.25 $m^3.s^{-1}$, where peak flow was 2.63 $m^3.s^{-1}$ in sample 8). This behavior suggests that first-flush occurred in the first set of samples, introducing pollutants more available to be carried in the nearest drainage area of point BA2 (incremental area). In sequence, on the second set of samples, the peak of concentration occurred after the peak flow, suggesting the influence of upstream pollutants, in other words, from BA1 plus WWTP influence. In the first set of samples, the concentration order was Fe > Ca > Mg > Al > Mn > Cu, while on the second set of sample, the concentration order was Ca > Fe > Mg > Al > Mn > Cu. The increase of representativeness of Al and

Figure 70 – EMC curves of total metals during event 2 in BA1 and BA2

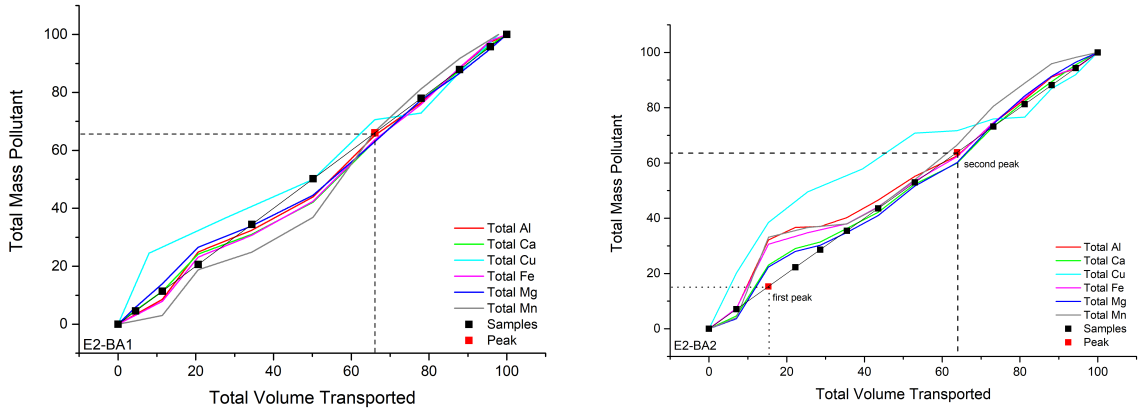

(a) EMC curve BA1

(b) EMC curve BA2

Fe can be related to the WWTP influence, which generally uses Iron Chloride ($FeCl_3$) and Aluminum Sulfate ($Al_2(SO_3)_3$) as coagulant in the sewage treatment process.

EMC values indicate amount of pollutant transported during an rainfall episodes. EMC for Ca and Mg were bigger in BA1 than in BA2, whereas EMC of Al, Fe, Cu and Mn were bigger in BA2 than in BA1. However, when EMC curves are analyzed, it is possible to identify the proportion of the pollutant carried until the peak of events. Thus, Table 32 summarizes EMC proportion in the peak samples and Figure 70 shows EMC curves of the event 2 for the total metals analyzed.

Table 32 – Proportion (%) of the pollutant carried into the river until peak flow in BA1 and BA2

Site	Peak sample	Flow	Al	Ca	Cu	Fe	Mg	Mn
BA1	Sample 6	2.72	65.25	64.38	67.37	64.59	64.37	64.02
BA2	Sample 2	1.99	19.07	17.12	21.77	18.91	16.69	18.38
	Sample 8	2.63	62.18	61.61	71.20	62.17	61.81	63.83

According to the Figure 70 it is possible to observed that, the curves in BA1 were close to central line, in zone B. In the beginning of the event, Cu have concavity above central line, in the zone A, while others elements have slight concavity down the central line. This suggests that during the begin of the event there was more expressive input of Cu from near sources, but in general the pollutant transport along rainfall episodes have the same proportion of the amount of water transported. Until event peak, it was transported, in average, 65% of the metals.

For BA2, Cu have the same behavior observed in BA1, with concavity above central line, indicating that there were, proportionally, more pollutant being inputted than water transported. For the other elements, the interesting signal of introduction it is observed after the first peak (sample 2). After that, and during the second peak, EMC curves were close to the central line. This indicate that the first peak have bigger contribution than the second one, which can be associated to the first-flush in the initial wash-off occurred in the first peak, after some days without rainfall and, consequently, pollutant accumulation. At the first peak, in sample 2, in average was carried about 19% of the all metals transported, and until the second peak, in sample 6, this amount increases to 64%.

EMC curves classification predominantly in zone B indicates that the effects of first-flush are not as pronounced for, mainly in BA1, probably due to the type of land use (more vegetation than urbanized areas). For BA2, there is a slight occurrence of first-flush in the beginning of the event, associated to

the more urbanized and impervious areas, as well as, WWTP influence. In addition, the occurrence of pollution transport along with water transport, indicates that these elements are carried by the flow, favored by rain episodes, being associated to the diffuse pathways.

Thus, Figure 71 shows the difference between BA2 and BA1, which correspond to the incremental area of metals during event 2. Although the behavior and transport of metals was favored by the rainfall episodes, the difference in EMC of BA1 and BA2 drainage areas shows the great influence of the geological composition of the region, where Ca and Mg had negative values, and Al, Fe, Cu and Mn had positive values

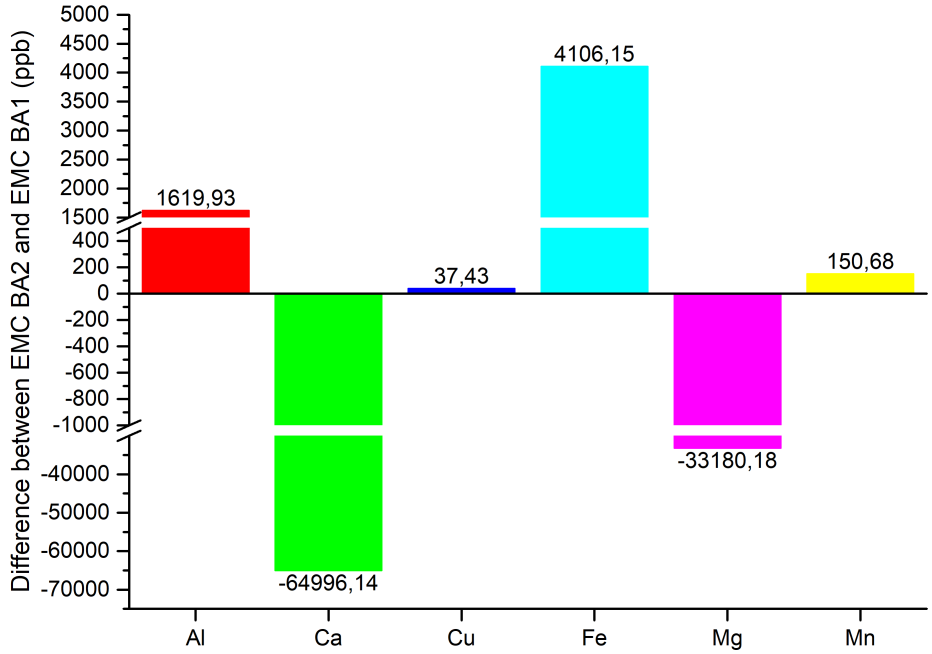

Figure 71 – Metals EMC of incremental area on the event 2

SOURCE: The Author (2020)

Thus, Ca and Mg from BA1 had bigger influence in the BA2 than just the incremental area, probably due to the composition of the soil formation and the erosion process in BA1, which have less urbanized areas. The others elements had bigger influence from the incremental area than from BA1, which can be associated to influence of the WWTP in the transported of Al and Fe, for example, during rainfall episodes.

4.5.4 SUMMARY

In this section, it was possible to observe the dissolved and total metals dynamics during rainfall episodes. Dissolved fraction had bigger concentration in baseline than during rainfall episodes. The most significative elements were Ca and Mg, mainly in BA1 than in BA2. Total fraction had opposite influence, with bigger concentration during rainfall episodes, than during baseline. The relation between turbidity, flow and metals analyzed helps to corroborate the influence of particles in the metals affinity and transport. Additionally, there was verified that total metals have almost the same introduction in rivers, regardless the hydrological characteristics of the events. The high correlation between Ca and Mg, and Fe and Al suggest that these elements have the same sources of contribution

As observed in EMC curves, the beginning of the event have the bigger influence on metals transported, where about 65% of the total pollutant were transported until the peak event. Additionally, first-flush phenomena was not evident, probably due to the drainage area characteristics, where the occurrence of these macro inorganic elements are predominantly natural. Therefore, this group of elements can be related to non point sources of pollution, mainly to understand the environment dynamics.

4.6 SUMMARY OF THE CHAPTER

In this chapter, the five sub-section of results generated in this work were presented. The first sub-topic, hydrological characteristics, can be considered "mother-section", because it is the rainfall attributes that determines pollutant transport of pollutants, as well as, the land use composition that determines the types of pollutants present. So, in that section, quantitative aspects of the monitored rainfall events were presented, being possible to generate some scenarios such as: fast and short rainfall event (E1), fast and intense rainfall event (E2), consecutive rainfalls events (E3 and E4), and a long and mild event (E5).

In the second sub-section, traditional water quality parameters were presented, in polutographs, EMC values and curves, and loads. In that section, it was possible to explore the dynamics of land use considering the parameters most commonly used in the classification of water bodies (e.g. N and P), as well as, parameter characteristic of NPS transport (e.g. SS and turbidity) and PS contribution (e.g. COD). From these data, it was already possible to observe the significant influence that the incremental area has on water quality during rainfall events.

In the third sub-section, DOM dynamics was presented, which identifies OM characteristics introduced during the rainfall and possible sources. Rainfall events showed a refractory composition character and NPS processes are predominant.

Emerging contaminants were presented in the fourth sub-section, in terms of occurrence and behavior during rainfall events. This set of parameters aims to identify urban influence on the watershed, considering that EmerC are elements directly related to human activities, such as pharmaceutical and caffeine. Another important aspect is the understanding of the occurrence of these elements during extreme events, since some compounds have a short half-life or have more hydrophobic characteristics. Therefore, the appearance of these compounds, highlights relevant elements for the water resources management, such as i) inefficient sanitary sewage collection system or the lack of; ii) impacts of urban occupation expansion; iii) PS influence during rainfall events; iv) input of EmerC into the water body that may represent adverse effects on biota in the medium- and long-term.

Finally, in the fifth sub-section, metals dynamics were presented, in terms of quantity, predominant fraction and behavior during rainfall events. This set of parameters helped to identify behavior of elements from geological formation, showing how NPS can behave in the system. In addition, the distinct occurrence of particulate and dissolved fraction during quantification support the understanding of how much the particle transport has a strong contribution effect during rainfall events, being possible to carry adsorbed pollution downstream.

Thus, the association of these characteristics helps to try to recognize environment dynamic from many perspectives, considering multiple influences and responses of the system. Additionally, in order to proceed an proper analysis, the baseline conditions profile is fundamental, to establish how much the "mother-section" has influence in the other sections. However, considering the lack of studies that address NPS issues considering the same strategy presented here, it is difficult to make appropriate comparisons and discussion. Thus, Figure 72 shows a scheme of the main references linked to each section presented.

Each research was fundamental to understand NPS process and classic behavior on the study areas presented. However, it is complex to make specific comparison and generalization in a multiple and delicate environment interface, mainly because each rainfall episode has different cause-effect relation through the watershed. Researches which evaluated hydrological characteristics generally is focused in one specific WQP that well represent rainfall events influences, such as nitrate or turbidity (CHEN et al., 2018b; PÉREZ-GUTIÉRREZ et al., 2020). Researches which considers conventional WQP and DOM evaluation during rainfall episodes (YANG et al., 2015; FRANK; GOEPPERT; GOLDSCHEIDER,

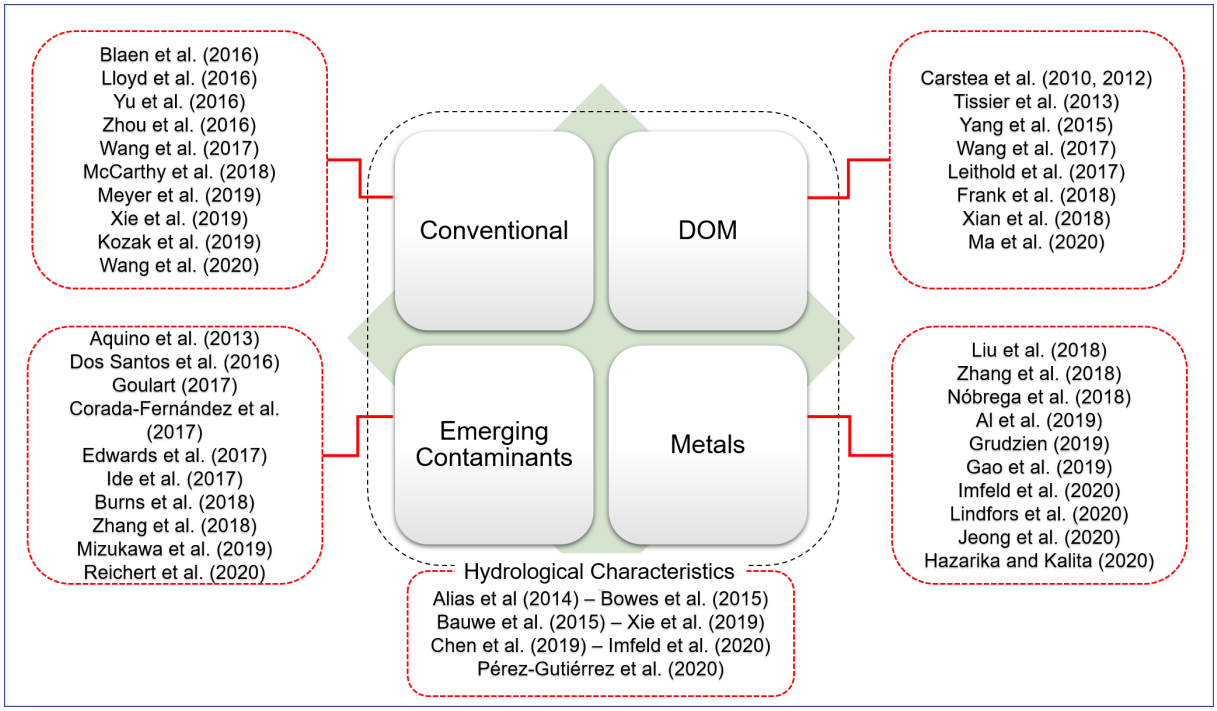

Figure 72 – Scheme of the similar researches associated to the results sub-sections presented

2018; KOZAK et al., 2019; MEYER et al., 2019), generally present more data discretization, due to the use of high-frequency structure, however without association with land use and consecutive monitoring sites. And, researches which consider EmerC and metals normally perform spatial assessment or simple quantification, without considered NPS pollution.

Therefore, the main contribution of this thesis was to present the influence of the land uses changes in river water quality during rainfall episodes, where small land use variation increase pollution inputs. This contribution was possible due to the baseline profile, and mainly as result of the novelty in to consider two consecutive, and close, monitoring sites, being possible to connect the cause-effect and pollution-source-pathways relation. The data generated in this thesis can be helpful to mathematical models purposes, to establish sources of pollution and understanding about NPS processes, to reflect about the next step of water resources management improving, such as legal requirements and BMPs program.

5 FINAL REFLECTIONS

It is necessary to reduce the distance between what is said and what is done, until, at a given moment, your speech is your practice.

Paulo Freire

In the context of this research distinct land use have significant influence on pollutant contribution by surface runoff in the watershed, considering the impact from rainfall events. Based upon automatic sampling, the strategy of increasing temporal resolution, associated to the incremental area approach was possible to observe different contribution from two distinct monitored drainage area. Therefore, the main research questions associated no NPS sources previously stated are addressed, as presented next.

5.1 HOW IS THE IMPACT OF LAND USE?

The different types of land use in each drainage area reflects on distinct pollutant availability, and, consequently river water quality. Some important aspects are presented below.

First of all, in BA1 vegetated areas (35.9 km^2) and pasture areas (14.0 km^2) have bigger proportion of area than other land use as, for example, urbanization (3.4 km^2). Whereas in the incremental area up to BA2, the amount of vegetated area (18.4 km^2) and pasture (11.2 km^2) is smaller, and urbanization grows (10.6 km^2). Therefore, point BA1 has more proportion of pervious areas, at the same time that exposed areas can facilitate erosive processes. For point BA2, water infiltration decreases due to the increasing impervious areas, favoring superficial runoff.

In hydrological terms, these differences affect physical process of the river during the rainfall episodes. Figure 73 shows average values of the hydrological characteristics measured on the rainfall episodes monitored during this study. For example, point BA1 had, on average, less amount of rainfall received than BA2 (28.27 mm and 49.32 mm respectively), which reflects in the lower volumes of water transported in BA1 (2.17 m^3 in total, of which 1.77 m^3 were via surface runoff) than in BA2 (6.67 mm^3 in total, of which 4.98 mm^3 were via surface runoff). However, the average rainfall intensity of the measured rainfall episodes were higher in BA1 (4.00 $mm.h^{-1}$) than in BA2 (1.66 $mm.h^{-1}$), which is associated to the cross section area at each monitoring point, reflecting in the longer rising time and critical time in BA2 (8.03 hours and 20.96 hours, respectively) than in BA1 (1.53 hours and 1.86 hours).

The response that the river has under the different characteristics of the monitored rainfall episodes was similar with low standard deviation, with average respectively for BA1 and BA2, of Q_{base} (0.34 ± 0.08 m^3 s^{-1} and 1.36 ± 0.13 m^3 s^{-1}), Q_{max} (3.13 ± 1.48 m^3 s^{-1} and 4.33 ± 2.19 m^3 s^{-1}), ΔQ (2.79 ± 1.40 and 2.97 ± 2.07) and Bt (2.08 ± 1.16 days and 2.92 ± 1.15 days). However, considering that point BA1, which has land use with a greater tendency for soil infiltration, revealed a larger Cot than BA2 (18h versus 16h) that has land use that shows greater tendency for runoff. This indicates that in BA1, after the end of the rainfall event, it takes longer time for the hydrograph recession to reach inflection point than BA2, probably associated to the more saturated soil in BA1 than in BA2, where it is more impervious, requiring more time for the assimilation of water bodies. Additionally, it should be noted that consecutive rainfall episodes increases the river's response effect of Bt values.

In terms of water quality, distinct distribution of land use in BA1 (more vegetation) and BA2 (more urbanized), implies different potential influences from sources and the transport of pollutants.

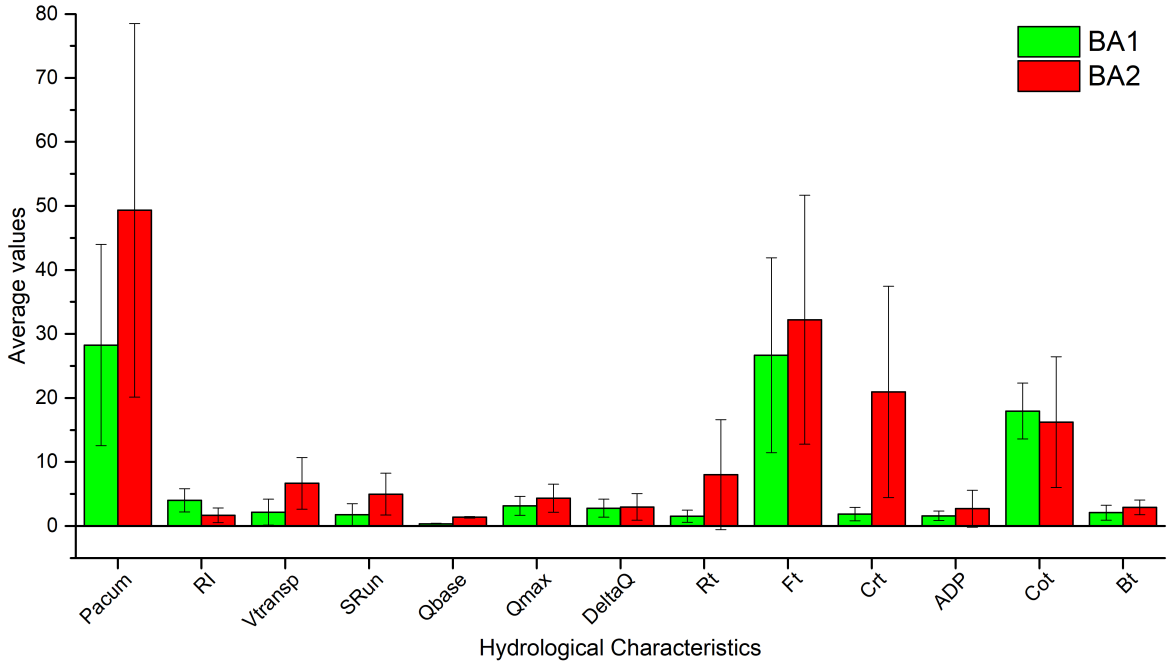

Figure 73 – Average values of hydrological characteristics measured in BA1 and BA2

LEGEND: P_{accum} - Accumulated precipitation (mm); RI - Rainfall intensity ($mm.h^{-1}$); V_{transp} - Volume of water transported (m^3); SRun - Surface runoff (m^3); Q_{base} - Base flow ($m^3.s^{-1}$); Q_{max} - Maximum flow ($m^3.s^{-1}$); ΔQ - Difference between Q_{max} and Q_{base} ($m^3.s^{-1}$); Rt - Rising time (h); Ft - Falling time (h); Crt - Critical time (hours); ADP - Antecedent Dry Periods (day); Cot - Concentration time (hours); Bt - Base time (days)

For example, BA1 can be characterized with a drainage area that receives greater influence from NPS during rainfall events, such as: subsurface runoff, facilitated erosion processes and runoff to a lesser extent. Differently, BA2 receives influence NPS from upstream, with a higher proportion of urbanization, favoring surface runoff, and a PS of discharge at the WWTP, imposing a mixture of multiple sources of pollution.

Therefore, land use composition have influence on pollution availability and build-up. Pervious area favours infiltration, as well as, impervious area favours pollution accumulation. Thus, considering that, in areas with bigger proportions of pervious area than impervious, the hydrological characteristics involving specifically rainfall have more influence on the pollution transport. Whereas, in the opposite with more proportion of impervious area, the period without rainfall have more influence on pollution impacts, due to accumulation, than distinct rainfall duration and intensity. These conjuncture corroborate hypothesis 1 and 2.

5.2 HOW MUCH POLLUTANT LOAD IS CARRIED INTO THE RIVER DURING THE RAINFALL EPISODES?

The flux transported to the river system during rainfall events is directly related to land use, since higher loads are expected in BA2 (more urbanized) than in BA1 (less urbanized), exemplified in Figure 74. The load estimates of conventional water quality parameters increase from BA1 to BA2. DOC, TN, TP and PO_4^{3-} have the smallest increasing proportion, ranging from 2 to 8 times, while COD, N-NH_4^+ and SS increase more than 10 times. COD and N-NH_4^+ are very characteristic of WWTP emmision, which suggests the great influence of this PS in the pollutants discharge during the rainfall episodes.

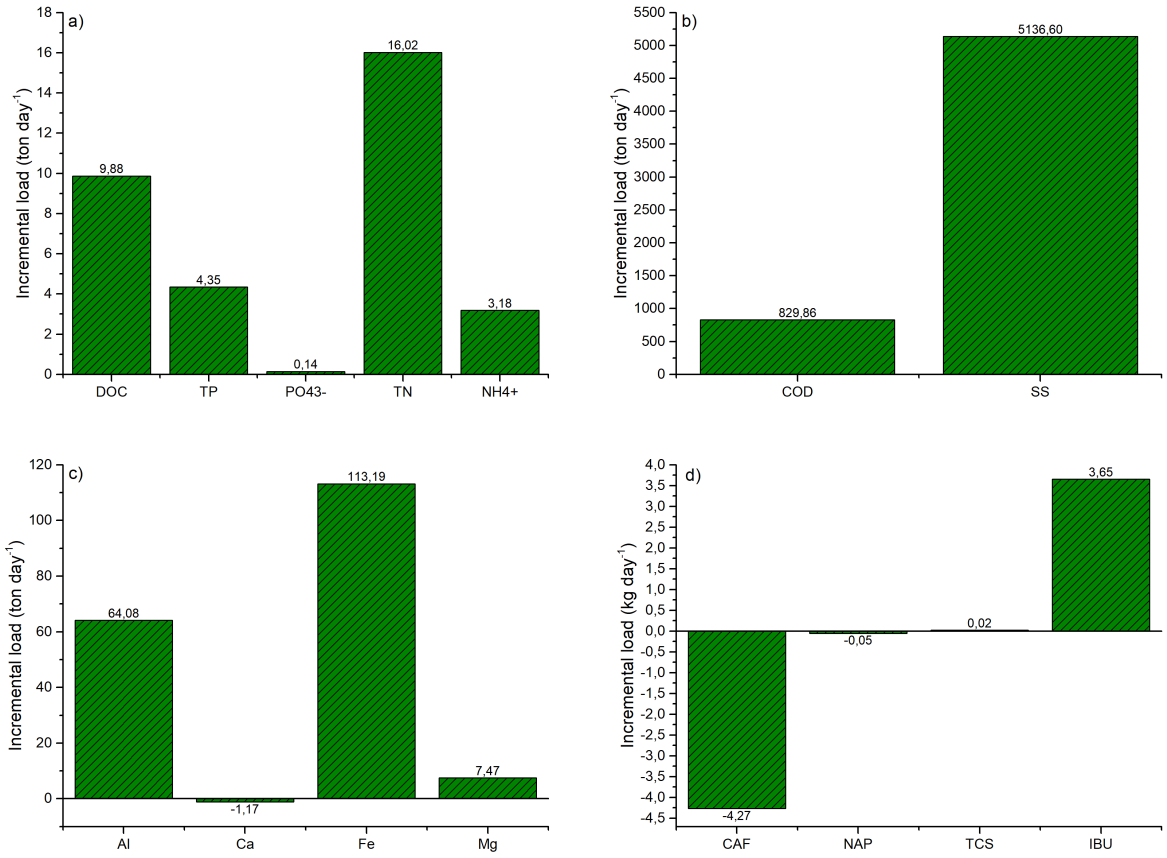

Figure 74 – Average incremental load (ton day^{-1}) of the water quality parameters analyzed in this study: a) conventional - part I; b) conventional - part II; c) emerging contaminants; d) total metals

Similarly, total metal loads for Al, Fe and Mg increased between BA1 and BA2, while Ca load decreased, suggesting that this bigger contribution of Al and Fe may be related to WWTP discharges, which use coagulants in the sewage treatment process that contains Al and Fe. Additionally, the geochemical formation has a great influence on point BA1.

The emerging contaminants loads have lower standardized occurrence than the other elements. TCS and IBU load increased (respectively 1 and 3.4 times) from BA1 to BA2, while CAF and NAP had load decrease (respectively 0.5 and 1 time). However, these distinct variation between the monitoring sites indicates: i) higher CAF load in BA1 suggests that even low urban area has an influence on input of anthropogenic pollutants into the river via diffuse pathways; ii) the use of medications (NAP is anti-inflammatory drug) by the population living in the drainage area at point BA1, which is carried to the river without proper treatment, either through percolation/accumulation in the soil via septic tanks, either by irregular discharge of sewage into the river, or by failures in the sewage collection network, resulting in greater loads introduced in BA1 than in BA2; iii) WWTP influence on emerging contaminant discharge into the river, with the biggest load increase of IBU, which is a typical anti-inflammatory drug used in Brazil, not well degraded in treatment processes. On the other hand, the DOM dynamics measured by spectroscopy techniques is not able to transform loads, because the technique itself represents a qualitative assessment of the possible/predominant organic structure present. Thus, in general, it is possible to determine that humic compounds (refractory or more complex organic chain) are predominant in relation to protein compounds (labile or more simplified organic chain), at both monitoring points. Among them, BA2 had higher fluorescence intensity than BA1. Therefore, although traditional compounds show a

possible influence of labile material from WWTP (such as, N-NH_4^+), rainfall episodes have the ability to introduce more refractory compounds into the system. For BA1, these compounds may come from erosive processes and/or degraded organic material, while in BA2 they may come from washing-off surface area around plus WWTP overflow plus BA1 influence.

Finally, Table 33 summarizes average flux in day and in year for BA1 and BA2. In descending order of loads calculated, classification was SS > COD > Fe > Al > TN > DOC > Mg > TP > IBU > N-NH_4^+ > PO_4^{3-} > TCS > NAP > Ca > CAF, where the last three compounds had negative incremental load between points.

Table 33 – Calculated loads for conventional water quality parameters, total metals and emerging compounds in BA1 and BA2

	ton day^{-1}	
	BA1	BA2
DOC	6.11	15.98
COD	74.10	903.95
TP	0.90	5.25
PO_4^{3-}	0.02	0.16
TN	2.12	18.14
N-NH_4^+	0.35	3.53
SS	196.27	5,332.87
Al	28.45	92.53
Ca	156.63	155.46
Fe	54.80	167.99
Mg	97.46	104.93
CAF*	8.07	3.80
NAP*	1.25	1.20
TCS*	0.47	0.49
IBU*	1.55	5.21

NOTE: * - loads in $kg.day^{-1}$

Therefore, corroborating hypothesis 3, average loads were distinct in both monitoring sites, with bigger values in BA2 than in BA1. This difference were observed, generally, in all water quality parameters, and related to the distinct pollution sources in each drainage area monitored. Moreover, the hypothesis 4 has not been confirmed, because caffeine were detected in all samples analyzed in BA1. This indicates the great influence of the small urban proportions on that drainage area and the lack of efficient sewage collecting to reduce the emerging contaminant load into the river without a proper treatment.

5.3 HOW DISTANT ARE WE FROM THE BASELINE CONDITIONS?

One way of measuring the NPS contribution is observing the differences relatively to the baseline water quality conditions, that can occur in two ways: (i) "positive", which indicates that rainfall effects (5% of the time) are greater than the baseline influences (95% of the time), and (ii) "negative", which indicates that baseline effects are greater than the rainfall influences. These influences are distinct and dependent of the hydrological characteristics and the water quality parameter analyzed.

For conventional parameters most of them indicated positive values, revealing that rainfall episodes introduces compounds such as TN, TP, COD, DOC and, mainly, SS into the river. The conventional parameters measured in the dissolved fraction have a smaller increase than the parameters

Figure 75 – Relative differences between rainfall events EMC and baseline EMC for a) conventional parameters - part I, b) conventional parameters - part II, c) emerging contaminants, d) dissolved metals, e) total metals

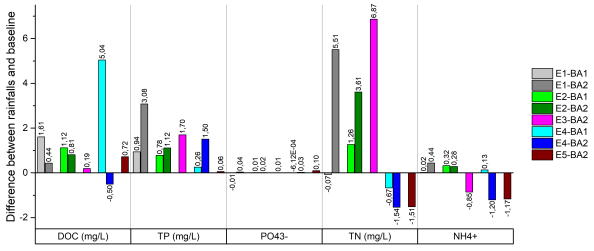

(a) Conventional Parameters - Part I

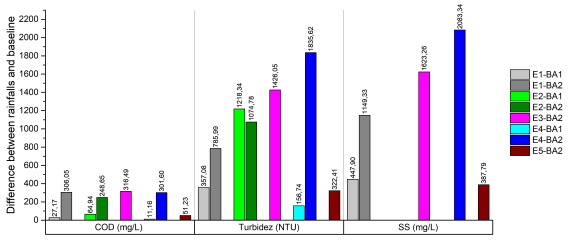

(b) Conventional Parameters - Part II

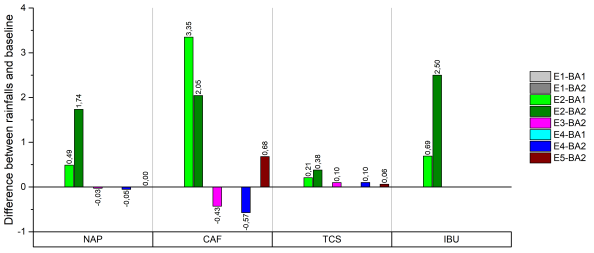

(c) Emerging Contaminants

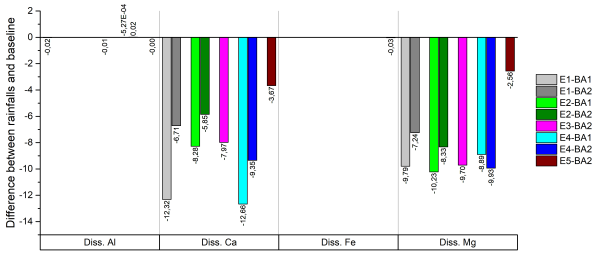

(d) Dissolved Metals

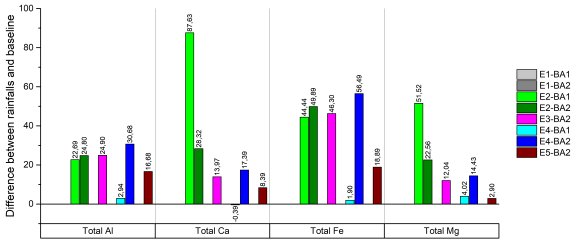

(e) Total Metals

measured in the total fraction (particulate), as for example is the case of DOC (lower difference) and COD (bigger difference) and TP (lower difference) and PO_4^{3-} (bigger difference). In addition, rainfall events E3 and E4, that were consecutive to event E2 in October 2018, may have favored the negative values of TN and NH_4^+, due to dilution effects.

For metals, two opposite behavior is observed. The first is associated with negative values for all metals analyzed in the dissolved fraction, suggesting that for this form, the contribution of baseline is more intense than during rainfalls episodes. Therefore, the second and opposite is associated with the positive values calculated in the total fraction of metals, suggesting that the rainfall events exerts a greater influence on the transport of these elements to the water body than the baseline. This fact is also directly associated with the carrying of particles (erosion processes) during rainfall events.

Therefore, for each set of elements analyzed there is a different behavior. Thus, in addition to choosing the most suitable element to characterize a transport process or behavior, it can be emphasized that hydrological characteristics are essential in estimating the dynamics of the environment. Different river conditions correspond to different rainfall responses in quantity and quality. This is intrinsic to the process. That is why the effects and responses are so complex and need a bigger and more complete data set that can help to understand the whole system.

5.4 WHERE DOES THE POLLUTION GO?

Rainfall occurrence can be associated with the surface washing off and, consequently, discharge into the river drainage river. Suspended solids and turbidity are the main visual parameters attributed to this washing off. These solids, which are also called particles, in general, adsorb pollutants.

The pollutants adhered to the particles can be considered unreactive, as they are not in ionized form, however they can be very sensitive to changes of the pH or redox potential for instance. In other side, the pollutants that do not adhere to the particles can be considered dissolved elements, or even elements available for interactions in the system, which are in their ionic form. However, it does not mean that the pollutants adhered to the particles do not produce a long-term problem.

Figure 76 shows the box plot of the some elements analyzed in this work, in their particulate and dissolved fraction. For total forms of COD, TP, TN and metals, there are dissolved forms of DOC, PO43-, NH4 + and dissolved metals, respectively. It can be observed that total fraction are bigger than dissolved fraction, as expected. Moreover, total fraction had more dispersion in the data than dissolved fraction, which can be associated to the random inputs received by the river during rainfalls. Dissolved fraction is standardized with filtration on 0.45 μm membrane, being representative of the same portion.

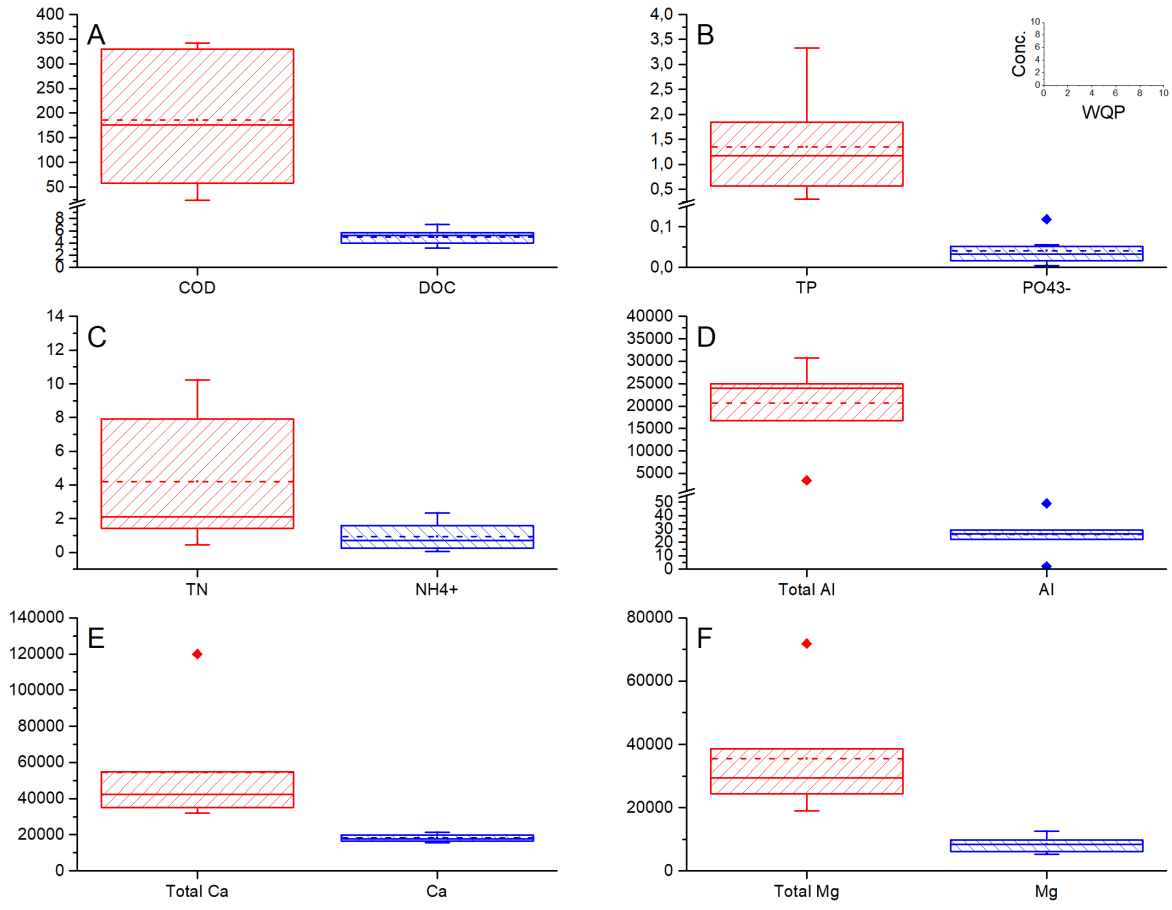

Figure 76 – Box plots of the total and dissolved fraction of a) carbon, b) phosphorus, c) nitrogen, d) aluminium, e) calcium, and f) magnesium measured during rainfall episodes

SOURCE: The Author (2020)
NOTE: unit of sub figures a, b and c are mg L^{-1}, and units in sub figures d, e and f are ppb

Ca, Mg and nitrogen had the lower increase, which were 3 times, 4 times and 5 times, respectively. This suggests that these elements are common in the environment. Ca and Mg represent geological

formation, and nitrogen represents natural and artificial sources, as for example primary productivity and wastewater effluent, which have significative inputs during dry periods. Otherwise, carbon and phosphorus increases about 37 and 33 times, respectively, whereas Al increase more than 1,200 times, suggesting that these elements are less common in the environment. Carbon, phosphorus and aluminium input are bigger during rainfall than during baseline, probably associated to the point source of pollution after BA1.

Therefore, more than 67% of these elements which are introduced in rivers during rainfall are total fraction or particulate form, probably in a inert stage. However, variations on environmental conditions can cause a chemical imbalance that favors desorption. Pearson's correlation shows that turbidity have positive and strong correlation with COD (Pearson 0.81, p-value < 0.05), TP (Pearson 0.86, p-value < 0.05), Total Al (Pearson 0.91, p-value < 0.05) and Total Fe (Pearson 0.95, p-value < 0.05) , suggesting that these elements are associated to turbidity, and consequently to suspended solids. Moreover, another positive, strong and known correlation, such as total Al and total Fe (Pearson 0.96, p-value < 0.05), total Ca and total Mg (Pearson 0.99, p-value < 0.05), TP and total Al (Pearson 0.74, p-value < 0.05), and TP and COD (Pearson 0.95, p-value < 0.05), indicating the occurrence of the both elements during rainfall episodes.

Dissolved Ca and Mg also have positive and strong correlation (Pearson 0.76, p-value < 0.05), as previously observed. Then, beside the bigger proportion of pollutant can be input into the system associated to the particles, the dissolved elements (or ionic ones) are also important and must be controlled. Emerging contaminants, for example, are measured in dissolved form. Some contaminants have a low potential for adsorption to particles, however none of the contaminants are expected to experience water volatility, and verification of their occurrence and possible quantification is paramount. The potential of emerging bio-contaminants to concentrate varies from low to high, depending on their class and category, but all have the potential to affect biota.

Finally, it is important to highlight that sampling strategy during rainfall events was extremely facilitated with the use of the automatic sampler, which were programmed to perform sample collect according to the water level variation. Manual collections are also possible, but with less quality of temporal resolution on the hydrograph rising and falling limb. Therefore, for the development of this type of approach and analysis, the equipment is essential, and always must be improved.

5.5 FUTURE STRATEGY RESEARCH QUESTIONS

This research allowed opening opportunities and motivation for improving the understanding about NPS of pollution emerged, in the context of monitoring and assessment for water resources planning and management.

First of all, is the need for *improving analytical techniques applied to the monitoring and management of water resources*. Chemistry is a powerful science for understanding many environmental processes. Therefore, complimentary techniques, strategies and logistics will assist in the specific investigation of those. For example, spectroscopy and chromatography allows quantitative and qualitative analysis of the element and/or molecule. The information generated, in concentration units, when applied to engineering problems, in flow units, increases the understanding of the dynamics of the water system. In the context of this research the monitoring need to continue.

In this sense, with proper chemistry association, *the soil characterization in the watershed* becomes extremely relevant. The benefit of is to proper identify elements naturally available geologically in the study area, allowing to develop perception regard, for example, inorganic elements mobility and organic elements affinity. Thus, transport mechanisms, such as pollutant dispersion, and exchanges between

sediment-water-air interfaces could be better explored and understood. In addition, considering that each environment has its particularities, to outline chemical patterns and their environmental interactions, can be used as a basis for other watershed with similar characteristics, as well as, for mathematical modelling application for river systems.

Another perspective is associated to developing an experimental plan similar to this work, however considering *smaller drainage areas and using singular land use*, in order to generate specific conclusions about transport processes and mechanisms including flow contribution and export coefficient loads of these elements.

It is possible to use remote sensing and geoprocessing tools in more detail, such as: i) effects of urbanization with increased runoff and accumulation of pollution by vehicular emissions; ii) effects of agricultural and farming activities that favor nutrient leaching, erosion processes, decreased soil infiltration, application of additional chemical elements; iii) atmospheric deposition impacts. These kind of information can also be used and to contribute to the application of mathematical models of environmental systems. However, it is worth noting that the bigger and extensive applications are also valid and necessary, considering that the systems are always complex and dynamic.

Finally, the *physical effects of pollutants inputs into the river during rainfall events*, both in particulate and dissolved forms, can be better explored. There is understood that occurs the entry, but not necessarily the exit. The occurrence of subsequent rainfalls favour the re-suspension and movement of particles, which at first are inert but which may have an influence on the aquatic system balance. Thus, studies on sediment transport during rain episodes are recommended, considering the introduction of these elements, re-suspension of the sediment that already exists, and its sedimentation downstream.

6 APPENDIX

Here will be presented all extra information related of this thesis, which can be used in order to clarify any existing questions.

6.1 MATERIALS AND METHODS

6.1.1 QUALITY CONTROL OF EMERGING CONTAMINANTS ANALYSIS

Table 34 – Selectivity data of the emerging compounds measured in this thesis

Compound	Fragmentation (m/z)	Energy of colision (eV)	Retention Time (min)
IBU	295 – 280	10	8.858 ± 0.096
FenP	270.1 – 196	5	13.000 ± 0.007
AS	267.1 – 209	10	7.732 ± 0.038
BuP	266.5 – 210	5	10.263 ± 0.006
PrP	252 – 195	15	9.162 ± 0.006
EtP	238.2 – 223.1	5	8.193 ± 0.005
AAS	195 – 177	10	7.877 ± 0.060
MeP	224.1 – 209.1	5	7.540 ± 0.003
CAF	194 – 109	10	11.303 ± 0.035
TCS	362 – 347	5	14.898 ± 0.007
MTL	223.3 – 72	10	14.600 ± 0.086
NAP	302.2 – 185	10	14.214 ± 0.014
BeP	300 – 193.1	10	15.366 ± 0.008
PRL	144 – 115	15	15.614 ± 0.265
NAD	210.4 – 420.2	10	19.637 ± 0.292
EE2	425.2 – 193.1	15	23.369 ± 0.131
E2	416.3 – 326.2	10	22.003 ± 0.011
STI	394.5 – 255.3	10	28.819 ± 0.213
CPL	217.1 – 121.2	30	23.761 ± 0.027
EPL	215.2 – 158.9	35	26.246 ± 0.046
FNF	360 – 273.1	15	20.357 ± 0.017
Bsi	357.5 – 121.1	30	29.507 ± 0.013
E1	342.2 – 257.2	15	21.379 ± 0.015
CTL	329.1 – 121.1	30	27.295 ± 0.008
CNL	231.2 – 121.1	30	27.424 ± 0.014

SOURCE: Kramer (2016)

6.1.2 QUALITY CONTROL OF INORGANIC ELEMENTS ANALYSIS

Table 35 – Linearity and sensitivity of the emerging compounds measured in this thesis

Compound	Calibration Curve	Correlation Coeficient (r)
IBU	y = 91213.33x - 7544.65	0.9914
FenP	y = 495.52x - 9.45	0.9974
AS	y = 641533.79x - 40958.87	0.9912
BuP	y = 12209.32x - 1019.63	0.9889
PrP	y = 371798.25x - 5889.82	0.9951
EtP	y = 1062008.42x - 52764.81	0.9954
AAS	y = 989472.68x + 56814.08	0.9914
MeP	y = 2827479.43x - 56011.37	0.9907
CAF	y = 1378101.53x - 107909.49	0.9945
TCS	y = 519226.26x - 13642.20	0.9962
MTL	y = 21011.94x - 1161.41	0.9838
NAP	y = 396978.30x - 15365.40	0.9885
BeP	y = 687779.00x - 72634.49	0.9936
PRL	y = 7459.89x + 123.72	0.9894
NAD	y = 3948.11x - 244.46	0.9888
EE2	y = 45349.52x - 1005.17	0.9986
E2	y = 116468.69x - 7909.83	0.9972
STI	y = 13903.42x - 800.56	0.9948
CPL	y = 37326.22x - 2683.96	0.9952
EPL	y = 13001.93x - 809.98	0.9958
FNF	y = 581311.16x - 26450.81	0.9977
Bsi	y = 30425.32x - 1104.45	0.9950
E1	y = 841406.61x - 46897.86	0.9982
CTL	y = 35996.18x - 2786.72	0.9939
CNL	y = 73569.63x - 3691.87	0.9924

SOURCE: The Author (2020)

6.1.3 FLUORESCENCE EXCITATION-EMISSION MATRIX CODE - FEEMC

Considering data-intensive and parametrization difficulties a mathematical routine (named Fluorescence Excitation-Emission Matrix Code – FEEMC) was developed for data manipulation and result of DOM analysis. The code is written in Python Language. Calculations are based on inner filter effects corrections (MCKNIGHT et al., 2001; CARSTEA, 2012) and Raman Units (r.u.) normalizations (MCKNIGHT et al., 2001) in order to avoid any sample interference (which can compromise data veracity).

Therefore, the excitation-emission matrix (EEM) analysis is based on DOC concentration, UV-Visible absorbance and fluorescence data of the used blanks and samples. The steps were performed by FEEMC in this order, necessarily:

1. Calculation of absorptivity to correct the inner filter effects (MCKNIGHT et al., 2001; CARSTEA, 2012). The calculation includes the emitted energy (absorbance from UV-Visible scan) in relation to the amount of carbon and a quartz cell correction (Equation 6.1) (MCKNIGHT et al., 2001):

$$Absorptivity = Absorbance * DOC * 0.005 \tag{6.1}$$

   where absorbance is the energy abosrved in the UV-VIS scan (nm), DOC is dissolved organic carbon of the sample (mg.L^{-1}), and 0.005 is the quartz cell length (m)

2. Calculation of Raman value from Ex $\lambda = 350$ nm from water EEM: it is necessary to integrate the area under wavelengths between 380 and 410 nm.

3. Generation of a normalization matrix: from the absorptivity value is calculated a new matrix with the same size of the sample and water matrices (135 lines x 41 columns). Calculations are made

Table 36 – Limits of detection (LOD) and quantification (LOQ) for the emerging components measured in samples of this thesis

Compound	LOD (μg L^{-1})	LOQ (μg L^{-1})
IBU	0.14	0.46
FenP	9.84	32.80
AS	0.15	0.50
BuP	4.88	16.28
PrP	0.03	0.10
EtP	0.12	0.41
AAS	0.42	1.40
MeP	0.13	0.42
CAF	0.04	0.13
TCS	0.02	0.05
MTL	2.06	6.86
NAP	0.02	0.07
BeP	0.03	0.11
PRL	2.30	7.66
NAD	4.56	15.18
EE2	0.21	0.69
E2	4.41	14.71
STI	5.30	17.68
CPL	0.49	1.64
EPL	5.03	16.76
FNF	0.05	0.17
Bsi	2.58	8.60
E1	0.05	0.16
CTL	2.30	7.66
CNL	0.16	0.53

SOURCE: The Author (2020)

Table 37 – Element identification, calibration curve and correlation coefficient for the inorganic analysis performed in ICP-OES

Element	Wavelength (nm)	Calibration Curve	Correlation coeficient (r)
Al	396.153	y = 61871x + 3033.1	0.9999
Cd	228.802	y = 22117x + 3219.4	0.9985
Co	228.616	y = 14041x + 3559.5	0.9919
Cr	267.716	y = 45618x + 8788.7	0.9944
Cu	327.393	y = 98846x + 5227.9	0.9996
Mn	257.61	y = 261915x + 78421	0.9950
Ni	231.604	y = 13941x + 910.55	0.9886
Pb	220.353	y = 2252.7x + 336.97	0.9974
Zn	206.2	y = 6250.8x + 3227.3	0.9950
Ca	317.933	y = 5710x + 11773	0.9993
Fe	238.204	y = 3865.2x + 9627.4	0.9985
Mg	285.213	y = 34378x + 24616	0.9988

SOURCE: The Author (2020)

crossing excitation and emission absorptivity according to Equation 6.2. In Python language, this is possible due to broadcasting effects in arrays operations, as follows:

$$L_n XC_n = (10^{-(Em_n + Ex_n)}) * raman \tag{6.2}$$

, where L is matrix lines, C is matrix columns, n is wavelength reference that is depending on matrix shape and resolution, Em is absorptivity value in emission wavelength, Ex is absorptivity

Table 38 – Limits of detection (LOD) and quantification (LOQ) for the inorganic elements (metals) measured in samples of this thesis

Element	Wavelength (nm)	LOD (ppb)	LOQ (ppb)
Al	396.153	2.864	9.547
Cd	228.802	1.599	5.329
Co	228.616	1.546	5.152
Cr	267.716	1.123	3.742
Cu	327.393	12.506	41.688
Mn	257.61	0.432	1.441
Ni	231.604	1.143	3.810
Pb	220.353	2.928	9.759
Zn	206.2	8.415	28.049
Ca	317.933	5.035	16.782
Fe	238.204	12.487	41.622
Mg	285.213	2.769	9.230

SOURCE: The Author (2020)

value in excitation wavelength, and raman is the value calculated in step 2.

4. Adjustment of sample matrices reducing water interference: sample matrix minus water matrix.
5. Correction of sample matrices: sample matrix divided by normalization matrix.

Step 1 and 2 are necessary, respectively, to correct inner effect and day interference as air humidity, temperature, equipment resolution, light, and others. It is important to highlight that all operations are possible if all matrices have, necessarily, the same shape. FEEMC open code, developed in python language is a part of an article submitted to a international journal.

Additionally, FEEMC is able to select specific peaks from 5 distinct regions in the EEM, which represent the present fluorescent organic compounds that are labile or protein-like (peaks T1, T2 and B) and refractory or humic-like (peaks A and C). These regions were based on studies of Coble (1996), Hudson, Baker and Reynolds (2007), which identified this correlation, and then, we expanded them to cover an additional and more representative area of interest observed previously.

BIBLIOGRAPHY

ÁGUAS, A. Agência Nacional de. *Cadernos de Capacitação em Recursos Hídricos: Planos de recursos hídricos e enquadramento dos corpos de água*. ISBN: 978-85-89629-96-6, 2013. Language: portuguese. 27

ÁGUAS, A. Agência Nacional de. *Cuidando das águas: soluções para melhorar a qualidade dos recursos hídricos*. [S.l.], 2013. Traduzido e adaptado do original "Clearing the waters: a focus on water quality solutions". Produzido em Nairobi, Kenya em março de 2010. 28

ÁGUAS, A. Agência Nacional de. *Conjuntura dos Recursos Hídricos no Brasil 2018: informe anual*. Brasília - DF, Brasil, 2018. Language: Portuguese 72p. 27

AICH, V.; ZIMMERMANN, A.; ELSENBEER, H. Quantification and interpretation of suspended-sediment discharge hysteresis patterns: How much data do we need? *Catena*, Elsevier, v. 122, p. 120–129, 2014. 37

ALI, S. A. et al. Investigation of the wash-off process using an innovative portable rainfall simulator allowing continuous monitoring of flow and turbidity at the urban surface outlet. *Science of the Total Environment*, Elsevier, v. 609, p. 17–26, 2017. 49

ALIAS, N. et al. Time as the critical factor in the investigation of the relationship between pollutant wash-off and rainfall characteristics. *Ecological engineering*, Elsevier, v. 64, p. 301–305, 2014. 37, 38, 39, 40, 44, 47

ALVAREZ-CAMPOS, O.; EVANYLO, G. *Inorganic Trace Elements*. <http://www.virginiabiosolids.com/>, 2020. 62

AMARANTE, O. P. d. et al. Validação de métodos analíticos: uma breve revisão. *Cad. Pesq*, v. 12, n. 1/2, p. 116–31, 2001. 88

ANA. *Atlas Esgotos - Despoluição de Bacias Hidrográficas, Relatório de Esgotamento Sanitário Municipal*. $http://portal1.snirh.gov.br/arquivos/Atlas_Esgoto/Parana2017. Accessed in October 27, 2019. 71$

ANA, A. N. d. *Cuidando das Águas: soluções para melhorar a qualidade dos recursos hídricos*. second. Brasília/DF - Brazil: Agência Nacional de Águas, Programa das Nações Unidas para o Meio Ambiente, 2013. ISBN: 978-85-8210-018-9. 34

ANVISA, A. N. d. V. S. *Guia para qualidade em Química Analítica: Uma assistência a Acreditação*. [S.l.]: Núcleo de assessoramento em comunicação social e institucional Brasília, 2004. 88

APHA. Standard methods for the examination of water and wastewater. *Water Environmental Federatio American Public Health Association and others*, 2012. Washington, DC, USA. 85, 87

AQUINO, S. F. d.; BRANDT, E. M. F.; CHERNICHARO, C. A. d. L. Remoção de fármacos e desreguladores endócrinos em estações de tratamento de esgoto: revisão da literatura. *Engenharia Sanitária e Ambiental*, SciELO Brasil, v. 18, n. 3, p. 187–204, 2013. 55

ARAUJO, E. S.; MAIA, Y. L. M. Análise de elementos traço e de metais na bacia hidrográfica do rio meia ponte na região metropolitana de goiânia. *Revista EVS-Revista de Ciências Ambientais e Saúde*, v. 35, n. 6, p. 1241–1265, 2008. 62

BAETTKER, E. et al. Applicability of conventional and non-conventional parameters for municipal landfill leachate characterization. *Chemosphere*, Elsevier, p. 126414, 2020. 49

BAIRD, C.; CANN, M. *Química ambiental*. Fourth edition. [S.l.]: Bookman, 2011. 63, 64

BARBOSA, A. E.; FERNANDES, J. N.; DAVID, L. M. Key issues for sustainable urban stormwater management. *Water research*, v. 46, n. 20, p. 6787–6798, 2012. 65, 66

BARBOSA, M. O. et al. Spatial and seasonal occurrence of micropollutants in four portuguese rivers and a case study for fluorescence excitation-emission matrices. *Science of The Total Environment*, v. 644, p. 1128–1140, 2018. 67

BAUWE, A. et al. Classifying hydrological events to quantify their impact on nitrate leaching across three spatial scales. *Journal of Hydrology*, Elsevier, v. 531, p. 589–601, 2015. 29, 48, 67, 69, 98

BEHMEL, S. et al. Water quality monitoring strategies—a review and future perspectives. *Science of the Total Environment*, Elsevier, v. 571, p. 1312–1329, 2016. 38

BENDER, M. A. et al. Phosphorus dynamics during storm events in a subtropical rural catchment in southern brazil. *Agriculture, Ecosystems & Environment*, Elsevier, v. 261, p. 93–102, 2018. 28, 66, 67, 69

BIEROZA, M.; HEATHWAITE, A. Seasonal variation in phosphorus concentration-discharge hysteresis inferred from high-frequency in situ monitoring. *Journal of Hydrology*, Elsevier, v. 524, p. 333–347, 2015. 40, 44, 45, 47, 48, 66, 67

BIRDWELL, J. E.; ENGEL, A. S. Characterization of dissolved organic matter in cave and spring waters using uv-vis absorbance and fluorescence spectroscopy. *Organic Geochemistry*, Elsevier, v. 41, n. 3, p. 270–280, 2010. 52, 53

BLAEN, P. J. et al. Real-time monitoring of nutrients and dissolved organic matter in rivers: Capturing event dynamics, technological opportunities and future directions. *Science of the Total Environment*, Elsevier, v. 569, p. 647–660, 2016. 37, 38, 39, 48, 67, 69, 79

BOWES, M. et al. Characterising phosphorus and nitrate inputs to a rural river using high-frequency concentration-flow relationships. *Science of the Total Environment*, Elsevier, v. 511, p. 608–620, 2015. 38, 40, 66, 67

BOWES, M. J.; SMITH, J. T.; NEAL, C. The value of high-resolution nutrient monitoring: A case study of the river frome, dorset, uk. *Journal of Hydrology*, Elsevier, v. 378, n. 1-2, p. 82–96, 2009. 39

BRAGA, S. M. *Uma nova abordagem para integração entre quantidade e qualidade da água para a avaliação da poluição difusa*. Tese (Doutorado) — Universidade Federal do Paraná, Programa de Pós-Graduação em Engenharia de Recursos Hídricos e Ambiental, 2013. 28, 36, 37, 39, 71, 79, 80

BRASIL, R. F. do. *Lei nº 6.938, de 31 de Agosto de 1981: Dispõe sobre a Política Nacional do Meio Ambiente, seus fins e mecanismos de formulação e aplicação, e dá outras providências*. 1981. 33

BRUNET, F. et al. Terrestrial and fluvial carbon fluxes in a tropical watershed: Nyong basin, cameroon. *Chemical Geology*, Elsevier, v. 265, n. 3-4, p. 563–572, 2009. 48

BU, H. et al. Relationships between land use patterns and water quality in the taizi river basin, china. *Ecological indicators*, Elsevier, v. 41, p. 187–197, 2014. 28, 34, 36, 48

BUFFLE, J. et al. Analysis and characterization of natural organic matters in freshwaters. *Schweizerische Zeitschrift für Hydrologie*, Springer, v. 44, n. 2, p. 325–362, 1982. 50

BURNS, E. E. et al. Temporal and spatial variation in pharmaceutical concentrations in an urban river system. *Water research*, Elsevier, v. 137, p. 72–85, 2018. 56

BUTTURINI, A. et al. Diversity and temporal sequences of forms of doc and no3- discharge responses in an intermittent stream: Predictable or random succession? *Journal of Geophysical Research: Biogeosciences*, Wiley Online Library, v. 113, n. G3, 2008. 44, 45

BUTTURINI, A. et al. Cross-site comparison of variability of doc and nitrate c–q hysteresis during the autumn–winter period in three mediterranean headwater streams: a synthetic approach. *Biogeochemistry*, v. 77, p. 327–349, feb 2006. 45

CARSTEA, E. M. Fluorescence spectroscopy as a potential tool for in-situ monitoring of dissolved organic matter in surface water systems. In: *Water pollution*. [S.l.]: InTech, 2012. 48, 49, 51, 53, 87, 166

CARSTEA, E. M. et al. Continuous fluorescence excitation-emission matrix monitoring of river organic matter. *Water research*, v. 44, n. 18, p. 5356–5366, 2010. 39, 49

CARSTEA, E. M. et al. Fluorescence spectroscopy for wastewater monitoring: a review. *Water Research*, v. 95, p. 205–219, 2016. 49

CHEN, L. et al. Influence of rainfall data scarcity on non-point source pollution prediction: Implications for physically based models. *Journal of Hydrology*, Elsevier, v. 562, p. 1–16, 2018. 30

CHEN, L. et al. Comparison between snowmelt-runoff and rainfall-runoff nonpoint source pollution in a typical urban catchment in beijing, china. *Environmental Science and Pollution Research*, Springer, v. 25, n. 3, p. 2377–2388, 2018. 27, 155

CHEN, N. et al. Phosphorus export during storm events from a human perturbed watershed, southeast china: Implications for coastal ecology. *Estuarine, Coastal and Shelf Science*, Elsevier, v. 166, p. 178–188, 2015. 28

CHIBA, W. et al. Seasonal study of contamination by metal in water and sediment in a sub-basin in the southeast of brazil. *Brazilian Journal of Biology*, SciELO Brasil, v. 71, n. 4, p. 833–843, 2011. 64

CLARET, F. et al. Generation of humic and fulvic acid from callovo-oxfordian clay under high alkaline conditions. *Science of the total environment*, Elsevier, v. 317, n. 1-3, p. 189–200, 2003. 49, 50

COBLE, P. G. Characterization of marine and terrestrial dom in seawater using excitation-emission matrix spectroscopy. *Marine chemistry*, Elsevier, v. 51, n. 4, p. 325–346, 1996. 52, 53, 168

COLIAR, C. das Bacias do Alto Iguaçu e afluente do A. R. *RESOLUÇÃO Nº 04 DO COMITÊ DAS BACIAS DO ALTO IGUAÇU E AFLUENTES DO ALTO RIBEIRA - COALIAR, de 11 de julho de 2013. http* : *//www.recursoshidricos.pr.gov.br/arquivos/File/CERH*$_{-2}$*2*$_{R}$*O/resolucao*$_{e}$*nquadramento*$_{c}$*oaliar.pdf*, 2013. Accessed October 27, 2019. 71

CONAMA. *Resolução N 357, de 17 de março de 2005.* [S.l.], 2005. 47, 118, 119, 120

CORADA-FERNÁNDEZ, C. et al. Effects of extreme rainfall events on the distribution of selected emerging contaminants in surface and groundwater: The guadalete river basin (sw, spain). *Science of the total environment*, Elsevier, v. 605, p. 770–783, 2017. 55, 67

CORY, R. M.; MCKNIGHT, D. M. Fluorescence spectroscopy reveals ubiquitous presence of oxidized and reduced quinones in dissolved organic matter. *Environmental science & technology*, ACS Publications, v. 39, n. 21, p. 8142–8149, 2005. 48, 52

DELPLA, I. et al. Impacts of rainfall events on runoff water quality in an agricultural environment in temperate areas. *Science of the total environment*, Elsevier, v. 409, n. 9, p. 1683–1688, 2011. 37, 39, 41, 48

DERRIEN, M. et al. Estimation of different source contributions to sediment organic matter in an agricultural-forested watershed using end member mixing analyses based on stable isotope ratios and fluorescence spectroscopy. *Science of The Total Environment*, Elsevier, v. 618, p. 569–578, 2018. 49, 53

DERRIEN, M. et al. Spectroscopic and molecular characterization of humic substances (hs) from soils and sediments in a watershed: comparative study of hs chemical fractions and the origins. *Environmental Science and Pollution Research*, Springer, v. 24, n. 20, p. 16933–16945, 2017. 49

DING, J. et al. Influences of the land use pattern on water quality in low-order streams of the dongjiang river basin, china: a multi-scale analysis. *Science of the Total Environment*, v. 551, p. 205–216, 2016. 35, 36, 39, 47, 48, 67

DONG, J. et al. Effects of rainfall events on behavior of tetracycline antibiotics in a receiving river: Seasonal differences in dominant processes and mechanisms. *Science of The Total Environment*, Elsevier, v. 692, p. 511–518, 2019. 29, 68, 69

DRUMMOND, S. B. M. *Análise Temporal de Poluentes Difusos no Rio Passaúna por Meio da Utilização de Amostrador Automático*. Dissertação (Mestrado) — Universidade Federal do Paraná, Programa de Pós-Graduação em Engenharia de Recursos Hídricos e Ambiental, Universidade Federal do Paraná, Curitiba/PR, 2020. Preliminary Version. 28, 39, 66, 67, 69, 80

EBELE, A. J.; ABDALLAH, M. A.-E.; HARRAD, S. Pharmaceuticals and personal care products (ppcps) in the freshwater aquatic environment. *Emerging Contaminants*, Elsevier, v. 3, n. 1, p. 1–16, 2017. 54, 55, 57

EDWARDS, Q. A. et al. Contaminants of emerging concern in surface waters in barbados, west indies. *Environmental monitoring and assessment*, Springer, v. 189, n. 12, p. 636, 2017. 57, 60

EEA, E. E. A. *Water and Marine Environment: Water use and environmental pressures*. https://www.eea.europa.eu/themes/water/european-waters/water-use-andenvironmental-pressures/water-use-and-environmental-pressures, 2018. Accessed in May 21, 2020. 34

ERLANDSSON, M. et al. Variability in spectral absorbance metrics across boreal lake waters. *Journal of Environmental Monitoring*, Royal Society of Chemistry, v. 14, n. 10, p. 2643–2652, 2012. 50

FERREIRA, D. B. Nonpoint pollution and best management practices assessment using geographic information systems data – application in the barigui basin, state of parana. *Graduation Project in Civil Engineering*, p. 127p., 2016. Hydraulics and Sanitation Department, Federal University of Parana. 71, 72

FILELLA, M. Freshwaters: which nom matters? *Environmental chemistry letters*, Springer, v. 7, n. 1, p. 21–35, 2009. 48

FILIPPE, T. C. *Cafeína, hormônios e produtos de cuidados pessoais no Rio Palmital - PR*. Dissertação (Mestrado) — Universidade Tecnológica Federal do Paraná, Programa de Pós-Graduação em Ciência e Tecnologia Ambiental, Curitiba/PR, 2018. 106p. 88, 137

FILL, H. D. et al. Balanço hídrico da bacia do rio barigüi, pr. *Raega-O Espaço Geográfico em Análise*, v. 9, 2005. 83, 84

FONTENELE, A. P. G.; PEDROTTI, J. J.; FORNARO, A. Evaluation of trace metals and major ions concentrations in rainwater in downtown são paulo city. *Química Nova*, SciELO Brasil, v. 32, n. 4, p. 839–844, 2009. 64

FRANK, S.; GOEPPERT, N.; GOLDSCHEIDER, N. Fluorescence-based multi-parameter approach to characterize dynamics of organic carbon, faecal bacteria and particles at alpine karst springs. *Science of The Total Environment*, v. 615, p. 1446–1459, 2018. 28, 29, 39, 48, 49, 53, 67, 69, 155, 156

FRIMMEL, F.; ABBT-BRAUN, G. Dissolved organic matter (dom) in natural environments. *Biophysicochemical processes involving natural nonliving organic matter in enviromental systems. Wiley, Hoboken*, p. 367–406, 2009. 48, 49, 50, 51

GAILLARDET, J.; VIERS, J.; DUPRÉ, B. Trace elements in river waters. *TrGeo*, v. 5, p. 605, 2003. 62, 63

GAO, B. et al. A novel method for evaluating the potential release of trace metals associated with rainfall leaching/runoff from urban soils. *Science of The Total Environment*, Elsevier, v. 664, p. 37–44, 2019. 64

GAO, Y. et al. Coupled effects of biogeochemical and hydrological processes on c, n, and p export during extreme rainfall events in a purple soil watershed in southwestern china. *Journal of hydrology*, v. 511, p. 692–702, 2014. 37

GARRIDO, E. et al. Monitoring of emerging pollutants in guadiamar river basin (south of spain): analytical method, spatial distribution and environmental risk assessment. *Environmental Science and Pollution Research*, Springer, v. 23, n. 24, p. 25127–25144, 2016. 57, 67

GASIM, M. B. et al. Flux of nutrients and heavy metals from the melai river sub-catchment into lake chini, pekan, pahang, malaysia. *Environmental earth sciences*, Springer, v. 68, n. 3, p. 889–897, 2013. 64

GIRI, S.; QIU, Z. Understanding the relationship of land uses and water quality in twenty first century: A review. *Journal of environmental management*, Elsevier, v. 173, p. 41–48, 2016. 28, 30, 34, 36

GONÇALVES, M. F. *VARIAÇÃO TEMPORAL E ESPACIAL DA PRESENÇA DOS METAIS PESADOS Cd, Cr, Ni, Pb, Zn NA BACIA DO RIO BARIGÜI E IDENTIFICAÇÃO DE SUAS FONTES POTENCIAIS*. Dissertação (Mestrado) — Universidade Federal do Paraná, Programa de Pós-Graduação em Engenharia de Recursos Hídricos e Ambiental, Curitiba, 2008. 152f. 70, 72

GOULART, F. D. A. B. *CONTAMINANTES EMERGENTES EM UM PAÍS EMERGENTE: Estudo de caso no Rio Barigui*. Dissertação (Mestrado) — UNIVERSIDADE TECNOLÓGICA FEDERAL DO PARANÁ, PROGRAMA DE PÓS-GRADUAÇÃO EM CIÊNCIA E TECNOLOGIA AMBIENTAL, Curitiba, 2017. 141f. 66, 67, 69, 137

GRAYSON, R. P.; HOLDEN, J. Improved automation of dissolved organic carbon sampling for organic-rich surface waters. *Science of the Total Environment*, Elsevier, v. 543, p. 44–51, 2016. 38, 53

GRIMALT, J. O. et al. Assessment of fecal sterols and ketones as indicators of urban sewage inputs to coastal waters. *Environmental Science & Technology*, ACS Publications, v. 24, n. 3, p. 357–363, 1990. 60

GRUDZIEN, J. P. *Utilização de amostrador automático experimental para a identificação do aporte de poluentes no Rio Passaúna*. Tese (Doutorado) — Universidade Federal do Paraná, Programa de Pós-Graduação em Engenharia de Recursos Hídricos e Ambiental. Universidade Federal do Paraná Curitiba, 2019. 201f. 28, 39, 66, 67, 69, 80

HALLIDAY, S. J. et al. The water quality of the river enborne, uk: Observations from high-frequency monitoring in a rural, lowland river system. *Water*, Multidisciplinary Digital Publishing Institute, v. 6, n. 1, p. 150–180, 2014. 38, 47, 48

HAYGARTH, P. M.; JARVIS, S. C. et al. *Agriculture, hydrology, and water quality*. [S.l.]: CABI Pub., 2002. 62

HAZARIKA, A. K.; KALITA, U. Incidence of heavy metals and river restoration assessment of a major south asian transboundary river. *Environmental Science and Pollution Research International*, Springer, 2020. 64

HE, W. et al. Differences in spectroscopic characteristics between dissolved and particulate organic matters in sediments: Insight into distribution behavior of sediment organic matter. *Science of The Total Environment*, Elsevier, v. 547, p. 1–8, 2016. 53

HERNÁNDEZ-CRESPO, C. et al. Influence of rainfall intensity and pollution build-up levels on water quality and quantity response of permeable pavements. *Science of The Total Environment*, Elsevier, v. 684, p. 303–313, 2019. 99, 100

HU, B. et al. The effect of anthropogenic impoundment on dissolved organic matter characteristics and copper binding affinity: Insights from fluorescence spectroscopy. *Chemosphere*, v. 188, p. 424–433, 2017. 49

HUDSON, N.; BAKER, A.; REYNOLDS, D. Fluorescence analysis of dissolved organic matter in natural, waste and polluted waters—a review. *River Research and Applications*, Wiley Online Library, v. 23, n. 6, p. 631–649, 2007. 51, 52, 168

HUGUET, A. et al. Properties of fluorescent dissolved organic matter in the gironde estuary. *Organic Geochemistry*, Elsevier, v. 40, n. 6, p. 706–719, 2009. 49, 52

IDE, A. H. et al. Occurrence of pharmaceutical products, female sex hormones and caffeine in a subtropical region in brazil. *CLEAN–Soil, Air, Water*, Wiley Online Library, v. 45, n. 9, p. 1700334, 2017. 59, 67

IMFELD, G. et al. Do rainfall characteristics affect the export of copper, zinc and synthetic pesticides in surface runoff from headwater catchments? *Science of The Total Environment*, Elsevier, v. 741, p. 140437, 2020. 67, 69

INAMDAR, S. et al. Fluorescence characteristics and sources of dissolved organic matter for stream water during storm events in a forested mid-atlantic watershed. *Journal of Geophysical Research: Biogeosciences*, v. 116, n. G3, 2011. 28, 49

JEONG, H. et al. Heavy metal pollution by road-deposited sediments and its contribution to total suspended solids in rainfall runoff from intensive industrial areas. *Environmental Pollution*, Elsevier, v. 265, p. 115028, 2020. 64

KLAPER, R.; WELCH, L. Emerging contaminant threats and the great lakes: existing science, estimating relative risk and determining policies. *Alliance for the Great Lakes*, 2011. 54

KNAPIK, H. G. et al. Applicability of fluorescence and absorbance spectroscopy to estimate organic pollution in rivers. *Environmental engineering science*, v. 31, n. 12, p. 653–663, 2014. 49, 50

KOZAK, C. *Water quality assessment and its effects on diffuse pollution considering a new water quality and quantity approach*. Dissertação (Mestrado) — Federal University of Paraná, Post-Graduate Program on Water Resources and Environmental Engineering, Federal University of Paraná. Curitiba, 2016. 265f. 28, 67

KOZAK, C. et al. Water quality dynamic during rainfall episodes: integrated approach to assess diffuse pollution using automatic sampling. *Environmental monitoring and assessment*, Springer, v. 191, n. 6, p. 402, 2019. 28, 30, 37, 39, 40, 47, 48, 66, 67, 69, 80, 155, 156

KRAMER, R. D. *Avaliação do desempenho ambiental de uma ETE considerando a presença dos contaminantes emergentes. In english: Environmental performance assessment of WWTP considering the presence of emerging contaminants.* Tese (Doutorado) — Federal University of Paraná, Graduate Program on Water Resources and Environmental Engineering, Federal University of Paraná. Curitiba, 2016. 201f. 59, 88, 137, 165

KRAUSE, S. et al. Frontiers in real-time ecohydrology–a paradigm shift in understanding complex environmental systems. *Ecohydrology*, Wiley Online Library, v. 8, n. 4, p. 529–537, 2015. 38, 79

LANGMUIR, D. *Issue paper on the environmental chemistry of metals*. [S.l.]: US Environmental Protection Agency, 2004. 63

LEE, H. et al. Design of stormwater monitoring programs. *Water research*, Elsevier, v. 41, n. 18, p. 4186–4196, 2007. 37, 39, 40

LEE, J. Y. et al. Characteristics of the event mean concentration (emc) from rainfall runoff on an urban highway. *Environmental Pollution*, Elsevier, v. 159, n. 4, p. 884–888, 2011. 48

LEE, M.-H. et al. Evaluating the contributions of different organic matter sources to urban river water during a storm event via optical indices and molecular composition. *Water research*, Elsevier, v. 165, p. 115006, 2019. 49, 53

LEE, S.-W. et al. Landscape ecological approach to the relationships of land use patterns in watersheds to water quality characteristics. *Landscape and Urban Planning*, Elsevier, v. 92, n. 2, p. 80–89, 2009. 34, 36

LEI, M. et al. Overview of emerging contaminants and associated human health effects. *BioMed research international*, Hindawi, v. 2015, 2015. 54, 55

LEITHOLD, J. et al. Quali-quantitative characterization of organic matter in urbanized drainage basins as a basis for the application of water resources management instruments. *RBRH*, v. 22, 2017. 49, 50, 53

LI, P.; HUR, J. Utilization of uv-vis spectroscopy and related data analyses for dissolved organic matter (dom) studies: A review. *Critical Reviews in Environmental Science and Technology*, Taylor & Francis, v. 47, n. 3, p. 131–154, 2017. 49, 50, 51

LIAO, Y. et al. An innovative method based on cloud model learning to identify high-risk pollution intervals of storm-flow on an urban catchment scale. *Water research*, Elsevier, v. 165, p. 115007, 2019. 98

LICHT, O. A. B. *A GEOQUÍMICA MULTIELEMENTAR NA GESTÃO AMBIENTAL: Identificação e caracterização de províncias geoquímicas naturais, alterações antrópicas da paisagem, áreas favoráveis à prospecção mineral e regiões de risco para a saúde no Estado do Paraná, Brasil*. Tese (Doutorado) — Universidade Federal do Paraná, Programa de Pós-Graduação em Geologia, 2001. 63

LIN, W. et al. Can water quality indicators and biomarkers be used to estimate real-time population? *Science of The Total Environment*, Elsevier, v. 660, p. 603–610, 2019. 60

LINDFORS, S. et al. Metal size distribution in rainfall and snowmelt-induced runoff from three urban catchments. *Science of the Total Environment*, Elsevier, v. 743, p. 140813, 2020. 64, 67, 68, 69

LIU, A. et al. Linking source characterisation and human health risk assessment of metals to rainfall characteristics. *Environmental Pollution*, Elsevier, v. 238, p. 866–873, 2018. 64

LLOYD, C. et al. Using hysteresis analysis of high-resolution water quality monitoring data, including uncertainty, to infer controls on nutrient and sediment transfer in catchments. *Science of the Total Environment*, Elsevier, v. 543, p. 388–404, 2016. 36, 38, 40, 46, 47, 48, 66, 67

MA, Y.; LI, S. Spatial and temporal comparisons of dissolved organic matter in river systems of the three gorges reservoir region using fluorescence and uv–visible spectroscopy. *Environmental Research*, Elsevier, p. 109925, 2020. 29, 51, 53, 67, 69

MACHADO, K. S. et al. Assessment of historical fecal contamination in curitiba, brazil, in the last 400 years using fecal sterols. *Science of the total environment*, Elsevier, v. 493, p. 1065–1072, 2014. 60

MAKAREWICZ, A. et al. Characteristics of chromophoric and fluorescent dissolved organic matter in the nordic seas. *Ocean Science*, v. 14, n. 3, 2018. 49

MAMOON, A. A. et al. First flush analysis using a rainfall simulator on a micro catchment in an arid climate. *Science of The Total Environment*, Elsevier, v. 693, p. 133552, 2019. 37, 44, 49, 67

MARTIN-NETO, L. et al. Epr, ft-ir, raman, uv–visible absorption, and fluorescence spectroscopies in studies of nom. *Biophysico-Chemical Processes Involving Natural Nonliving Organic Matter in Environmental Systems Biophys; John Wiley & Sons: Hoboken, NJ, USA*, p. 651–727, 2009. 49, 51

MATSUNAGA, T. et al. Temporal variations in metal enrichment in suspended particulate matter during rainfall events in a rural stream. *Limnology*, Springer, v. 15, n. 1, p. 13–25, 2014. 64

MCCARTHY, D. T. et al. Assessment of sampling strategies for estimation of site mean concentrations of stormwater pollutants. *Water research*, Elsevier, v. 129, p. 297–304, 2018. 28, 29, 36, 37, 43, 48, 66, 67

MCKNIGHT, D. M. et al. Spectrofluorometric characterization of dissolved organic matter for indication of precursor organic material and aromaticity. *Limnology and Oceanography*, Wiley Online Library, v. 46, n. 1, p. 38–48, 2001. 52, 87, 166

MELLO, K. de et al. Effects of land use and land cover on water quality of low-order streams in southeastern brazil: Watershed versus riparian zone. *Catena*, Elsevier, v. 167, p. 130–138, 2018. 30, 35

MENDOZA, W. G.; ZIKA, R. G. On the temporal variation of dom fluorescence on the southwest florida continental shelf. *Progress in Oceanography*, v. 120, p. 189–204, 2014. 49

MENESES, B. et al. Land use and land cover changes in zêzere watershed (portugal)—water quality implications. *Science of the Total Environment*, Elsevier, v. 527, p. 439–447, 2015. 34

METADIER, M.; BERTRAND-KRAJEWSKI, J.-L. The use of long-term on-line turbidity measurements for the calculation of urban stormwater pollutant concentrations, loads, pollutographs and intra-event fluxes. *Water research*, Elsevier, v. 46, n. 20, p. 6836–6856, 2012. 37, 39, 40, 41, 43, 115

MEYER, A. M. et al. Real-time monitoring of water quality to identify pollution pathways in small and middle scale rivers. *Science of the Total Environment*, Elsevier, v. 651, p. 2323–2333, 2019. 30, 41, 48, 65, 67, 155, 156

MINEROPAR. *Levantamento geoquímico multielementar do Estado do Paraná: geoquímica de solo; horizonte B. relatório final de projeto.* Available in $< http : //www.mineropar.pr.gov.br/arquivos/File/publicacoes/relatorios_concluidos/12_relatorios_concluidos.pdf >$, 2005. Language: Portuguese. 72, 73

MIZUKAWA, A. *AVALIAÇÃO DE CONTAMINANTES EMERGENTES NA ÁGUA E SEDIMENTO NA BACIA DO ALTO IGUAÇU/PR.* Tese (Doutorado) — Universidade Federal do Paraná, Programa de Pós-Graduação em Engenharia de Recursos Hídricos e Ambiental, Curitiba, 2014. 166f. 59, 60

MIZUKAWA, A. et al. Caffeine as a chemical tracer for contamination of urban rivers. *RBRH*, SciELO Brasil, v. 24, 2019. 58

MONTAGNER, C. C.; VIDAL, C.; ACAYABA, R. D. Contaminantes emergentes em matrizes aquáticas do brasil: cenário atual e aspectos analíticos, ecotoxicológicos e regulatórios. *Química nova*, SciELO Brasil, v. 40, n. 9, p. 1094–1110, 2017. 55, 56, 57, 58, 59

MORAETIS, D. et al. High-frequency monitoring for the identification of hydrological and biogeochemical processes in a mediterranean river basin. *Journal of Hydrology*, Elsevier, v. 389, n. 1-2, p. 127–136, 2010. 28

MUDGE, S. M.; SEGUEL, C. G. Organic contamination of san vicente bay, chile. *Marine Pollution Bulletin*, Elsevier, v. 38, n. 11, p. 1011–1021, 1999. 60

MÜLLER, A. et al. The pollution conveyed by urban runoff: A review of sources. *Science of The Total Environment*, Elsevier, p. 136125, 2019. 34

NEALE, P. A. et al. Natural versus wastewater derived dissolved organic carbon: Implications for the environmental fate of organic micropollutants. *Water research*, Elsevier, v. 45, n. 14, p. 4227–4237, 2011. 49

NICOLAU, R. et al. Base flow and stormwater net fluxes of carbon and trace metals to the mediterranean sea by an urbanized small river. *Water Research*, Elsevier, v. 46, n. 20, p. 6625–6637, 2012. 30, 64

NIH, N. I. o. H. *PubChem website: open chemistry database*. 2020. Accessed in July and August 2020. Available at: <https://pubchem.ncbi.nlm.nih.gov/>. 56, 57, 58, 59, 90, 91

NITSCHE, P. R. et al. *Atlas Climático do Estado do Paraná/ In English: Climate Atlas of Paraná State*. [S.l.], 2019. 210p. 74

NÓBREGA, R. L. et al. Impacts of land-use and land-cover change on stream hydrochemistry in the cerrado and amazon biomes. *Science of the Total Environment*, Elsevier, v. 635, p. 259–274, 2018. 30, 36, 48, 66, 67, 69

NOVOTNY, V. *Water quality: Diffuse pollution and watershed management*. [S.l.]: John Wiley & Sons, 2003. 28, 33, 34, 37, 42, 47

OECD. *Diffuse Pollution, Degraded Waters - Emerging Policy Solutions*. Oecd studies on water. Paris: [s.n.], 2017. 122 p. ISBN 9789264269057. Available at: <https://www.oecd-ilibrary.org/environment-/diffuse-pollution-degraded-waters_9789264269064>. 33, 34

OKAMURA, K. et al. Development of a 128-channel multi-water-sampling system for underwater platforms and its application to chemical and biological monitoring. *Methods in Oceanography*, Elsevier, v. 8, p. 75–90, 2013. 37

OLIVEIRA, L. M. de; MAILLARD, P.; PINTO, E. J. de A. Application of a land cover pollution index to model non-point pollution sources in a brazilian watershed. *Catena*, Elsevier, v. 150, p. 124–132, 2017. 30, 36, 67

OSAWA, R. A. et al. Determinação de fármacos anti-hipertensivos em águas superficiais na região metropolitana de curitiba. *Revista Brasileira de Recursos Hídricos*, v. 20, n. 4, p. 1039–1050, 2015. 57

PALLEIRO, L. et al. Dissolved and particulate metals in the mero river (nw spain): factors affecting concentrations and load during runoff events. *Communications in soil science and plant analysis*, Taylor & Francis, v. 43, n. 1-2, p. 88–94, 2012. 64

PENG, H.-Q. et al. Event mean concentration and first flush effect from different drainage systems and functional areas during storms. *Environmental Science and Pollution Research*, Springer, v. 23, n. 6, p. 5390–5398, 2016. 37

PÉREZ-GUTIÉRREZ, J. D. et al. Impact of rainfall characteristics on the no3–n concentration in a tailwater recovery ditch. *Agricultural Water Management*, Elsevier, v. 233, p. 106079, 2020. 98, 155

PEURAVUORI, J.; PIHLAJA, K. Molecular size distribution and spectroscopic properties of aquatic humic substances. *Analytica Chimica Acta*, Elsevier, v. 337, n. 2, p. 133–149, 1997. 50, 51

PITRAT, D. M. J. J. *Avaliação da contaminação por metais em rios: Estudo de caso da Bacia do Rio Passaúna*. Tese (Doutorado) — Universidade Federal do Paraná, Programa de Pós-Graduação em Engenharia de Recursos Hídricos e Ambiental, 2010. 63

PORTO, M.; PORTO, R. Gestão de bacias hidrográficas. *Estudos avançados*, SciELO Brasil, v. 22, n. 63, p. 43–60, 2008. 27, 28, 34, 36

QUIGLEY JANE CLARY, A. E. A. P. M. L. E. S. J. J. R. M. M.; O'BRIEN, J. *Urban stormwater BMP performance monitoring*. [S.l.], 2009. 36, 37, 38, 47, 48

RAIMUNDO, C. C. M. *Ocorrência de interferentes endócrinos e produtos farmacêuticos nas águas superficiais da bacia do rio Atibaia*. Tese (Doutorado) — Universidade Estadual de Campinas, Universidade Estadual de Campinas, Instituto de Química, 2007. 59

RAMOS, T. B. et al. Sediment and nutrient dynamics during storm events in the enxoé temporary river, southern portugal. *Catena*, Elsevier, v. 127, p. 177–190, 2015. 28, 30, 37, 45, 46

RANTAKARI, M. et al. Organic and inorganic carbon concentrations and fluxes from managed and unmanaged boreal first-order catchments. *Science of the Total Environment*, Elsevier, v. 408, n. 7, p. 1649–1658, 2010. 47, 48

REICHERT, G. et al. Emerging contaminants and antibiotic resistance in the different environmental matrices of latin america. *Environmental Pollution*, Elsevier, v. 255, p. 113140, 2019. 54, 57

REICHERT, G. et al. Determination of parabens, triclosan, and lipid regulators in a subtropical urban river: Effects of urban occupation. *Water, Air, & Soil Pollution*, Springer, v. 231, n. 3, p. 1–11, 2020. 57, 59, 67

ROSTAN, J.; CELLOT, B. On the use of uv spectrophotometry to assess dissolved organic carbon origin variations in the upper rhône river. *Aquatic Sciences*, Springer, v. 57, n. 1, p. 70–80, 1995. 50

RUHALA, S. S.; ZARNETSKE, J. P. Using in-situ optical sensors to study dissolved organic carbon dynamics of streams and watersheds: a review. *Science of the Total Environment*, Elsevier, v. 575, p. 713–723, 2017. 28, 38, 48

SANTOS, H. G. dos et al. *Sistema brasileiro de classificação de solos*. [S.l.: s.n.], 2018. 73

SANTOS, M. L. dos; LENZI, E.; COELHO, A. R. Ocorrência de metais pesados no curso inferior do rio ivaí, em decorrência do uso do solo em sua bacia hidrográfica. *Acta Scientiarum. Technology*, Universidade Estadual de Maringá, v. 30, n. 1, p. 99–107, 2008. 64

SANTOS, M. M. d. et al. Occurrence and risk assessment of parabens and triclosan in surface waters of southern brazil: a problem of emerging compounds in an emerging country. *RBRH*, SciELO Brasil, v. 21, n. 3, p. 603–617, 2016. 57, 58

SAUVÉ, S.; DESROSIERS, M. A review of what is an emerging contaminant. *Chemistry Central Journal*, BioMed Central, v. 8, n. 1, p. 1–7, 2014. 54

SENESI, N.; XING, B.; HUANG, P. M. *Biophysico-chemical processes involving natural nonliving organic matter in environmental systems*. [S.l.]: John Wiley & Sons, 2009. v. 2. 49

SHEN, W. et al. A framework for evaluating county-level non-point source pollution: Joint use of monitoring and model assessment. *Science of The Total Environment*, Elsevier, p. 137956, 2020. 28, 30, 66

SHI, Y. et al. Influence of land use and rainfall on the optical properties of dissolved organic matter in a key drinking water reservoir in china. *Science of the Total Environment*, Elsevier, v. 699, p. 134301, 2020. 67

SINGH, S.; INAMDAR, S.; MITCHELL, M. Changes in dissolved organic matter (dom) amount and composition along nested headwater stream locations during baseflow and stormflow. *Hydrological processes*, v. 29, n. 6, p. 1505–1520, 2015. 28

SODRÉ, F. F. Fontes difusas de poluição da Água: Características e métodos de controle. *Artigos Temáticos do AQQUA*, v. 1, p. 9–16, 2012. 34, 35

SPEIGHT, J. G. *Environmental Inorganic chemistry for engineers*. [S.l.]: Butterworth-Heinemann, 2017. 62, 63, 70

SPERLING, M. V. *Introdução à qualidade das águas e ao tratamento de esgotos*. [S.l.]: Editora UFMG, 2017. v. 1. 33, 47, 48, 146

STEPHENS, B. M.; MINOR, E. C. Dom characteristics along the continuum from river to receiving basin: a comparison of freshwater and saline transects. *Aquatic Sciences*, Springer, v. 72, n. 4, p. 403–417, 2010. 51

SUDERHSA. *Plano Diretor de Drenagem para a Bacia do Rio Iguaçu na Região Metropolitana de Curitiba*. [S.l.], 2002. Relatório Final: Capacidade do sistema atual e medidas de controle de cheias. Edição Final, CH2M Hill do Brasil Serviços de Engenharia Ltda. 70

TAKADA, H. et al. Transport of sludge-derived organic pollutants to deep-sea sediments at deep water dump site 106. *Environmental science & technology*, ACS Publications, v. 28, n. 6, p. 1062–1072, 1994. 60

TALIB, A.; RANDHIR, T. O. Managing emerging contaminants in watersheds: need for comprehensive, systems-based strategies. *Sustainability of Water Quality and Ecology*, Elsevier, v. 9, p. 1–8, 2017. 57

TAMANDARÉ, P. M. de A. *Plano Municipal de Saneamento Básico do Município de Almirante Tamandaré. http : //www.tamandare.pr.gov.br/uploads/8285f30d2ad035c5a5adfebd45d89d44.pdf*, 2015. Accessed in October 27, 2019. 71

TISSIER, G. et al. Seasonal changes of organic matter quality and quantity at the outlet of a forested karst system (la roche saint alban, french alps). *Journal of hydrology*, v. 482, p. 139–148, 2013. 49

UNEP; OECD. *OECD Screening Information Data Set (SIDS) for Caffeine, CAS 58-08-2*. [S.l.], 2003. 376 f. p. Available from, as of Jan 9, 2014. 58

UNESCO. *Emerging Pollutants in Water and Wastewater*. 2020. Accessed in August 26, 2020. Available at: <https://en.unesco.org/emergingpollutantsinwaterandwastewater>. 54

USEPA. *Report to Congress: Nonpoint Source Pollution in the U.S.* Washington D.C., 1984. 160p. 33, 34

USEPA. *Program Overview: Total Maximum Daily Loads (TMDL)*. 2018. Accessed in Jan/2018. Available at: <https://www.epa.gov/tmdl/program-overview-total-maximum-daily-loads-tmdl>. 28

USGS. *Emerging Contaminants*. 2020. Accessed in August 26, 2020. Available at: <https://www.usgs-.gov/mission-areas/water-resources/science/emerging-contaminants?qt-science_center_objects=0#qt-science_center_objects>. 54

VALLERO, D. A.; LETCHER, T. M. *Unraveling environmental disasters*. [S.l.]: Newnes, 2012. 62, 63

VISWANATHAN, V. C.; MOLSON, J.; SCHIRMER, M. Does river restoration affect diurnal and seasonal changes to surface water quality? a study along the thur river, switzerland. *Science of the Total Environment*, Elsevier, v. 532, p. 91–102, 2015. 37, 48, 67

WANG, X. et al. Evaluation and estimation of surface water quality in an arid region based on eem-parafac and 3d fluorescence spectral index: A case study of the ebinur lake watershed, china. *Catena*, Elsevier, v. 155, p. 62–74, 2017. 48, 53, 67

WANG, Z.-J. et al. Rainfall driven nitrate transport in agricultural karst surface river system: Insight from high resolution hydrochemistry and nitrate isotopes. *Agriculture, Ecosystems & Environment*, Elsevier, v. 291, p. 106787, 2020. 48, 67

WESTERHOFF, P.; ANNING, D. Concentrations and characteristics of organic carbon in surface water in arizona: influence of urbanization. *Journal of hydrology*, Elsevier, v. 236, n. 3-4, p. 202–222, 2000. 50, 52

WHO, W. M. O. *Guide to Meteorological Instruments and Methods of Observation - WMO-No. 8*. Seventh edition. Geneva, Switzerland, 2008. 20, 77, 94, 96, 101, 102

WIJESIRI, B. et al. Influence of pollutant build-up on variability in wash-off from urban road surfaces. *Science of the Total Environment*, Elsevier, v. 527, p. 344–350, 2015. 40

WILLIAMS, G. P. Sediment concentration versus water discharge during single hydrologic events in rivers. *Journal of Hydrology*, Elsevier, v. 111, n. 1-4, p. 89–106, 1989. 44

WISE, J. L. et al. Dissolved organic matter dynamics in storm water runoff in a dryland urban region. *Journal of arid environments*, Elsevier, v. 165, p. 55–63, 2019. 37, 39, 67

WQA. *Contaminants of Emerging Concern*. 2020. Accessed in August 26, 2020. Available at: <https://www.wqa.org/whats-in-your-water/emerging-contaminants>. 54

XIA, F. et al. A comprehensive analysis and source apportionment of metals in riverine sediments of a rural-urban watershed. *Journal of hazardous materials*, Elsevier, v. 381, p. 121230, 2020. 64

XIAN, Q. et al. Concentration and spectroscopic characteristics of dom in surface runoff and fracture flow in a cropland plot of a loamy soil. *Science of The Total Environment*, v. 622, p. 385–393, 2018. 53

XIE, H. et al. Intra-and inter-event characteristics and controlling factors of agricultural nonpoint source pollution under different types of rainfall-runoff events. *Catena*, Elsevier, v. 182, p. 104105, 2019. 39, 40, 48, 67, 92, 98, 102

YAN, R.; LI, L.; GAO, J. Framework for quantifying rural nps pollution of a humid lowland catchment in taihu basin, eastern china. *Science of the total environment*, Elsevier, v. 688, p. 983–993, 2019. 27, 30

YANG, L. et al. Tracking the evolution of stream dom source during storm events using end member mixing analysis based on dom quality. *Journal of Hydrology*, v. 523, p. 333–341, 2015. 49, 67, 69, 155, 156

YANG, Y. et al. Dissolved organic matter in relation to nutrients (n and p) and heavy metals in surface runoff water as affected by temporal variation and land uses–a case study from indian river area, south florida, usa. *Agricultural water management*, Elsevier, v. 118, p. 38–49, 2013. 64

YU, S. et al. Effect of land use types on stream water quality under seasonal variation and topographic characteristics in the wei river basin, china. *Ecological indicators*, Elsevier, v. 60, p. 202–212, 2016. 28, 35, 36, 39, 47, 48, 67

ZHANG, L. et al. Characterizing fluvial heavy metal pollutions under different rainfall conditions: Implication for aquatic environment protection. *Science of the Total Environment*, Elsevier, v. 635, p. 1495–1506, 2018. 64, 67, 68, 69

ZHANG, Z. et al. Risk estimation and annual fluxes of emerging contaminants from a scottish priority catchment to the estuary and north sea. *Environmental geochemistry and health*, Springer, v. 40, n. 5, p. 1987–2005, 2018. 29, 57, 67, 68, 69

ZHAO, Y. et al. Evaluation of cdom sources and their links with water quality in the lakes of northeast china using fluorescence spectroscopy. *Journal of Hydrology*, Elsevier, v. 550, p. 80–91, 2017. 49

ZHOU, P. et al. New insight into the correlations between land use and water quality in a coastal watershed of china: Does point source pollution weaken it? *Science of The Total Environment*, Elsevier, v. 543, p. 591–600, 2016. 34, 36, 47, 48, 67

ZHOU, Y. et al. Dissolved organic matter fluorescence at wavelength 275/342 nm as a key indicator for detection of point-source contamination in a large chinese drinking water lake. *Chemosphere*, Elsevier, v. 144, p. 503–509, 2016. 49

ZHOU, Y. et al. Potential rainfall-intensity and ph-driven shifts in the apparent fluorescent composition of dissolved organic matter in rainwater. *Environmental Pollution*, v. 224, p. 638–648, 2017. 28, 67

ZUCCO, E. et al. Metodologia para estimativa das concentrações em cursos de água para vazões de referência: uma ferramenta de suporte e apoio ao sistema de gestão de bacias hidrográficas. *REGA*, v. 9, n. 1, p. 25–37, 2012. 27

ZULIANI, D. Q. et al. Elementos-traço em águas, sedimentos e solos da bacia do rio das mortes, minas gerais. *HOLOS*, Instituto Federal de Educação, Ciência e Tecnologia do Rio Grande do Norte, v. 4, p. 308–326, 2017. 62, 64

ZULKIFLI, S. N.; RAHIM, H. A.; LAU, W. J. Detection of contaminants in water supply: A review on state-of-the-art monitoring technologies and their applications. *Sensors and Actuators B: Chemical*, Elsevier, 2017. 28, 36